VIBRATIONAL WAVE PACKETS: MOLECULAR STATE RECONSTRUCTION IN THE GAS PHASE AND MIXED QUANTUM/SEMICLASSICAL DESCRIPTIONS OF SMALL-MOLECULE DYNAMICS IN LOW-TEMPERATURE SOLID MEDIA

by

CRAIG THOMAS CHAPMAN

A DISSERTATION

Presented to the Department of Chemistry
and the Graduate School of the University of Oregon
in partial fulfillment of the requirements
for the degree of
Doctor of Philosophy

March 2010

University of Oregon Graduate School

Confirmation of Approval and Acceptance of Dissertation prepared by:

Craig Chapman

Title:

"Vibrational Wave Packets: Molecular State Reconstruction in the Gas Phase and Mixed Quantum/Semiclassical Descriptions of Small-Molecule Dynamics in Low-Tempurature Solid Media"

This dissertation has been accepted and approved in partial fulfillment of the requirements for the Doctor of Philosophy degree in the Department of Chemistry by:

David Herrick, Chairperson, Chemistry
Jeffrey Cina, Advisor, Chemistry
Thomas Dyke, Member, Chemistry
Michael Kellman, Member, Chemistry
Hailin Wang, Outside Member, Physics

and Richard Linton, Vice President for Research and Graduate Studies/Dean of the Graduate School for the University of Oregon.

March 20, 2010

Original approval signatures are on file with the Graduate School and the University of Oregon Libraries.

An Abstract of the Dissertation of

Craig Thomas Chapman for the degree of Doctor of Philosophy

in the Department of Chemistry to be taken March 2010

Title: VIBRATIONAL WAVE PACKETS: MOLECULAR STATE RECONSTRUCTION IN THE GAS PHASE AND MIXED QUANTUM/SEMICLASSICAL DESCRIPTIONS OF SMALL-MOLECULE DYNAMICS IN LOW-TEMPERATURE SOLID MEDIA

Approved: _____
Dr. Jeffrey A. Cina

We explore the reconstruction of B-state vibrational wave packets in I_2 from simulated two-color nonlinear wave packet interferometry data. As a simplification of earlier proposals, we make use of different vibrational energy ranges in the B-state—rather than different electronic potential surfaces—for the short-pulse preparation and propagation of both target and reference wave packets. Numerical results from noisy interferograms indicate that experimental reconstruction should be possible with high fidelity (>0.99).

Time-resolved coherent nonlinear optical experiments on small molecules in low-temperature host crystals are exposing valuable information on quantum mechanical dynamics in condensed media. We make use of generic features of these systems to

frame two simple, comprehensive theories that will enable the efficient calculation of their ultrafast spectroscopic signals and support their interpretation in terms of the underlying chemical dynamics. Both treatments rely on the identification of normal coordinates to unambiguously partition the well-structured guest-host complex into a system and a bath and expand the overall wave function as a sum of product states between fully anharmonic vibrational basis states for the system and approximate Gaussian wave packets for the bath degrees of freedom. The theories exploit the fact that ultrafast experiments typically drive large-amplitude motion in a few intramolecular degrees of freedom of higher frequency than the crystal phonons, while these intramolecular vibrations indirectly induce smaller-amplitude—but still perhaps coherent—motion among the lattice modes. The equations of motion for the time-dependent parameters of the bath wave packets are fairly compact in a fixed vibrational basis/Gaussian bath (FVB/GB) approach. An alternative adiabatic vibrational basis/Gaussian bath (AVB/GB) treatment leads to more complicated equations of motion involving adiabatic and nonadiabatic vector potentials.

Numerical tests of the FVB/GB are presented. We consider two bilinearly coupled harmonic oscillators with varying coupling strengths and initial conditions and show that the mixed quantum/semiclassical theory compares favorably with the exact results. Linear absorption spectra and wave-packet interferometry signals calculated using the theory are presented.

This dissertation includes previously published coauthored material.

CURRICULUM VITAE

NAME OF AUTHOR: Craig Thomas Chapman

PLACE OF BIRTH: Somers Point, NJ, USA

DATE OF BIRTH: August 25, 1980

GRADUATE AND UNDERGRADUATE SCHOOLS ATTENDED:

University of Oregon, Eugene, OR
The Richard Stockton College of New Jersey, Pomona, NJ

DEGREES AWARDED:

Doctor of Philosophy in Chemistry, University of Oregon, 2010
Bachelor of Science in Chemistry, The Richard Stockton College of New Jersey, 2003

AREAS OF SPECIAL INTEREST:

Vibrational wave packets
Quantum dynamics
Ultrafast spectroscopy

PROFESSIONAL EXPERIENCE:

Graduate Research Assistant, Department of Chemistry, University of Oregon, 2003-2010
Graduate Teaching Fellow, University of Oregon, 2003-2009
Research Assistant, National Science Foundation Research Experience for Undergraduates, 2001

PUBLICATIONS:

Heide N. Ibrahim, Craig T. Chapman, Hiroyuki Katsuki, Jeffrey A. Cina, and Kenji Ohmori, "Wave packet reconstruction on unknown potential surfaces by two-colour non-linear wave packet interferometry," Proceedings of the 17th International Conference on Ultrafast Phenomena, Springer, New York (2010)

Craig T. Chapman, Jeffrey A. Cina, "Semiclassical treatments for smallmolecule dynamics in low-temperature crystals using fixed and adiabatic vibrational bases," Journal of Chemical Physics, **127**, 114502 (2007)

Craig T. Chapman, Mary A. Rohrdanz, Jeffrey A. Cina, "Intermolecular communication and a vibrationally adiabatic basis treatment of smallmolecule dynamics in low temperature solids," Proceedings of the 15th International Conference on Ultrafast Phenomena, Springer, New York (2006)

Jeff Fiscus, Neil G. Pschirer, R. Hipp, Andrea M. Goforth, Craig T. Chapman, S. Shotwell, R. Layland, Mark D. Smith, Uwe H. F. Bunz, Hans-Conrad zur Loye, "Synthesis and structural characterization of five new coordination polymer chain structures using a new, Z-shaped ligand, 2,2 'bis(4-pyridylethynyl) tolane," Journal of Chemical Crystallography, **35**, 125 (2005)

Craig T. Chapman, Andrea M. Goforth, Neil G. Pschirer, Mark D. Smith, Uwe H. F. Bunz and Hans-Conrad zur Loye, "Synthesis and crystal structure of catenapoly[$Rh_2(OAc)_4(C_{27}H_{15}N_3)$]·$2CH_2Cl_2$, a novel Rh(II) organic/inorganic coordination polymer," Journal of Chemical Crystallography, **33**, 885 (2003)

Craig T. Chapman, Delia M. Ciurtin, Mark D. Smith and HansConrad zur Loye, "A new mixedmetal MnRh coordination polymer assembled from Mn-containing molecular building blocks and $Rh_2(OAc)_4$ dimers," Solid State Sciences, **4**, 1187 (2002)

ACKNOWLEDGMENTS

I would like to thank, first and foremost, my thesis advisor Dr. Jeff Cina for spending the better part of a decade teaching me how to live life as a scientist, to be systematic, and that no matter how many times you've derived an equation you're better off doing it one more time. All of my research rests on impeccable foundations laid by Dr. Mary Rohrdanz and Dr. Travis Humble, whose nonlinear wave-packet interferometry code served as a template for my own. Xiaolu Cheng was an indispensable resource in confirming numerical convergence of our theory, and in elucidating the assymetry of the equation of motion for the width parameter of our bath wave packets.

I would like to acknowledge the strong women in my life who have always emphasized that through hard work and perserverence anything is possible: Karen, Mary, Margaret, and Marilee. Of these women, I especially thank my future wife, Margaret, for her incomparable patience and support, late-night errands, and many trips to King Street Station. I am forever grateful. I also extend my grattitude to the National Railroad Passenger Corporation (Amtrak) for providing direct rail access between Eugene and Seattle.

The entirety of this dissertation, including relevant calculations, plotting, and typesetting, was performed using open source software released under the GNU General Public License.

Wouldn't it be nice...

TABLE OF CONTENTS

Chapter Page

Chapter Page

LIST OF FIGURES

Figure Page

CHAPTER I

INTRODUCTION

A Overview

Quantum mechanics has been an effective tool for interpreting and predicting the outcomes of experiments aimed at studying matter on the microscopic level, and has ultimately led to a more thorough understanding of the natural world. There have been many technological advances that have enabled the probing of atomic and molecular dynamics with ever greater precision and accuracy, most notably the ability to use coherent laser light to manipulate the spatio-temporal evolution of electrons and nuclei on chemically relevant scales. The concurrent development of ever faster CPU's has allowed advances in theoretical and computational descriptions of quantum dynamical processes to proceed to the point of intermittently surpassing experimental capabilities. The interplay between experimental and theoretical investigation is of the utmost importance; one cannot thrive without the other.

Of particular interest to the work presented herein is the elucidation and description of nuclear dynamics. Sequences of pulsed laser light can be used to transfer amplitude between molecular electronic states, creating linear superpositions of stationary vibrational eigenstates, or vibrational wave packets.[1] The wave packets then evolve according to the relevant nuclear Hamiltonian and their dynam-

ics can be analyzed using a plethora of techniques. With knowledge of the pulse profiles and subsequent wave packet evolution, one can potentially guide or control nuclear motion with limitations set only by available technology and Heisenberg's uncertainty principle.

An important quantum mechanical phenomenon with interesting consequences is the interference of wave functions. The wave functions describing a molecular system can interfere constructively or destructively depending on the relative phases of the constituent basis functions. This purely quantum mechanical effect can be exploited to gain information on a molecule spectroscopically using the technique of wave-packet interferometry (WPI). A WPI experiment entails creating and manipulating electronic, vibrational, and rotational coherences using two (linear WPI) or more (nonlinear or nl-WPI) laser pulses. The pulses imprint their phase onto the wave functions which can then interfere with each other to enhance or deplete the population of relevant quantum states.

The first linear WPI experiments involved a phase-locked optical pulse pair impinging on a sample of gaseous I_2, creating a superposition of wave packets on the B state.[2,3] The signal, found by measuring the time- and frequency-integrated fluorescence, is the portion of the B state population that is linear in each of the electric fields of the pulses. The signal can then be used to completely resolve the overlap of the two one-pulse wave packets.

Linear WPI has been used on a variety of other molecular systems. We point out a few representative examples here. Ohmori *et al.* were able to prepare arbitrary population distributions in a HgAr van der Waals complex using a pair of time-delayed UV pulses.[4] The ability to create such superpositions is important for coherently controlling the outcome of chemical reactions using lasers. Fushitani *et al.* used WPI on Cl_2 embedded in cryogenic Ar to control chromophore-bath

coupling.[5] By varying the inter-pulse delay and relative phase between the pulses they were able to selectively create wave packets consisting of excited Cl_2 without directly exciting the Ar host.

Nonlinear WPI, first developed conceptually by Humble and Cina,[6] uses two pairs of phase locked optical pulses to create wave packets that can evolve on various electronic states. One particularly important application of nl-WPI is molecular state reconstruction.[7] wherein a target wave packet that is to be determined is launched on an excited electronic surface *via* one of the pulses in the four-pulse sequence. The other three pulses are used to create a reference state that subsequently interferes with the one-pulse wave packet. The signal in a nl-WPI experiment is the portion of the population of the excited electronic state measured by time- and frequency-integrated fluorescence that is quadrilinear in the electric fields of the excitation pulses and bears a particular phase signature. A collection of reference states and signal values (one of each for a particular set of inter-pulse delays) can be used to determine the target state. We test a new scheme for molecular state reconstruction using nl-WPI wherein the target and reference packets evolve only on the X and B states of I_2, as opposed to previous descriptions that involved preparation and evolution of the target wave packet on a third, high-lying electronic surface.

In addition to studying vibrational wave packet dynamics for isolated molecules, it is possible, and in some instances quite necessary, to have a wave packet description of the environmental degrees of freedom with which the molecule of interest exchanges information. Matrix isolation spectroscopy, first introduced to study free radicals[8] and largely developed by Pimentel in the 1950's, can probe the dynamics of a chromophore embedded in a cryogenic, chemically-inert host and, with the help of a cogent and comprehensive theory, can be used to extract detailed information about the chromophore-bath interactions. Direct laser excitation of the

chromophore can give rise to coherent vibrational motion in the bath, necessitating that a meaningful theoretical treatment have a wave-packet description of the bath, leading to the requirement that approximate methods, with amplitude-level information, be formulated to treat the many-body system-bath dynamics.

The environmental degrees of freedom, although chemically inert, can directly influence the dynamics and chemical identity of embedded molecules. The *cis-trans* isomerization of nitrous acid (HONO) in cryogenic Kr was first observed experimentally by Pimentel,[9] but to date has not been observed in the gas phase. Recent theoretical efforts by Hamm *et al.* indicate that the host Kr matrix alters the energy levels of the HONO molecule in such a way as to enable tunneling of the proton.[10] Another example of bath-mediated dynamics is the class of proposed experiments entitled "intermolecular communication."[11] Rohrdanz and Cina formulated a method to interrogate the communication between an atom and a molecule on a one-dimensional chain with Ar atoms separating the two, using time-resolved coherent anti-Stokes Raman scattering. The bath directly relays information that has been encoded into the 'transmitter' from a laser pulse, to the molecular 'receiver' through a coherent lattice phonon. It is essential to have a theory of coherent bath motion in such situations.

There have been many experimental investigations of cryogenically isolated dihalogens.[12–14] They couple the simplicity and well-known characteristics of homonuclear diatomic halogens with the richness of information to be had from quantum many-body interactions. There are still fundamental issues in need of theoretical exposition that, upon successful interpretation, can lead to a deeper understanding of the quantum mechanical nature of matter. Entanglement, collisional coherence transfer, vibrational and electronic decoherence, vibrational energy relaxation and transfer are all phenomena that can be meaningfully addressed both theoretically

and experimentally within the framework of matrix isolation.

The work presented in this dissertation is meant to illustrate the richness of information that can be obtained from, and wide applicability of, quantum dynamical descriptions of nuclear wave packet dynamics and the need for close collaboration between experimentalists and theoreticians.

B Outline

The main scientific findings in this dissertation are presented in three chapters. Chapter II investigates a new scheme for molecular state reconstruction *via* nl-WPI that uses the X and B states of I_2, and will be submitted for publication as a coauthored paper in an altered form. Coauthors will include Kenji Ohmori, Heide Ibrahim, Travis Humble, and Jeffrey Cina. Chapter II is expository in nature and lays the theoretical foundation for the fixed vibrational basis/Gaussian bath (FVB/GB) and adiabatic vibrational basis/Gaussian bath (AVB/GB) theories for treating the dynamics of small molecules embedded in cryogenic media, and has been published as a coauthored paper with Jeffrey Cina in *J. Chem. Phys.* **127**, 114502 (2007). The FVB/GB theory is tested numerically in Chapter IV, and will be submitted for publication in an altered form. Coauthors include Xiaolu Cheng and Jeffrey Cina. There are four appendices. Appendix A presents nl-WPI signals as well as target and reconstructed wave functions for various delays between the third and fourth pulses of the four-pulse sequence. Appendix B contains the equations of motion for the bath wave packet parameters evolving according to the FVB/GB theory, while the equations of motion under the AVB/GB are in Appendix C. Computational details, including computer code used to carry out a representative FVB/GB calculation, are included in Appendix D.

Notes

[1] Mukamel. S. *Principles of Nonlinear Optical Spectroscopy*; Oxford University Press. 1999.

[2] Scherer, N. F.; Carlson, R. J.; Matro, A.; Du, M.; Ruggiero, A. J.; Romero-Rochin, V.; Cina, J. A.; Fleming, G. R.; Rice, S. A. *J. Chem. Phys.* **1991**, *95*, 1487.

[3] Scherer, N. F.; Matro, A.; Ziegler, L. D.; Du, M.; Carlson, R. J.; Cina, J. A.; Fleming, G. R. *J. Chem. Phys.* **1992**, *96*, 4180.

[4] Ohmori, K.; Sato, Y.; Nikitin, E. E.; Rice, S. A. *Phys. Rev. Lett.* **2003**, *91*, 243003.

[5] Fushitani, M.; Bargheer, M.; Guhr, M.; Ibrahim, H.; Schwentner, N. *J. Phys. B: At. Mol. Opt. Phys.* **2008**, *41*, 074013.

[6] Cina, J. A.; Harris, R. A. *J. Chem. Phys.* **1994**, *100*, 2531.

[7] Humble, T. S.; Cina, J. A. *J. Phys. Chem. B* **2006**, *110*, 18879.

[8] Whittle, E.; Dows, D. A.; Pimentel, G. C. *J. Chem. Phys.* **1954**, *22*, 1943.

[9] Pimentel, G. C. *J. Am. Chem. Soc.* **1958**, *80*, 62.

[10] Schanz, R.; Boţan, V.; Hamm, P. *J. Chem. Phys.* **2005**, *122*, 044509.

[11] Rohrdanz, M. A.; Cina, J. A. *Mol. Phys.* **2006**, *104*, 1161.

[12] Goldschleger, I. U.; Senekerimyan, V.; Krage, M. S.; Seferyan, H.; Janda, K. C.; Apkarian, V. A. *J. Chem. Phys.* **2006**, *124*, 204507.

[13] Fushitani, M.; Bargheer, M.; Gühr, M.; Schwentner, N. *Phy. Chem. Chem. Phys.* **2005**, *7*, 3143.

[14] Bihary, Z.; Karavitis, M.; Apkarian, V. A. *J. Chem. Phys.* **2004**, *120*, 8144.

CHAPTER II

MOLECULAR STATE RECONSTRUCTION VIA NONLINEAR WAVE-PACKET INTERFEROMETRY

Dr. Kenji Ohmori and Dr. Heide Ibrahim initially raised the possibility of performing molecular state reconstructions using nonlinear wave-packet interferometry involving only two electronics states. I implemented this scheme numerically, with help from Dr. Jeff Cina, using Dr. Travis Humble's original nonlinear wave-packet interferometry/state reconstruction code as a template.

A Introduction

We explore the reconstruction of B-state vibrational wave packets in I_2 from simulated two-color nonlinear wave packet interferometry data. As a simplification of earlier proposals, we make use of different vibrational energy ranges in the B-state—rather than different electronic potential surfaces—for the short-pulse preparation and propagation of both target and reference wave packets. Numerical results from noisy interferograms indicate that experimental reconstruction should be possible with high fidelity (>0.99).

Time-resolved coherent multidimensional electronic spectroscopy can reveal amplitude-level molecular information on chemically relevant time scales. In particular, wave packet interferometry (WPI) has been used by several groups to char-

acterize atomic and molecular systems. Recent theoretical studies have shown that linear[1–4] and nonlinear WPI[5] (nl-WPI) data provides sufficient information to allow the robust reconstruction of time-dependent target wave packets launched by one pulse in the WPI sequence, in the latter case despite imperfect knowledge of the underlying electronic potential surface. The most detailed study to date demonstrated the reconstruction of rovibrational states of the lithium dimer using two phase-locked pulse pairs that access different electronic states. This chapter explores a simplification of this process by considering the possibility of determining a target wave packet not on a third, potentially poorly characterized, electronic surface, but in the upper region of the same surface used to generate the family of reference wave packets. Specifically, we investigate the systematic reconstruction of time-dependent nuclear wave functions in high-lying regions of the B $^3\Pi_{0_u^+}$ state of I_2 using reference wave packets that have evolved in lower-lying regions of the B state as well as the X $^1\Sigma_g^+$ state. These states have been studied extensively and are well characterized.[6,7]

B Nonlinear Wave-Packet Interferometry

In a nl-WPI experiment there are two pairs of optical phase-controlled ultrashort pulses, here a red pair (pulses 1 and 2) and a blue pair (pulses 3 and 4). The time delays between the first and second pulses, t_{21}, and between the second and third pulses, t_{32}, are varied for a given fixed delay between the third and fourth pulses, t_{43} (see inset of Figure 2.1). The signal is the portion of the population of the excited electronic state measured by time- and frequency-integrated fluorescence that is quadrilinear in the electric fields of the excitation pulses and bears a particular phase signature. Here, specifically, wave-packet reconstruction is based

on the contribution to the excited state population proportional to the overlap, $\langle (421)_B \mid (3)_B \rangle = \langle ref|tar \rangle$, of a wave packet that has been acted on by the third pulse (the target) with ones that have been acted on by the first, second, and fourth pulses (the reference). In this scheme the first pulse-pair acts on an initial state, creating a vibrationally excited wave packet in the ground electronic state. The third pulse interacts with the initial state and creates the target state proportional to $|(3)_B\rangle$ on the upper part of the B potential. Finally, the fourth pulse interacts with the evolving wave packet bilinear in E_1 and E_2, creating a reference packet proportional to $|(421)_B\rangle$. The nl-WPI signal, $\langle ref|tar \rangle$, from a collection of reference packets—one for each pair of (t_{21}, t_{32})—can be used to reconstruct the target state.

We use the RKR potential parameters of LeRoy[6] (X state) and Barrow and Yee[7] (B state), which are plotted along with the pulse sequence in Figure 2.1. As a first approximation we treat the dipole moment as a $\mu(r)$ = constant for all internuclear separations. The laser electric fields were written as

$$\begin{aligned} E_j(t) &= A(t - t_j)\cos\Phi_j(t - t_j) \\ &= Ae^{-(t-t_j)^2/2\sigma_j^2}\cos[\Omega_j \cdot (t - t_j) + \Phi_j] \end{aligned} \tag{2.1}$$

for $j = 1 - 4$; all pulses have the same amplitude, A, and temporal envelope, $\exp[-(t - t_j)^2/2{\sigma_j}^2]$, where t_j is the arrival time of the j^{th} pulse, and σ_j is the pulse duration. We set σ_j = 20 fs (47.1 fs FWHM amplitude, 33.3 fs FWHM intensity) for all of the pulses. The carrier angular frequency for the first two pulses is taken to be resonant with the $|X\rangle|\nu = 0\rangle \rightarrow |B\rangle|\nu = 20\rangle$ transition, $\Omega_1 = \Omega_2 = 2\pi c \cdot (17921\text{cm}^{-1})$ (558 nm), while the carrier angular frequency for the second pair is resonant with the $|X\rangle|\nu = 0\rangle \rightarrow |B\rangle|\nu = 40\rangle$ transition, $\Omega_3 = \Omega_4 =$

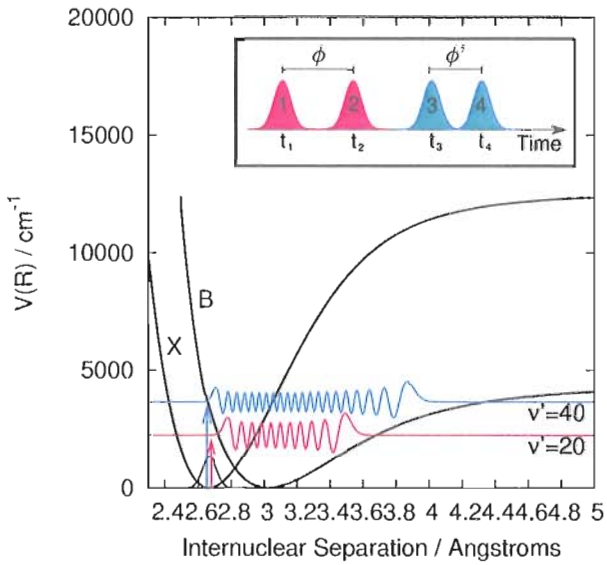

Figure 2.1: The X and B potentials of I_2 are plotted as functions of internuclear separation with the electronic energy removed. The pulse sequence (inset) for a nl-WPI experiment involves two phase-locked pulse pairs. The first pair is resonant with the $|\nu = 0\rangle$ to $|\nu' = 20\rangle$ transition, with relative phase ϕ, and is used to create a vibrationally excited wave packet on the X potential surface, while the second pair is resonant with the $|\nu = 0\rangle$ to $|\nu' = 40\rangle$ transition, with relative phase ϕ'. The first pulse of the second pulse pair generates the target wave packet from the vibrational ground state. The second pulse of the the second pulse pair generates the reference wave packet from the moving X-state packet prepared by the first pulse-pair. The time delays t_{21} and t_{32} are variably delayed for a fixed t_{43}.

$2\pi c \cdot (19493\text{cm}^{-1})$ (513 nm). The absolute phases Φ_j are unknown, but the relative phases $\Phi_2 - \Phi_1$ and $\Phi_4 - \Phi_3$ are under experimental control. Phase locking the first pulse pair dictates the optical phase shift $\phi = \Phi_2 - \Phi_1 - \omega_L t_{21}$ be held constant as t_{21} is scanned. Likewise phase locking the second pulse pair specifies a phase shift $\phi' = \Phi_4 - \Phi_3 - \omega_L' t_{43}$. Here the lock frequency for the first (second) pulse-pair, ω_L (ω_L'), is the carrier frequency of both pulses in that pair.

The one- and three-pulse wave packets whose overlap for a given set of inter-pulse delays constitutes the calculated signal are

$$|(3)_B\rangle = e^{-iH_B t_{43}} P_3^{BX} |0_X\rangle, \tag{2.2}$$

and

$$|(421)_B\rangle = P_4^{BX} e^{-iH_X t_{42}} P_2^{XB} e^{-iH_B t_{21}} P_1^{BX} e^{iH_X t_{31}} |0_X\rangle, \tag{2.3}$$

respectively. Here $P_j^{\alpha\beta}$ is a reduced pulse propagator[5] for the j^{th} pulse transferring amplitude from the electronic state β to state α, and $|0_X\rangle$ is the ground vibrational state of the X electronic state. The target states are related to the one-pulse packets by a phase factor, $|(3)_B\rangle = e^{i\phi_3(\omega_L')+i\omega_L' t_{43}} |tar\rangle$. The reference states are similarly related to the three-pulse packets, $|(421)_B\rangle = e^{i\phi_3(\omega_L')+i\omega_L' t_{43}} |ref\rangle = e^{i\phi_4(\omega_L')} |ref\rangle$. In both cases the phase factor is introduced to eliminate dependence on the uncontrolled absolute phases of the pulses. Here $\phi_j(\omega) - \omega t_j$ is the spectral phase of the Fourier component of the j^{th} pulse at frequency ω. Note that $|tar\rangle$ and $|ref\rangle$ are defined such that ϕ and ϕ' are equal to zero.

C Molecular State Reconstruction

For the reconstruction process we write the signal, $\mathbf{z} = \langle(421)_B|(3)_B\rangle$ as a vector of length M, with elements z_m and each $m \equiv (t_{21}, t_{32})$ corresponding to a different combination of delays. Working in the vibrational eigenbasis of the ground electronic state* we can write $z_m = \sum_\nu \langle ref|\nu\rangle\langle\nu|tar\rangle$. Reconstruction consists of solving the equation

$$\mathbf{z} = \mathbf{R}\mathbf{t}, \tag{2.4}$$

where the M by N reference matrix has elements $R_{m\nu} = \langle ref|\nu\rangle$ and the N-dimensional target state vector has elements $t_\nu = \langle\nu|tar\rangle$. A pseudoinverse of the reference matrix, $\mathbf{R}_T^{-1}$ can be found *via* singular value decomposition and back substitution,[8] which involves factoring the reference matrix as $\mathbf{R} = \mathbf{U}\mathbf{W}\mathbf{V}^\dagger$, where $\mathbf{V}$ is

*The vibrational energy eigenbasis proved to more computationally efficient in the present calculations than the discrete position basis used in a previous Reference 5.

a unitary N by N matrix, $\mathbf{U}$ is an M by N row-unitary matrix, and $\mathbf{W}$ is a diagonal matrix with real positive singular values along its diagonal. We set a tolerance T, such that the modified inverse of $\mathbf{W}$ has elements

$$(\mathbf{W}_T{}^{-1})_{jj} = \begin{cases} 1/W_{jj} & \text{if} \quad W_{jj}/W_{\max} > T \\ 0 & \text{otherwise} \end{cases} \tag{2.5}$$

where W_{max} is the largest singular value. We can then write $\mathbf{R}_T^{-1} = \mathbf{V}\mathbf{W}_T{}^{-1}\mathbf{U}^\dagger$ to find an approximate solution to Eqn. (2.4) given by $\mathbf{r} = \mathbf{R}_T^{-1}\mathbf{z} \cong \mathbf{t}$. The fidelity, $f = \frac{|\mathbf{r}^\dagger \cdot \mathbf{t}|}{|\mathbf{r}||\mathbf{t}|}$, which lies between 0 and 1, assesses the accuracy of the reconstruction.

In an effort to more realistically mimic experimental conditions, we add noise to the signal before performing the reconstruction. We add to each point in the interferogram a value of noise, x, that is randomly chosen from the distribution $\rho(x) = e^{-x^2/2\sigma^2}$, where σ is 5% of the maximum of the absolute value of the complex signal.

In a recent probe-detected wave-packet interferometry study, Katsuki *et al.* were able to visualize interference fringes of I_2 wave packets in samples prepared in a molecular jet.[9] The rotational temperature of the sample was ~15 K. At that temperature the rotational period is tens of ps, two orders of magnitude longer than the vibrational period in the ground state, and much longer than the maximum inter-pulse delay used in the calculations being presented here. We therefore neglect rotational dynamics in the exploratory calculations reported here.

For an initial state we use the ground vibrational state of the X electronic state, $|0_X\rangle$, ignoring any population in higher levels due to thermal excitation. Both t_{21} and t_{32} are varied from 0 to 1500 fs in increments of 10 fs, and we consider two target propagation times at present, t_{43} = 15 fs and 60 fs. The real and imaginary

parts of the resulting two-dimensional interferogram for $t_{43} = 15$ fs are shown in Figure 2.2. The periodicity in signal intensity with t_{21} is related to the vibrational

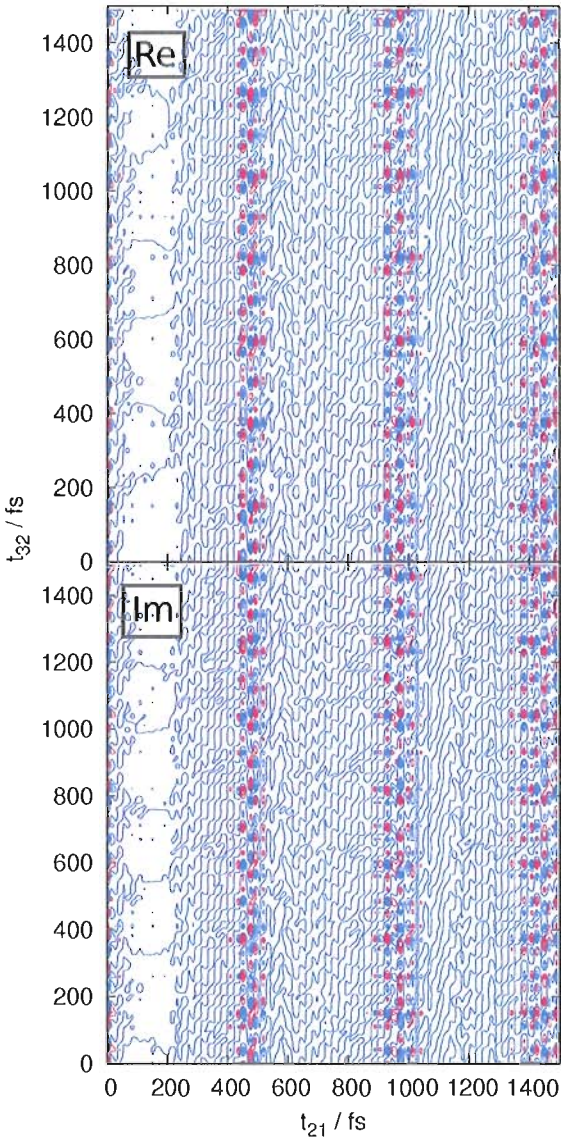

Figure 2.2: Real (upper panel) and imaginary (lower panel) components of the noise-free interferogram from vibrating, nonrotating I_2 plotted as a function of interpulse delays t_{21} and t_{32} for fixed $t_{43} = 15$ fs. The positive (red lines) and negative (blue lines) are separated by $1/25^{\text{th}}$ of the maximum absolute value of the signal. Periodicity along the t_{21} axis reflects wave-packet motion in the B state, while that along the t_{32} axis is due to motion in the X state.

period of the B state around $\nu = 20$ ($\tau_B \approx 490$ fs), while a less visually apparent periodicity along the t_{32} axis is due to vibrational motion in the X state ($\tau_X \approx 254$ fs).

The amplitudes and phases of the target and reconstructed states are plotted in Figure 2.4. The fidelity of reconstruction from the noisy signal is $f = 0.99343$

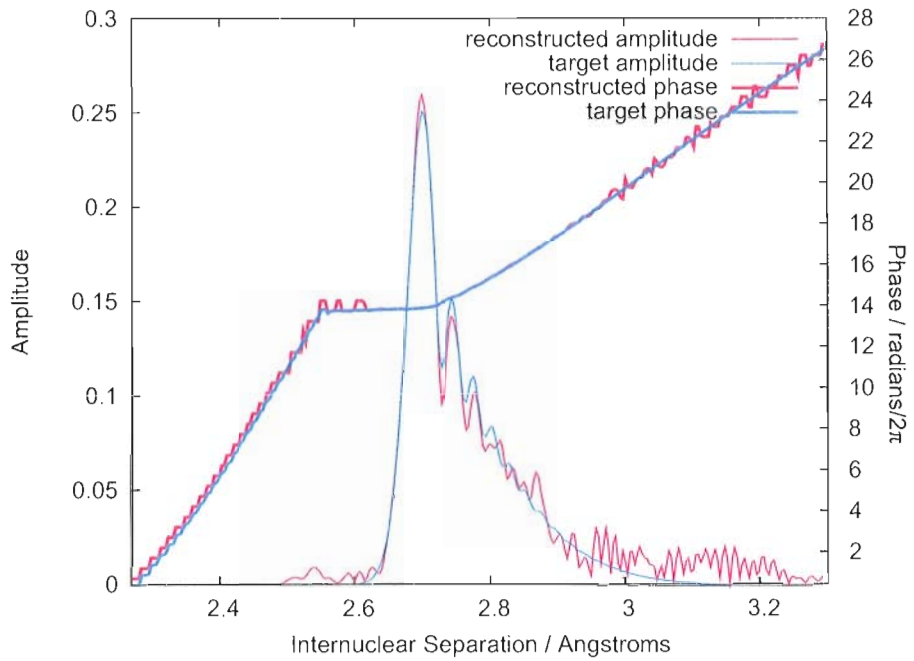

Figure 2.3: The phase (right hand scale) and amplitude (left hand scale) of the target (blue lines) and reconstructed (red lines) states for $t_{43} = 15$ fs. Reconstruction is performed with a fidelity $f = 0.993433$ using an optimal tolerance 0.03767.

(compared to unit fidelity from a noiseless signal). After 15 fs, the target wave packet has gained momentum and begun to move away from the Franck-Condon region centered at 2.666 Å. The success of the reconstruction, despite minor disagreements in the amplitudes at relatively small (<2.6 Å) and large (>3 Å) internuclear separations, is due in large part to the accurate reproduction of the phase, especially in regions where there is considerable amplitude. As pointed out in reference 5, discrepancies in the amplitude alone of the reconstructed wave packet affect the fidelity

only at second order. The reconstructed local phase is

$$\theta_{rec}(r) = \tan^{-1}(\psi''_{rec}(r)/\psi'_{rec}(r)), \tag{2.6}$$

where $\psi_{rec}(r) = \psi'_{rec} + i\psi''_{rec}(r)$ and $\theta_{rec}(r)$ is bounded by $\pm\pi$. We shift $\theta_{rec}(r)$ by integer multiples of 2π so that $-\pi < \theta_{rec}(r) - \theta_{target}(r) < \pi$ without altering the reconstructed wave function or the fidelity.

Writing $\psi(r) = |\psi(r)|e^{i\theta(r)}$, we note that $\hbar\partial\theta/\partial r \approx p(r)$ can be identified as an approximate local momentum. In the range 2.5-2.7 Å the phase profile is nearly flat, indicating that the trailing edge of the target wave packet has yet to gain significant momentum. Portions of the wave packet at the leading edge, with separations greater than 2.7 Å, however, have begun to acquire momentum in the direction of increasing internuclear separation, as seen by the positive slope in the phase function.

A complication presents itself when using inter-pulse delays shorter than the pulse duration. Pulse propagators were used in calculating the effect of the laser pulses on each wave packet. A pulse propagator reduces the effect of a finite duration pulse on a state vector to the action of a single matrix-vector multiplication. In determining the nuclear matrix elements of the various pulse propagators, one time-evolves the relevant state ket on the originating potential surface for the full duration of the pulse and subsequently back-propagates the resulting wave packet on the final surface until the arrival time of that pulse. The unpropagated wave packet produced by the instantaneous action of a pulse propagator serves only as an initial condition that will yield the correct wave packet once it is propagated under the appropriate bare nuclear Hamiltonian for a time longer than the pulse duration. The target state that is reconstructed in Figure 2.3, for instance, has evolved on

the upper portion of the B state for approximately half of the pulse duration, so that it may not necessarily reflect the target state that would be produced under experimental conditions.

As the target state is allowed to evolve for longer times in the B state it loses some of its amplitude fringes and takes the more Gaussian-like shape seen in Figure 2.4. The reconstruction in this case (t_{43} = 60 fs) is more accurate, with

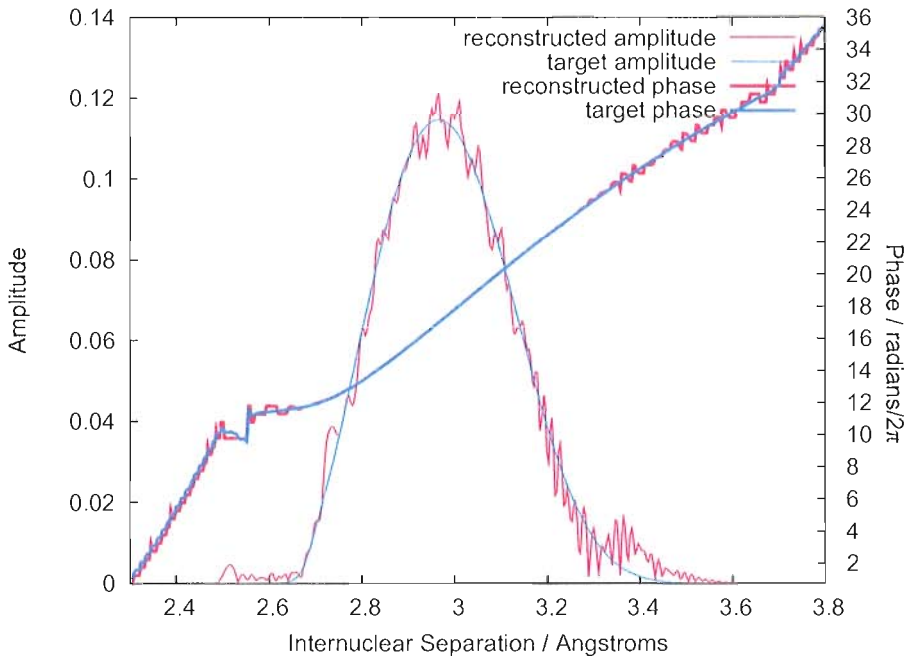

Figure 2.4: The phase (right hand scale) and amplitude (left hand scale) of the target (blue lines) and reconstructed (red lines) states for $t_{43} = 60$ fs. Reconstruction is performed with a fidelity $f = 0.997217$ using an optimal tolerance 0.00957.

$f = 0.997217$, than with $t_{43} = 15$ fs. The small gain in fidelity may be attributable to the more complicated form of the amplitude accompanying a shorter t_{43}.

The signal for $t_{43} = 60$ fs (see Appendix A) has smaller amplitude than that calculated for $t_{43} = 15$ fs. As the target wave packet moves out of the Franck-Condon region it enters a part of the potential that is less accessible to the reference states, due to the spectral selectivity of the pulses involved in creating $|ref\rangle$. Shorter

pulses could afford the bandwidth necessary to maintain a large signal amplitude, but would interfere with the spectral separation between the red and blue pulse pairs that enables isolation of signal contributions proportional to $\langle(421)_B|(3)_B\rangle$. Noise-free signals and plots of reconstructed and target states for t_{43} = 0, 30, 45, 60, 75, 650, and 715 fs are presented in Appendix A.

There are two contributions to the signal from a nl-WPI experiment that have the phase signature we seek, $\langle(421)_B|(3)_B\rangle$ and $\langle(431)_B|(2)_B\rangle$. The contribution of the latter to the signals presented in this chapter and on possible experimentally collected signals can be ignored. Given the pulse carrier frequencies previously mentioned, the transfer of amplitude from the low-lying region of the B state to the X state by the third pulse will be possible only for t_{31}'s that are near integer multiples of the B state period. Furthermore the transfer will be highly inefficient due to the small amplitude of $|20_B\rangle$ in the region of internuclear distance where $V_B(r) - V_X(r) \approx \hbar\Omega_3$. The fluorescence could also be filtered to collect only photons with energy sufficiently less than $E = V_B(r'_{20}) - V_X(r'_{20})$, where r'_n is the outer turning point of the $|n_B\rangle$ state, so that $\langle r|(2)_B\rangle$ is negligible in the emission-window region. In situations where the excited potential surface is dissociative, one could use time-of-flight mass spectroscopy to determine the relative contribution of the two overlaps with the relevant phase signature.[10]

An interesting issue for further investigation will be the robustness of molecular state reconstruction with partial neglect of information concerning the high-lying portion of the B-state, which contributes to the target, but not reference, wave-packet propagation. Such an investigation would be analogous to earlier studies of two-color, three-state nl-WPI which found that one can make even fairly crude approximations to the form of the final-state potential in calculating the reference wave packets and still successfully reconstruct a target wave packet. Using a linear

approximation to the difference potential, for instance, Humble and Cina were able to perform reconstructions of Li dimers with fidelity $f = 0.9907$.

In conclusion, we have demonstrated the possibility of reconstructing vibrational wave packets on I_2 from collections of wave packets evolving on the X and B states. This differs from previously formulated schemes for state reconstruction *via* nl-WPI in that we use only two electronic states. This simplification entails preparing reference states that have evolved on the lower portion of the B state, as well as the X state, to reconstruct a target state that is prepared on and allowed to evolve on the upper portion of the B state. Reconstructions from a noisy simulated signal were performed with high fidelity (>99%) and prove to be promising experimentally.

In addition to reconstructing molecular states using collections of vibrational wave packets in isolated molecules, we are also interested in the wave packet dynamics of interacting molecules in the condensed phase. Isolated gas phase molecules evolve with minimal intermolecular interactions. In the condensed phase, however, these interactions play a significant and inextricable role in the dynamics of directly probed chromophores. An ideal family of molecular systems whose vibrational and electronic degrees of freedom can be studied using wave packet techniques are small molecules embedded in cryogenic matrices. The chromophore and host dynamics are intimately connected, and an accurate description of not only the chromophore, but the host as well, is needed to simulate and interpret coherent spectroscopic experiments on these systems.

Notes

[1] Scherer, N. F.; Carlson, R. J.; Matro, A.; Du, M.; Ruggiero, A. J.; Romero-Rochin, V.; Cina, J. A.; Fleming, G. R.; Rice, S. A. *J. Chem. Phys.* **1991**, *95*, 1487.

[2] Scherer, N. F.; Matro, A.; Ziegler, L. D.; Du, M.; Carlson, R. J.; Cina, J. A.; Fleming, G. R. *J. Chem. Phys.* **1992**, *96*, 4180.

[3] Leichtle, C.; Schleich, W. P.; Averbukh, I. S.; Shapiro, M. *Phys. Rev. Lett.* **1998**, *80*, 1418.

[4] Averbukh, I. S.; Shapiro, M.; Leichtle, C.; Schleich, W. P. *Phys. Rev. A* **1999**, *59*, 2163–2173.

[5] Humble, T. S.; Cina, J. A. *J. Phys. Chem. B* **2006**, *110*, 18879.

[6] LeRoy, R. J. *J. Chem. Phys.* **1970**, *52*, 2678.

[7] Barrow, R. F.; Yee, K. K. *J. Chem. Soc. Faraday Trans. 2* **1973**, *69*, 684.

[8] Press, W.; Teukolsky, S.; Vetterling, W.; Flannery, B. *Numerical Recipes in C*, 2nd ed.; Cambridge University Press: Cambridge, UK, 1992.

[9] Katsuki, H.; Chiba, H.; Girard, B.; Meier, C.: Ohmori, K. *Science* **2006**, *311*, 1589.

[10] Breunig, H. G.; Urbasch, G.; Weitzel, K.-M. *J. Chem. Phys.* **2008**, *128*, 121101.

CHAPTER III

THEORETICAL FOUNDATIONS OF THE FIXED AND ADIABATIC VIBRATIONAL BASIS/GAUSSIAN BATH TREATMENTS

A Introduction

Ultrafast coherent spectroscopic experiments performed in conjunction with matrix isolation of a small-molecule chromophore reveal fundamental information about many-body molecular interactions of a quantum mechanical nature. Photo-induced molecular electronic excitations,[1,2] vibrations,[3–9] or chemical reactions[10,11] interact dissipatively with the surrounding medium. Entanglement may ensue between the chromophore and medium degrees of freedom, leading to both decoherence and energy loss by the "system." During the dynamics leading to equilibration, an initially pure electronic or nuclear reduced density matrix may become mixed in character. In the structured environment of a low temperature crystal, it is not uncommon for coherence transfer to occur between system and bath so that coherent molecular motion in the system leads to the onset of coherent motion in the "bath."[12–14]

The use of cryogenic noble-gas host matrices affords an opportunity to perform experiments on many-body systems in well-characterized nearly pure states, and has several generic features that can be exploited in constructing a new theoretical framework. A well-defined initial structure obviates the need for averaging over different equilibrium geometries and, at cryogenic temperatures, the entire guest-host complex can often be assumed to reside in its overall ground state prior to short-pulse laser excitation, with the neglect of any population in higher-lying states due to the low but nonzero temperature. The experimentally probed chromophore motion is oftentimes somewhat removed from the density of states of the lattice phonons—being significantly higher in frequency than the Debye frequency of the host crystal—and weakly coupled to them. Moreover, the ultrashort pulses of laser excitation and probing are usually chosen to be electronically or vibrationally resonant with transitions of the guest molecule. Its internal degrees of freedom are thus externally driven to large-amplitude coherent motion. Non-resonantly coupled modes of the surrounding medium become excited only indirectly through the transfer of energy, and possibly coherence, from the directly excited intramolecular degrees of freedom.

Here we put forward a theoretical approach that takes advantage of these factors. It will enable the systematic simulation of ultrafast coherent spectroscopic signals from small molecules embedded in solid matrices. We make a system-bath decomposition of the full nuclear Hamiltonian, with the system comprising the directly excited chromophore modes while the remaining degrees of freedom are relegated to the bath. The system's eigenstates—which are to be calculated numerically—serve as an anharmonic vibrational basis in which to express the composite state ket, and the bath wave packets act as time-dependent expansion coefficients.

There is some freedom in defining the vibrational basis, and we present two

options. The first uses the vibrational basis obtained when the bath is held fixed in its equilibrium (i.e. minimum-potential-energy) configuration. The fixed vibrational basis (FVB) is therefore independent of the time-varying coordinates of the bath. The second uses an adiabatic vibrational basis (AVB), which is parametrized by the bath coordinate variables. In both cases, the small-amplitude motion of the bath is treated semiclassically, with a differently propagating multidimensional Gaussian wave packet accompanying each vibrational level. Following Heller's general prescription for semiclassical dynamics under locally quadratic approximations (LQA) to the relevant Hamiltonians,[15] equations of motion for the parameters specifying the bath wave packets are derived for both vibrational bases.

The semiclassical approaches developed in this paper represent alternative generalizations to an earlier treatment that applied the LQA to all modes of a cryogenic complex by treating the time-dependent nuclear wave functions in various electronic states as multidimensional Gaussian wave packets describing *all* solute and solvent nuclear degrees of freedom.[16] Using that "universal" semiclassical method, Rohrdanz demonstrated the basic principle of intermolecular communication by lattice phonons. She observed abrupt changes in the calculated time-resolved coherent anti-Stokes Raman scattering (tr-CARS) signal from an I_2 molecule isolated in a one-dimensional Ar crystal arising from the arrival of a coherent lattice wave launched by the short-pulse electronic excitation and dynamical solvation of a Ca atom several lattice sites away. Those calculations[16] can also be regarded as providing a practical initial demonstration of the more advanced methods outlined here. As we shall explain, the new theories, while sharing many desirable features with the universal semiclassical approximation, are designed to overcome certain limitations of the earlier theory for treating large amplitude intramolecular vibrational motion.

In the next section, we outline the theoretical framework for the two new

approaches and derive the corresponding parameter equations of motion. In the final section, we make some comparisons between the FVB-Gaussian bath (FVB/GB) and AVB-Gaussian bath (AVB/GB) theories, and spell out their relationship to other semiclassical and system-bath approaches. We briefly describe their application to the calculation of nonlinear optical signals from chromophores embedded in low-temperature crystals in conjunction with a pulse-propagator-based treatment of the short-pulse interactions. Appendix B contains the parameter equations of motion for the FVB/GB theory and Appendix C contains the parameter equations of motion for the AVB/GB theory.

B Theory

B.1 System-Bath Decomposition

The nuclear Hamiltonian for a many-body molecular system with amplitude in a single electronic state* is

$$H = \frac{1}{2}\mathsf{p}^T \cdot M \cdot \mathsf{p} + V(\mathsf{r}) \tag{3.1}$$

where $\mathsf{p} = \text{column}(\mathsf{p}_1, \ldots \mathsf{p}_N)$ is the momentum vector, with $\mathsf{p}_i = \text{column}(\mathsf{p}_{ix}, \mathsf{p}_{iy}, \mathsf{p}_{iz})$; $M_{i\alpha,j\beta} = \frac{1}{m_i}\delta_{ij}\delta_{\alpha\beta}$; m_i is the mass of the i^{th} nucleus; $V(\mathsf{r})$ is the potential; and $\mathsf{r} = \text{column}(\mathsf{r}_1, \ldots \mathsf{r}_N)$ is the position vector, with $\mathsf{r}_i = \text{column}(\mathsf{x}_i, \mathsf{y}_i, \mathsf{z}_i)$.

We shall reexpress the full nuclear Hamiltonian in terms of normal coordinates to provide a systematic basis for our subsequent system-bath decomposition,

*Although we consider explicitly the dynamics in only one electronic state, it is to be understood that the same type of treatment could be applied in several electronic levels simultaneously. Thus the theory is directly applicable to coherent electronic spectroscopy signals, such as time-resolved coherent anti-Stokes Raman scattering (tr-CARS) and wave-packet interferometry (WPI).

recapitulating the standard steps in such a transformation[17] in order to be precise about our definitions and notation. We transform preliminarily to mass-weighted Cartesian momenta, $\Pi = D \cdot \mathsf{p}$, and coordinates, $R = D^{-1} \cdot \left(\mathsf{r} - \mathsf{r}^{(0)}\right)$, where $D = \sqrt{M}$ and $\mathsf{r}^{(0)}$ is a minimum-energy configuration (perhaps determined in practice from a classical molecular dynamics simulation[16]). In terms of the mass-weighted coordinates and momenta, the nuclear Hamiltonian takes the form

$$H = \frac{1}{2}\Pi^T \cdot \Pi + V\left(D \cdot R + \mathsf{r}^{(0)}\right). \tag{3.2}$$

For the purpose of identifying normal coordinates, we temporarily expand the potential through second order as $V \cong V(\mathsf{r}^{(0)}) + \frac{1}{2}R^T \cdot (\nabla_R \nabla_R^T V) \cdot R$ and diagonalize the force-constant matrix

$$(\nabla_R \nabla_R^T V) \cdot \Lambda = \Lambda \cdot \lambda. \tag{3.3}$$

The columns of the orthogonal transformation matrix Λ are the eigenvectors of the force constant matrix; the corresponding eigenvalues are arranged in order of decreasing size along the diagonal of λ.

The normal coordinates and momenta for our system are theref3-ore given by $\xi = \Lambda^T \cdot R$ and $\pi = \Lambda^T \cdot \Pi$, respectively. In terms of these operators, the full nuclear Hamiltonian can be expressed as

$$H = \frac{1}{2}\pi^T \cdot \pi + V\left(D \cdot \Lambda \cdot \xi + \mathsf{r}^{(0)}\right). \tag{3.4}$$

Although the potential energy is written as a function of the normal coordinates, it should be emphasized that all intra- and intermode anharmonicities have thus far been retained; a quadratic approximation to the potential is *not* being made.

In the application of our framework to small-molecule dynamics within matri-

ces, it is useful to mimic a macroscopic host crystal by applying "periodic boundary conditions" to a sample cell small enough to be computationally tractable. This is accomplished by requiring that $V(\mathsf{r})$ be periodic in the length L of the sample cube (which contains one solute chromophore and tens or hundreds of solvent atoms). The cell length must be at least twice the range of intermolecular forces to prevent an atom from interacting with either itself or more than one copy of another atom.[†]

Under periodic boundary conditions, there is no potential energy change associated with overall spatial translation of the sample, but overall rigid rotation is hindered. We therefore assume that only the last three elements of the diagonal matrix λ —the eigenvalues associated with center-of-mass translation—are strictly vanishing. The Hamiltonian can be separated into center-of-mass kinetic energy and internal components, $H = \frac{1}{2}\pi_{CM}^T \cdot \pi_{CM} + h$, where $\pi_{CM} = \text{column}(\pi_{3N-2}, \pi_{3N-1}, \pi_{3N})$, and the internal Hamiltonian h is independent of $\xi_{CM} = \text{column}(\xi_{3N-2}, \xi_{3N-1}, \xi_{3N})$.

In order to simplify the description, we specialize to the case of a diatomic solute whose single high-frequency internal vibration is to be driven to large-amplitude. The highest-frequency normal coordinate ξ_1 should have the largest component of intramolecular solute vibration, so we decompose the internal Hamiltonian into system (vibrational) and bath (phonon) components plus interactions:

$$h = h_s(q) + h_b(Q) + u(q, Q). \tag{3.5}$$

[†]It would be readily possible to include explicit multi-body forces within our framework, but we specialize to pair-wise additive atom-atom potentials $V(\mathsf{r}) = \sum_{i>j} v_{ij}(\mathsf{r}_i - \mathsf{r}_j)$ for the sake of simplicity. Periodicity is enforced by taking $v_{ij}(\mathsf{r}_i - \mathsf{r}_j) = \sum_{lmn} f_{ij}(\mathsf{x}_i - \mathsf{x}_j + lL, \mathsf{y}_i - \mathsf{y}_j + mL, \mathsf{z}_i - \mathsf{z}_j + nL)$ for the pair potentials, where f_{ij} can be nonzero only when all its arguments have magnitude smaller than $L/2$; the coordinate values range continuously from minus infinity to plus infinity (which will be a useful feature for our wave-packet-based theory) but only the single term in the sum over l, m, and n with $l = -\text{nearest integer}[(\mathsf{x}_i - \mathsf{x}_j)/L]$, and analogously for m and n, can possibly be nonzero.

The system Hamiltonian is

$$h_s = \frac{p^2}{2} + u_s(q), \tag{3.6}$$

the bath Hamiltonian is

$$h_b = \frac{1}{2} P^T \cdot P + u_b(Q), \tag{3.7}$$

and $u(q,Q)$ describes the system-bath interaction. In these operators, $q = \xi_1$, $p = \pi_1$, $Q = \text{column}(\xi_2, \ldots \xi_{3N-3})$, and $P = \text{column}(\pi_2, \ldots \pi_{3N-3})$. The system and bath potentials are $u_s(q) = V\left(D \cdot \Lambda \cdot \text{column}(q, 0, \ldots 0) + \mathsf{r}^{(0)}\right)$ and $u_b(Q) = V\left(D \cdot \Lambda \cdot \text{column}(0,Q,0,0,0) + \mathsf{r}^{(0)}\right) - V\left(\mathsf{r}^{(0)}\right)$, respectively; we have defined the latter so that $u_b(0) = 0$. The system-bath interaction is thus defined by

$$u(q,Q) = V\left(D \cdot \Lambda \cdot \text{column}(q,Q,0,0,0) + \mathsf{r}^{(0)}\right) - u_s(q) - u_b(Q). \tag{3.8}$$

The system dynamics is to be rigorously calculated, while the bath can be treated by a number of methods to varying degrees of approximation. In general, the action of the bath is twofold: to dissipate vibrational excitation from the system through the transfer of vibrational quanta, and to dephase the system vibration by modulating its energy level spacings. To quantify the action of these two processes, a reduced description of the vibrational state would suffice. For application to time-resolved Raman and other coherent optical spectroscopieswhose signals involve the overlap between nuclear states of both the system *and the bath* accompanying different electronic states of the resonantly excited chromophorewe also need at least an approximate amplitude-level description of the quantum mechanical state of the bath degrees of freedom.

Although we are currently specializing to the case of a single-mode-system, our general approach could be applied straightforwardly to a several-mode system.

In particular, if the system vibration induces large amplitude motion in any bath mode, the system can be expanded to include that coordinate so that weak coupling to the remaining bath modes still applies. Our system-bath separation based on normal coordinates has a beneficial feature relative to a heuristic identification of intramolecular and solvent degrees of freedom. Model calculations within Redfield and other relaxation theories often assume bilinear coupling between system and bath coordinates.[18,19] In our approach on the other hand, all second-order terms in the potential energy are squares of single-mode system or bath position operators; the lowest-order contributions to the system-bath interaction potential are *third order*, and comprise terms proportional to q^2Q_i, qQ_i^2, and qQ_iQ_j. Postponing the onset of system-bath interaction to higher order in this way should extend the range of applicability of *any* theory based on weak system-bath coupling.

B.2 Fixed Vibrational Basis/Gaussian Bath Approach (FVB/GB)

a Fixed Vibrational Basis States

We shall consider two different approaches to calculating the dynamics under the Hamiltonian . The first of these makes use of the fixed vibrational basis accompanying a ref3-erence configuration of the bath, say Q = 0. We write the time-dependent nuclear ket as a sum of tensor products states,

$$|\psi(t)\rangle = \sum_{\nu} |\nu\rangle\, |\psi_\nu(t)\rangle, \tag{3.9}$$

where $|\nu\rangle$ are the fixed vibrational basis states obeying $h_s\,|\nu\rangle = \varepsilon_\nu\,|\nu\rangle$, and the expansion coefficients, $|\psi_\nu\rangle = \langle\nu \mid \psi\rangle$, are pure bath kets. Weak system-bath coupling along with the small-amplitude nature of the bath vibrations make the fixed vibrational basis expansion a natural form for $|\psi(t)\rangle$. It is to be expected that the bath

kets $|\psi_\nu(t)\rangle$ will not differ very greatly from each other or from the ground state of h_b in any single bath-mode component.[‡]

Temporal evolution of the overall nuclear ket is governed by the time-dependent Schrdinger equation

$$i\frac{\partial}{\partial t}|\psi(t)\rangle = h|\psi(t)\rangle\,. \tag{3.10}$$

($\hbar \equiv 1$ hereafter). It can be seen from Eqn. (3.9) that all of $|\psi(t)\rangle$'s time dependence is carried by the bath kets. Using Eqns. (3.5) and (3.9), and projecting onto state $|\nu\rangle$, yields the equation of motion for the bath wave packet,

$$i\frac{\partial}{\partial t}|\psi_\nu(t)\rangle = (\varepsilon_\nu + h_b + u_{\nu\nu})|\psi_\nu(t)\rangle + \sum_{\bar{\nu}\neq\nu} u_{\nu\bar{\nu}}|\psi_{\bar{\nu}}(t)\rangle\,, \tag{3.11}$$

where $u_{\nu\bar{\nu}} \equiv \langle\nu|\,u(\hat{q},\hat{Q})\,|\bar{\nu}\rangle$. The transfer of amplitude between bath kets accompanying different vibrational states is governed by the coupling operator, $u(\hat{q},\hat{Q})$, and the corresponding changes in population are responsible for vibrational energy relaxation. Dephasing of the system vibration occurs as a result of loss of overlap between the bath kets accompanying different vibrational states.

b Gaussian Bath Wave Packets Accompanying Fixed Vibrational States

The displacements of the lattice atoms in the vicinity of the guest molecule, indirectly induced by the latter's external vibrational excitation, may in some instances be fairly large. But their displacements should be describable as superpositions of small-amplitude displacements in many low-frequency spatially extended modes. Thus we may assume that the amplitude of motion in all the bath modes

[‡]Some inner products $\langle\psi_\nu \mid \psi_{\bar{\nu}}\rangle$, with $\nu \neq \bar{\nu}$, may nonetheless approach zero due to the cumulative effect of small losses of overlap in many bath modes, as is necessary to account for vibrational decoherence.

will be fairly small.

We do not wish to restrict our treatment to a strictly harmonic description of the bath, however. Among other limitations, such an approximation would prevent the bath degrees of freedom from interacting with each other, except indirectly through the system. A *locally quadratic* treatment goes further, by allowing third and higher-order coupling terms among bath modes and between the system and the bath. We theref3-ore adopt a locally quadratic approximation (LQA) to the bath potential, approximating $u_b(Q) + u(q, Q)$ as a locally second order function of Q based on its slopes and curvatures at the spatial center $eq : 3.12 Q_\nu = \langle \psi_\nu(t) | \hat{Q} | \psi_\nu(t) \rangle$ of the Gaussian wave packet

$$\langle Q \mid \psi_\nu(t) \rangle = \exp\left[i(Q - Q_\nu)^T \cdot \alpha_\nu \cdot (Q - Q_\nu) + i P_\nu^T \cdot (Q - Q_\nu) + i\gamma_\nu \right]. \quad (3.12)$$

The time dependence of the wave packet (3.12) resides in the parameters: $\alpha_\nu = \alpha'_\nu + i\alpha''_\nu$, a complex-symmetric matrix whose elements determine the spatial widths of the packet; the position expectation value Q_ν; the momentum vector $P_\nu = \langle \psi_\nu(t) | \hat{P} | \psi_\nu(t) \rangle$; and the complex scalar $\gamma_\nu = \gamma'_\nu + i\gamma''_\nu$, whose real part specifies the phase of the packet and whose imaginary part relates to its norm

In order to find the equations of motion for the parameters of the bath wave packets under the LQA,[15] Eqn. (3.11) is written in the position representation with the *ansatz* (3.12) for $\langle Q \mid \psi_\nu(t) \rangle$; the operators on the RHS are expanded through second order in the elements of $(Q - Q_\nu)$, and the time derivative on the LHS is evaluated with the help of the chain rule. Coupled equations of motion for the parameters are then obtained by equating the coefficients of like powers of $(Q - Q_\nu)$ on both sides of the equation. The summand in (3.11) involves vibrational matrix elements of the system-bath interaction operating on the $\bar{\nu}^{th}$ bath wave packet. In

the $\bar{\nu} \neq \nu$ terms responsible for vibrational relaxation, we write $\langle Q \mid \psi_{\bar{\nu}} \rangle$ as $\langle Q \mid \psi_{\nu} \rangle$ times a Q -dependent "correction factor,"

$$\langle Q \mid \psi_{\bar{\nu}} \rangle = e^{if(\nu,\bar{\nu})} g\left(Q;\nu,\bar{\nu}\right) \langle Q \mid \psi_{\nu} \rangle \,, \tag{3.13}$$

with

$$f\left(\nu,\bar{\nu}\right) = \left(Q_{\nu} - Q_{\bar{\nu}}\right)^{T} \cdot \alpha_{\bar{\nu}} \cdot \left(Q_{\nu} - Q_{\bar{\nu}}\right) + \left(Q_{\nu} - Q_{\bar{\nu}}\right)^{T} \cdot P_{\bar{\nu}} + \gamma_{\bar{\nu}} - \gamma_{\nu} \tag{3.14}$$

and

$$\begin{aligned} g\left(Q;\nu,\bar{\nu}\right) \cong 1 + i\left(Q - Q_{\nu}\right)^{T} \cdot \left[2\alpha_{\bar{\nu}} \cdot \left(Q_{\nu} - Q_{\bar{\nu}}\right) + P_{\bar{\nu}} - P_{\nu}\right] + \left(Q - Q_{\nu}\right)^{T} \\ \cdot \Big[i\alpha_{\bar{\nu}} - i\alpha_{\nu} - (1/2)(2\alpha_{\bar{\nu}} \cdot \left(Q_{\nu} - Q_{\bar{\nu}}\right) + P_{\bar{\nu}} - P_{\nu})(2(Q_{\nu} - Q_{\bar{\nu}})^{T} \\ \cdot \alpha_{\bar{\nu}} + P_{\bar{\nu}}^{T} - P_{\nu}^{T}) \Big] \cdot \left(Q - Q_{\nu}\right) . \end{aligned} \tag{3.15}$$

The function $g\left(Q;\nu,\bar{\nu}\right)$ is written as a second-order polynomial in $\left(Q - Q_{\nu}\right)$ as an algebraic convenience in isolating equal-order terms and canceling the common factors $\langle Q \mid \psi_{\nu} \rangle$. But the quantitative validity of the approximation (3.15) rests on the assumptioncentral to our LQA treatment of the baththat the various $\langle Q \mid \psi_{\nu} \rangle$ are similar enough and the vibrational transition rates low enough that each retains a Gaussian form. The equations of motion for the bath parameters α_{ν}, P_{ν}, Q_{ν}, and γ_{ν} can now be found and are stated in their entirety in Appendix B.

B.3 Adiabatic Vibrational Basis/Gaussian Bath Approach (AVB/GB)

a Adiabatic Vibrational Basis States

The system-bath decomposition and FVB/GB approximation described above do not automatically take advantage of the high-frequency nature of the system vibration. We set the stage for an alternative treatment that makes full use of this time-scale difference by reexpressing the overall nuclear state in terms of an adiabatic vibrational basis. The adiabatic basis states are eigenkets of the vibrational Hamiltonian

$$h_{vib}(Q) = h_s + u_b(Q) + u(q, Q) \tag{3.16}$$

parametrized by the bath-coordinate operator and obeying

$$h_{vib}(Q)\,|\nu(Q)\rangle = \varepsilon_\nu(Q)\,|\nu(Q)\rangle \tag{3.17}$$

with $\nu = 0, 1, 2, \ldots$. When the bath kinetic energy operator is reintroduced, the eigenvalues in Eqn. (3.17) will play the role of potential energy surfaces on which the bath degrees of freedom evolve, and between which vibrationally nonadiabatic transitions may occur. These bath potential surfaces are analogous to the adiabatic potential energy surfaces on which the nuclei evolve in the usual electronic Born-Oppenheimer approximation.[20,21] We emphasize, however, that we will avoid making an adiabatic approximation *per se*. Nonadiabatic effects are included in the system dynamics and will be needed to account for vibrational relaxation and dephasing processes.

The advantage of adopting an adiabatic vibrational basis description of the system states derives from the time-scale separation that is assumed to exist between the laser-driven vibrational system and the indirectly excited bath, the weak-

coupling nature of their interaction, and the small-amplitude range of bath motion. Even though the time-scale difference between system and bath may be insufficient to justify an adiabatic approximation, these features should all tend to decrease the number of adiabatic vibrational basis states required and slow the rate of nonadiabatic transitions between them.

Implementation of the adiabatic-vibrational-basis treatment for a small molecule solute in a crystalline host cannot proceed directly, however, as would an analogous electronically-adiabatic-basis description of the dynamics of a small, isolated molecule with a handful of nuclear coordinates. For it would be entirely impracticable to specify the vibrational eigenkets and eigenenergies for a dense array of Q values. The dimension of this space is $3N-4$, with N on the order of hundreds; the number of points required, say $\sim 10^{3N-4}$, would lead to computationally prohibitive basis-set storage requirements.

The vibrational kets and energies could instead be sought as functions of a much smaller list of collective bath coordinates as follows. By grouping the system-bath coupling by powers of the vibrational coordinate

$$u(q,Q)=\sum_{k=1}^{k_{\max}} q^k \sigma_k(Q) \tag{3.18}$$

one could specify the force on the system with $k_{\max}$ collective bath parameters σ_k. It would be necessary only to specify $|\nu(u_b;\sigma_1,\ \ldots\ \sigma_{k_{\max}})\rangle$ and $\varepsilon_\nu(u_b;\sigma_1,\ \ldots\ \sigma_{k_{\max}})$ for an array of perhaps $\sim 10^{k_{max}+1}$ points in a much lower-dimensional parameter space. But even if the expansion (3.18) is truncated at low order in the system coordinate, the number of parameter sets required could easily run into the thousands. Although this number may not be strictly prohibitive, storing multiple vibrational states and energies for such an array of points could nevertheless place rather strong demands

on computer memory.

As an alternative to cataloging the adiabatic vibrational basis states and energies for parameter values $Q = (Q_1, \ldots Q_{3N-4})$ or $(u_b; \sigma_1, \ldots \sigma_{k_{\max}})$ distributed on a discrete array, we can instead obtain them as explicit functions of either set of parameters, which can be evaluated as needed during a calculation rather than stored. We can accomplish such a description with the help of time-independent perturbation theory.[21] Let

$$h_{vib}(Q) = h_{vib}^{(0)}(Q) + \delta u(q, Q), \tag{3.19}$$

with

$$h_{vib}^{(0)}(Q) = h_s + u_b(Q) + \sum_{\nu} |\nu\rangle \langle\nu| u(q, Q) |\nu\rangle \langle\nu| \tag{3.20}$$

and

$$\delta u(q, Q) = u(q, Q) - \sum_{\nu} |\nu\rangle \langle\nu| u(q, Q) |\nu\rangle \langle\nu|. \tag{3.21}$$

The ref3-erence states $|\nu\rangle \equiv |\nu(Q = 0)\rangle$ obey $h_{vib}^{(0)}(Q) |\nu\rangle = \varepsilon_\nu^{(0)}(Q) |\nu\rangle$, with

$$\varepsilon_\nu^{(0)}(Q) = \varepsilon_\nu + u_b(Q) + \langle v| u(q, Q) |\nu\rangle, \tag{3.22}$$

where $\varepsilon_\nu \equiv \varepsilon_\nu(Q = 0)$.[§] Using Eqn. (3.18), the perturbation operator (3.21) becomes

$$\delta u(q, Q) = \sum_{k=1}^{k_{\max}} \left(q^k - \sum_{\nu} |\nu\rangle \langle\nu| q^k |\nu\rangle \langle\nu| \right) \sigma_k(Q) \tag{3.23}$$

[§]The reference states of the adiabatic vibrational basis treatment are identical to the fixed vibrational basis states introduced previously. In some instances it may be sufficient to make use of a smaller number of the former than of the latter in carrying out the two different approaches.

which has vanishing diagonal matrix elements

$$\delta u_{\nu\nu} \equiv \langle \nu | \, \delta u \, | \nu \rangle = 0 \tag{3.24}$$

and off-diagonal matrix elements given as functions of Q by

$$\delta u_{\bar{\nu}\nu}(Q) \equiv \langle \bar{\nu} | \, \delta u \, | \nu \rangle = \sum_{k=1}^{k_{\max}} \langle \bar{\nu} | \, q^k \, | \nu \rangle \, \sigma_k(Q). \tag{3.25}$$

Making use of standard expressions from stationary-state perturbation theory,[21] we obtain the adiabatic potential energy of the bath

$$\varepsilon_\nu(Q) = \varepsilon_\nu^{(0)}(Q) + \varepsilon_\nu^{(1)}(Q) + \varepsilon_\nu^{(2)}(Q) + \cdots \tag{3.26}$$

with $\varepsilon_\nu^{(0)}(Q)$ given by Eqn. (3.22), $\varepsilon_\nu^{(1)}(Q) = 0$ from Eqn. (3.24), and

$$\varepsilon_\nu^{(2)}(Q) = -\sum_{\bar{\nu} \neq \nu} \frac{|\delta u_{\bar{\nu}\nu}(Q)|^2}{(\varepsilon_{\bar{\nu}}^{(0)}(Q) - \varepsilon_\nu^{(0)}(Q))}. \tag{3.27}$$

We define a unitary operator relating the adiabatic states to the ref3-erence states,

$$|\nu(Q)\rangle \equiv U(Q) \, |\nu\rangle \, . \tag{3.28}$$

$U(Q)$ can be approximated with a perturbation series

$$U(Q) = U^{(0)}(Q) + U^{(1)}(Q) + U^{(2)}(Q) + \cdots, \tag{3.29}$$

where

$$U^{(0)}(Q) = 1 \tag{3.30}$$

$$U^{(1)}(Q) = -\sum_{\nu}\sum_{\bar{\nu}\neq\nu} |\bar{\nu}\rangle \frac{\delta u_{\bar{\nu}\nu}(Q)}{\varepsilon^{(0)}_{\bar{\nu}}(Q) - \varepsilon^{(0)}_{\nu}(Q)} \langle\nu| \tag{3.31}$$

$$U^{(2)}(Q) = \sum_{\nu}\sum_{\bar{\nu}\neq\nu} |\bar{\bar{\nu}}\rangle \frac{1}{(\varepsilon^{(0)}_{\bar{\bar{\nu}}}(Q) - \varepsilon^{(0)}_{\nu}(Q))} \sum_{\bar{\nu}\neq\nu} \frac{\delta u_{\bar{\bar{\nu}}\bar{\nu}}(Q)\delta u_{\bar{\nu}\nu}(Q)}{(\varepsilon^{(0)}_{\bar{\nu}}(Q) - \varepsilon^{(0)}_{\nu}(Q))} \langle\nu|$$
$$- |\nu\rangle\langle\nu| \frac{1}{2} \sum_{\bar{\nu}\neq\nu} \frac{|\delta u_{\bar{\nu}\nu}(Q)|^2}{(\varepsilon^{(0)}_{\bar{\nu}}(Q) - \varepsilon^{(0)}_{\nu}(Q))^2}. \tag{3.32}$$

The practical virtue of the expansions (3.26) and (3.29)—carried to unspecified orders to be determined by the sample-specific coupling strengths and relative frequencies of the bath modes and the system vibrationis that they provide adiabatic vibrational energies and eigenstates as explicit functions of the bath coordinates.

The adiabatic vibrational states (3.28) are defined within an arbitrary phase function of Q. The transformation $U(Q)$ is consequently defined within a Q-dependent phase-factor matrix that is diagonal in the basis $\{|\nu\rangle\}$. In our perturbative expressions (3.30) through (3.32), those phase functions were chosen so that all the $\langle\nu \mid \nu(Q)\rangle$ are real and consequently $\langle\nu| U^{(n)}(Q) |\nu\rangle = \langle\nu| \left[U^{(n)}(Q)\right]^\dagger |\nu\rangle$. This condition on the unitary operator (3.29) will determine the gauge of an induced vector potential appearing in the Schrödinger equation for the bath dynamics (see Eqns. (3.34) and (3.35) below).[22] [24]

b Time Evolution in the Adiabatic Vibrational Basis Treatment

The composite nuclear ket describing the evolving state of the coupled system and bath is written as $U(\hat{Q})$ times a sum of system-bath tensor product states

$$|\psi(t)\rangle = \sum_{\nu} \left|\nu(\hat{Q})\right\rangle |\varphi_{\nu}(t)\rangle = U(\hat{Q}) \sum_{\nu} |\nu\rangle |\varphi_{\nu}(t)\rangle \tag{3.33}$$

where $|\varphi_v\rangle = \langle\nu(\hat{Q})|\psi\rangle = \langle\nu| U^{\dagger}(\hat{Q}) |\psi\rangle$ is the bath wave packet accompanying the ν^{th} adiabatic vibrational state. We use a circumflex to emphasize the bath-position-operator-dependence of the unitary transformation. Substituting $h = (1/2)\,\hat{P}^T \cdot \hat{P} + h_{vib}(\hat{Q})$ (see Eqns. (3.5) and (3.16)) and Eqn. (3.33) into the time-dependent Schrödinger equation, using Eqn. (3.17), and projecting onto state $|\nu(\hat{Q})\rangle$, yields the equation of motion for the bath wave packet

$$i\frac{\partial}{\partial t} |\varphi_{\nu}(t)\rangle = \sum_{\bar{\nu}} \langle\nu| \left[\frac{1}{2}\left(\hat{P} + A(\hat{Q})\right)^T \cdot \left(\hat{P} + A(\hat{Q})\right) + \varepsilon_{\bar{\nu}}(\hat{Q})\right] |\bar{\nu}\rangle |\varphi_{\bar{\nu}}(t)\rangle . \tag{3.34}$$

The vector potential in Eqn. (3.34) is given by

$$A(Q) = -iU^{\dagger}(Q)\,\nabla U(Q) \tag{3.35}$$

and arises as a result of the commutation relation $PU = UP - i\nabla U$. The gradient in Eqn. (3.35) is taken with respect to bath coordinate variables, and the bath momentum operator in the position representation is $\langle Q|\,\hat{P}\,|\varphi_{\nu}\rangle = -i\nabla\,\langle Q \mid \varphi_{\nu}\rangle$. Our choice of phase function in the perturbative expansion (3.29) for $U(Q)$ specifies the gauge of the vector potential (3.35). Note that in Eqn. (3.33), the time dependence of $|\psi(t)\rangle$ is once again carried by the bath packets alone, as it was in the fixed vibrational basis approach.

c Gaussian Bath Wave Packets for the Adiabatic Vibrational States

We adopt a Gaussian *ansatz* for the bath wave packets $\langle Q \,|\varphi_v(t)\rangle$ and proceed as in Section B.2 of this chapter to find the equations of motion for the wave-packet parameters. The vibrational eigenenergies are now functions of the bath coordinates; locally quadratic expansions for these bath potential functions will be obtained in practice from perturbative expressions like Eqn. (3.26). Bath wave packets accompanying different adiabatic vibrational states are coupled through the nonadiabatic portion of the vector potential, rather than through the potential energy operator.

To see how to handle the vector-potential-containing terms in the Gaussian wave-packet theory, we can imagine writing the unitary transformation (3.28) as $U(Q) = e^{iF(Q)}$ where F is a Hermitian operator in the vibrational Hilbert space parametrized by the bath coordinates. In keeping with the Gaussian form of the bath wave packets, we would expand $F(Q)$ quadratically. This observation indicates that a consistent treatment should adopt a locally *linear* approximation to the vector potential,

$$A(Q) \cong A(Q_\nu) + (Q - Q_\nu)^T \cdot \nabla A(Q_\nu) \,. \tag{3.36}$$

Using Eqns. (3.26), (3.34), and (3.36), it becomes a straightforwardbut somewhat involvedexercise to derive equations of motion for the AVB/GB parameters. The resulting expressions are presented in Appendix C.¶

¶See Appendix C for the equations of motion governing the time evolution of Gaussian wave packet parameters expanded in an adiabatic vibrational basis.

C Discussion

C.1 Relationship to Other Work

We have formulated two different semiclassical descriptions of the dynamics of matrix-isolated small molecules undergoing large amplitude, high frequency motion. Both theories partition the nuclear Hamiltonian in a given electronic state into system, bath, and interaction terms in order to define a vibrational basis in which to expand the state ket; both arrive at equations of motion for the parameters of bath wave packets that are constrained to take the form of Gaussians. The two treatments differ in their adoption of a fixed vibrational basis (FVB/GB theory) or an adiabatic vibrational basis (AVB/GB).

The FVB/GB theory is analogous in structure to applications of Heller's original LQA to the short-time dynamics of Gaussian nuclear wave packets in various fixed electronic states (i.e., electronic basis states assumed independent of nuclear coordinates).[25-28] In our theory, the bath-coordinate-independent vibrational states play a role analogous to the electronic basis states in Heller's theory, and the bath coordinates play the role assumed by all of the nuclear coordinates in those problems. In many applications of the LQA to chemical dynamics, continuous-wave laser fields drive transitions between different electronic states. In the applications of interest for the present theory, vibrationally off-diagonal elements of the system-bath interaction join pulsed laser fields in effecting the transfer of amplitude between different vibrational (or electronic) states. With its incorporation of explicitly bath-coordinate-dependent adiabatic vibrational basis states, our AVB/GB theory is analogous to an earlier generalization of Heller's theory to incorporate adiabatic electronic states that are parameterized by nuclear coordinates.[23]

The vibrational-basis theories spelled out in this chapter should help over-

come a significant limitation of the LQA in application to the spectroscopy and dynamics of small molecules in cryogenic matrices. In a recent study of intermolecular communication between atomic and molecular chromophores embedded in a rare-gas host crystal, Rohrdanz[16] demonstrated that tr-CARS can be a sensitive probe of signals transmitted by coherent phonons over nanometer distance scales. Those calculations applied the LQA universally, to all lattice and intramolecular modes of the system. In part because of the LQA's tendency to disobey energy conservation over many periods of large-amplitude motion in the anharmonic potential well of the iodine molecule used as the "receiver" in that study, fairly strict limits has to be placed on some of the pulse durations and inter-pulse delays. In addition, the universal LQA did not conserve energy for times long enough to investigate intermolecular communication over longer distances or the temporal decay of the tr-CARS signal due to vibrational dephasing. Replacing the LQA by a numerically calculated vibrational basis for the large-amplitude anharmonic modes should greatly extend the range of systems and timescales that can be quantitatively simulated.

The calculations of ref3-. 16 demonstrate the basic applicability of Gaussian-wave-packet-based semiclassical theory to the calculation of time-resolved nonlinear optical signals from matrix-isolated molecules undergoing coherent internal vibration. Since that paper applied the LQA to *all* modes, it represents the limit of the present theories in which the "system" is zero-dimensional and all nuclear degrees of freedom are treated the same way that the present theories treat just the bath. The new approaches will have to pay the modest price of roughly $(N_{sys}N_{bath})^3$ scaling, where N_{sys} is the size of the basis set for the vibrational subsystem ($N_{sys} = 1$ in the old theory) and N_{bath} is the number of bath degrees of freedom. This is the approximate scaling required for computational propagation of the equations of

motion in both the FVB/GB and AVB/GB theories to obtain the time-dependent parameters of the bath wave packets. Rohrdanz's work[16] nonetheless provides an extensive illustration of the basic method, including the description of E-field interactions with pulse propagators and the calculation of spectroscopic observables from nuclear wave-packet overlaps.

The ultimate practical limitations of the FVB/GB and AVB/GB in terms of system size, strength of system-environment coupling, maximum pulse durations, and length of run consistent with energy conservation, will of course be system-specific and are more difficult to estimate than the approximate overall scaling. Based on our experience with the universal semiclassical theory,[16] is our expectation that these new theories may provide reliable results for the dynamics of appropriate systems comprising tens or hundreds of atoms over timescales on the order of tens of picoseconds.

The assumed small-amplitude motion of the lattice coordinates constituting the bath in both FVB/GB and AVB/GB theories justifies their treatment of the bath wave function accompanying each vibrational state as a single multi-dimensional Gaussian wave packet. Swarms of Gaussian wave packets have been used previously to describe the nuclear degrees of freedom in molecules undergoing electronically nonadiabatic processes.[29] In those applications, the dynamics in different electronic states is not typically assumed to be small in amplitude or roughly similar to each other. Nor is the net nuclear wave function accompanying a given electronic state generally assumed to be approximately Gaussian.

Since their inception three decades ago as computational and interpretive tools for molecular spectroscopy, Gaussian wave-packet methods[30] have been extensively generalized and tested.[31–34] These methods have found applications in many areas of spectroscopy and dynamics and, in a temperature-propagation formula-

tion,[35,36] have also been of use in calculations of statistical properties. In the latter context, thermal Gaussians can serve as a more efficient, approximate alternative to rigorous but costly path-integral Monte Carlo techniques. In a second stage of development of the theories outlined here, we intend to make use of some techniques that were adopted in the statistical applications. In particular, Frantsuzov and Mandelshtam[35] demonstrated the use of variationally derived thermal Gaussian propagation, which is known to be more stable than propagation by the LQA.[31] The enabling element in their approach is the representation of intermolecular potentials as sums of Gaussians or polynomials, so that the integrals involving these potentials that appear in the Bloch equation (imaginary-time equation of motion) can be calculated analytically, rather than numerically. Combined with our strategy of treating high-frequency intramolecular (and, possibly, local) modes in a fixed or adiabatic vibrational basis, application of Frantsuzov and Mandelshtam's approach should help expand the range of allowable pulse durations, the length of stable propagation, and the allowable amplitude of lattice motion.

The use of a vibrational basis approach to describe many-body condensed phase dynamics has a significant advantage over reduced dynamical treatments[37] such as Redfield theory as it is usually applied to condensed-phase dynamics,[19,38] in that it can readily be used in the numerical simulation of coherent optical spectroscopic signals involving electronic as well as nuclear coherences. The calculation of such signals requires the evaluation of wave packets simultaneously evolving in multiple electronic states, while in a reduced dynamical description it is not immediately obvious how to take long-lived electronic coherences into account.

Our new treatment can be compared with an interesting theory recently put forward by Martens and co-workers.[39] Aimed primarily at the dephasing of small-molecule vibrations in molecular crystals (rather than longer-time relaxation

processes including energy dissipation and wave-packet revivals[1,40,41]), that work adopted a vibrationally adiabatic *approximation* (the nonadiabatic processes responsible for vibrational relaxation were omitted), incorporated system-bath coupling by low-order perturbation theory, and relied on a classical approximation to the bath dynamics. Within its scope, the theory behaved reasonably well, providing dephasing times for specific vibrational coherences of I_2 in Ar in rough agreement with the experimental values.

Other theories to which our approach can meaningfully be compared include generalized master-equation treatments,[42] quantized Hamilton dynamics,[43,44] and a variety of procedures based on forward-backward semiclassical dynamics[45] or any of the various quantum corrections to the relevant classical correlation functions.[46] Because our theory targets spectroscopic *signals* governed by small-molecule dynamics in molecular crystals, it may have some advantages that do not apply to admittedly more general semiclassical theories aimed at calculating *nonlinear optical response functions*, in their entirety, for chromophores in liquid environments. Principal among these is the assumption that the initial state of our system has a well-defined structure describable by a localized multi-dimensional wave function or density matrix.[47] Monte Carlo sampling of starting phase-space trajectory points, which for a liquid sample may account for multiple initial structures, is not required. This sampling step multiplies the computational cost of popular computational schemes for liquid-phase optical response functions based on the Herman-Kluk propagator, which in any case adopt dynamical approximations based on high (liquid-like) temperature.[48-50]

Both of our vibrational-basis/Gaussian bath theories offer rare opportunities to monitor the quantum mechanical dynamics of a certain class of macroscopic systems prepared in *pure, nonequilibrium states*. If the system vibration and its

surroundings are driven from their collective ground state by a short optical pulse that is resonant with the small-molecule vibration, the overall state remains pure (i.e. described by a single state-ket) and certainly does not correspond initially to the system mode in canonical equilibrium with its low- (but now nonzero-) temperature surroundings. The theories outlined here afford the means to track the ensuing dynamics of system and bath with a well-defined—albeit approximate—prescription for the time-development of the overall state-ket of system and bath.

In this connection, it is worth making ref3-erence to some interesting recent work on quantum mechanical entanglement and the foundations of statistical mechanics.[51,52] Popescu, Short, and Winter considered the reduced density operator of a small (sub-) system in contact with a larger environment when the "universe" (system plus environment) is in a pure state that is chosen at random within some overall constraints. They quantified the proximity between the actual reduced system state (defined by tracing the pure-state universe density operator over the environmental degrees of freedom) and the system density operator corresponding to canonical equilibrium (obtained by tracing over the environment the density operator of the universe having equal *a priori* population of all states within the constraint space). Their remarkable finding is that for *almost any* randomly chosen pure state of the universe, the instantaneous reduced system density operator is very nearly indistinguishable from that corresponding to canonical equilibrium. The results of Popescu and co-workers[51,52] thus obviate the need for the conventional assumption of equal *a priori* probabilities of "universe" states within a constraint space (of energy or some other quantities) as a foundational concept for statistical mechanics; virtually the same instantaneous subsystem distribution is obtained from almost any randomly chosen pure state of the universe (provided the subsystem constitutes a small enough piece of the universe).

Stated another way, the work of Popescu, Short, and Winter shows that pure states of the suitably constrained system-plus-environment in which the system is not in equilibrium with its surroundings are *very much fewer* in number than pure states in which it is in equilibrium. It must be assumed by extension that these unusual states typically make their way to and spend most of their subsequent evolution in states for which the subsystem is "in equilibrium." Although it will be of great interest to study this "pure-state equilibration" process in simplified model systems, it should also be worthwhile to view the approach to equilibrium in this way using actual molecular many-body systems. The fact that small molecules in low-temperature matrices can externally be driven from their ground states into a wide variety of disequilibrium pure states suggests these systems as ideal candidates for the experimental study of pure-state equilibration.

C.2 Signals and Observables

Aside from the simulation of time-resolved nonlinear optical signals for molecular many-body systems under our vibrational basis/Gaussian bath theories, the time evolution of some other physical observables for the sample, which can be compactly expressed in terms of bath-packet parameters, can also be monitored. Here we give a few examples of quantities that can reveal key features to the many-body nuclear dynamics, without regard for specific experimental strategies for measuring these "observables." We will return in future work to the explicit numerical computation of tr-CARS, pump-probe, and other nonlinear optical signals from small molecules in cryogenic matrices.

The time evolution of the average value of the vibrational energy $\langle h_s \rangle$ tracks the dissipation of vibrational energy into bath potential and kinetic energy, and

system-bath interaction. This quantity is readily calculable in the FVB/GB theory and takes the form

$$\langle h_s \rangle = \langle \psi(t) | \, h_s \, | \psi(t) \rangle = \sum_\nu \varepsilon_\nu \int dQ |\langle Q \mid \psi_\nu \rangle|^2. \tag{3.37}$$

Eqn.(3.37) can be evaluated straightforwardly from the Gaussian probability densities $|\langle Q \mid \psi_\nu \rangle|^2 = \exp\left\{ -2\gamma''_\nu - (Q - Q_\nu)^T \cdot 2\alpha''_\nu \cdot (Q - Q_\nu) \right\}$. Under the AVB/GB theory, we would consider instead the time evolution of the average adiabatic vibrational energy $\langle h_{vib}(\hat{Q}) \rangle$, which tracks the dissipation of vibrational energy along with bath potential energy into bath kinetic energy. This quantity is given by

$$\left\langle h_{vib}(\hat{Q}) \right\rangle = \langle \psi(t) | \, h_{vib}(\hat{Q}) \, | \psi(t) \rangle = \sum_\nu \int dQ |\langle Q \mid \varphi_\nu \rangle|^2 \varepsilon_\nu(Q). \tag{3.38}$$

By expanding $\varepsilon_\nu(Q)$ of Eqn. (3.26) in powers of Q, the adiabatic vibrational energy can be evaluated in terms of the various moments of the probability densities $|\langle Q \mid \varphi_\nu \rangle|^2$.

The expectation value of the system coordinate is sensitive to vibrational dephasing, which can occur even in the absence of vibrational energy loss. It is given in the fixed vibrational basis by

$$\langle \hat{q} \rangle = \sum_{\bar{\nu},\nu} q_{\bar{\nu}\nu} \int dQ \, \langle \psi_{\bar{\nu}}(t) \mid Q \rangle \, \langle Q \mid \psi_\nu(t) \rangle. \tag{3.39}$$

The required matrix elements of q between vibrational eigenstates are to be calculated numerically, and the wave-packet overlap integrals can be evaluated according

to

$$\int dQ \, \langle \psi_{\bar{\nu}}(t) \mid Q \rangle \, \langle Q \mid \psi_{\nu}(t) \rangle = \sqrt{\frac{\pi^{3N-4}}{\det \mathsf{A}}} \exp\left\{ \frac{1}{4} \mathsf{B}^T \cdot \mathsf{A}^{-1} \cdot \mathsf{B} + \mathsf{C} \right\}, \tag{3.40}$$

where

$$\mathsf{A} = i\alpha_{\bar{\nu}}^{*} - i\alpha_{\nu} \tag{3.41}$$

$$\mathsf{B} = i \left(2\alpha_{\bar{\nu}}^{*} \cdot Q_{\bar{\nu}} - 2\alpha_{\nu} \cdot Q_{\nu} - P_{\bar{\nu}} + P_{\nu} \right) \tag{3.42}$$

$$\mathsf{C} = i \left(-Q_{\bar{\nu}}^{T} \cdot \alpha_{\bar{\nu}}^{*} \cdot Q_{\bar{\nu}} + Q_{\nu}^{T} \cdot \alpha_{\nu} \cdot Q_{\nu} + P_{\bar{\nu}}^{T} \cdot Q_{\bar{\nu}} - P_{\nu}^{T} \cdot Q_{\nu} - \gamma_{\bar{\nu}}^{*} + \gamma_{\nu} \right). \tag{3.43}$$

The same quantity expressed using an adiabatic vibrational basis is

$$\begin{aligned} \langle \hat{q} \rangle = & \sum_{\bar{\nu},\nu} \int dQ \, \langle \varphi_{\bar{\nu}}(t) \mid Q \rangle \, \langle Q \mid \varphi_{\nu}(t) \rangle \\ & \times \sum_{\bar{\bar{\nu}},\bar{\bar{\nu}}} \langle \bar{\nu} | U^{\dagger}(Q) \, | \bar{\bar{\nu}} \rangle \, q_{\bar{\bar{\nu}}\bar{\bar{\nu}}} \left\langle \bar{\bar{\nu}} \right| U(Q) \, | \nu \rangle . \end{aligned} \tag{3.44}$$

With the matrix elements of U and $U^{\dagger}$ written as power series expansions in Q, the calculation reduces to the evaluation of various parameter derivatives of a closed-form Gaussian integral according to

$$\begin{aligned} \langle \varphi_{\bar{\nu}} | \, Q^m \, | \varphi_{\nu} \rangle &= \left(\frac{\partial}{\partial \mathsf{B}} \right)^m \langle \varphi_{\bar{\nu}} \mid \varphi_{\nu} \rangle = \left(\frac{\partial}{\partial \mathsf{B}} \right)^m \int dQ e^{-Q^T \cdot \mathsf{A} \cdot Q + Q^T \cdot \mathsf{B} + \mathsf{C}} \\ &= \left(\frac{\partial}{\partial \mathsf{B}} \right)^m \sqrt{\frac{\pi^{3N-4}}{\det \mathsf{A}}} \exp\left\{ \frac{1}{4} \mathsf{B}^T \cdot \mathsf{A}^{-1} \cdot \mathsf{B} + \mathsf{C} \right\}. \end{aligned} \tag{3.45}$$

In the application of the FVB/GB or AVB/GB theories to pump-probe, tr-

CARS, or wave-packet interferometry signals, the continuous changes in the bath-wave-packet parameters described by the parameter equations of motion will have to be augmented by abrupt changes in those parameters due to the action of individual finite-duration laser pulses. These parameter changes will be accounted with pulse propagators.[53] Analytical expressions derived within the semiclassical Franck-Condon approximation,[16,54] will be applied to components of the pulse propagators acting on the low-frequency bath, whereas low-dimensional numerical expressions (obtained through split-operator calculations) will be obtained for the higher-frequency intramolecular vibrations. This approach will enable the accurate description of shaped or transform-limited pulses with realistic durations on the order of tens or hundreds of femtoseconds.

Notes

[1] Fushitani, M.; Bargheer, M.; Gühr, M.; Schwentner, N. *Phy. Chem. Chem. Phys.* **2005**, *7*, 3143.

[2] Bihary, Z.; Karavitis, M.; Apkarian, V. A. *J. Chem. Phys.* **2004**, *120*, 8144.

[3] Karavitis, M.; Zadoyan, R.; Apkarian, V. A. *J. Chem. Phys.* **2001**, *114*, 4131.

[4] Karavitis, M.; Apkarian, V. A. *J. Chem. Phys.* **2004**, *120*, 292.

[5] Kiviniemi, T.; Aumanen, J.; Myllyperkiö, P.; Apkarian, V. A.; Pettersson, M. *J. Chem. Phys.* **2005**, *123*, 064509.

[6] Apkarian, V. A.; Schwentner, N. *Chem. Rev.* **1999**, *99*, 1481.

[7] Karavitis, M.; Segale, D.; Bihary, Z.; Pettersson, M.; Apkarian, V. A. *Low Temp. Phys.* **2003**, *29*, 814–821.

[8] Gühr, M.; Schwentner, N. *J. Chem. Phys.* **2005**, *123*, 244506.

[9] Karavitis, M.; Kumada, T.; Goldschleger, I. U.; Apkarian, V. A. *Phys. Chem. Chem. Phys.* **2005**, *7*, 791.

[10] Poulin, P. R.; Nelson, K. A. *Science* **2006**, *313*, 1756.

[11] Momose, T.; Fushitani, M.; Hoshina, H. *International Reviews in Physical Chemistry* **2005**, *24*, 533.

[12] Gühr, M.; Bargheer, M.; Schwentner, N. *Phys. Rev. Lett.* **2003**, *91*, 085504.

[13] Gühr, M.; Bargheer, M.; Schwentner, N. *Phys. Chem. Chem. Phys.* **2004**, *7*, 760.

[14] Bihary, Z.; Zadoyan, R.; Karavitis, M.; Apkarian, V. A. *J. Chem. Phys.* **2004**, *120*, 7576.

[15] Heller, E. J. *J. Chem. Phys.* **1975**, *62*, 1544.

[16] Rohrdanz, M. A.; Cina, J. A. *Mol. Phys.* **2006**, *104*, 1161.

[17] Bernath, P. F. *Spectra of Atoms and Molecules*; Oxford University Press, NY, 1995.

[18] Bader, J. S.; Berne, B. J. *J. Chem. Phys.* **1994**, *100*, 8359.

[19] Ungar, L. W.; Cina, J. A. *J. Phys. Chem. A* **1998**, *102*, 7382.

[20] Born, M.; Oppenheimer, J. R. *Ann. Phys.* **1927**, *84*, year.

[21] Messiah, A. *Quantum Mechanics*; Dover Pulications, Mineola, New York, 1999.

[22] Mead, C. A. *Rev. Mod. Phys.* **1992**, *64*, 51.

[23] Cina, J. A.; T. J. Smith, J.; Romero-Rochin, V. *Adv. Chem. Phys.* **1993**, *83*, 1.

[24] Moody, J.; Shapere, A.; Wilczek, F. *Phys. Rev. Lett.* **1986**, *56*, 893.

[25] Heller, E. J. *J. Chem. Phys.* **1978**, *68*, 2066.

[26] Lee, S.-Y.; Heller, E. J. *J. Chem. Phys.* **1982**, *76*, 3035.

[27] Heller, E. J.; Sundberg, R. L.; Tannor, D. *J. Phys. Chem.* **1982**, *86*, 1822.

[28] Myers, A. B.; Harris, R. A.; Mathies, R. A. *J. Chem. Phys.* **1983**, *79*, 603.

[29] Martinez, T. J. *Acc. Chem. Res.* **2006**, *39*, 119.

[30] Heller, E. J. *Acc. Chem. Res.* **1981**, *14*, 368.

[31] Sawada, S.; Metiu, H. *J. Chem. Phys.* **1986**, *84*, 227–238.

[32] Coalson, R. D.; Karplus, M. *J. Chem. Phys.* **1990**, *93*, 3919.

[33] Buch, V. *J. Chem. Phys.* **2002**, *117*, 4738.

[34] Buch, V. *J. Chem. Phys.* **2004**, *121*, 6961.

[35] Frantsuzov, P. A.; Mandelshtam, V. A. *J. Chem. Phys.* **2004**, *121*, 9247.

[36] Frantsuzov, P.; Neumaier, A.; Mandelshtam, V. A. *Chem. Phys. Lett.* **2003**, *381*, 117.

[37] Silbey, R.; Harris, R. A. *J. Phys. Chem.* **1989**, *93*, 7062.

[38] Pollard, W. T.; Felts, A. K.; Friesner, R. A. *Adv. Chem. Phys.* **1996**, *93*, 77.

[39] Riga, J. M.; Fredj, E.; Martens, C. C. *J. Chem. Phys.* **2005**, *122*, 174107.

[40] Katsuki, H.; Chiba, H.; Girard, B.; Meier, C.; Ohmori, K. *Science* **2006**, *311*, 1589.

[41] Ohmori, K.; Katsuki, H.; Chiba, H.; Honda, M.; Hagihara, Y.; Fujiwara. K.; Sato, Y.; Ueda, K. *Phys. Rev. Lett.* **2006**, *96*, 093002.

[42] Shi, Q.; Geva, E. *J. Chem. Phys.* **2004**, *120*, 10647.

[43] Prezhdo, O. V.; Pereverzev, Y. V. *J. Chem. Phys.* **2002**, *116*, 4450.

[44] Prezhdo, O. *Theor. Chem. Acc.* **2006**, *116*, 206.

[45] Miller, W. H. *J. Chem. Phys.* **2006**, *125*, 132305.

[46] Lawrence, C. P.; Nakayama, A.; Makri, N.; Skinner, J. L. *J. Chem. Phys.* **2004**. *120*, 6621.

[47] Yan, Y. J.; Mukamel, S. *J. Chem. Phys.* **1988**, *88*, 5735.

[48] Ovchinnikov, M.; Apkarian, V. A. *J. Chem. Phys.* **1998**, *108*, 2277.

[49] Ovchinnikov, M.; Apkarian, V. A.; Voth, G. A. *J. Chem. Phys.* **2001**, *114*, 7130.

[50] Kuhn, O.; Makri, N. *J. Phys. Chem. A* **1999**, *103*, 9487.

[51] Popescu, S.; Short, A. J.; Winter, A. *Nature Physics* **2006**, *2*, 754.

[52] Popescu, S.; Short, A. J.; Winter, A. *http://arxiv.org/abs/quant-ph/0511225v3* **2006**.

[53] Smith, T. J.; Cina, J. A. *J. Chem. Phys.* **1996**, *104*, 1272.

[54] Shen, Y.-C.; Cina, J. A. *J. Chem. Phys.* **1999**, *110*, 9793.

CHAPTER IV

NUMERICAL TESTS OF THE FIXED VIBRATIONAL BASIS/GAUSSIAN BATH TREATMENT

Xiaolu Cheng brought the assymetric nature of the originally published equations of motion for the real and imaginary parts of α_ν to light, and helped in elucidating the non-Gaussian nature of bath wave packets accompanying high-lying vibrational levels. Dr. Jeff Cina aided in every step.

A Introduction

The behavior of small molecules in solid crystals, including electronic[1,2] and vibrational dynamics,[3-9] as well as chemical reactions[10,11] is affected in a fundamental way by interactions with the environment and can be studied using myriad time-resolved optical experiments.[1,2,12] Accurate and efficient simulations of the resultant spectroscopic signals are needed to aid in their interpretation and to expose the nature of the underlying many-body quantum mechanics. Due to the exponential scaling with system size of computational effort required for such simulations, it is not feasible to perform exact calculations of the dynamics of tens or hundreds of atoms. However, there are several key features of systems involving chromophores embedded in cryogenic noble-gas hosts that can be exploited to develop a computa-

tionally efficient, yet comprehensive approach to treating their dynamics. Ultrafast experiments often drive a few high-frequency intramolecular degrees of freedom to large-amplitude motion. The host lattice phonons can be disturbed from their equilibrium configuration through coupling to either or both the nuclear or electronic degrees of freedom of the directly-excited chromophore. The excitation of the chromophore motion of interest has been seen to induce coherent motion in the host. This necessitates an approximate theoretical treatment of the many–body dynamics that can retain the quantum nature of both the chromophore *and* the host.

To this end we have developed a theory that treats the system exactly quantum mechanically while the bath is treated semi-classically as a collection of multidimensional Gaussian wave packets. This theory will enable us to simulate ultrafast coherent spectroscopic signals from small molecules embedded in solid matrices.

This chapter includes several parts: the first section provides a short review of the theory; in the second section, we point out a few clarifications of the theory; in the third section, we implement the theory numerically on a simple test case of coupled harmonic oscillators; in the fourth section, we calculate linear wave-packet interferometry signals from several test cases using the fixed vibration basis/Gaussian bath (FVB/GB) approach.

B Outline of FVB/GB

A comprehensive exposition of the FVB/GB theory has been given in the previous chapter, but we shall summarize several of the key elements here. To elucidate the treatment of small molecule dynamics *via* FVB/GB, we consider a pair of coupled oscillators whose dynamics is governed by a well-defined vibrational Hamiltonian. In the types of systems we will be treating with FVB/GB there is a

significant time-scale separation between the characteristic frequencies of the oscillators. Of particular interest are dihalogen vibrations in cryogenic rare-gas matrices, molecular iodine embedded in Ar, for instance. The vibrational frequency of gas-phase I_2, which is slightly blue-shifted from the cryogenically isolated molecule, is ~ 215 cm^{-1} and the Debye frequency of solid Ar is 64 cm^{-1}, making this system a suitable candidate for treatment using FVB/GB.

We proceed by identifying the mass-weighted normal coordinates and momenta of the sample. We designate the mode with the largest component of the intermolecular motion of interest (as well as the highest frequency) as the "system" with coordinate q and momentum p, while the other modes will constitute the "bath" with a collective multidimensional coordinate Q and momentum P.

We consider a test case in which the bath is composed of a single low-frequency oscillator. A high-frequency oscillator will comprise the system and will represent a generalized chromophore motion of interest, such as those probed by ultrafast coherent spectroscopies. In the general case of a large multi-dimensional solid-phase bath whose frequency distribution forms a near-continuum, with an upper limit given by the Debye frequency of the lattice, the bath modes contribute to decoherence of the chromophore vibration by modulating its energy level spacings, thereby disrupting the delicate phase relations between the wave packet's constituent vibrational levels, and also induce vibrational relaxation in the chromophore by the absorption and dissipation of vibrational quanta.[13] While appeal to decoherence and relaxation rates is not appropriate in our two-dimensional model, we can nonetheless examine the system dynamics under the influence of the bath and vice versa.

Expressing the full nuclear Hamiltonian for a given electonic state, h, in terms of the system and bath coordinates and momenta we have

$$h = \frac{\hat{p}^2}{2} + \frac{\hat{P}^2}{2} + V(\hat{q}, \hat{Q}). \tag{4.1}$$

We decompose the potential energy term into system and bath portions, $u_s(\hat{q})$ and $u_b(\hat{Q})$, respectively, and the interaction potential $u(\hat{q}, \hat{Q})$, and write the Hamiltonian (4.1) as a sum:

$$h = h_s(\hat{q}, \hat{p}) + h_b\left(\hat{Q}, \hat{P}\right) + u\left(\hat{q}, \hat{Q}\right) \quad . \tag{4.2}$$

Since the partitioning of the system and bath is based on the normal modes of the sample, the bilinear coupling terms vanish by definition, leaving the lowest-order contribution to u at third order (i.e. consisting of terms proportional to $\hat{q}^2\hat{Q}$ and $\hat{q}\hat{Q}^2$). In the calculations presented below, however, we will nevertheless adopt a bilinear form for the coupling ($u \propto qQ$) in order to frame a simple, exactly soluble model problem on which to test the FVB/GB theory.

Our treatment begins by finding the vibrational eigenstates at a fixed reference configuration of the bath, say $Q = 0$. An arbitrary time-dependent nuclear ket of the sample can then be written as a sum of tensor product states,

$$|\Psi(t)\rangle = \sum_\nu |\nu\rangle \langle \nu \mid \Psi(t)\rangle = \sum_\nu |\nu\rangle |\psi_\nu(t)\rangle \quad , \tag{4.3}$$

where the $|\nu\rangle$ are fixed vibrational states obeying $h_s|\nu\rangle = \varepsilon_\nu |\nu\rangle$, and the $|\psi_\nu\rangle = \langle \nu \mid \Psi\rangle$ are time-dependent bath wave packets accompanying each system vibrational eigenstate. The time-evolution of the total wave function (4.3) is governed by the time-dependent Schrödinger equation,

$$i\frac{\partial}{\partial t}|\Psi(t)\rangle = h|\Psi(t)\rangle \tag{4.4}$$

($\hbar = 1$ throughout). Using Eqns. (4.2) and (4.3), and projecting onto state $|\nu\rangle$, we get the exact equation of motion for the bath wave packet,

$$i\frac{\partial}{\partial t}|\psi_\nu(t)\rangle = (\varepsilon_\nu + h_b + u_{\nu\nu})|\psi_\nu(t)\rangle + \sum_{\bar{\nu}\neq\nu} u_{\nu\bar{\nu}}|\psi_{\bar{\nu}}(t)\rangle \quad , \tag{4.5}$$

where $u_{\nu\bar{\nu}} = u_{\nu\bar{\nu}}(\hat{Q}) = \langle\nu|\, u(\hat{q},\hat{Q})\,|\bar{\nu}\rangle$.

The molecular systems studied in the experiments we will be simulating consist of low-temperature solids containing isolated chromophores that are externally driven to large-amplitude motion within an extended bath. The bath itself may be disturbed from its equilibrium configuration either through Franck-Condon active bath modes or through nuclear coupling to the system. While some of the bath nuclei may undergo large-amplitude displacements, the motion of any single atom does not greatly contribute to the overall displacement of any single bath mode. Given this fact, along with the absence of thermal population at low temperatures, it is appropriate to assume that the bath wave packet never varies greatly from its ground-state wave function. We therefore make a Gaussian ansatz for the form of the distinct bath wave packets accompanying each vibrational level:

$$\langle Q \mid \psi_\nu\rangle = \exp\left[i(Q-Q_\nu)^T\cdot\alpha_\nu\cdot(Q-Q_\nu) + iP_\nu^T\cdot(Q-Q_\nu) + i\gamma_\nu\right] \quad . \tag{4.6}$$

The explicit time-dependence is carried by the ν-indexed quantities, all of which are scalars in the present case of a one-dimensional bath. The momentum expectation value is given by $P_\nu = \langle\psi_\nu|\hat{P}|\psi_\nu\rangle/\langle\psi_\nu|\psi_\nu\rangle$ while the wave packet's spatial center is $Q_\nu = \langle\psi_\nu|\hat{Q}|\psi_\nu\rangle/\langle\psi_\nu|\psi_\nu\rangle$. The imaginary part of the complex scalar $\alpha_\nu = \alpha'_\nu + i\alpha''_\nu$ indicates the bath wave packet's spatial width, while its real part is related to the position-momentum correlation. The imaginary part of γ_ν is related to the popu-

lation of the ν^{th} vibrational level, $\langle\psi_\nu|\psi_\nu\rangle = e^{-2\gamma''_\nu}\sqrt{\pi/\alpha''_\nu}$, and its real part gives the phase of the wave function. In the case of a multidimensional bath, α_ν would become a matrix quantity and P_ν and Q_ν would become vectors while γ_ν would remain a scalar. In order for the wave packets to retain their Gaussian form while propagating in an arbitrary potential that may contain anharmonicities, as will be considered in future studies, we would enforce a locally quadratic approximation to the Hamiltonian[14] wherein the bath-coordinate-dependent quantities are expanded through second order in $\hat{Q} - Q_\nu$. To obtain equations of motion for the bath wave packet parameters accompanying the ν^{th} vibrational level we must express the summand in Eqn. (4.5) in terms of $|\psi_\nu(t)\rangle$, rather than$|\psi_{\bar{\nu}}(t)\rangle$, which can be done by writing

$$\langle Q|\, u_{\nu\bar{\nu}}(\hat{Q})\,|\psi_{\bar{\nu}}\rangle = u_{\nu\bar{\nu}}(Q)\frac{\langle Q \mid \psi_{\bar{\nu}}\rangle}{\langle Q \mid \psi_\nu\rangle}\,\langle Q \mid \psi_\nu\rangle \quad . \tag{4.7}$$

In order to remain consistent with the locally quadratic approximation, and as an algebraic convenience, it is necessary to expand the quantity $u_{\nu\bar{\nu}}(Q)\frac{\langle Q|\psi_{\bar{\nu}}\rangle}{\langle Q|\psi_\nu\rangle}$ through second order in $\hat{Q} - Q_\nu$. This approximation is justified insofar as we anticipate the bath wave packets accompanying different vibrational levels will not differ greatly from one another, so that the ratio $\langle Q|\psi_{\bar{\nu}}\rangle/\langle Q|\psi_\nu\rangle$ does not differ greatly a constant value.

Our approach grants us access to information that is not available when using a reduced density matrix treatment of a coupled system and bath. In particular we are able to ascertain detailed information about states of the bath that are associated with different system vibrational levels, such as Q_ν and P_ν, among others. The reduced density matrix of the system, $\rho_s = Tr_b\sigma$, is found by taking the trace over the bath degrees of freedom of the full density matrix, $\sigma = |\Psi\rangle\langle\Psi|$. Likewise the reduced density matrix of the bath, ρ_b can be found by tracing over the sys-

tem degrees of freedom. Expectation values of a general bath observable, $\hat{O}_b$ can then be found using $\langle \hat{O}_b \rangle = Tr(\rho_b \hat{O}_b)$. In this formalism we can find system and bath quantities such as $\langle \hat{q} \rangle$, and $\langle \hat{Q} \rangle$, but there is no system- or bath-only operator whose expectation value yields $Q_\nu = \langle \Psi | (|\nu\rangle\langle\nu| \hat{Q}) | \Psi \rangle$, or any other ν-indexed bath quantity, thus making such information inaccessible in the reduced density matrix approach.

B.1 Accuracy and Precision Considerations

Successful integration of the bath wave packet parameters requires a sufficiently accurate numerical integration routine. We applied several techniques and found a 4^{th} order Runge-Kutta method with a fixed time step to be sufficient for our purposes. Although other methods including using a variable time step were computationally less expensive, they led to accumulation of numerical error in advance of a breakdown of the FVB/GB. Additional computational details can be found in Appendix D.

B.2 Comparison of Exact Parameter Evaluation with FVB/GB

A Gaussian wave packet propagating in a quadratic potential will remain Gaussian, and the semi-classical equations of motion derived by Heller[14] become exact. The accuracy of the propagation relies on the validity of the LQA which is compromised with the onset of potential anharmonicity and can become inexact rapidly when considering vibrations of diatomic molecules such as I_2. As such we seek to compare our results with numerically exact solutions to the time-dependent wave packet parameters calculated *via* a method that could, in principle, include anharmonicities without resorting to approximations such as the locally quadratic

approximation. While our test case consists of a composite system whose dynamics can be exactly described using Gaussian wave packets evolving in a quadratic potential, we seek a comparison with a more general approach. In carrying out this comparison we construct and diagonalize the matrix representation of the 2-D Hamiltonian:

$$h = \omega\left(\hat{a}^\dagger\hat{a} + \frac{1}{2}\right) + \Omega\left(\hat{A}^\dagger\hat{A} + \frac{1}{2}\right) + J\left(\hat{a}^\dagger + \hat{a}\right)\left(\hat{A}^\dagger + \hat{A}\right) \tag{4.8}$$

where $\hat{a}$ and $\hat{A}$ are the creation and annihilation operators corresponding to a Hamiltonian with no displacements in the system or bath equilibrium positions and non-zero system-bath coupling. The matrix elements of (4.8) are

$$\begin{aligned} &h_{\nu\bar{\nu}n\bar{n}} = \delta_{\nu,\bar{\nu}}\delta_{n,\bar{n}}\left[\left(\nu + \tfrac{1}{2}\right) + \left(n + \tfrac{1}{2}\right)\right] \\ &+J\left[\tfrac{1}{\sqrt{2\omega}}\left(\delta_{\nu,\bar{\nu}+1}\sqrt{\bar{\nu}+1} + \delta_{\nu,\bar{\nu}-1}\sqrt{\nu}\right) + \tfrac{1}{\sqrt{2\Omega}}\left(\delta_{n,\bar{n}+1}\sqrt{\bar{n}+1} + \delta_{n.\bar{n}-1}\sqrt{n}\right)\right]. \end{aligned} \tag{4.9}$$

In truncating the basis of h we consider only combinations of system and bath states that fall below an upper limit on the vibrational energy in the composite system-plus-bath. The eigenvectors of h are sums of tensor products of system and bath states

$$h\left|k\right\rangle = \varepsilon_k\left|k\right\rangle = \sum_{\nu,n} c_{\nu n}^{(k)}\left|\nu\right\rangle\left|n\right\rangle \quad , \tag{4.10}$$

where $c_{\nu n}^{(k)} = \langle\nu|\left\langle n \mid k\right\rangle$. Our initial wave function (4.26) can be written in terms of the eigenvectors of h:

$$\left|\Psi(t=0)\right\rangle = \sum_{\nu k} c_\nu c_{\nu 0}^{(k)*}\left|k\right\rangle \quad , \tag{4.11}$$

and the wave function (4.11) can be readily propagated given the exact eigen-energies of each state $|k\rangle$,

$$|\Psi(t)\rangle = \sum_{\nu k} e^{-i\epsilon_k t} c_\nu c_{\nu 0}^{(k)*} |k\rangle \quad . \tag{4.12}$$

To compare the dynamics simulated *via* FVB/GB treatment with the numerically exact results we need expressions for the FVB/GB wave-packet parameters in terms of exactly calculable observables. The average values of the position and momentum for the various bath wave packets can be written:

$$\langle \psi_\nu | \hat{Q} | \psi_\nu \rangle = Q_\nu \langle \psi_\nu | \psi_\nu \rangle \tag{4.13}$$

$$\langle \psi_\nu | \hat{P} | \psi_\nu \rangle = P_\nu \langle \psi_\nu | \psi_\nu \rangle \quad . \tag{4.14}$$

The quantities Q_ν and P_ν along with the vibrational populations are found using FVB/GB while the matrix elements of bath operators can be obtained from the numerically exact calculation. The parameter α''_ν can be related to the RMS width of the ν^{th} bath packet:

$$\Delta Q_\nu = \sqrt{\frac{\langle \psi_\nu | (\hat{Q} - Q_\nu)^2 | \psi_\nu \rangle}{\langle \psi_\nu | \psi_\nu \rangle}} = \sqrt{\frac{\langle \psi_\nu | \hat{Q}^2 | \psi_\nu \rangle}{\langle \psi_\nu | \psi_\nu \rangle} - {Q_\nu}^2 \langle \psi_\nu | \psi_\nu \rangle} \quad , \tag{4.15}$$

The second moment of the bath coordinate is

$$\frac{\langle \psi_\nu | \hat{Q}^2 | \psi_\nu \rangle}{\langle \psi_\nu | \psi_\nu \rangle} = \left(\frac{1}{4\alpha''_\nu} + {Q_\nu}^2 \right) \quad , \tag{4.16}$$

whence we see that:

$$\alpha''_\nu = \frac{1}{4} \left[\frac{\langle \psi_\nu | \hat{Q}^2 | \psi_\nu \rangle}{\langle \psi_\nu | \psi_\nu \rangle} - \left(\frac{\langle \psi_\nu | \hat{Q} | \psi_\nu \rangle}{\langle \psi_\nu | \psi_\nu \rangle} \right)^2 \right]^{-1} \quad . \tag{4.17}$$

The imaginary part of γ_ν can be found through its relation to the population of the ν^{th} vibrational state:

$$\langle\psi_\nu|\psi_\nu\rangle = \exp\left[-2\gamma_\nu''\right]\sqrt{\frac{\pi}{2\alpha_\nu''}} \quad . \tag{4.18}$$

The real part of alpha can be found by considering the quantity:

$$\frac{\langle\psi_\nu|\left(\hat{Q}\hat{P}+\hat{P}\hat{Q}\right)|\psi_\nu\rangle}{\langle\psi_\nu|\psi_\nu\rangle} = -\frac{\alpha_\nu'}{\alpha_\nu''} - 2P_\nu Q_\nu \quad . \tag{4.19}$$

B.3 Are the Bath Wave Packets Strictly Gaussian?

By expanding the composite state ket in the system vibrational basis and assuming a Gaussian form for the accompanying bath wave packets we place a physically unjustified restriction on the wave function in the name of functional utility in the hopes that any inaccuracies will be small compared to the wide applicability of the theory. We approximate the superposition of bath states accompanying any given vibrational state as having a Gaussian spatial probability distribution. It can be shown that the bath wave packet accompanying the $\nu = 0$ vibrational level is indeed Gaussian for coupled harmonic oscillators, while those accompanying higher levels are products polynomials in Q and a Gaussian wave packet.

A composite system-bath Gaussian wave packet can be written:

$$\langle qQ|\Psi\rangle = \exp[-c_1Q^2 - c_2q^2 + c_3qQ + c_4q + c_5Q + c_6] \tag{4.20}$$

where c_i is a time-dependent parameter and is determined by the system and bath frequencies and displacements. This wave function can be expanded in a vibrational basis according to Eqn. (4.3). The vibrational basis states in this case are harmonic

oscillator eigenfunctions,

$$\langle q|\nu\rangle = \sqrt{\frac{\beta}{2^{\nu}\nu!\pi^{1/2}}}e^{-\beta^2 q^2/2}H_{\nu}(\beta q) \tag{4.21}$$

where $\beta = \sqrt{\omega}$, and $H_{\nu}(x)$ is the ν^{th} Hermite polynomial. The bath wave packets can be written:

$$\begin{aligned}\langle Q|\psi_{\nu}\rangle &= \int_{-\infty}^{\infty} dq\langle\nu|q\rangle\langle q|\langle Q|\Psi\rangle \\ &\propto \int_{-\infty}^{\infty} dq H_{\nu}(\beta q)\exp[c_1Q^2 + c_2q^2 + c_3qQ + c_4q + c_5Q + c_6] \quad .\end{aligned} \tag{4.22}$$

Using Eqns. (4.21) and (4.22), the bath wave packet accompanying the $|\nu = 0\rangle$ state is

$$\begin{aligned}\langle Q|\psi_0\rangle &\propto e^{-c_1Q^2+c_5Q+c_6}\int_{-\infty}^{\infty} dq e^{-c_2q^2+c_3qQ} \\ &\propto \sqrt{\frac{\pi}{c_2}}e^{-c_1Q^2+c_5Q+c_6}e^{(c_3Q+c_4)^2/4c_2}\end{aligned} \tag{4.23}$$

whose form is Guassian. For the bath packet accompanying $|\nu = 1\rangle$, though, we have

$$\begin{aligned}\langle Q|\psi_1\rangle &\propto e^{-c_1Q^2+c_5Q+c_6}\int_{-\infty}^{\infty} dq\, q e^{-c_2q^2+c_3qQ} \\ &\propto e^{-c_1Q^2+c_5Q+c_6}e^{(c_3Q+c_4)^2/4c_2}(c_3Q + c_4) \quad ,\end{aligned} \tag{4.24}$$

which is no longer Gaussian. Continuing the analysis, one finds that the bath wave packets accompanying higher lying vibrational levels consist of Gaussians multiplied

by consecutively higher-order polynomials in Q.

The degree to which the rigorous bath wave packets deviate from a Gaussian form depends on the preparation of the initial state $|\Psi\rangle$. In the types of experiments we are interested in simulating the composite state, prior to excitation by short laser pulses, is a product of the ground vibrational states. Excitation by pulses whose duration is much shorter than any relevant vibrational time scale renders the resultant state nearly Gaussian and consequently accurately modeled by FVB/GB.

C Bilinearly Coupled Harmonic Oscillators

C.1 Test System

To test the efficacy of the FVB/GB treatment of vibrational dynamics on a system amenable to exact treatment, we consider two bilinearly coupled harmonic oscillators between which bilinear coupling remains, i.e. a normal coordinate analysis is not carried out. In future applications we shall retain all anharmonicities, as well as eliminate bilinear couplings by carrying out a normal mode analysis on a multidimensional composite system-plus-bath. In a realistic molecular sample the system and bath, both of which may contain multiple modes, are coupled through indeterminant order, making an exact calculation of the dynamics unfeasible. By considering a case whose dynamics is tractable we are able to effectively gauge the accuracy of our equations of motion which will serve as a basis for confidence in applying the FVB/GB treatment to samples whose rigorous dynamics are intractable. These test calculations will also provide a sense of what will be required computationally to treat larger multi-dimensional molecular systems.

Our test Hamiltonian is:

$$h = \frac{p^2}{2} + \frac{\omega^2}{2}(q - q_e)^2 + \frac{P^2}{2} + \frac{\Omega^2}{2}(Q - Q_e)^2 + J\,(q - q_e)\,(Q - Q_e) \quad , \qquad (4.25)$$

with equilibrium positions of the system, q_e, and the bath, Q_e. We set $\omega = 1$, $\Omega = 1/2$, and will consider two different coupling strengths, $J = 0.001$ and $J = 0.05$. We take our initial wave function to be a product of the system- and bath-only ground states, displaced along the system coordinate by an amount equivalent to the width of the packet in the system coordinate:

$$|\Psi(t = 0)\rangle = \hat{D}(\delta)\,|\nu = 0\rangle\,|n = 0\rangle = \sum_{\nu} c_\nu |\nu\rangle |n = 0\rangle \quad , \qquad (4.26)$$

where $h_b\,|n\rangle = \varepsilon_n\,|n\rangle$, and $\hat{D}(\delta) = e^{-i\hat{p}\delta}$. This displacement increases amplitude in bath wave packets accompanying higher lying system vibrational levels and can alter their phases by a factor of π, depending on the sign of δ, while leaving their widths, spatial centers, and momenta identical to those of $|\psi_0\rangle$. The system-bath coupling is then turned on and the displaced wave function (4.26) is allowed to evolve in this modified potential.

The changes in population induced by displacement along the system coordinate occurs much in the same way as an electronic transition induced by a laser pulse whose duration is short enough to obey the Franck-Condon approximation induces changes in population of the relevant electronic states without altering the shape of the nuclear probability density distribution. In the situation being considered the analogous nuclear potential accompanying the ground electronic state would be that of an uncoupled system and bath with the ground state $|\nu = 0\rangle|n = 0\rangle$, and potential minimum set to $(q_e = 0, Q_e = 0)$. The nuclear potential in the excited

electronic state would have a non-zero coupling along with a negative displacement of the system's equilibrium position. After a vertical electronic excitation of the ground state wave function to the excited electronic state it is allowed to propagate under the excited state nuclear Hamiltonian,

$$h_e = \frac{p^2}{2} + \frac{\omega^2}{2}(q - q_e)^2 + \frac{P^2}{2} + \frac{\Omega^2}{2}Q^2 + J\,(q - q_e)\,Q \quad , \tag{4.27}$$

with $q_e = -1$. The propagated time-dependent wave function is expanded in the basis of the ground electronic state vibrational levels, $|\Psi\rangle = \sum_\nu |\nu\rangle\,|\psi_\nu\rangle$, where $h_g\,|\nu\rangle = \epsilon_\nu\,|\nu\rangle$.

D Observables and Parameters

D.1 Weak Coupling

To quantify the comparison between FVB/GB propagation and the exact results we consider the time dependent wave packet parameters and several observables. First we consider the weak-coupling case with $J = 0.001$. A plot of the spatial centers of several wave packets is shown in Figure 4.1.

We find that the FVB/GB treatment reproduces the exact results quantitatively, in this case, and does so for many system vibrational periods. The FVB/GB and numerically exact results for parameters in the weak coupling case are overlain in the plots giving the appearance of a single trace. The periodicity exhibited arises from the natural high- and low-frequencies of the composite system, i.e. the frequencies of the coupled two-oscillator composite system whose normal modes have frequencies ω and Ω, respectively. The momentum of each wave packet exhibits similar features and is shown in Figure 4.2.

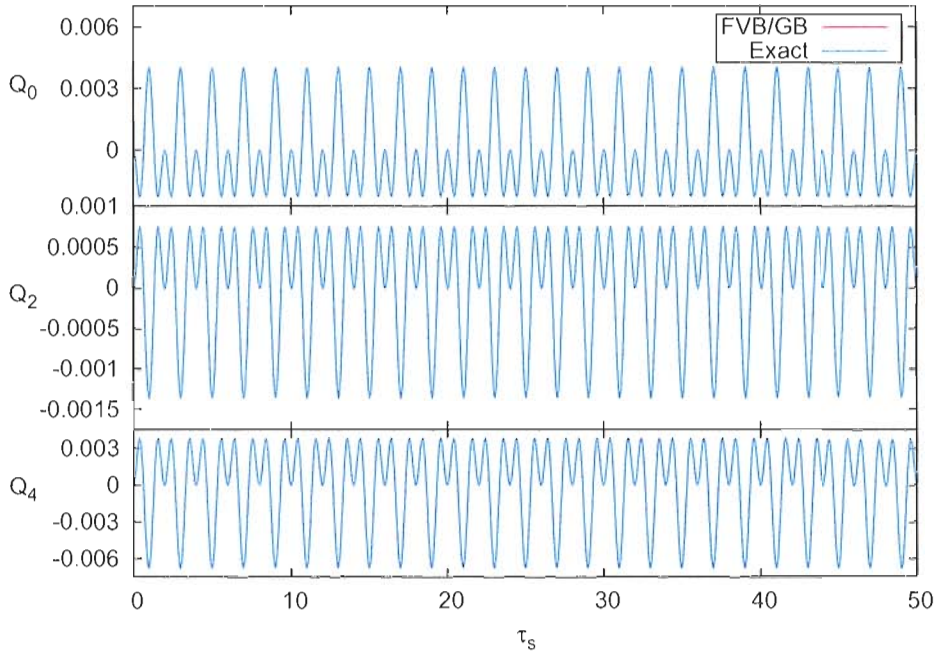

Figure 4.1: A plot of the spatial centers of the bath wave packets accompanying the $\nu = 0$ (top), $\nu = 2$ (center), and $\nu = 4$ (bottom) vibrational levels versus time (in units of the high-frequency normal coordinate's vibrational period, τ_s, calculated using the FVB/GB approach and numerically exact methods in the weak coupling case. Initial conditions are presented in Section D.1

The width parameters for the same vibrational levels are plotted in Figure 4.3. We see significant deviations in the width of each packet that exhibits an inverse relationship with the population of the vibrational level with which the packet is associated. These variations suggest that it would be inappropriate to make any further assumptions concerning their evolution beyond a locally quadratic approximation, such as is done when employing frozen, or fixed-width, Gaussians. The populations of several vibrational levels are shown in Figure 4.1.

Noticeable fluctuations in the population are seen as it is transferred between adjacent vibrational levels ν and $\bar{\nu} = \nu \pm 1$ While the total population is not conserved as described in Section D.5 it fluctuates only slightly about its initial value of $\langle \Psi | \Psi \rangle = 1$.

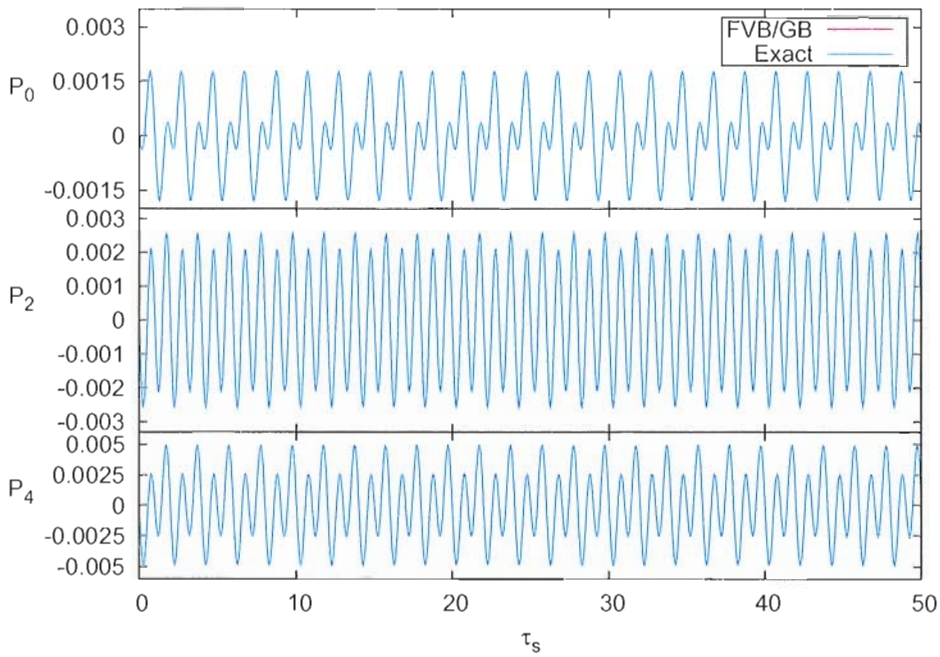

Figure 4.2: A plot of the momentum expectation values of the bath wave packets accompanying the $\nu = 0$ (top), $\nu = 2$ (center), and $\nu = 4$ (bottom) vibrational levels calculated using the FVB/GB approach and numerically exact methods.

D.2 Moderate Coupling

When the coupling constant is increased to $J = 0.05$ and the system is otherwise prepared in the same manner as the weak-coupling case the FVB/GB can be seen to break down after several intramolecular vibrations. Figure 4.5 shows the spatial centers of the $\nu = 0, 2, 4$ bath packets. The FVB/GB parameter propagation starts to show significant deviations from the exactly calculated values after approximately $\tau_s = 20$ for $\nu = 2, 4$, while remaining stable for $\nu = 0$. The breakdown occurs at slightly shorter times for the higher-lying $\nu = 4$ packet than it does for the $\nu = 2$ packet. The same trend is exhibited for the momenta (Figure 4.6), width parameters (Figure 4.7), and populations (Figure 4.8). While no plots are shown for neither α'_ν nor γ'_ν, they exhibit the same trends as the other parameters in both the weak- and moderate-coupling cases.

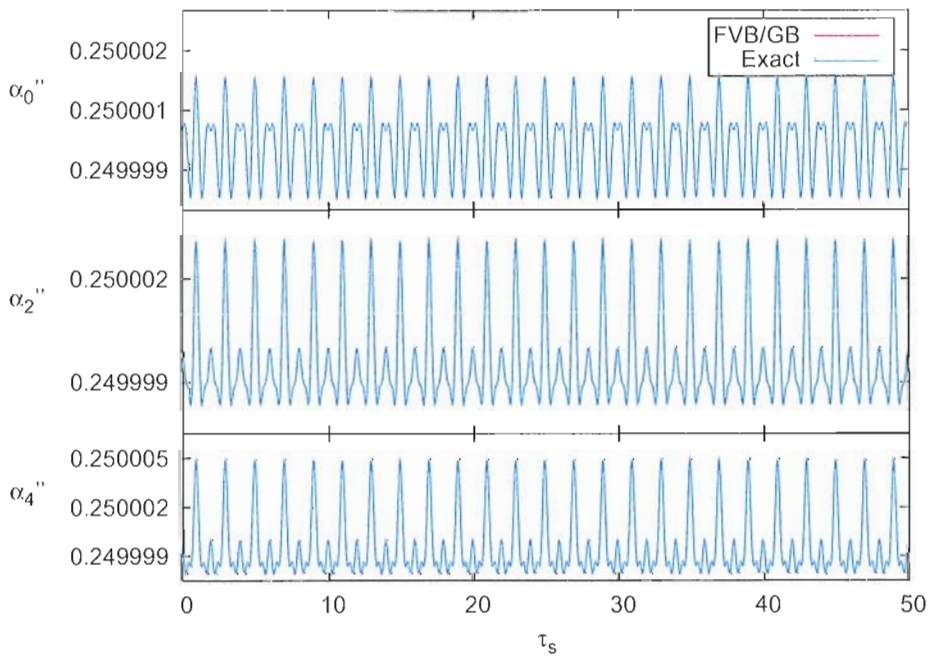

Figure 4.3: A plot of the width parameter α_ν'' of the bath wave packets accompany the $\nu = 0$ (top), $\nu = 2$ (center), and $\nu = 4$ (bottom) vibrational levels calculated using the FVB/GB approach and numerically exact methods.

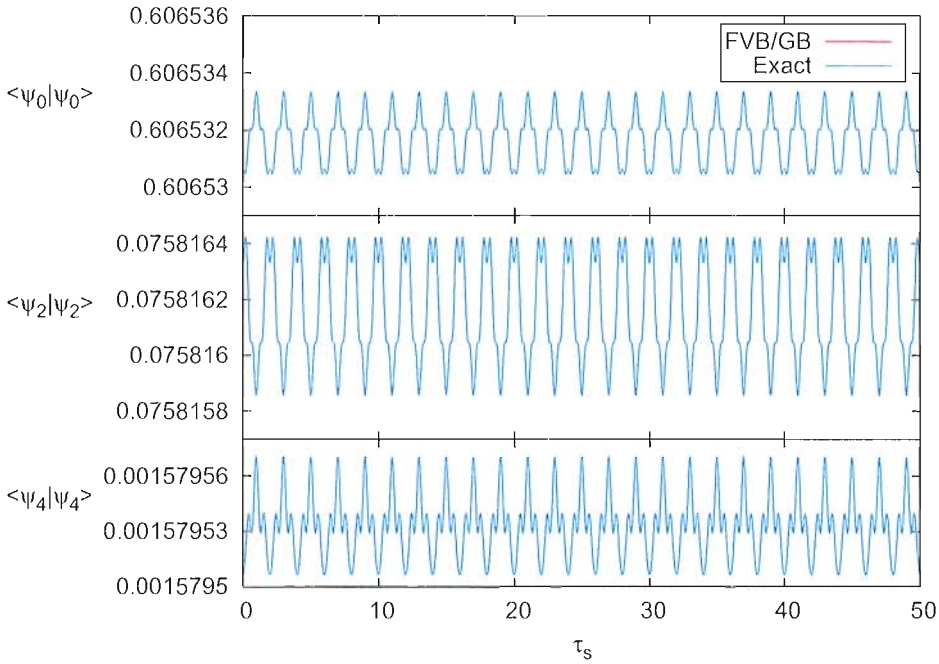

Figure 4.4: Populations of the vibrational levels $\nu = 0$ (top), $\nu = 2$ (center), and $\nu = 4$ (bottom), calculated using the FVB/GB approach and numerically exact methods.

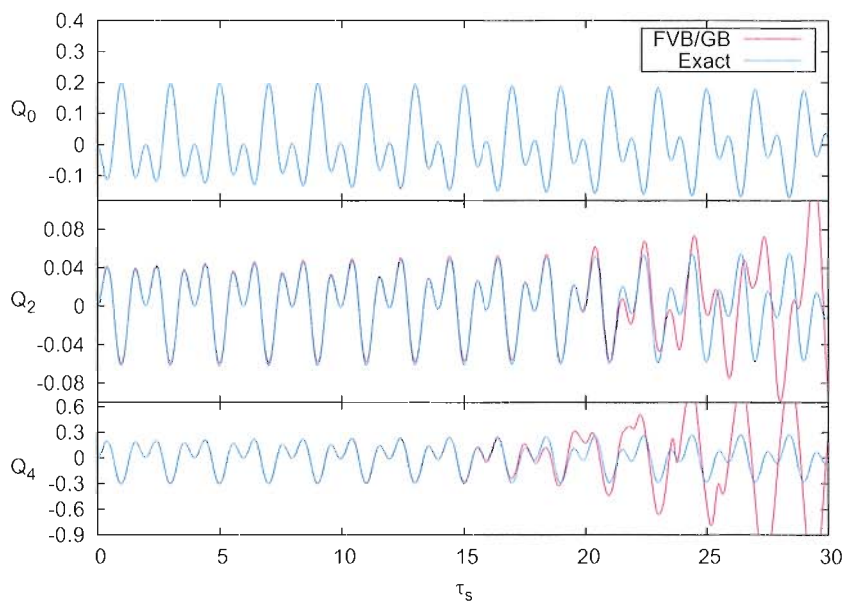

Figure 4.5: A plot of the spatial centers of the bath wave packets accompany the $\nu = 0$ (top), $\nu = 2$ (center), and $\nu = 4$ (bottom) vibrational levels calculated using the FVB/GB approach and numerically exact methods.

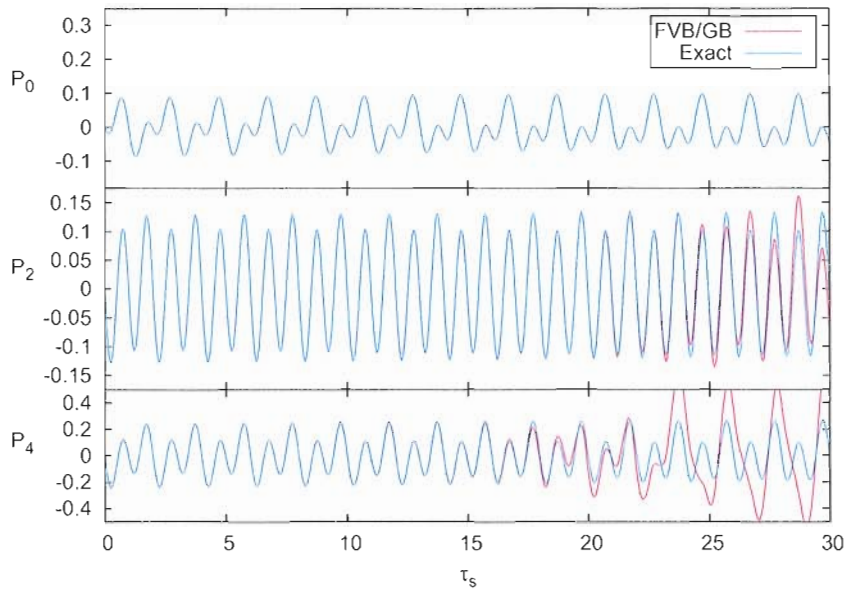

Figure 4.6: A plot of the momentum expectation values of the bath wave packets accompany the $\nu = 0$ (top), $\nu = 2$ (center), and $\nu = 4$ (bottom) vibrational levels calculated using the FVB/GB approach and numerically exact methods.

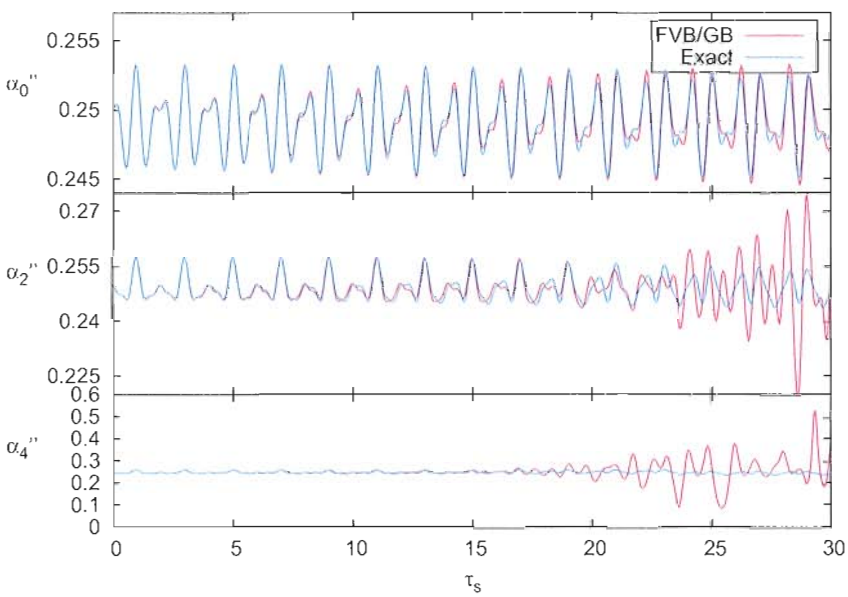

Figure 4.7: A plot of the width parameter α''_ν of the bath wave packets accompany the $\nu = 0$ (top), $\nu = 2$ (center), and $\nu = 4$ (bottom) vibrational levels calculated using the FVB/GB approach and numerically exact methods.

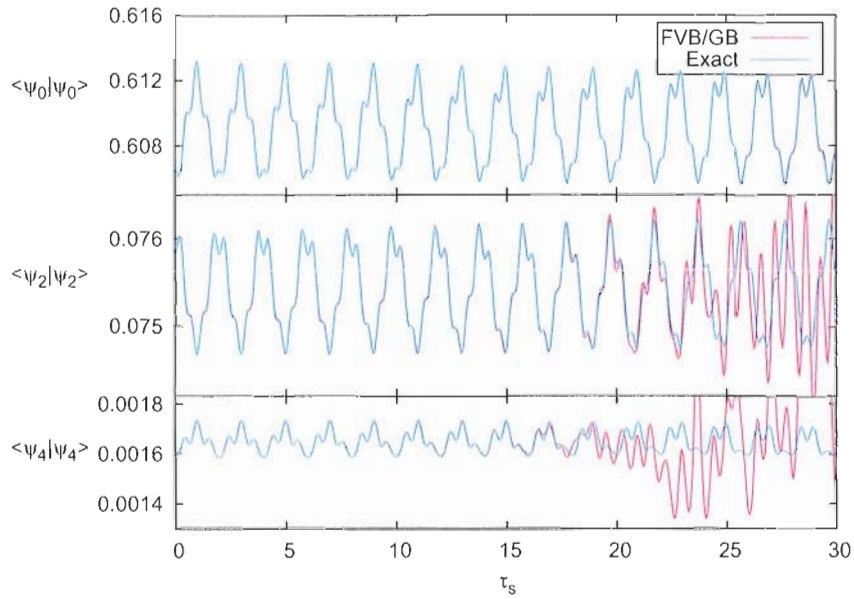

Figure 4.8: Populations of the $\nu = 0$ (top), $\nu = 2$ (center), and $\nu = 4$ (bottom) vibrational levels calculated using the FVB/GB approach and numerically exact methods.

D.3 Fidelity

A measure of the accuracy of the FVB/GB propagation can be found in the fidelity, defined as

$$f_\nu = \frac{|\langle\tilde{\psi}_\nu|\psi_\nu\rangle|}{\sqrt{\langle\tilde{\psi}_\nu|\tilde{\psi}_\nu\rangle\langle\psi_\nu|\psi_\nu\rangle}} \tag{1.28}$$

where $|\tilde{\psi}_\nu\rangle$ is the bath wave packet whose parameters have been calculated exactly. The fidelity can take values from 0 to 1, plots of which are shown in Figure 4.9 for the weak coupling case and Figure 4.10 for the strong coupling case. As

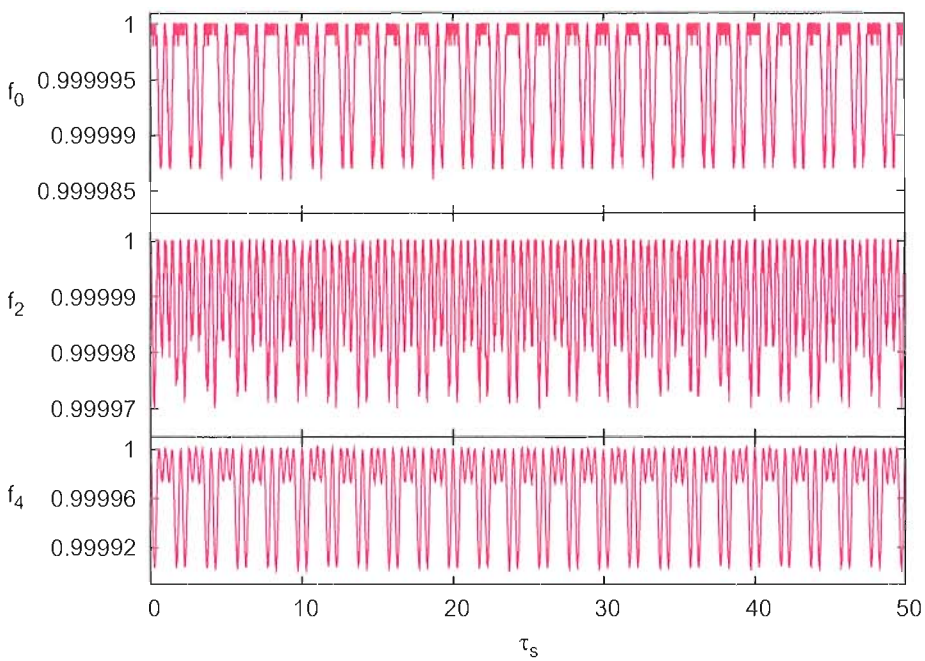

Figure 4.9: A plot of the fidelity of the $\nu = 0$ (top), $\nu = 2$ (center), and $\nu = 4$ (bottom) vibrational levels calculated using the FVB/GB approach and numerically exact methods.

Figure 4.9 illustrates the FVB/GB reproduces the exact bath wave packet nearly quantitatively, the fidelity taking values as small as $f_\nu < 2 \times 10^{-5}$ for $\nu = 0$, increasing to $f_\nu < 8 \times 10^{-5}$ for $\nu = 1$, and increasing further as the vibrational quantum number approaches the edge of the truncated basis. As shown in Figure

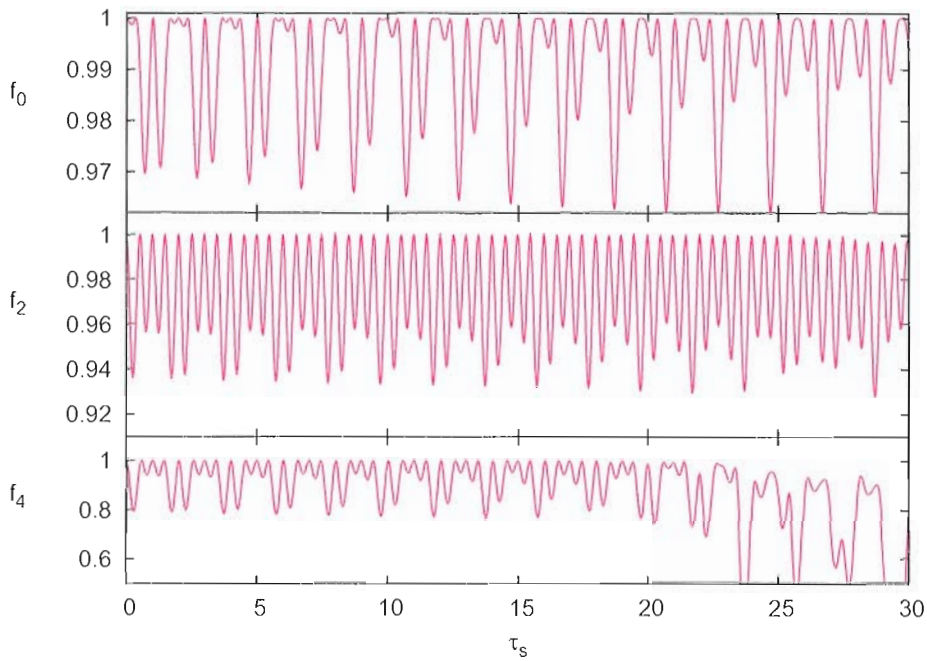

Figure 4.10: A plot of the fidelity of the $\nu = 0$ (top), $\nu = 2$ (center), and $\nu = 4$ (bottom) vibrational levels calculated using the FVB/GB approach and numerically exact methods.

4.10 it is immediately evident that the accuracy of the FVB/GB is compromised by stronger system-bath coupling. In increasing the coupling by 1.5 orders of magnitude the fidelity drops to $f_\nu < 0.98$ for $\nu = 0$, and $f_\nu < 0.8$ for $\nu = 4$.

D.4 Numerical vs. Theoretical Breakdown

As mentioned above Figures 4.5 — 4.8 illustrate a departure of the FVB/GB propagation from the exact results at approximately 20 system vibrational periods for some of the bath packets in the moderate-coupling case. To determine whether this disagreement is numerical in nature or if it arises as a result of the approximate nature of our theory we investigated the necessary computational effort required to achieve numerical convergence. Using several propagation methods we found that even after the FVB/GB results were converged disagreement with the exact results

still manifested themselves, setting an upper limit on the amount of time during which meaningful results can be derived from our theory. Nevertheless the stability of FVB/GB propagation should not pose a significant problem in the simulation of ultrafast spectroscopic signals whose decay time is determined by short-lived electronic coherences such as pump-probe and WPI. These electronic coherences are especially sensitive to the environment in the condensed phase and last for only hundreds of femtoseconds, long enough for a molecule such as I_2 in Ar to undergo a few intramolecular vibrations. Our ability to investigate processes that occur on time scales that are long relative to nuclear motion, such as vibrational dephasing and vibrational relaxation, may be hindered by this upper limit. The vibrational coherence of I_2 (X-state) in Kr, as measured by time-resolved coherent Anti-Stokes Raman scattering spectroscopy, can last for as long as 110 ps during which time the iodine molecule undergoes hundreds of intramolecular vibrations.

D.5 Population Nonconservation

The time derivative of total population is

$$\frac{d}{dt}\langle\Psi(t)|\Psi(t)\rangle = \sum_{\nu}\left(\left\langle\dot{\psi}_\nu|\psi_\nu\right\rangle + \left\langle\psi_\nu|\dot{\psi}_\nu\right\rangle\right). \tag{4.29}$$

The evolution of the bath wave packets is governed by Eqn. (4.5), whence we see

$$\frac{d}{dt}\langle\Psi(t)\mid\Psi(t)\rangle = i\sum_{\nu}\sum_{\bar{\nu}\neq\nu}\left\{\langle\psi_\nu|\,u^\dagger{}_{\nu\bar{\nu}}\,|\psi_{\bar{\nu}}\rangle - \langle\psi_\nu|\,u_{\nu\bar{\nu}}\,|\psi_{\bar{\nu}}\rangle\right\}. \tag{4.30}$$

The system-bath interaction potential $u(\hat{q},\hat{Q})$ is Hermitian, so the time derivative of Eqn. (4.30) is identically zero. The exact temporal evolution of the bath wave packets preserves the squared norm, however, in the FVB/GB treatment, norm

preservation becomes approximate. To see this, let

$$r_{\nu\bar{\nu}} = 2\mathrm{Im}\left\langle \psi_\nu \right| u_{\nu\bar{\nu}} \left| \psi_{\bar{\nu}} \right\rangle . \tag{4.31}$$

The time derivative of total population is

$$\sum_\nu \dot{p}_\nu = \frac{d}{dt}\left\langle \Psi(t) \mid \Psi(t) \right\rangle = \sum_\nu \sum_{\bar{\nu}\neq\nu} r_{\nu\bar{\nu}} = \sum_{\nu,\bar{\nu}}{}' (r_{\nu\bar{\nu}} + r_{\bar{\nu}\nu}). \tag{4.32}$$

where $\sum'$ denotes a sum over pairs of vibrational levels for $\nu < \bar{\nu}$. $r_{\nu\bar{\nu}}$ is antisymmetric, which guarantees the conservation of the total population. In the FVB/GB theory, the antisymmetry of $r_{\nu\bar{\nu}}$ is compromised because $r_{\nu\bar{\nu}}$ and $r_{\bar{\nu}\nu}$ are subject to slightly different approximations. As a result, $(r_{\nu\bar{\nu}} + r_{\bar{\nu}\nu})$ need not vanish exactly, and the norm conservation becomes approximate. This occurs because, as mentioned previously, in calculating $r_{\nu\bar{\nu}} = 2\mathrm{Im}\left\langle \psi_\nu \right| u_{\nu\bar{\nu}}(Q) \left| \psi_{\bar{\nu}} \right\rangle$, we write $\left\langle Q \right| u_{\nu\bar{\nu}}(Q) \left| \psi_{\bar{\nu}} \right\rangle = u_{\nu\bar{\nu}}(Q)\frac{\langle Q|\psi_{\bar{\nu}}\rangle}{\langle Q|\psi_\nu\rangle}\left\langle Q \mid \psi_\nu \right\rangle$ and expand $u_{\nu\bar{\nu}}(Q)\frac{\langle Q|\psi_{\bar{\nu}}\rangle}{\langle Q|\psi_\nu\rangle}$ about Q_ν through second order in $Q - Q_\nu$, so that $\left\langle Q \mid \psi_\nu \right\rangle$ will retain its Gaussian form. On the other hand, $r_{\bar{\nu}\nu} = 2\mathrm{Im}\left\langle \psi_{\bar{\nu}} \right| u_{\bar{\nu}\nu}(Q) \left| \psi_\nu \right\rangle$ is evaluated by expanding $u_{\bar{\nu}\nu}(Q)\frac{\langle Q|\psi_\nu\rangle}{\langle Q|\psi_{\bar{\nu}}\rangle}$ about $Q_{\bar{\nu}}$, through second order in $Q - Q_{\bar{\nu}}$. This treatment makes $r_{\nu\bar{\nu}} \neq -r_{\bar{\nu}\nu}$, and therefore total population is not exactly conserved in such calculations. Nonetheless, this approximation is acceptable to some extent. When Q_ν and $Q_{\bar{\nu}}$ are widely separated, $\left\langle Q \mid \psi_\nu \right\rangle$ and $\left\langle Q \mid \psi_{\bar{\nu}} \right\rangle$ are spatially non-overlapping. In this limit,$r_{\nu\bar{\nu}} \cong 0$, so that the rate of transfer of population between states ν and $\bar{\nu}$ is negligible, and these transitions do nothing to undermine norm conservation . When $Q_\nu \cong Q_{\bar{\nu}}$, the approximations made in expanding $r_{\nu\bar{\nu}}$ and $r_{\bar{\nu}\nu}$ very much the same. In this case, $r_{\nu\bar{\nu}}$ becomes more nearly antisymmetric and population is approximately conserved.

D.6 Symmetry of α_ν

In the case being considered the one dimensional bath lends itself to a complex scalar $\alpha_\nu = \alpha'_\nu + i\alpha''_\nu$. The real part describes the correlation between position and momentum while the imaginary part determines the spatial width of the packet. Its time evolution is governed by coupled equations given in Appendix B. For a multidimensional bath α_ν is a matrix and the time derivative of neither α'_ν nor α''_ν, as previously published,[15] are symmetric, and therefore the symmetry of α_ν itself will be undermined during spatio-temporal evolution. While performing numerical tests using a multi-dimensional bath, the non-symmetry of α'_ν and α''_ν caused the determinants of these matrices to approach zero, making the computation of their inverses difficult. To avoid unnecessary numerical difficulty, α'_ν and α''_ν were adjusted to be symmetric, and are presented in Appendix B. In generalizing from a one-dimensional bath to one containing many bath modes, parameter equations of motion of the form

$$Q^2\dot{\alpha} = Q^2\beta \tag{4.33}$$

are changed to

$$Q^T \cdot \dot{\alpha} \cdot Q = Q^T \cdot \beta \cdot Q \tag{4.34}$$

where α can be the scalar (one-dimensional bath, Eqn. (4.33)) or matrix (multidimensional bath, Eqn. (4.33)) representation of either α'_ν or α''_ν, and β is a real scalar in Eqn. (4.33) and a real matrix in Eqn. (4.34). According to Eqn. (4.33) $\dot{\alpha} = \beta$, but the same is not true for Eqn. (4.34). In the latter case we symmetrize the time-derivative of α by setting $\dot{\alpha} = \frac{1}{2}(\beta + \beta^T)$. Note that this correction does not change the value of any calculated observables. In Eqn. (4.34) $\dot{\alpha}$ and β have the

same diagonal elements,

$$\beta_{jj} = \frac{1}{2}(\beta_{jj} + \beta^T{}_{jj}); \tag{4.35}$$

and they have different off-diagonal elements, but the sums of transposed elements are the same,

$$\beta_{jk} + \beta_{kj} = \frac{1}{2}(\beta_{jk} + \beta^T{}_{kj}) + \frac{1}{2}(\beta_{jk} + \beta^T{}_{kj}). \tag{4.36}$$

No single off-diagonal element has any physical implication, but the diagonal elements and the sums of matched off-diagonal elements do have genuine physical significance. Recall our Gaussian ansatz, Eqn. (4.6), the quadratic part of which can be written

$$\begin{aligned} &\exp\left[i(Q-Q_\nu)^T \cdot \alpha_\nu \cdot (Q-Q_\nu)\right] = \\ &\exp\left[i\sum_l (Q-Q_\nu)_l^{\,2} \cdot (\alpha_\nu)_{ll} + i\sum_{l<m} (Q-Q_\nu)_l \cdot [(\alpha_\nu)_{lm} + (\alpha_\nu)_{ml}] \cdot (Q-Q_\nu)_m\right]. \end{aligned} \tag{4.37}$$

The symmetrization of $\dot{\alpha}_\nu$ does not alter the diagonal elements or sums of transposed off-diagonal elements from the non-symmetrized expressions, thus the bath wave packets retain their form.

E Wave Packet Interferometry using FVB/GB

E.1 Linear Wave Packet Interferometry Signal

To illustrate how the FVB/GB can be used to simulate ultrafast spectroscopic signals we consider linear wave packet interferometry (WPI). Linear WPI involves a pair of laser pulses impinging on a molecular system, each of which transfers population to an excited electronic state. The resultant calculated signal from a

linear WPI experiment is proportional to this population that is linear in each of the fields,

$$S(t) = \langle (2)_e | (1)_e \rangle \ , \tag{4.38}$$

where $|(j)_e\rangle$ is the wave packet created on the excited electronic state by the j^{thS} pulse. The first pulse creates a wave packet on the excited electronic surface with the phase imprint of the pulse. During the variable interpulse delay $t_{21} = t_2 - t_1$ the wave packet evolves according to the excited state Hamiltonian. At t_2 the second pulse arrives and creates another wave packet on the excited surface that can interfere with the first. If the inter-pulse delay is such that the first wave packet has returned to the point at which it was launched at the time the second pulse arrives, the interference can, depending on the relative phase between the two pulses, ϕ, be constructive ($\phi = 0$) or destructive ($\phi = \pi$). The signal (4.38) goes through maxima when the interference is fully constructive, leading to an enhancement of the excited state population, and minima when the interference is destructive.

We can calculate a signal by taking the product of the linear absorption spectrum with the double pulse spectrum. The intensity of the linear absorption spectrum arising from a system residing in a state $|e\rangle|N\rangle$ can be written:

$$I(\omega) = \sum_{\bar{M}} |\mu_{eg} \langle \bar{M}|N\rangle|^2 \delta(\omega - \omega_{\bar{M}N}) \tag{4.39}$$

where $\omega_{\bar{M}N} = (E_{\bar{M}} - E_N)/\hbar$, $\mu_{eg} = \langle e|\mu|g\rangle$ is the dipole operator element connecting the ground and excited electronic state in the dipole approximation, and $|\bar{M}\rangle$ is a vibrational eigenstate of the excited electronic state. It is also possible to express the absorption spectrum in terms of an inverse Fourier transform of the overlap of an initial wave function with one that is propagating under the excited state

Hamiltonian h_e:[16]

$$I(\omega) = \frac{\mu^2}{2\pi} \int_{-\infty}^{\infty} dt \ \langle \psi(0)| \, e^{-i(\omega - h_e + \epsilon_{\nu=0})t} \, |\psi(0)\rangle \ . \tag{4.40}$$

which can be written as a sum of integrals over negative and positive time. In the integral ranging from $-\infty$ to 0 we make the variable change $dt' = -dt$, and exchange the limits of integration leading to an expression for the real-valued absorption spectrum:

$$I(\omega) = \frac{\mu^2}{\pi} \mathrm{Re}[\int_{0}^{\infty} dt \ \langle \psi(0)| \, e^{-i(\omega - h_e + \epsilon_{\nu=0})t} \, |\psi(0)\rangle] \ . \tag{4.41}$$

This approach is more readily suited for calculating the absorption spectrum of large, multidimensional systems where explicit determination of the eigenstates and corresponding energies is an unfeasible task, as is the case with the types of systems we will be considering in the near future. The time-dependent wave packets in Eqn. (4.40) can be propagated using any number of methods, including FVB/GB, and the integral (4.41) can be calculated, allowing for a simulation of the WPI signal as a function of the interpulse delay and relative phase, ϕ,

$$S(\Delta t, \phi) = ... \tag{4.42}$$

Below we consider several excited state Hamiltonians and present their absorption spectra and the resulting WPI signals.

E.2 Case A

The first case we consider entails a displacement of the equilibrium position of the system, q_e, in the excited state while the equilibrium configuration of the bath

and the coupling are both set to 0 in the ground and excited state. The relevant Hamiltonians are

$$h_g = \frac{p^2}{2} + \frac{\omega^2}{2}q^2 + \frac{P^2}{2} + \frac{\Omega^2}{2}Q^2, \tag{4.43}$$

and

$$h_e = \frac{p^2}{2} + \frac{\omega^2}{2}(q - q_e)^2 + \frac{P^2}{2} + \frac{\Omega^2}{2}Q^2 \tag{4.44}$$

with q_e set such that it coincides with the classical inner turning point of the $\nu = 1$ vibrational state. We set $\omega = 1$ and $\Omega = 1/3$. A positive value of q_e introduces a non-zero initial value of γ'_ν. Contour plots of the potentials are shown in Figure 4.11. The resulting absorption spectrum calculated using Eqns. (4.39) and (4.40) are plotted in Figure 4.12. The frequency resolution of the FVB/GB spectrum

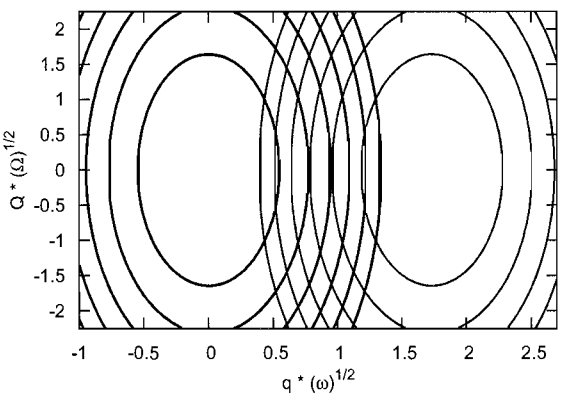

Figure 4.11: Case A: Contours of the nuclear potentials accompanying the ground and excited electronic states of two uncoupled harmonic oscillators. The ground state equilibrium configuration is centered at (0,0) while that of the excited state is at $(\sqrt{3}, 0)$

is limited by the amount of time that the bath wave packets can be propagated while still remaining realistic, at least for the vibrational levels with significant population, whose relative contribution to $\langle\Psi(0)|\Psi(t)\rangle$ is greater than those with very little population. For the case of no system-bath coupling the FVB/GB becomes

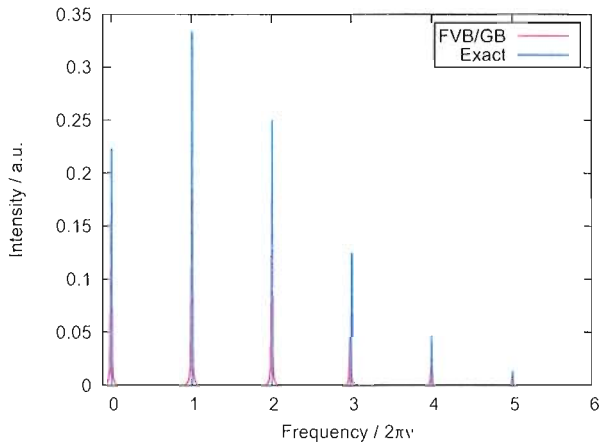

Figure 4.12: The linear absorption spectrum of two uncoupled harmonic oscillators, corresponding to case A presented in the text. Only the system is Franck-Condon active, leading to the evenly spaced lines with separation of $h\nu$. The absorption maxima is centered around the $\nu = 0$ to $\nu' = 1$ transition.

exact and thus remains theoretically stable, enabling an accurate calculation of the linear absorption spectrum. Only system transitions are involved in the peaks in Figure 4.12 since no bath motion is induced by the system vibration in the excited electronic state, and hence the bath contribution to the overlap $\langle\Psi(0)|\Psi(t)\rangle$ in Eqn. (4.40) remains constant. The FVB/GB accurately predicts the overall shape of the spectrum as well as the peak spacing. A maximum occurs at $2\pi\nu = 1$ arising from the $|\nu = 0\rangle|n = 0\rangle \rightarrow |\bar{\nu} = 1\rangle|\bar{n} = 0\rangle$ transition, consistent with the chosen value of q_e. The small width in the FVB/GB peaks arises from artificially setting the upper limit of integration in (4.41) to a finite value. When there is no system-bath coupling in the excited electronic state the propagation becomes numerically exact and remains numerically stable for many hundreds of vibrational periods, resulting in minimal peak widths. For subsequent cases with nonzero coupling the FVB/GB breaks down theoretically, which requires the introduction of a phenomenological exponential decay of $\langle\Psi(0)|\Psi(t)\rangle$ such that this overlap goes to zero before instability sets in. This decay mimics electronic dephasing and ensures the absorption

spectra are calculated using only numerically and theoretically meaningful results. in these cases the peak widths are slightly more exagerated.

The linear WPI signal is plotted in Figure 4.13 as a function of interpulse delay and relative phase. For this and subsequent cases presented below. all pulses

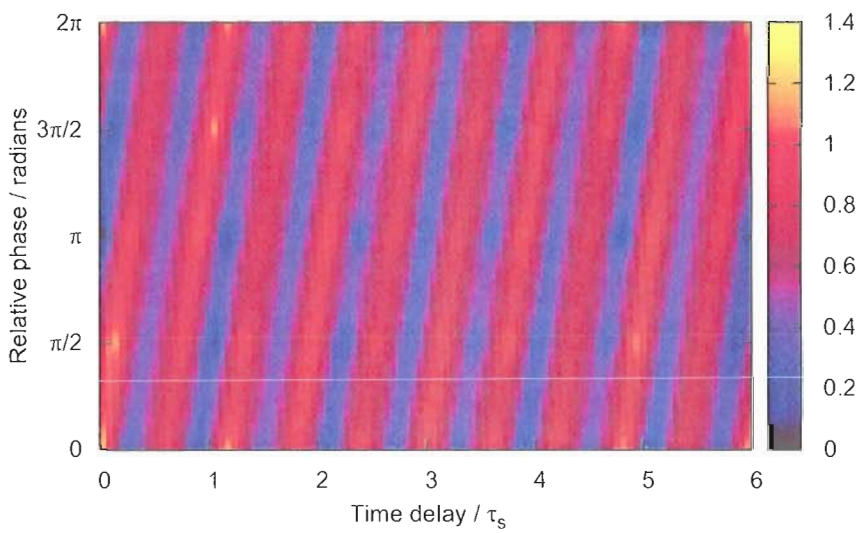

Figure 4.13: The linear WPI signal for two uncoupled harmonic oscillators with frequencies $\omega = 1$, and $\Omega = 1/3$. plotted as a function of the interpulse delay (units of system vibrational period. τ_s) and relative phase.

have Gaussian temporal envelopes with durations $\sigma = 0.2\tau_s$. where τ_s is the period of the uncoupled system vibration. and the carrier frequencies are resonant with the $|\nu = 0\rangle|n = 0\rangle \rightarrow |\bar{\nu} = 1\rangle|\bar{n} = 0\rangle$ transition. The interpulse delay is varied from 0 to $6\tau_s$. while the relative phase is varied from 0 to 2π. Maxima in the signal can be seen for delay and phase combinations that lead to maximal overlap of the fringe pattern in the pulse intensity profile and the absorption spectra.

At $3\tau_s$ the system wave packet and all of the bath wave packets accompanying various vibrational levels have returned to the point in phase space at which they

were placed by the action of the first pulse. When the second pulse acts on the wave-packets with a relative phase $\phi = 0$, they interfere constructively. As the phase is varied for this pulse delay we see complete destructive interference at $\phi = \pi$, where the phase imprint from the first pulse is completely out of phase with that from the second pulse.

E.3 Case B

The second case involves a identical values of q_e and Q_e as in the previous case, only now we set the system-bath coupling constant to $J = 0.05$. The ground state Hamiltonian is the same as Eqn. (4.43) but the excited state Hamiltonian takes the same form as Eqn. (4.27). The potentials are similar to those used in Section C.1, but differ in the sign and magnitude of q_e and Ω. Figure 4.14 shows isoenergy contours of the potentials. The nonzero coupling in the excited electronic

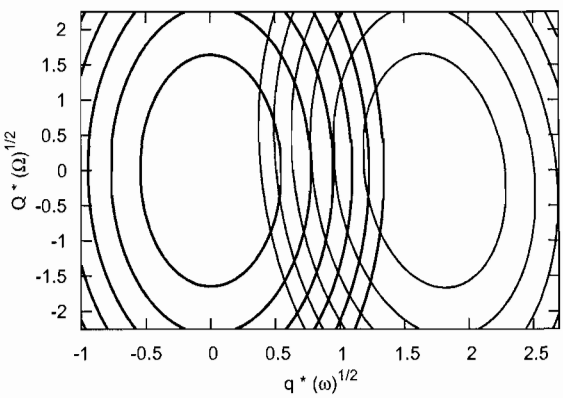

Figure 4.14: Case B: Contours of the nuclear potentials accompanying the ground and excited electronic states of two bilinearly coupled ($J = 0.05$) harmonic oscillators, The ground state equilibrium configuration is centered at (0.0) while that of the excited state is at ($\sqrt{3}$,0).

state causes the bath to become Franck-Condon active, giving rise to peaks in the absorption spectrum that involve concerted absorption by both the system and bath.

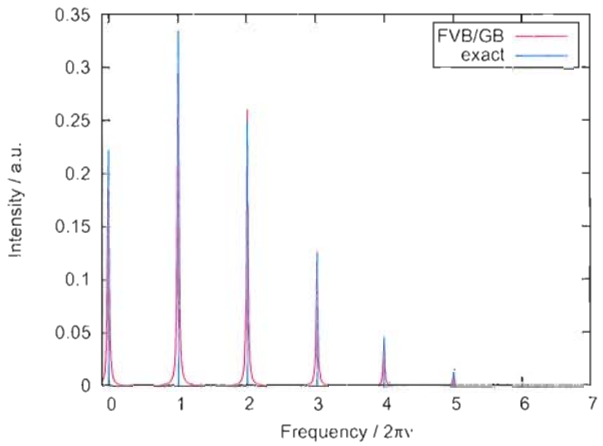

Figure 4.15: The linear absorption spectrum of two coupled harmonic oscillators, corresponding to case B presented in the text. The system coordinate is displaced relative to the ground electronic state equilibrium configuration. The bath is undisplaced. Both the system and bath are Franck-Condon due to nonzero coupling. The absorption maxima is centered around the $|00\rangle$ to $|10\rangle$ transition.

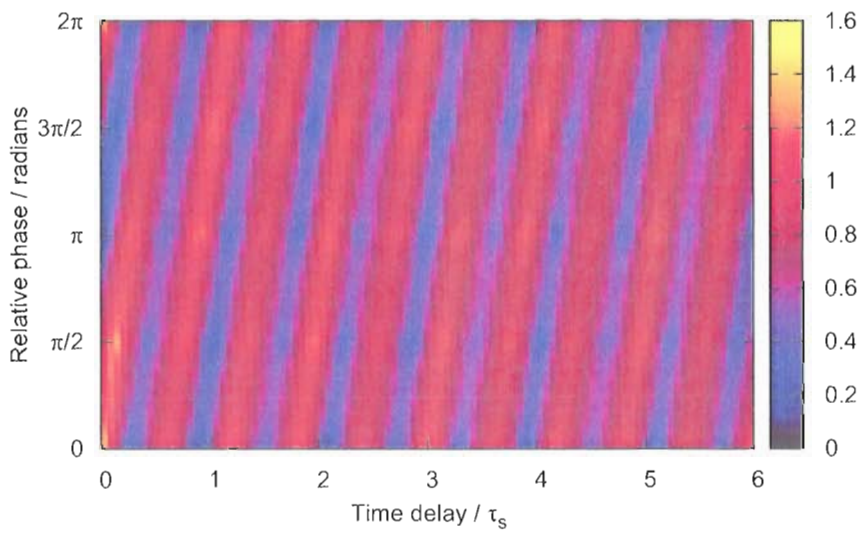

Figure 4.16: The linear WPI signal for two bilinearly coupled (J=0.05) harmonic oscillators with frequencies $\omega = 1$, and $\Omega = 1/3$, plotted as a function of the interpulse delay (units of system vibrational period, τ_s) and relative phase.

For example we should expect to see a peak corresponding to the $|g\rangle|\nu = 0\rangle|n = 0\rangle \rightarrow |e\rangle|\nu = 1\rangle|n = 1\rangle$ transition. Figure 4.15 shows the absorption spectrum calculated using both Eqns. (4.39) and (4.40). In both cases peaks that involve system and bath absorption are present. The linear WPI signal for this case is plotted in Figure 4.16 . The spectrum shares similarities with the spectrum of case A; the introduction of coupling does little to change the spectra.

E.4 Case C

The third case to consider involves the same h_g as in cases A and B, but now both the system and bath equilibrium positions are displaced in h_e. The system potential in the excited electronic state is translated relative to the ground state potential by an amount $\delta q = \sqrt{3}$ so that the minima of the excited state potential is at the outer turning point of the $|g\rangle|\nu = 1\rangle$ level. The bath is also displaced by $\delta Q = \sqrt{3}$ which corresponds to the outer turning point of the $|g\rangle|n = 0\rangle$ level. The system and bath are uncoupled in case C in both the ground and excited electronic states. The potentials involved are shown in Figure 4.17. The displacement in the bath equilibrium position in the excited state leads to a significant increase in the intensity of the bath absorption peaks, as seen in Figure 4.18. The calculated linear WPI signal is shown in Figure 4.19. While the periodicity of general intensity fringes is the same as in Figure 4.13 and Figure 4.16, much of the contrast in intensity has been decreased relative to cases A and B. The presence of strong bath absorption peaks excludes the possibility of completely destructive interference for many of the delay and phase combinations that led to the minima in cases A and B.

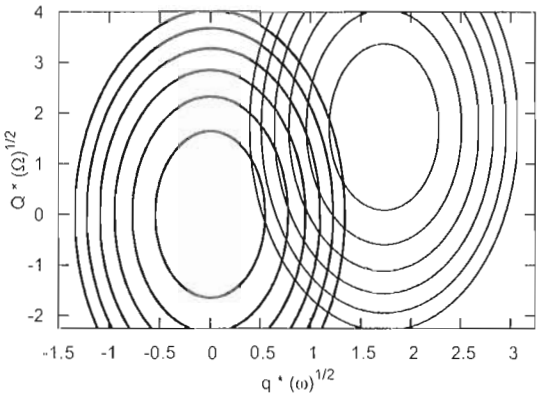

Figure 4.17: Case C: Contours of the nuclear potentials accompanying the ground and excited electronic states of two uncoupled harmonic oscillators. The ground state equilibrium configuration is centered at (0,0) while that of the excited state is at $(\sqrt{3}, \sqrt{3})$

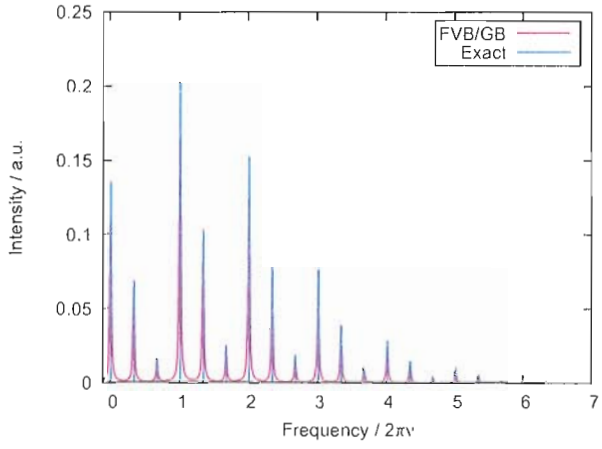

Figure 4.18: The linear absorption spectrum of two uncoupled harmonic oscillators, corresponding to case C presented in the text. Both the system and bath coordinates are displaced relative to their ground electronic state equilibrium configurations.

E.5 Case D

In addition to displacements in the system and bath potential in the excited state relative to the ground state, case D involves an excited state bilinear coupling $J = 0.05$. The displacements are, as in case C, $\delta q = \sqrt{3}$ and $\delta Q = \sqrt{3}$. The system and bath remain uncoupled in the ground state. The relevant potentials are shown

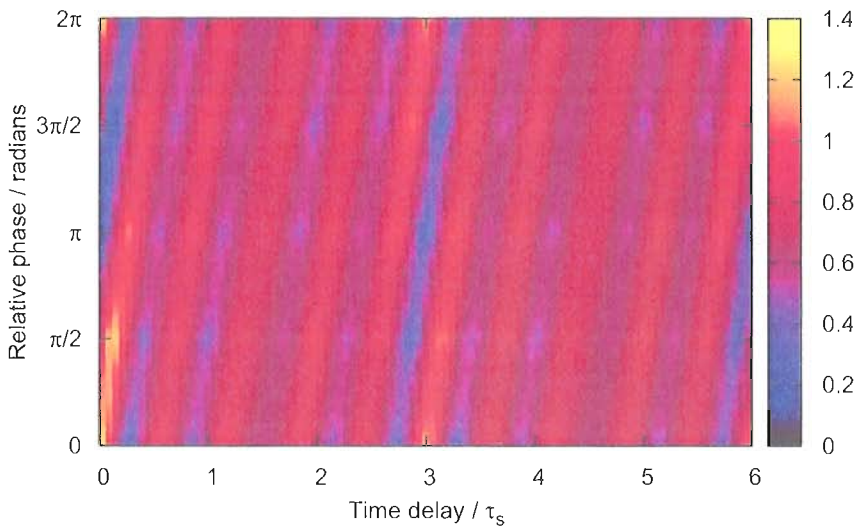

Figure 4.19: The linear WPI signal for two uncoupled harmonic oscillators with frequencies $\omega = 1$, and $\Omega = 1/3$. plotted as a function of the interpulse delay (units of system vibrational period, τ_s) and relative phase. Both the system and bath coordinates are displaced relative to their ground electronic state equilibrium configurations, in accord with the parameters for case C presented in the text.

in Figure 1.20. The absorption spectrum shown in Figure 4.21 is similar to that of case C but differs in the relative intensities of the peaks. This difference is due to the nonzero coupling in the excited state which has the effect of increasing or decreasing Franck-Condon factors. Figure 4.22 shows the calculated WPI signal for case D. As in Figure 1.19 contrast in the intensity is decreased relative to cases A and B for reasons stated in Section E.4.

E.6 Comparison of Cases A & B and C & D

The effect of coupling on the absorption spectra of two otherwise similar molecular systems can be addressed analytically in the case of coupled harmonic oscillators. The excited state Hamiltonians for cases A and B differ only in that

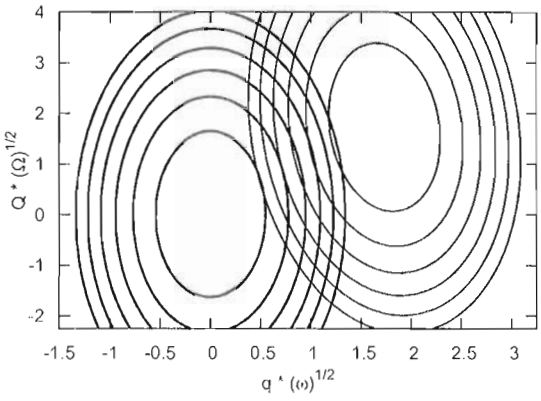

Figure 4.20: Case D: Contours of the nuclear potentials accompanying the ground and excited electronic states of two bilinearly coupled (J=0.05) harmonic oscillators. The ground state equilibrium configuration is centered at (0,0) while that of the excited state is at $(\sqrt{3}.\sqrt{3})$.

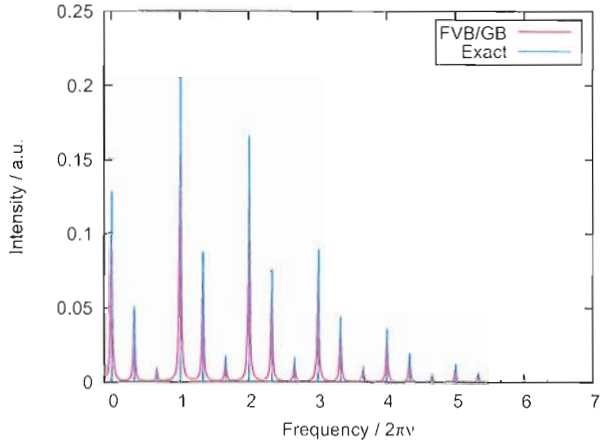

Figure 4.21: The linear absorption spectrum of two coupled harmonic oscillators, corresponding to case D presented in the text. Both the system and bath coordinates are displaced relative to their ground electronic state equilibrium configurations, and are Franck-Condon active with contributions from the nonzero coupling and displacements.

$J = 0$ in case A, while $J = 0.05$ in case B, the same is true for cases C and D. The excited state potential displacements in the system and bath are equivalent in each set of cases. The difference in peak intensities for a given transition in the presence and absence of coupling is related to the difference in Franck-Condon

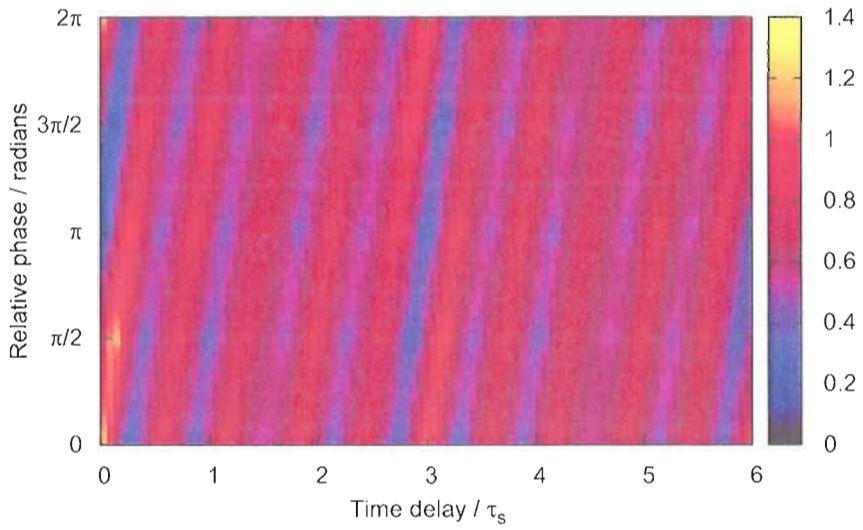

Figure 4.22: The linear WPI signal for two coupled (J=0.05) harmonic oscillators with frequencies $\omega = 1$, and $\Omega = 1/3$, plotted as a function of the interpulse delay (units of system vibrational period, τ_s) and relative phase. Both the system and bath coordinates are displaced relative to their ground electronic state equilibrium configurations, in accord with the parameters for case D presented in the text.

factors, $|\langle 00|\bar{\nu}\bar{n}\rangle_A| - |\langle 00|\bar{\nu}\bar{n}\rangle_B|$, where $h_e^{(A)}\,|\bar{\nu}\bar{n}\rangle_A = (\epsilon_{\bar{\nu}}^{(A)} + \epsilon_{\bar{n}}^{(A)})\,|\bar{\nu}\bar{n}\rangle_A$ for case A with corresponding expressions for the other cases, and $|00\rangle$ is the ground vibrational state of h_g in Eqn. (4.43). The eigenstates of the excited Hamiltonians are related to those of the ground state through combinations of squeezing, $\hat{\sigma}(\eta,\theta)$, rotation, $\hat{R}(\theta)$, and displacement operators, $\hat{D}_s(\delta)$ and $\hat{D}_b(\delta)$.

$$\hat{\sigma}(\eta,\theta) = \exp\left[\left(\tfrac{\eta_1}{2}\cos^2\theta + \tfrac{\eta_2}{2}\sin^2\theta\right)\left(a^\dagger a^\dagger - aa\right) + \left(\tfrac{\eta_1}{2}\sin^2\theta + \tfrac{\eta_2}{2}\cos^2\theta\right)\left(A^\dagger A^\dagger - AA\right)\right.$$
$$\left. + (\eta_1 - \eta_2)\cos\theta\sin\theta\left[\left(\sqrt{\tfrac{\omega}{\Omega}} + \sqrt{\tfrac{\Omega}{\omega}}\right)\left(a^\dagger A^\dagger - aA\right) + \left(\sqrt{\tfrac{\omega}{\Omega}} - \sqrt{\tfrac{\Omega}{\omega}}\right)\left(a^\dagger A - aA^\dagger\right)\right]\right] \tag{4.45}$$

$$\hat{R}(\theta) = \exp\left[\frac{\theta}{2}\left\{\left(\sqrt{\frac{\Omega}{\omega}} - \sqrt{\frac{\omega}{\Omega}}\right)\left(a^\dagger A^\dagger - aA\right) + \left(\sqrt{\frac{\Omega}{\omega}} + \sqrt{\frac{\omega}{\Omega}}\right)\left(aA^\dagger - a^\dagger A\right)\right\}\right] \tag{4.46}$$

$$\hat{D}_s(\delta) = \exp\left[-i\hat{p}\delta\right] \tag{4.47}$$

$$\hat{D}_b(\delta) = \exp[-i\hat{P}\delta], \tag{4.48}$$

where η_j is the squeezing parameter for the system (j=1) or bath (j=2), θ is the angle of relative rotation between the principle axes in the uncoupled and coupled scenarios, a (A) and $a^\dagger$ ($A^\dagger$) are the annihilation and creation operators for the uncoupled eigenstates of the system (bath) Hamiltonian. The parameters η_j and θ are determined by the coupling constant J. Both $\hat{\sigma}$ and $\hat{R}$ operate on the system and the bath, while $\hat{D}_s$ ($\hat{D}_b$) acts only on the system (bath). The eigenstates of the various coupled Hamiltonians can be written:

$$\begin{aligned}
|\bar{\nu} = \nu, \bar{N} = N\rangle_A &= \hat{D}_s|\nu N\rangle \\
|\bar{\nu} = \nu, \bar{N} = N\rangle_B &= \hat{\sigma}\hat{R}\hat{D}_s|\nu N\rangle \\
|\bar{\nu} = \nu, \bar{N} = N\rangle_C &= \hat{D}_s\hat{D}_b|\nu N\rangle \\
|\bar{\nu} = \nu, \bar{N} = N\rangle_D &= \hat{\sigma}\hat{R}\hat{D}_s\hat{D}_b|\nu N\rangle.
\end{aligned} \tag{4.49}$$

The omitted arguments for the operators are the same for all cases in which they appear.

Figure 4.23 and Figure 4.24 plot the exact absorption spectra of cases A vs. B and C vs. D, respectively. The change in intensity for a given transition can be calculated using

$$\Delta_{\nu N}^{(ij)} = |\langle 00|\bar{\nu}\bar{N}\rangle_i|^2 - |\langle 00|\bar{\nu}\bar{N}\rangle_j|^2. \tag{4.50}$$

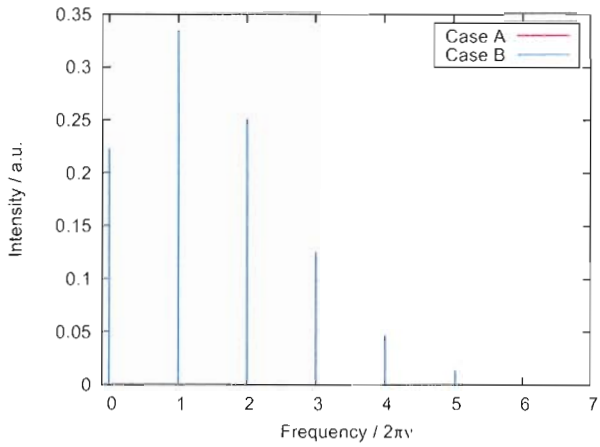

Figure 4.23: A comparison of the exactly numerically calculated absorption spectra for cases A and B.

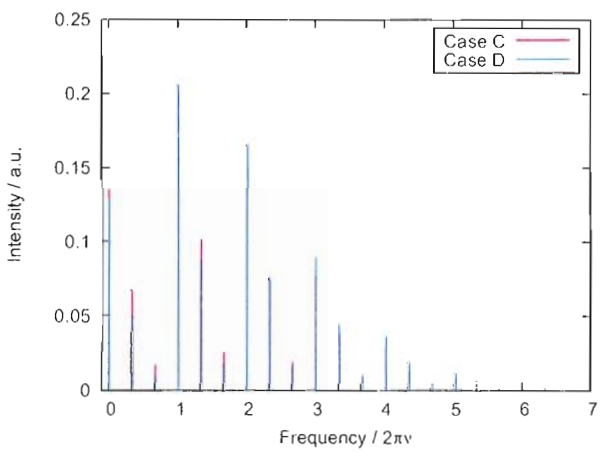

Figure 4.24: A comparison of the exactly numerically calculated absorption spectra for cases C and D.

For Δ_{AB} and Δ_{CD} we have

$$\begin{aligned}\Delta_{\nu N}^{(AB)} &= |\langle 00|\hat{D}_s|\nu N\rangle|^2 - |\langle 00|\hat{\sigma}\hat{R}\hat{D}_s|\nu N\rangle|^2 \\ &= -|\langle 00|\hat{\sigma}\hat{R}\hat{D}_s|\nu N\rangle|^2, \qquad (4.51)\end{aligned}$$

$$\Delta_{\nu N}^{(CD)} = |\langle 00|\hat{D}_s\hat{D}_b|\nu N\rangle|^2 - |\langle 00|\hat{\sigma}\hat{R}\hat{D}_s\hat{D}_b|\nu N\rangle|^2. \qquad (4.52)$$

To find how the intensity of a given peak will change with the introduction

of coupling becomes a task of calculating numerical values for the matrix elements featured in the above equations.

F Discussion

In cases B, C, and D above the Franck-Condon active bath gives rise to 'side bands' accompanying each absorption peak corresponding to a system transition. In the case of a one-dimensional bath considered here the bands' are composed of single peaks with considerable spacing between them, but in the case of a multi-dimensional bath the bands are composed of many infinitesimally closely spaced lines whose distribution is governed by the density of states. The ability to selectively excite the system or the bath using interferometry has been of recent experimental interest.[17] Using the interference fringes of a double pulse pair Schwenter and co-workers were able to electronically excite molecular bromine embedded in cryogenic Kr while minimizing bath absorption, measured by probing the fluorescence from a high-lying electronic level that is populated using a third laser pulse.

In other recent spectroscopic experiments whose signal relies on coherence between electronic states of a dihalogen in a cryogenic matrix evidence of coherent bath motion appears after electronic decoherence reduces the contribution to the signal from the chromophore vibration. Persistent low-frequency oscillations of the signal can be found in pump-probe spectra of a variety of dihalogen:rare gas motifs that last for tens of ps, long after electronic decoherence (tens of fs) has set in. These oscillations have been attributed to a local zone-boundary phonon (ZBP) whose mechanism of excitation still remains ambiguous with two probable origins: 1) Nuclear-nuclear coupling of the system and bath, and 2) electron-phonon coupling as embodied in the displacive excitation of coherent phonons (DECP). The relative

contribution of each scheme can be investigated using FVB/GB by altering potential parameters in the ground and excited states of model systems that closely mimic real molecules. A first step in this direction is taken when considering cases B-D in the previous section.

Even though the bath is not displaced in the excited state in case B an electronic excitation of the ground state wave function leads to small-amplitude bath motion through coupling to the system's nuclear coordinate. This type of system is analogous to one that would give rise to ZBP through nuclear coupling without appealing to the mechanism embodied in DECP. In case C the appearance of bath peaks in the absorption spectrum, shown in Figure 4.18, are due solely to the displacement in the bath mode in the excited state relative to the ground state. Since the system and bath are uncoupled in both electronic states an excitation of the ground state wave function leads to harmonic motion in both the system and the bath about their respective excited equilibrium positions. The analogous situation for a diatomic molecule embedded in a low-temperature matrix would be one in which motion in the bath can be wholly attributed to DECP since spatio-temporal evolution of the system after the excitation process does not affect that of the bath. Upon excitation a force is exerted on both the system and bath nuclear coordinates, but their subsequent trajectories do not alter the others. Collision-induced coherence transfer can be ruled out as a source of coherent bath motion in this case. Case D involves both nuclear-nuclear coupling and electron-phonon coupling as sources of bath motion. Using a multidimensional bath one could perform FVB/GB calculations on cases analogous to B, C, and D while manipulating coupling strengths and displacements and monitor the bath dynamics for ZBP to determine the relative contributions of the two previously mentioned excitation mechanisms.

G Conclusions

Numerical implementations of the FVB/GB theory, presented in the previous chapter, show agreeable results when compared with numerically exact calculations. We successfully applied the theory to a pair of bilinearly coupled harmonic oscillators with varying coupling strengths, bath frequencies, and initial conditions. In the weak coupling case ($J = 0.001$) the theory agrees quantitatively with the exact results for hundreds of system vibrational periods. When the coupling strength is increased ($J = 0.05$) the theory breaks down after approximately 20 system vibrational periods, which should be long enough to simulate any ultrafast spectroscopic experiment whose signal relies on the existence of electronic coherence.

The linear absorption spectra for several system-bath configurations were calculated using wave packet that had been propagated using the FVB/GB theory. Peak placements and amplitudes were reproduced with very good agreement to the exactly calculated spectra. In a recapitulation of the absorption spectra, linear WPI signals were calculated using a pair of variably time-delayed pulses while also varying their relative phase, showing the theory's ability to produce results which may aid in the elucidation of phenomena encoded in experimental signals.

Future applications of the theory will entail using realistic molecular potentials, and a multidimensional bath to investigate vibrational and electronic decoherence in dihalogen:rare gas systems. With the inclusion of many bath modes a physical explanation for the launching of ZBP can be rigorously and systematically formulated, and should serve as a focal point for future experimental investigations.

Notes

[1] Fushitani, M.; Bargheer, M.; Gühr, M.; Schwentner, N. *Phy. Chem. Chem. Phys.* **2005**, *7*, 3143.

[2] Bihary, Z.; Karavitis, M.; Apkarian, V. A. *J. Chem. Phys.* **2004**, *120*, 8144.

[3] Karavitis, M.; Zadoyan, R.; Apkarian, V. A. *J. Chem. Phys.* **2001**, *114*, 4131.

[4] Karavitis, M.; Apkarian, V. A. *J. Chem. Phys.* **2004**, *120*, 292.

[5] Kiviniemi, T.; Aumanen, J.; Myllyperkiö, P.; Apkarian, V. A.; Pettersson, M. *J. Chem. Phys.* **2005**, *123*, 064509.

[6] Apkarian, V. A.; Schwentner, N. *Chem. Rev.* **1999**, *99*, 1481.

[7] Karavitis, M.; Segale, D.; Bihary, Z.; Pettersson, M.; Apkarian, V. A. *Low Temp. Phys.* **2003**, *29*, 814–821.

[8] Gühr, M.; Schwentner, N. *J. Chem. Phys.* **2005**, *123*, 244506.

[9] Karavitis, M.; Kumada, T.; Goldschleger, I. U.; Apkarian, V. A. *Phys. Chem. Chem. Phys.* **2005**, *7*, 791.

[10] Poulin, P. R.; Nelson, K. A. *Science* **2006**, *313*, 1756.

[11] Momose, T.; Fushitani, M.; Hoshina, H. *International Reviews in Physical Chemistry* **2005**, *24*, 533.

[12] Goldschleger, I. U.; Senekerimyan, V.; Krage, M. S.; Seferyan, H.; Janda, K. C.; Apkarian, V. A. *J. Chem. Phys.* **2006**, *124*, 204507.

[13] Oxtoby, D. W. **2007**, 487.

[14] Heller, E. J. *J. Chem. Phys.* **1975**, *62*, 1544.

[15] Chapman, C. T.; Cina, J. A. *J. Chem. Phys.* **2007**, *127*, 114502.

[16] Heller, E. J. *J. Chem. Phys.* **1978**, *68*, 2066.

[17] Fushitani, M.; Bargheer, M.; Guhr, M.; Ibrahim, H.; Schwentner, N. *J. Phys. B: At. Mol. Opt. Phys.* **2008**, *41*, 074013.

APPENDIX A

NONLINEAR WAVE PACKET INTERFEROMETRY SIGNALS AND RECONSTRUCTED WAVE PACKETS FOR VARIOUS t_{43}'S

Noise-free signals and plots of target and reconstructed states for t_{43} = 0, 30, 45, 60, 75, 650, and 715 fs are presented below.

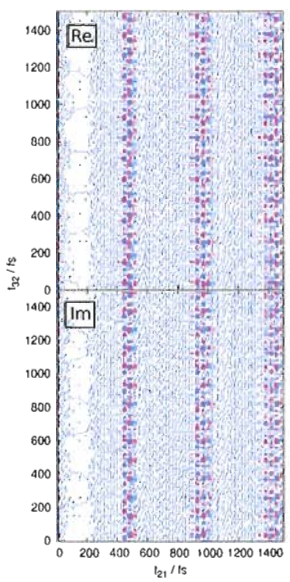

Figure A.1: Real (upper panel) and imaginary (lower panel) components of the noise-free interferogram from vibrating, nonrotating I_2 plotted as a function of interpulse delays t_{21} and t_{32} for a fixed t_{43} = 0 fs. The positive (red lines) and negative (blue lines) are separated by $1/25^{th}$ of the maximum absolute value of the signal.

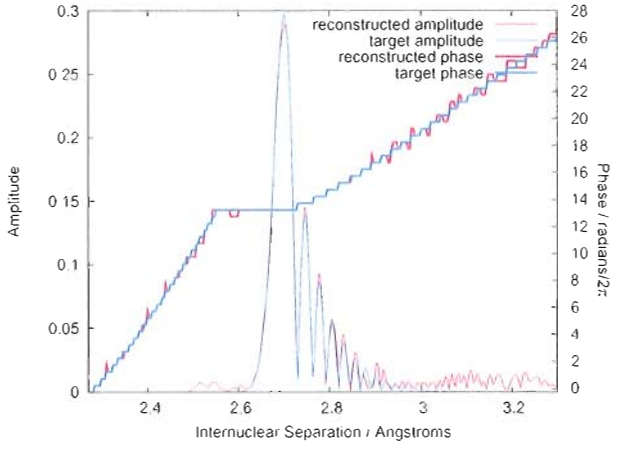

Figure A.2: The phase (right hand scale) and amplitude (left hand scale) of the target (blue lines) and reconstructed (red lines) states for $t_{43} = 0$ fs. Reconstruction is performed with a fidelity $f = 0.996942$ using an optimal tolerance 0.03787.

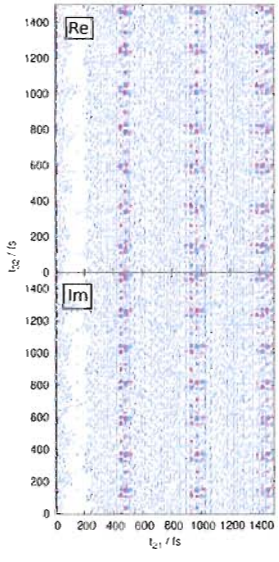

Figure A.3: Real (upper panel) and imaginary (lower panel) components of the noise-free interferogram from vibrating, nonrotating I_2 plotted as a function of interpulse delays t_{21} and t_{32} for a fixed $t_{43} = 30$ fs. The positive (red lines) and negative (blue lines) are separated by $1/25^{th}$ of the maximum absolute value of the signal.

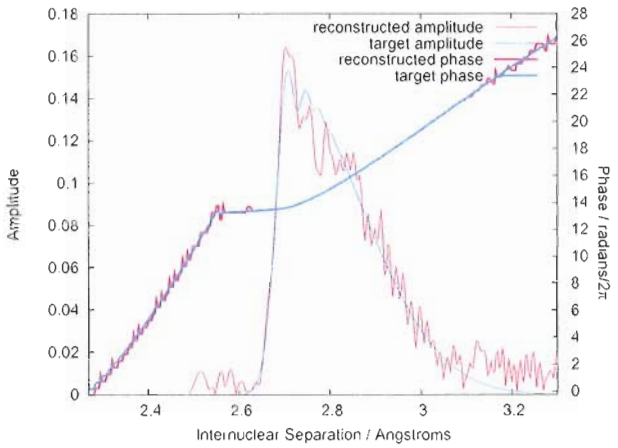

Figure A.4: The phase (right hand scale) and amplitude (left hand scale) of the target (blue lines) and reconstructed (red lines) states for $t_{43} = 30$ fs. Reconstruction is performed with a fidelity $f = 0.989948$ using an optimal tolerance 0.01691.

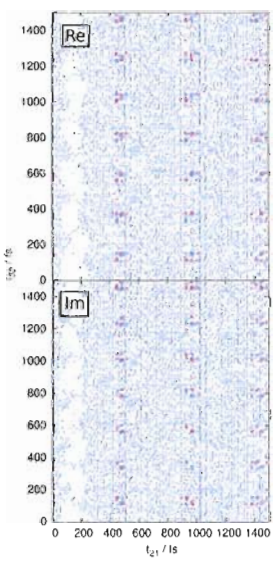

Figure A.5: Real (upper panel) and imaginary (lower panel) components of the noise-free interferogram from vibrating, nonrotating I_2 plotted as a function of interpulse delays t_{21} and t_{32} for a fixed $t_{43} = 45$ fs. The positive (red lines) and negative (blue lines) are separated by $1/25^{th}$ of the maximum absolute value of the signal.

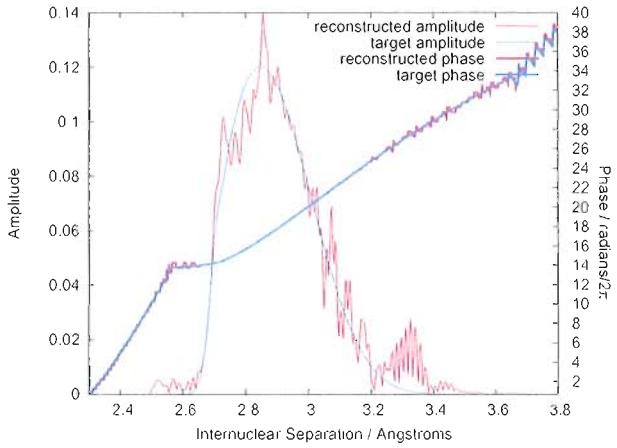

Figure A.6: The phase (right hand scale) and amplitude (left hand scale) of the target (blue lines) and reconstructed (red lines) states for $t_{43} = 45$ fs. Reconstruction is performed with a fidelity $f = 0.990238$ using an optimal tolerance 0.01713.

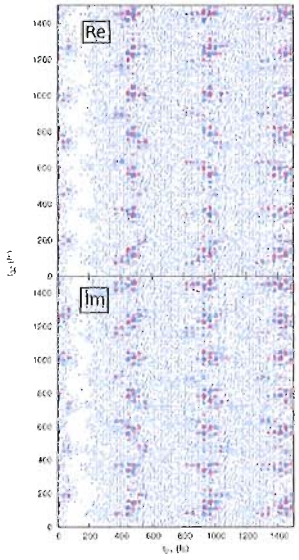

Figure A.7: Real (upper panel) and imaginary (lower panel) components of the noise-free interferogram from vibrating, nonrotating I_2 plotted as a function of interpulse delays t_{21} and t_{32} for a fixed $t_{43} = 60$ fs. The positive (red lines) and negative (blue lines) are separated by $1/25^{th}$ of the maximum absolute value of the signal. The signal scale is 1/4 of that shown for $t_{43} < 60$ fs.

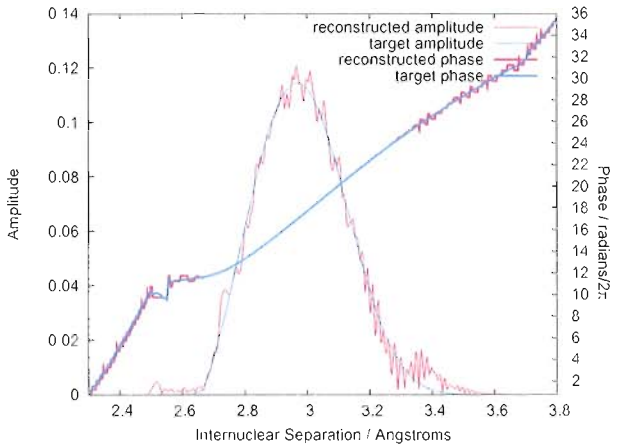

Figure A.8: The phase (right hand scale) and amplitude (left hand scale) of the target (blue lines) and reconstructed (red lines) states for $t_{43} = 60$ fs. Reconstruction is performed with a fidelity $f = 0.997217$ using an optimal tolerance 0.00957.

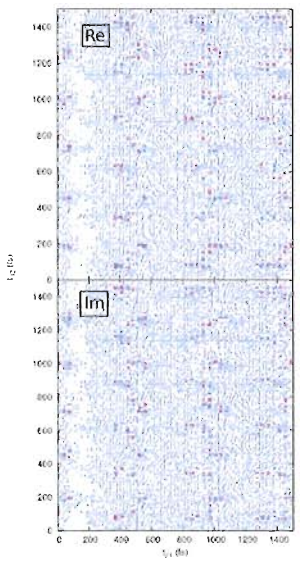

Figure A.9: Real (upper panel) and imaginary (lower panel) components of the noise-free interferogram from vibrating, nonrotating I_2 plotted as a function of interpulse delays t_{21} and t_{32} for a fixed $t_{43} = 75$ fs. The positive (red lines) and negative (blue lines) are separated by $1/25^{th}$ of the maximum absolute value of the signal. The signal scale is 1/4 of that shown for $t_{43} < 60$ fs.

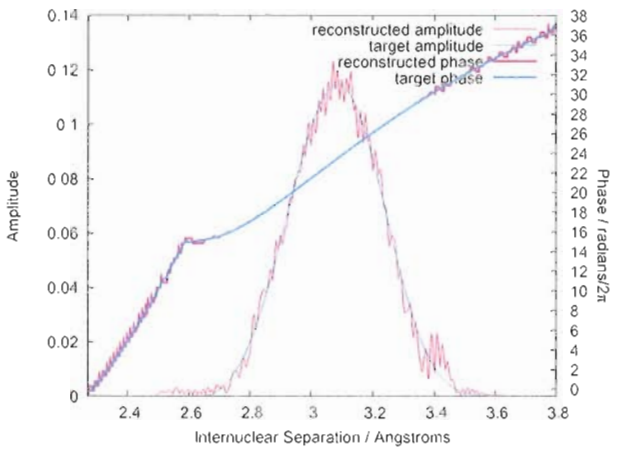

Figure A.10: The phase (right hand scale) and amplitude (left hand scale) of the target (blue lines) and reconstructed (red lines) states for $t_{43} = 75$ fs. Reconstruction is performed with a fidelity $f = 0.997217$ using an optimal tolerance 0.00957.

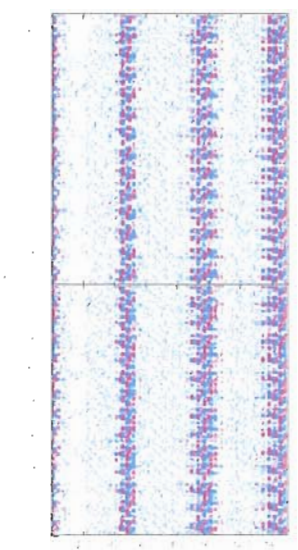

Figure A.11: Real (upper panel) and imaginary (lower panel) components of the noise-free interferogram from vibrating, nonrotating I_2 plotted as a function of interpulse delays t_{21} and t_{32} for a fixed $t_{43} = 650$ fs. The positive (red lines) and negative (blue lines) are separated by $1/25^{th}$ of the maximum absolute value of the signal. The signal scale is 1/4 of that shown for $t_{43} < 60$ fs.

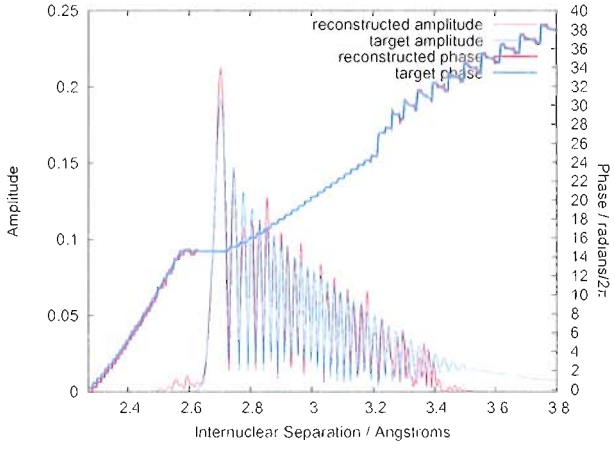

Figure A.12: The phase (right hand scale) and amplitude (left hand scale) of the target (blue lines) and reconstructed (red lines) states for $t_{43} = 650$ fs. Reconstruction is performed with a fidelity $f = 0.980823$ using an optimal tolerance 0.01345.

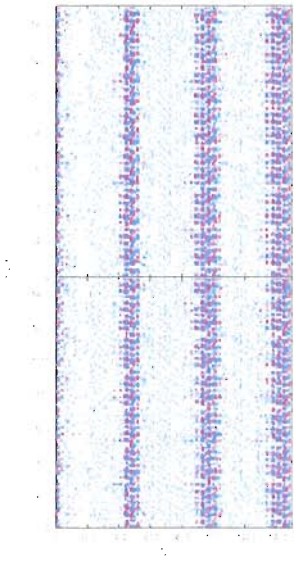

Figure A.13: Real (upper panel) and imaginary (lower panel) components of the noise-free interferogram from vibrating, nonrotating I_2 plotted as a function of interpulse delays t_{21} and t_{32} for a fixed $t_{43} = 715$ fs. The positive (red lines) and negative (blue lines) are separated by $1/25^{th}$ of the maximum absolute value of the signal. The signal scale is 1/4 of that shown for $t_{43} < 60$ fs.

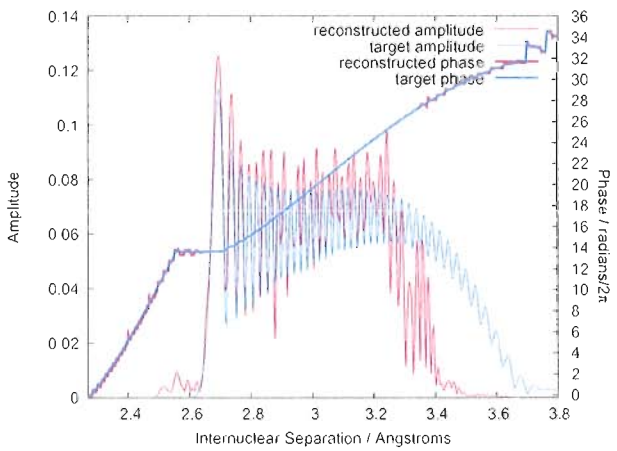

Figure A.14: The phase (right hand scale) and amplitude (left hand scale) of the target (blue lines) and reconstructed (red lines) states for $t_{43} = 715$ fs. Reconstruction is performed with a fidelity $f = 0.939553$ using a tolerance of 0.01139.

APPENDIX B

EQUATIONS OF MOTION FOR BATH WAVE-PACKET PARAMETERS IN A FIXED VIBRATIONAL BASIS

Here we give the equations of motion for the parameters determining the bath wave packets of Eqn. (3.12) in the FVB/GB theory, obtained by the procedure outlined in Ch. III Sec. B.2.b. We identify the real and imaginary parts of the complex parameters with single and double primes, respectively. All coordinate derivatives, as well as the quantities u_b, $u_{\nu\nu}$, and $u_{\nu\bar{\nu}}$, are to be evaluated at Q_ν.

$$\begin{aligned}\dot{\gamma}'_\nu = &\frac{1}{2}P_\nu^T \cdot P_\nu - \varepsilon_\nu - u_b - u_{\nu\nu} - Tr\,\{\alpha''_\nu\} + \sum_{\bar{\nu}\neq\nu} e^{-f''(\nu,\bar{\nu})}\,\{\cos f'(\nu,\bar{\nu})\,[-u_{\nu\bar{\nu}} \\ &+ u_{\nu\bar{\nu}}(Q_\nu - Q_{\bar{\nu}})^T \cdot \alpha'_{\bar{\nu}} \cdot (\alpha''_\nu)^{-1} \cdot P_\nu + \frac{1}{2}u_{\nu\bar{\nu}}(P_{\bar{\nu}} - P_\nu)^T \cdot (\alpha''_\nu)^{-1} \cdot P_\nu] \\ &+ \sin f'(\nu,\bar{\nu})\left[\frac{1}{2}(\nabla^T u_{\nu\bar{\nu}}) \cdot (\alpha''_\nu)^{-1} \cdot P_\nu - u_{\nu\bar{\nu}}(Q_\nu - Q_{\bar{\nu}})^T \cdot \alpha''_{\bar{\nu}} \cdot (\alpha''_\nu)^{-1} \cdot P_\nu\right]\}\end{aligned} \tag{B.1}$$

$$\dot{\gamma}''_\nu = Tr\,\{\alpha'_\nu\} - \sum_{\bar{\nu}\neq\nu} e^{-f''(\nu,\bar{\nu})} u_{\nu\bar{\nu}} \sin f'(\nu,\bar{\nu}) \tag{B.2}$$

$$\begin{aligned}\dot{Q}_\nu = &P_\nu + \frac{1}{2}(\alpha''_\nu)^{-1} \cdot \sum_{\bar{\nu}\neq\nu} e^{-f''(\nu,\bar{\nu})}\{\cos f'(\nu,\bar{\nu})[(2\alpha'_{\bar{\nu}} \cdot (Q_\nu - Q_{\bar{\nu}}) + P_{\bar{\nu}} - P_\nu)u_{\nu\bar{\nu}}] \\ &+ \sin f'(\nu,\bar{\nu})[\nabla u_{\nu\bar{\nu}} - 2u_{\nu\bar{\nu}}\alpha''_{\bar{\nu}} \cdot (Q_\nu - Q_{\bar{\nu}})]\}\end{aligned} \tag{B.3}$$

$$\dot{P}_\nu = -\nabla(u_b + u_{\nu\nu}) - \sum_{\bar{\nu}\neq\nu} e^{-f''(\nu,\bar{\nu})}\{\cos f'(\nu,\bar{\nu})[\nabla u_{\nu\bar{\nu}} - 2u_{\nu\bar{\nu}}\alpha''_{\bar{\nu}}\cdot(Q_\nu - Q_{\bar{\nu}})$$
$$- u_{\nu\bar{\nu}}\alpha'_\nu\cdot(\alpha''_\nu)^{-1}\cdot(2\alpha'_{\bar{\nu}}\cdot(Q_\nu - Q_{\bar{\nu}}) + P_{\bar{\nu}} - P_\nu)] - \sin f'(\nu,\bar{\nu})[u_{\nu\bar{\nu}}(2\alpha'_{\bar{\nu}}$$
$$\cdot(Q_\nu - Q_{\bar{\nu}}) + P_{\bar{\nu}} - P_\nu) - \alpha'_\nu\cdot(\alpha''_\nu)^{-1}\cdot(2u_{\nu\bar{\nu}}\alpha''_{\bar{\nu}}\cdot(Q_\nu - Q_{\bar{\nu}}) - \nabla u_{\nu\bar{\nu}})]\} \quad \text{(B.4)}$$

$$\dot{\alpha}'_\nu = -\frac{1}{2}\nabla\nabla^T(u_b + u_{\nu\nu}) - 2\alpha'_\nu\cdot\alpha'_\nu + 2\alpha''_\nu\cdot\alpha''_\nu - \sum_{\bar{\nu}\neq\nu} e^{-f''(\nu,\bar{\nu})}\{\cos f'(\nu,\bar{\nu})$$
$$\times[\nabla\nabla^T\frac{u_{\nu\bar{\nu}}}{2} + u_{\nu\bar{\nu}}(\alpha''_\nu - \alpha''_{\bar{\nu}}) - \frac{1}{2}u_{\nu\bar{\nu}}(2\alpha'_{\bar{\nu}}\cdot(Q_\nu - Q_{\bar{\nu}}) + P_{\bar{\nu}} - P_\nu)(2(Q_\nu$$
$$- Q_{\bar{\nu}})^T\cdot\alpha'_{\bar{\nu}} + P^T_{\bar{\nu}} - P^T_\nu) + 2u_{\nu\bar{\nu}}(\alpha''_{\bar{\nu}}\cdot(Q_\nu - Q_{\bar{\nu}}))((Q_\nu - Q_{\bar{\nu}})^T\cdot\alpha''_{\bar{\nu}})$$
$$- (\nabla u_{\nu\bar{\nu}})(Q_\nu - Q_{\bar{\nu}})^T\cdot\alpha''_{\bar{\nu}} - \alpha''_{\bar{\nu}}\cdot(Q_\nu - Q_{\bar{\nu}})\cdot(\nabla^T u_{\nu\bar{\nu}})] - \sin f'(\nu,\bar{\nu})$$
$$\times[u_{\nu\bar{\nu}}(\alpha'_{\bar{\nu}} - \alpha'_\nu) - u_{\nu\bar{\nu}}(\alpha''_{\bar{\nu}}\cdot(Q_\nu - Q_{\bar{\nu}}))(2(Q_\nu - Q_{\bar{\nu}})^T\cdot\alpha'_{\bar{\nu}} + P^T_{\bar{\nu}} - P^T_\nu)$$
$$- u_{\nu\bar{\nu}}(2\alpha'_{\bar{\nu}}\cdot(Q_\nu - Q_{\bar{\nu}}) + P_{\bar{\nu}} - P_\nu)((Q_\nu - Q_{\bar{\nu}})^T\cdot\alpha''_{\bar{\nu}}) + \frac{1}{2}(\nabla u_{\nu\bar{\nu}})(2(Q_\nu$$
$$- Q_{\bar{\nu}})^T\cdot\alpha'_{\bar{\nu}} + P^T_{\bar{\nu}} - P^T_\nu) + \frac{1}{2}(2\alpha'_{\bar{\nu}}\cdot(Q_\nu - Q_{\bar{\nu}}) + P_{\bar{\nu}} - P_\nu)\cdot(\nabla^T u_{\nu\bar{\nu}})]\} \quad \text{(B.5)}$$

$$\dot{\alpha}''_\nu = -2\alpha'_\nu\cdot\alpha''_\nu - 2\alpha''_\nu\cdot\alpha'_\nu - \sum_{\bar{\nu}\neq\nu} e^{-f''(\nu,\bar{\nu})}\{\cos f'(\nu,\bar{\nu})[u_{\nu\bar{\nu}}(\alpha'_{\bar{\nu}} - \alpha'_\nu)$$
$$- u_{\nu\bar{\nu}}(2\alpha'_{\bar{\nu}}\cdot(Q_\nu - Q_{\bar{\nu}}) + P_{\bar{\nu}} - P_\nu)((Q_\nu - Q_{\bar{\nu}})^T\cdot\alpha''_{\bar{\nu}}) - u_{\nu\bar{\nu}}(\alpha''_{\bar{\nu}}\cdot(Q_\nu - Q_{\bar{\nu}}))$$
$$\times(2(Q_\nu - Q_{\bar{\nu}})^T\cdot\alpha'_{\bar{\nu}} + P^T_{\bar{\nu}} - P^T_\nu) + \frac{1}{2}(\nabla u_{\nu\bar{\nu}})(2(Q_\nu - Q_{\bar{\nu}})^T\cdot\alpha'_{\bar{\nu}} + P^T_{\bar{\nu}} - P^T_\nu)$$
$$+ \frac{1}{2}(2\alpha'_{\bar{\nu}}\cdot(Q_\nu - Q_{\bar{\nu}}) + P_{\bar{\nu}} - P_\nu)(\nabla^T u_{\nu\bar{\nu}})] + \sin f'(\nu,\bar{\nu})[\frac{1}{2}\nabla\nabla^T u_{\nu\bar{\nu}}$$
$$+ u_{\nu\bar{\nu}}(\alpha''_\nu - \alpha''_{\bar{\nu}}) - \frac{1}{2}u_{\nu\bar{\nu}}(2\alpha'_{\bar{\nu}}\cdot(Q_\nu - Q_{\bar{\nu}}) + P_{\bar{\nu}} - P_\nu)(2(Q_\nu - Q_{\bar{\nu}})^T\cdot\alpha'_{\bar{\nu}} + P^T_{\bar{\nu}}$$
$$- P^T_\nu) + 2u_{\nu\bar{\nu}}(\alpha''_{\bar{\nu}}\cdot(Q_\nu - Q_{\bar{\nu}}))((Q_\nu - Q_{\bar{\nu}})^T\cdot\alpha''_{\bar{\nu}}) - (\nabla u_{\nu\bar{\nu}})(Q_\nu - Q_{\bar{\nu}})^T\cdot\alpha''_{\bar{\nu}}$$
$$- \alpha''_{\bar{\nu}}\cdot(Q_\nu - Q_{\bar{\nu}})(\nabla^T u_{\nu\bar{\nu}})]\} \quad \text{(B.6)}$$

APPENDIX C

EQUATIONS OF MOTION FOR BATH WAVE-PACKET PARAMETERS IN AN ADIBATIC VIBRATIONAL BASIS

Here we give the equations of motion for the parameters determining the bath wave packets, whose form is forced to remain Gaussian according to which

$$\langle Q \mid \varphi_\nu(t)\rangle = \exp\left[i(Q-Q_\nu)^T \cdot \alpha_\nu \cdot (Q-Q_\nu) + iP_\nu^T \cdot (Q-Q_\nu) + i\gamma_\nu\right]. \quad \text{(C.1)}$$

In the adiabatic vibrational basis the time-dependent Schrödinger equation governing the time-evolution of the bath wave packets is

$$i\frac{\partial}{\partial t}\left|\varphi_\nu(t)\right\rangle = \sum_{\bar{\nu}} \langle\nu| \left[\frac{1}{2}\left(\hat{P} + A(\hat{Q})\right)^T \cdot \left(\hat{P} + A(\hat{Q})\right) + \varepsilon_{\bar{\nu}}(\hat{Q})\right] |\bar{\nu}\rangle \left|\varphi_{\bar{\nu}}(t)\right\rangle. \quad \text{(C.2)}$$

The procedure for deriving individual parameter equations of motion is outlined in Ch. III Sec. B.3.c. The real and imaginary parts of complex quantities are denoted using single and double primes, respectively. All derivatives are taken with respect to the bath coordinates and are to be evaluated, along with the quantities ε_ν and $A_{\nu\bar{\nu}}$, at Q_ν.

$$\dot{\gamma}'_{\nu} = \frac{1}{2} P_{\nu}^{T} \cdot P_{\nu} - \varepsilon_{\nu} - Tr[\alpha''_{\nu}] - \frac{1}{2} \sum_{\bar{\nu}} e^{-f''(\nu,\bar{\nu})} \cos f'(\nu,\bar{\nu}) \{ \nabla^{T} \cdot A''_{\nu\bar{\nu}} + 2A'^{T}_{\nu\bar{\nu}}$$

$$\cdot (2\alpha'_{\bar{\nu}} \cdot (Q_{\nu} - Q_{\bar{\nu}}) + P_{\bar{\nu}}) - 4A''^{T}_{\nu\bar{\nu}} \cdot \alpha''_{\bar{\nu}} \cdot (Q_{\nu} - Q_{\bar{\nu}}) + \sum_{\bar{\bar{\nu}}} (A'^{T}_{\nu\bar{\bar{\nu}}} \cdot A_{\bar{\bar{\nu}}\bar{\nu}}' - A''^{T}_{\nu\bar{\bar{\nu}}}$$

$$\cdot A_{\bar{\bar{\nu}}\bar{\nu}}'') \} + \frac{1}{2} P_{\nu}^{T} \cdot \alpha'^{\prime-1}_{\nu} \cdot \sum_{\bar{\nu}} e^{-f''(\nu,\bar{\nu})} \cos f'(\nu,\bar{\nu}) \{ 2\alpha'_{\bar{\nu}} \cdot A''_{\nu\bar{\nu}} + 2\alpha''_{\bar{\nu}} \cdot A'_{\nu\bar{\nu}}$$

$$+ 2\alpha'_{\bar{\nu}} \cdot (Q_{\nu} - Q_{\bar{\nu}})(P_{\bar{\nu}}^{T} \cdot A'_{\nu\bar{\nu}}) - 2\alpha''_{\bar{\nu}} \cdot (Q_{\nu} - Q_{\bar{\nu}})(P_{\bar{\nu}}^{T} \cdot A''_{\nu\bar{\nu}}) + (P_{\bar{\nu}} - P_{\nu})$$

$$\times (P_{\bar{\nu}}^{T} \cdot A'_{\nu\bar{\nu}}) - 4\alpha''_{\bar{\nu}} \cdot (Q_{\nu} - Q_{\bar{\nu}})((Q_{\nu} - Q_{\bar{\nu}})^{T} \cdot \alpha'_{\bar{\nu}} \cdot A''_{\nu\bar{\nu}}) - 4\alpha''_{\bar{\nu}} \cdot (Q_{\nu} - Q_{\bar{\nu}})((Q_{\nu}$$

$$- Q_{\bar{\nu}})^{T} \cdot \alpha''_{\bar{\nu}} \cdot A'_{\nu\bar{\nu}}) + 4\alpha'_{\bar{\nu}} \cdot (Q_{\nu} - Q_{\bar{\nu}})((Q_{\nu} - Q_{\bar{\nu}})^{T} \cdot \alpha'_{\bar{\nu}} \cdot A'_{\nu\bar{\nu}}) - 4\alpha'_{\bar{\nu}} \cdot (Q_{\nu}$$

$$- Q_{\bar{\nu}})((Q_{\nu} - Q_{\bar{\nu}})^{T} \cdot \alpha''_{\bar{\nu}} \cdot A''_{\nu\bar{\nu}}) + 2(P_{\bar{\nu}} - P_{\nu})((Q_{\nu} - Q_{\bar{\nu}})^{T} \cdot \alpha'_{\bar{\nu}} \cdot A'_{\nu\bar{\nu}}) - 2(P_{\bar{\nu}}$$

$$- P_{\nu})((Q_{\nu} - Q_{\bar{\nu}})^{T} \cdot \alpha''_{\bar{\nu}} \cdot A''_{\nu\bar{\nu}}) + 2\nabla A'_{\nu\bar{\nu}} \cdot \alpha''_{\bar{\nu}} \cdot (Q_{\nu} - Q_{\bar{\nu}}) + \nabla A''_{\nu\bar{\nu}} \cdot (2\alpha'_{\bar{\nu}} \cdot (Q_{\nu}$$

$$- Q_{\bar{\nu}}) + P_{\bar{\nu}}) + \alpha'_{\bar{\nu}} \cdot (Q_{\nu} - Q_{\bar{\nu}})(\nabla^{T} \cdot A''_{\nu\bar{\nu}}) + \alpha''_{\bar{\nu}} \cdot (Q_{\nu} - Q_{\bar{\nu}})(\nabla^{T} \cdot A'_{\nu\bar{\nu}})$$

$$+ \frac{1}{2}(P_{\bar{\nu}} - P_{\nu})(\nabla^{T} \cdot A''_{\nu\bar{\nu}}) + \frac{1}{2} \sum_{\bar{\bar{\nu}}} (-2\alpha''_{\bar{\nu}} \cdot (Q_{\nu} - Q_{\bar{\nu}})(A'^{T}_{\nu\bar{\bar{\nu}}} \cdot A_{\bar{\bar{\nu}}\bar{\nu}}'') - 2\alpha''_{\bar{\nu}} \cdot (Q_{\nu}$$

$$- Q_{\bar{\nu}})(A''^{T}_{\nu\bar{\bar{\nu}}} \cdot A_{\bar{\bar{\nu}}\bar{\nu}}') + 2\alpha'_{\bar{\nu}} \cdot (Q_{\nu} - Q_{\bar{\nu}})(A'^{T}_{\nu\bar{\bar{\nu}}} \cdot A_{\bar{\bar{\nu}}\bar{\nu}}') - 2\alpha'_{\bar{\nu}} \cdot (Q_{\nu} - Q_{\bar{\nu}})(A''^{T}_{\nu\bar{\bar{\nu}}}$$

$$\cdot A_{\bar{\bar{\nu}}\bar{\nu}}'') + (P_{\bar{\nu}} - P_{\nu})(A'^{T}_{\nu\bar{\bar{\nu}}} \cdot A_{\bar{\bar{\nu}}\bar{\nu}}') - (P_{\bar{\nu}} - P_{\nu})(A''^{T}_{\nu\bar{\bar{\nu}}} \cdot A_{\bar{\bar{\nu}}\bar{\nu}}'') + (\nabla A'^{T}_{\nu\bar{\bar{\nu}}}) \cdot A_{\bar{\bar{\nu}}\bar{\nu}}''$$

$$+ (\nabla A''^{T}_{\nu\bar{\bar{\nu}}}) \cdot A_{\bar{\bar{\nu}}\bar{\nu}}' + (\nabla A''^{T}_{\bar{\bar{\nu}}\bar{\nu}}) \cdot A_{\nu\bar{\bar{\nu}}}' + (\nabla A'^{T}_{\bar{\bar{\nu}}\bar{\nu}}) \cdot A_{\nu\bar{\bar{\nu}}}'') \}$$

$$+ \frac{1}{2} \sum_{\bar{\nu}} e^{-f''(\nu,\bar{\nu})} \sin f'(\nu,\bar{\nu}) \{ -\nabla^{T} \cdot A'_{\nu\bar{\nu}} + 4A'^{T}_{\nu\bar{\nu}} \cdot \alpha''_{\bar{\nu}} \cdot (Q_{\nu} - Q_{\bar{\nu}}) + 2A''^{T}_{\nu\bar{\nu}}$$

$$\cdot (2\alpha'_{\bar{\nu}} \cdot (Q_{\nu} - Q_{\bar{\nu}}) + P_{\bar{\nu}}) + \sum_{\bar{\bar{\nu}}} (A'^{T}_{\nu\bar{\bar{\nu}}} \cdot A_{\bar{\bar{\nu}}\bar{\nu}}'' + A''^{T}_{\nu\bar{\bar{\nu}}} \cdot A_{\bar{\bar{\nu}}\bar{\nu}}') \} + \frac{1}{2} P_{\nu}^{T} \cdot \alpha'^{\prime-1}_{\nu}$$

$$\cdot \sum_{\bar{\nu}} e^{-f''(\nu,\bar{\nu})} \sin f'(\nu,\bar{\nu}) \{ 2\alpha'_{\bar{\nu}} \cdot A'_{\nu\bar{\nu}} - 2\alpha''_{\bar{\nu}} \cdot A''_{\nu\bar{\nu}} - 2\alpha''_{\bar{\nu}} \cdot (Q_{\nu} - Q_{\bar{\nu}})(P_{\bar{\nu}}^{T} \cdot A'_{\nu\bar{\nu}})$$

$$- 2\alpha'_{\bar{\nu}} \cdot (Q_{\nu} - Q_{\bar{\nu}})(P_{\bar{\nu}}^{T} \cdot A''_{\nu\bar{\nu}}) - (P_{\bar{\nu}} - P_{\nu})(P_{\bar{\nu}}^{T} \cdot A''_{\nu\bar{\nu}}) + 4\alpha''_{\bar{\nu}} \cdot (Q_{\nu} - Q_{\bar{\nu}})$$

$$\times ((Q_{\nu} - Q_{\bar{\nu}})^{T} \cdot \alpha''_{\bar{\nu}} \cdot A''_{\nu\bar{\nu}}) - 4\alpha''_{\bar{\nu}} \cdot (Q_{\nu} - Q_{\bar{\nu}})((Q_{\nu} - Q_{\bar{\nu}})^{T} \cdot \alpha'_{\bar{\nu}} \cdot A'_{\nu\bar{\nu}})$$

$$- 4\alpha'_{\bar{\nu}} \cdot (Q_{\nu} - Q_{\bar{\nu}})((Q_{\nu} - Q_{\bar{\nu}})^{T} \cdot \alpha''_{\bar{\nu}} \cdot A'_{\nu\bar{\nu}}) - 4\alpha'_{\bar{\nu}} \cdot (Q_{\nu} - Q_{\bar{\nu}})((Q_{\nu} - Q_{\bar{\nu}})^{T} \cdot \alpha'_{\bar{\nu}})$$

$$\cdot A''_{\nu\bar{\nu}} - 2(P_{\bar{\nu}} - P_{\nu})((Q_{\nu} - Q_{\bar{\nu}})^{T} \cdot \alpha'_{\bar{\nu}} \cdot A''_{\nu\bar{\nu}}) - 2(P_{\bar{\nu}} - P_{\nu})((Q_{\nu} - Q_{\bar{\nu}})^{T} \cdot \alpha''_{\bar{\nu}} \cdot A'_{\nu\bar{\nu}})$$

$$+ \frac{1}{2}(\nabla A'_{\nu\bar{\nu}}) \cdot (2\alpha'_{\bar{\nu}} \cdot (Q_{\nu} - Q_{\bar{\nu}}) + P_{\bar{\nu}}) - 2(\nabla A''_{\nu\bar{\nu}}) \cdot \alpha''_{\bar{\nu}} \cdot (Q_{\nu} - Q_{\bar{\nu}}) + \alpha'_{\bar{\nu}} \cdot (Q_{\nu}$$

$$
\begin{aligned}
&- Q_{\bar{\nu}})(\nabla^T \cdot A'_{\nu\bar{\nu}}) - \alpha''_{\bar{\nu}} \cdot (Q_\nu - Q_{\bar{\nu}})(\nabla^T \cdot A''_{\nu\bar{\nu}}) + \frac{1}{2}(P_{\bar{\nu}} - P_\nu)(\nabla^T \cdot A'_{\nu\bar{\nu}}) \\
&+ \frac{1}{2}\sum_{\bar{\bar{\nu}}}(2\alpha''_{\bar{\nu}} \cdot (Q_\nu - Q_{\bar{\nu}})({A''_{\nu\bar{\bar{\nu}}}}^T \cdot A_{\bar{\bar{\nu}}\bar{\nu}}'') - 2\alpha''_{\bar{\nu}} \cdot (Q_\nu - Q_{\bar{\nu}})({A'_{\nu\bar{\bar{\nu}}}}^T \cdot A_{\bar{\bar{\nu}}\bar{\nu}}') - 2\alpha'_{\bar{\nu}} \\
&\cdot (Q_\nu - Q_{\bar{\nu}})({A'_{\nu\bar{\bar{\nu}}}}^T \cdot A_{\bar{\bar{\nu}}\bar{\nu}}'') - 2\alpha'_{\bar{\nu}} \cdot (Q_\nu - Q_{\bar{\nu}})({A''_{\nu\bar{\bar{\nu}}}}^T \cdot A_{\bar{\bar{\nu}}\bar{\nu}}') - (P_{\bar{\nu}} - P_\nu)({A''_{\nu\bar{\bar{\nu}}}}^T \\
&\cdot A_{\bar{\bar{\nu}}\bar{\nu}}') - (P_{\bar{\nu}} - P_\nu)({A'_{\nu\bar{\bar{\nu}}}}^T \cdot A_{\bar{\bar{\nu}}\bar{\nu}}'') + (\nabla {A'_{\nu\bar{\bar{\nu}}}}^T) \cdot A_{\bar{\bar{\nu}}\bar{\nu}}' - (\nabla {A''_{\nu\bar{\bar{\nu}}}}^T) \cdot A_{\bar{\bar{\nu}}\bar{\nu}}'' + (\nabla {A'_{\bar{\bar{\nu}}\bar{\nu}}}^T) \\
&\cdot A_{\nu\bar{\bar{\nu}}}' - (\nabla {A''_{\bar{\bar{\nu}}\bar{\nu}}}^T) \cdot A_{\nu\bar{\bar{\nu}}}'')\}
\end{aligned} \tag{C.3}
$$

$$
\begin{aligned}
&\dot{\gamma}''_\nu = Tr[\alpha'_\nu] - \sum_{\bar{\nu}} e^{-f''(\nu,\bar{\nu})}[\cos f'(\nu,\bar{\nu})\{-\frac{1}{2}\nabla^T \cdot A'_{\nu\bar{\nu}} + 2{A'_{\nu\bar{\nu}}}^T \cdot \alpha''_{\bar{\nu}} \cdot (Q_\nu - Q_{\bar{\nu}}) \\
&+ {A''_{\nu\bar{\nu}}}^T \cdot (2\alpha'_{\bar{\nu}} \cdot (Q_\nu - Q_{\bar{\nu}}) + P_{\bar{\nu}}) + \frac{1}{2}\sum_{\bar{\bar{\nu}}}({A'_{\nu\bar{\bar{\nu}}}}^T \cdot A_{\bar{\bar{\nu}}\bar{\nu}}'' + {A''_{\nu\bar{\bar{\nu}}}}^T \cdot A_{\bar{\bar{\nu}}\bar{\nu}}')\} \\
&+ \sin f'(\nu,\bar{\nu})\{\frac{1}{2}\nabla^T \cdot A''_{\nu\bar{\nu}} + A'_{\nu\bar{\nu}} \cdot (2\alpha'_{\bar{\nu}} \cdot (Q_\nu - Q_{\bar{\nu}}) + P_{\bar{\nu}}) - 2A''_{\nu\bar{\nu}} \cdot \alpha''_{\bar{\nu}} \\
&\cdot (Q_\nu - Q_{\bar{\nu}}) + \frac{1}{2}\sum_{\bar{\bar{\nu}}}({A'_{\nu\bar{\bar{\nu}}}}^T \cdot A_{\bar{\bar{\nu}}\bar{\nu}}' - {A''_{\nu\bar{\bar{\nu}}}}^T \cdot A_{\bar{\bar{\nu}}\bar{\nu}}'')\}]
\end{aligned} \tag{C.4}
$$

$$
\begin{aligned}
&\dot{Q}_\nu = P_\nu + \frac{1}{2}(\alpha''_\nu)^{-1} \cdot \sum_{\bar{\nu}} e^{-f''(\nu,\bar{\nu})}[\cos f'(\nu,\bar{\nu})\{2\alpha'_{\bar{\nu}} \cdot A''_{\nu\bar{\nu}} + 2\alpha''_{\bar{\nu}} \cdot A'_{\nu\bar{\nu}} \\
&+ 2\alpha'_{\bar{\nu}} \cdot (Q_\nu - Q_{\bar{\nu}})(P^T_{\bar{\nu}} \cdot A'_{\nu\bar{\nu}}) - 2\alpha''_{\bar{\nu}} \cdot (Q_\nu - Q_{\bar{\nu}})(P^T_{\bar{\nu}} \cdot A''_{\nu\bar{\nu}}) + (P_{\bar{\nu}} - P_\nu) \\
&\times (P^T_{\bar{\nu}} \cdot A'_{\nu\bar{\nu}}) - 4\alpha''_{\bar{\nu}} \cdot (Q_\nu - Q_{\bar{\nu}})((Q_\nu - Q_{\bar{\nu}})^T \cdot \alpha'_{\bar{\nu}} \cdot A''_{\nu\bar{\nu}}) - 4\alpha''_{\bar{\nu}} \cdot (Q_\nu - Q_{\bar{\nu}})((Q_\nu \\
&- Q_{\bar{\nu}})^T \cdot \alpha''_{\bar{\nu}} \cdot A'_{\nu\bar{\nu}}) + 4\alpha'_{\bar{\nu}} \cdot (Q_\nu - Q_{\bar{\nu}})((Q_\nu - Q_{\bar{\nu}})^T \cdot \alpha'_{\bar{\nu}} \cdot A'_{\nu\bar{\nu}}) - 4\alpha'_{\bar{\nu}} \cdot (Q_\nu \\
&- Q_{\bar{\nu}})((Q_\nu - Q_{\bar{\nu}})^T \cdot \alpha''_{\bar{\nu}} \cdot A''_{\nu\bar{\nu}}) + 2(P_{\bar{\nu}} - P_\nu)((Q_\nu - Q_{\bar{\nu}})^T \cdot \alpha'_{\bar{\nu}} \cdot A'_{\nu\bar{\nu}}) - 2(P_{\bar{\nu}} \\
&- P_\nu)((Q_\nu - Q_{\bar{\nu}})^T \cdot \alpha''_{\bar{\nu}} \cdot A''_{\nu\bar{\nu}}) + 2\nabla A'_{\nu\bar{\nu}} \cdot \alpha''_{\bar{\nu}} \cdot (Q_\nu - Q_{\bar{\nu}}) + \nabla A''_{\nu\bar{\nu}} \cdot (2\alpha'_{\bar{\nu}} \cdot (Q_\nu \\
&- Q_{\bar{\nu}}) + P_{\bar{\nu}}) + \alpha'_{\bar{\nu}} \cdot (Q_\nu - Q_{\bar{\nu}})(\nabla^T \cdot A''_{\nu\bar{\nu}}) + \alpha''_{\bar{\nu}} \cdot (Q_\nu - Q_{\bar{\nu}})(\nabla^T \cdot A'_{\nu\bar{\nu}}) \\
&+ \frac{1}{2}(P_{\bar{\nu}} - P_\nu)(\nabla^T \cdot A''_{\nu\bar{\nu}}) + \frac{1}{2}\sum_{\bar{\bar{\nu}}}(-2\alpha''_{\bar{\nu}} \cdot (Q_\nu - Q_{\bar{\nu}})({A'_{\nu\bar{\bar{\nu}}}}^T \cdot A_{\bar{\bar{\nu}}\bar{\nu}}'') - 2\alpha''_{\bar{\nu}} \cdot (Q_\nu \\
&- Q_{\bar{\nu}})({A''_{\nu\bar{\bar{\nu}}}}^T \cdot A_{\bar{\bar{\nu}}\bar{\nu}}') + 2\alpha'_{\bar{\nu}} \cdot (Q_\nu - Q_{\bar{\nu}})({A'_{\nu\bar{\bar{\nu}}}}^T \cdot A_{\bar{\bar{\nu}}\bar{\nu}}') - 2\alpha'_{\bar{\nu}} \cdot (Q_\nu - Q_{\bar{\nu}})({A''_{\nu\bar{\bar{\nu}}}}^T
\end{aligned}
$$

$$\cdot A_{\bar{\nu}\bar{\nu}}{}'') + (P_{\bar{\nu}} - P_{\nu})(A'_{\nu\bar{\nu}}{}^{T} \cdot A_{\bar{\nu}\bar{\nu}}{}') - (P_{\bar{\nu}} - P_{\nu})(A''_{\nu\bar{\nu}}{}^{T} \cdot A_{\bar{\nu}\bar{\nu}}{}'') + (\nabla A'_{\nu\bar{\nu}}{}^{T}) \cdot A_{\bar{\nu}\bar{\nu}}{}''$$

$$+ (\nabla A''_{\nu\bar{\nu}}{}^{T}) \cdot A_{\bar{\nu}\bar{\nu}}{}' + (\nabla A''_{\bar{\nu}\bar{\nu}}{}^{T}) \cdot A_{\nu\bar{\nu}}{}' + (\nabla A'_{\bar{\nu}\bar{\nu}}{}^{T}) \cdot A_{\nu\bar{\nu}}{}'')\}$$

$$+ \sin f'(\nu.\bar{\nu})\{2\alpha'_{\bar{\nu}} \cdot A'_{\nu\bar{\nu}} - 2\alpha''_{\bar{\nu}} \cdot A''_{\nu\bar{\nu}} - 2\alpha''_{\bar{\nu}} \cdot (Q_{\nu} - Q_{\bar{\nu}})(P^{T}_{\bar{\nu}} \cdot A'_{\nu\bar{\nu}})$$

$$- 2\alpha'_{\bar{\nu}} \cdot (Q_{\nu} - Q_{\bar{\nu}})(P^{T}_{\bar{\nu}} \cdot A''_{\nu\bar{\nu}}) - (P_{\bar{\nu}} - P_{\nu})(P^{T}_{\bar{\nu}} \cdot A''_{\nu\bar{\nu}}) + 4\alpha''_{\bar{\nu}} \cdot (Q_{\nu} - Q_{\bar{\nu}})$$

$$\times ((Q_{\nu} - Q_{\bar{\nu}})^{T} \cdot \alpha''_{\bar{\nu}} \cdot A''_{\nu\bar{\nu}}) - 4\alpha''_{\bar{\nu}} \cdot (Q_{\nu} - Q_{\bar{\nu}})((Q_{\nu} - Q_{\bar{\nu}})^{T} \cdot \alpha'_{\bar{\nu}} \cdot A'_{\nu\bar{\nu}})$$

$$- 4\alpha'_{\bar{\nu}} \cdot (Q_{\nu} - Q_{\bar{\nu}})((Q_{\nu} - Q_{\bar{\nu}})^{T} \cdot \alpha''_{\bar{\nu}} \cdot A'_{\nu\bar{\nu}}) - 4\alpha'_{\bar{\nu}} \cdot (Q_{\nu} - Q_{\bar{\nu}})((Q_{\nu} - Q_{\bar{\nu}})^{T} \cdot \alpha'_{\bar{\nu}})$$

$$\cdot A''_{\nu\bar{\nu}} - 2(P_{\bar{\nu}} - P_{\nu})((Q_{\nu} - Q_{\bar{\nu}})^{T} \cdot \alpha'_{\bar{\nu}} \cdot A''_{\nu\bar{\nu}}) - 2(P_{\bar{\nu}} - P_{\nu})((Q_{\nu} - Q_{\bar{\nu}})^{T} \cdot \alpha''_{\bar{\nu}} \cdot A'_{\nu\bar{\nu}})$$

$$+ \frac{1}{2}(\nabla A'_{\nu\bar{\nu}}) \cdot (2\alpha'_{\bar{\nu}} \cdot (Q_{\nu} - Q_{\bar{\nu}}) + P_{\bar{\nu}}) - 2(\nabla A''_{\nu\bar{\nu}}) \cdot \alpha''_{\bar{\nu}} \cdot (Q_{\nu} - Q_{\bar{\nu}}) + \alpha'_{\bar{\nu}} \cdot (Q_{\nu}$$

$$- Q_{\bar{\nu}})(\nabla^{T} \cdot A'_{\nu\bar{\nu}}) - \alpha''_{\bar{\nu}} \cdot (Q_{\nu} - Q_{\bar{\nu}})(\nabla^{T} \cdot A''_{\nu\bar{\nu}}) + \frac{1}{2}(P_{\bar{\nu}} - P_{\nu})(\nabla^{T} \cdot A'_{\nu\bar{\nu}})$$

$$+ \frac{1}{2}\sum_{\bar{\bar{\nu}}}(2\alpha''_{\bar{\nu}} \cdot (Q_{\nu} - Q_{\bar{\nu}})(A''_{\nu\bar{\bar{\nu}}}{}^{T} \cdot A_{\bar{\bar{\nu}}\bar{\nu}}{}'') - 2\alpha''_{\bar{\nu}} \cdot (Q_{\nu} - Q_{\bar{\nu}})(A'_{\nu\bar{\bar{\nu}}}{}^{T} \cdot A_{\bar{\bar{\nu}}\bar{\nu}}{}') - 2\alpha'_{\bar{\nu}}$$

$$\cdot (Q_{\nu} - Q_{\bar{\nu}})(A'_{\nu\bar{\bar{\nu}}}{}^{T} \cdot A_{\bar{\bar{\nu}}\bar{\nu}}{}'') - 2\alpha'_{\bar{\nu}} \cdot (Q_{\nu} - Q_{\bar{\nu}})(A''_{\nu\bar{\bar{\nu}}}{}^{T} \cdot A_{\bar{\bar{\nu}}\bar{\nu}}{}') - (P_{\bar{\nu}} - P_{\nu})(A''_{\nu\bar{\bar{\nu}}}{}^{T}$$

$$\cdot A_{\bar{\bar{\nu}}\bar{\nu}}{}') - (P_{\bar{\nu}} - P_{\nu})(A'_{\nu\bar{\bar{\nu}}}{}^{T} \cdot A_{\bar{\bar{\nu}}\bar{\nu}}{}'') + (\nabla A'_{\nu\bar{\bar{\nu}}}{}^{T}) \cdot A_{\bar{\bar{\nu}}\bar{\nu}}{}' - (\nabla A''_{\nu\bar{\bar{\nu}}}{}^{T}) \cdot A_{\bar{\bar{\nu}}\bar{\nu}}{}'' + (\nabla A'_{\bar{\bar{\nu}}\bar{\nu}}{}^{T})$$

$$\cdot A_{\nu\bar{\bar{\nu}}}{}' - (\nabla A''_{\bar{\bar{\nu}}\bar{\nu}}{}^{T}) \cdot A_{\nu\bar{\bar{\nu}}}{}'')\}] \tag{C.5}$$

$$\dot{P}_{\nu} = -\nabla\varepsilon_{\nu} - \sum_{\bar{\nu}} e^{-f''(\nu,\bar{\nu})} \cos f'(\nu,\bar{\nu})\{2\alpha'_{\bar{\nu}} \cdot A'_{\nu\bar{\nu}} - 2\alpha''_{\bar{\nu}} \cdot A''_{\nu\bar{\nu}} - 2\alpha''_{\bar{\nu}} \cdot (Q_{\nu} - Q_{\bar{\nu}})$$

$$\cdot (P^{T}_{\bar{\nu}} \cdot A'_{\nu\bar{\nu}}) - 2\alpha'_{\bar{\nu}} \cdot (Q_{\nu} - Q_{\bar{\nu}})(P^{T}_{\bar{\nu}} \cdot A''_{\nu\bar{\nu}}) - (P_{\bar{\nu}} - P_{\nu})(P^{T}_{\bar{\nu}} \cdot A''_{\nu\bar{\nu}}) + 4\alpha''_{\bar{\nu}} \cdot (Q_{\nu}$$

$$- Q_{\bar{\nu}})((Q_{\nu} - Q_{\bar{\nu}})^{T} \cdot \alpha''_{\bar{\nu}} \cdot A''_{\nu\bar{\nu}}) - 4\alpha''_{\bar{\nu}} \cdot (Q_{\nu} - Q_{\bar{\nu}})((Q_{\nu} - Q_{\bar{\nu}})^{T} \cdot \alpha'_{\bar{\nu}} \cdot A'_{\nu\bar{\nu}})$$

$$- 4\alpha'_{\bar{\nu}} \cdot (Q_{\nu} - Q_{\bar{\nu}})((Q_{\nu} - Q_{\bar{\nu}})^{T} \cdot \alpha''_{\bar{\nu}} \cdot A'_{\nu\bar{\nu}}) - 4\alpha'_{\bar{\nu}} \cdot (Q_{\nu} - Q_{\bar{\nu}})((Q_{\nu} - Q_{\bar{\nu}})^{T} \cdot \alpha'_{\bar{\nu}}$$

$$\cdot A''_{\nu\bar{\nu}}) - 2(P_{\bar{\nu}} - P_{\nu})((Q_{\nu} - Q_{\bar{\nu}})^{T} \cdot \alpha'_{\bar{\nu}} \cdot A''_{\nu\bar{\nu}}) - 2(P_{\bar{\nu}} - P_{\nu})((Q_{\nu} - Q_{\bar{\nu}})^{T} \cdot \alpha''_{\bar{\nu}}$$

$$\cdot A'_{\nu\bar{\nu}}) + (\nabla A'_{\nu\bar{\nu}}) \cdot (2\alpha'_{\bar{\nu}} \cdot (Q_{\nu} - Q_{\bar{\nu}}) + P_{\bar{\nu}}) - 2(\nabla A''_{\nu\bar{\nu}}) \cdot \alpha''_{\bar{\nu}} \cdot (Q_{\nu} - Q_{\bar{\nu}}) + \alpha'_{\bar{\nu}}$$

$$\cdot (Q_{\nu} - Q_{\bar{\nu}})(\nabla^{T} \cdot A'_{\nu\bar{\nu}}) - \alpha''_{\bar{\nu}} \cdot (Q_{\nu} - Q_{\bar{\nu}})(\nabla^{T} \cdot A''_{\nu\bar{\nu}}) + \frac{1}{2}(P_{\bar{\nu}} - P_{\nu})(\nabla^{T} \cdot A'_{\nu\bar{\nu}})$$

$$+ \frac{1}{2}\sum_{\bar{\bar{\nu}}}(2\alpha''_{\bar{\nu}} \cdot (Q_{\nu} - Q_{\bar{\nu}})(A''_{\nu\bar{\bar{\nu}}}{}^{T} \cdot A_{\bar{\bar{\nu}}\bar{\nu}}{}'') - 2\alpha''_{\bar{\nu}} \cdot (Q_{\nu} - Q_{\bar{\nu}})(A'_{\nu\bar{\bar{\nu}}}{}^{T} \cdot A_{\bar{\bar{\nu}}\bar{\nu}}{}') - 2\alpha'_{\bar{\nu}}$$

$$\cdot (Q_\nu - Q_{\bar\nu})({A'_{\nu\bar\nu}}^T \cdot A_{\bar\nu\bar\nu}'') - 2\alpha'_{\bar\nu} \cdot (Q_\nu - Q_{\bar\nu})({A''_{\nu\bar\nu}}^T \cdot A_{\bar\nu\bar\nu}') - (P_{\bar\nu} - P_\nu)({A''_{\nu\bar\nu}}^T \cdot A_{\bar\nu\bar\nu}')$$

$$- (P_{\bar\nu} - P_\nu)({A'_{\nu\bar\nu}}^T \cdot A_{\bar\nu\bar\nu}'') + (\nabla {A'_{\nu\bar\nu}}^T) \cdot A_{\bar\nu\bar\nu}' - (\nabla {A''_{\nu\bar\nu}}^T) \cdot A_{\bar\nu\bar\nu}'' + (\nabla {A'_{\bar\nu\bar\nu}}^T) \cdot A_{\nu\bar\nu}'$$

$$- (\nabla {A''_{\bar\nu\bar\nu}}^T) \cdot A_{\nu\bar\nu}'')\} + \alpha'_\nu \cdot {\alpha'_\nu}'^{-1} \cdot \sum_{\bar\nu} e^{-f''(\nu,\bar\nu)} \cos f'(\nu.\bar\nu)\{2\alpha'_{\bar\nu} \cdot A''_{\nu\bar\nu} + 2\alpha''_{\bar\nu}$$

$$\cdot A'_{\nu\bar\nu} + 2\alpha'_{\bar\nu} \cdot (Q_\nu - Q_{\bar\nu})(P_{\bar\nu}^T \cdot A'_{\nu\bar\nu}) - 2\alpha''_{\bar\nu} \cdot (Q_\nu - Q_{\bar\nu})(P_{\bar\nu}^T \cdot A''_{\nu\bar\nu}) + (P_{\bar\nu} - P_\nu)$$

$$\times (P_{\bar\nu}^T \cdot A'_{\nu\bar\nu}) - 4\alpha''_{\bar\nu} \cdot (Q_\nu - Q_{\bar\nu})((Q_\nu - Q_{\bar\nu})^T \cdot \alpha'_{\bar\nu} \cdot A''_{\nu\bar\nu}) - 4\alpha''_{\bar\nu} \cdot (Q_\nu - Q_{\bar\nu})$$

$$\times ((Q_\nu - Q_{\bar\nu})^T \cdot \alpha''_{\bar\nu} \cdot A'_{\nu\bar\nu}) + 4\alpha'_{\bar\nu} \cdot (Q_\nu - Q_{\bar\nu})((Q_\nu - Q_{\bar\nu})^T \cdot \alpha'_{\bar\nu} \cdot A'_{\nu\bar\nu}) - 4\alpha'_{\bar\nu}$$

$$\cdot (Q_\nu - Q_{\bar\nu})((Q_\nu - Q_{\bar\nu})^T \cdot \alpha''_{\bar\nu} \cdot A''_{\nu\bar\nu}) + 2(P_{\bar\nu} - P_\nu)((Q_\nu - Q_{\bar\nu})^T \cdot \alpha'_{\bar\nu} \cdot A'_{\nu\bar\nu}) - 2(P_{\bar\nu}$$

$$- P_\nu)((Q_\nu - Q_{\bar\nu})^T \cdot \alpha''_{\bar\nu} \cdot A''_{\nu\bar\nu}) + 2\nabla A'_{\nu\bar\nu} \cdot \alpha''_{\bar\nu} \cdot (Q_\nu - Q_{\bar\nu}) + \nabla A''_{\nu\bar\nu} \cdot (2\alpha'_{\bar\nu} \cdot (Q_\nu$$

$$- Q_{\bar\nu}) + P_{\bar\nu}) + \alpha'_{\bar\nu} \cdot (Q_\nu - Q_{\bar\nu})(\nabla^T \cdot A''_{\nu\bar\nu}) + \alpha''_{\bar\nu} \cdot (Q_\nu - Q_{\bar\nu})(\nabla^T \cdot A'_{\nu\bar\nu})$$

$$+ \frac{1}{2}(P_{\bar\nu} - P_\nu)(\nabla^T \cdot A''_{\nu\bar\nu}) + \frac{1}{2}\sum_{\bar{\bar\nu}}(-2\alpha''_{\bar\nu} \cdot (Q_\nu - Q_{\bar\nu})({A'_{\nu\bar{\bar\nu}}}^T \cdot A_{\bar{\bar\nu}\bar\nu}'') - 2\alpha''_{\bar\nu} \cdot (Q_\nu$$

$$- Q_{\bar\nu})({A''_{\nu\bar{\bar\nu}}}^T \cdot A_{\bar{\bar\nu}\bar\nu}') + 2\alpha'_{\bar\nu} \cdot (Q_\nu - Q_{\bar\nu})({A'_{\nu\bar{\bar\nu}}}^T \cdot A_{\bar{\bar\nu}\bar\nu}') - 2\alpha'_{\bar\nu} \cdot (Q_\nu - Q_{\bar\nu})({A''_{\nu\bar{\bar\nu}}}^T$$

$$\cdot A_{\bar{\bar\nu}\bar\nu}'') + (P_{\bar\nu} - P_\nu)({A'_{\nu\bar{\bar\nu}}}^T \cdot A_{\bar{\bar\nu}\bar\nu}') - (P_{\bar\nu} - P_\nu)({A''_{\nu\bar{\bar\nu}}}^T \cdot A_{\bar{\bar\nu}\bar\nu}'') + (\nabla {A'_{\nu\bar{\bar\nu}}}^T) \cdot A_{\bar{\bar\nu}\bar\nu}''$$

$$+ (\nabla {A''_{\nu\bar{\bar\nu}}}^T) \cdot A_{\bar{\bar\nu}\bar\nu}' + (\nabla {A''_{\bar{\bar\nu}\bar\nu}}^T) \cdot A_{\nu\bar{\bar\nu}}' + (\nabla {A'_{\bar{\bar\nu}\bar\nu}}^T) \cdot A_{\nu\bar{\bar\nu}}'')\} + \sum_{\bar\nu} e^{-f''(\nu,\bar\nu)} \sin f'(\nu.\bar\nu)$$

$$\times \{2\alpha'_{\bar\nu} \cdot A''_{\nu\bar\nu} + 2\alpha''_{\bar\nu} \cdot A'_{\nu\bar\nu} + 2\alpha'_{\bar\nu} \cdot (Q_\nu - Q_{\bar\nu})(P_{\bar\nu}^T \cdot A'_{\nu\bar\nu}) - 2\alpha''_{\bar\nu} \cdot (Q_\nu - Q_{\bar\nu})$$

$$\times (P_{\bar\nu}^T \cdot A''_{\nu\bar\nu}) + (P_{\bar\nu} - P_\nu)(P_{\bar\nu}^T \cdot A'_{\nu\bar\nu}) - 4\alpha''_{\bar\nu} \cdot (Q_\nu - Q_{\bar\nu})((Q_\nu - Q_{\bar\nu})^T \cdot \alpha'_{\bar\nu} \cdot A''_{\nu\bar\nu})$$

$$- 4\alpha''_{\bar\nu} \cdot (Q_\nu - Q_{\bar\nu})((Q_\nu - Q_{\bar\nu})^T \cdot \alpha''_{\bar\nu} \cdot A'_{\nu\bar\nu}) + 4\alpha'_{\bar\nu} \cdot (Q_\nu - Q_{\bar\nu})((Q_\nu - Q_{\bar\nu})^T$$

$$\cdot \alpha'_{\bar\nu} \cdot A'_{\nu\bar\nu}) - 4\alpha'_{\bar\nu} \cdot (Q_\nu - Q_{\bar\nu})((Q_\nu - Q_{\bar\nu})^T \cdot \alpha''_{\bar\nu} \cdot A''_{\nu\bar\nu}) + 2(P_{\bar\nu} - P_\nu)((Q_\nu - Q_{\bar\nu})^T$$

$$\cdot \alpha'_{\bar\nu} \cdot A'_{\nu\bar\nu}) - 2(P_{\bar\nu} - P_\nu)((Q_\nu - Q_{\bar\nu})^T \cdot \alpha''_{\bar\nu} \cdot A''_{\nu\bar\nu}) + 2\nabla A'_{\nu\bar\nu} \cdot \alpha''_{\bar\nu} \cdot (Q_\nu - Q_{\bar\nu})$$

$$+ \nabla A''_{\nu\bar\nu} \cdot (2\alpha'_{\bar\nu} \cdot (Q_\nu - Q_{\bar\nu}) + P_{\bar\nu}) + \alpha'_{\bar\nu} \cdot (Q_\nu - Q_{\bar\nu})(\nabla^T \cdot A''_{\nu\bar\nu})$$

$$+ \alpha''_{\bar\nu} \cdot (Q_\nu - Q_{\bar\nu})(\nabla^T \cdot A'_{\nu\bar\nu}) + \frac{1}{2}(P_{\bar\nu} - P_\nu)(\nabla^T \cdot A''_{\nu\bar\nu}) + \frac{1}{2}\sum_{\bar{\bar\nu}}(-2\alpha''_{\bar\nu} \cdot (Q_\nu$$

$$- Q_{\bar\nu})({A'_{\nu\bar{\bar\nu}}}^T \cdot A_{\bar{\bar\nu}\bar\nu}'') - 2\alpha''_{\bar\nu} \cdot (Q_\nu - Q_{\bar\nu})({A''_{\nu\bar{\bar\nu}}}^T \cdot A_{\bar{\bar\nu}\bar\nu}') + 2\alpha'_{\bar\nu} \cdot (Q_\nu - Q_{\bar\nu})({A'_{\nu\bar{\bar\nu}}}^T$$

$$\cdot A_{\bar{\bar\nu}\bar\nu}') - 2\alpha'_{\bar\nu} \cdot (Q_\nu - Q_{\bar\nu})({A''_{\nu\bar{\bar\nu}}}^T \cdot A_{\bar{\bar\nu}\bar\nu}'') + (P_{\bar\nu} - P_\nu)({A'_{\nu\bar{\bar\nu}}}^T \cdot A_{\bar{\bar\nu}\bar\nu}') - (P_{\bar\nu} - P_\nu)$$

$$\times ({A''_{\nu\bar{\bar\nu}}}^T \cdot A_{\bar{\bar\nu}\bar\nu}'') + (\nabla {A'_{\nu\bar{\bar\nu}}}^T) \cdot A_{\bar{\bar\nu}\bar\nu}'' + (\nabla {A''_{\nu\bar{\bar\nu}}}^T) \cdot A_{\bar{\bar\nu}\bar\nu}' + (\nabla {A''_{\bar{\bar\nu}\bar\nu}}^T) \cdot A_{\nu\bar{\bar\nu}}' + (\nabla {A'_{\bar{\bar\nu}\bar\nu}}^T)$$

$$
\begin{aligned}
&- \alpha'_\nu \cdot {\alpha'_\nu}^{\prime -1} \cdot A_{\nu\bar{\nu}}{}'')\} \\
&\cdot \sum_{\bar{\nu}} e^{-f''(\nu,\bar{\nu})} \sin f'(\nu,\bar{\nu})\{2\alpha'_{\bar{\nu}} \cdot A'_{\nu\bar{\nu}} - 2\alpha''_{\bar{\nu}} \cdot A''_{\nu\bar{\nu}} - 2\alpha''_{\bar{\nu}} \cdot (Q_\nu - Q_{\bar{\nu}}) \\
&\times (P_{\bar{\nu}}^T \cdot A'_{\nu\bar{\nu}}) - 2\alpha'_{\bar{\nu}} \cdot (Q_\nu - Q_{\bar{\nu}})(P_{\bar{\nu}}^T \cdot A''_{\nu\bar{\nu}}) - (P_{\bar{\nu}} - P_\nu)(P_{\bar{\nu}}^T \cdot A''_{\nu\bar{\nu}}) + 4\alpha''_{\bar{\nu}} \cdot (Q_\nu \\
&- Q_{\bar{\nu}})((Q_\nu - Q_{\bar{\nu}})^T \cdot \alpha''_{\bar{\nu}} \cdot A''_{\nu\bar{\nu}}) - 4\alpha''_{\bar{\nu}} \cdot (Q_\nu - Q_{\bar{\nu}})((Q_\nu - Q_{\bar{\nu}})^T \cdot \alpha'_{\bar{\nu}} \cdot A'_{\nu\bar{\nu}}) \\
&- 4\alpha'_{\bar{\nu}} \cdot (Q_\nu - Q_{\bar{\nu}})((Q_\nu - Q_{\bar{\nu}})^T \cdot \alpha''_{\bar{\nu}} \cdot A'_{\nu\bar{\nu}}) - 4\alpha'_{\bar{\nu}} \cdot (Q_\nu - Q_{\bar{\nu}})((Q_\nu - Q_{\bar{\nu}})^T \cdot \alpha'_{\bar{\nu}}) \\
&\cdot A''_{\nu\bar{\nu}} - 2(P_{\bar{\nu}} - P_\nu)((Q_\nu - Q_{\bar{\nu}})^T \cdot \alpha'_{\bar{\nu}} \cdot A''_{\nu\bar{\nu}}) - 2(P_{\bar{\nu}} - P_\nu)((Q_\nu - Q_{\bar{\nu}})^T \cdot \alpha''_{\bar{\nu}} \\
&\cdot A'_{\nu\bar{\nu}}) + \frac{1}{2}(\nabla A'_{\nu\bar{\nu}}) \cdot (2\alpha'_{\bar{\nu}} \cdot (Q_\nu - Q_{\bar{\nu}}) + P_{\bar{\nu}}) - 2(\nabla A''_{\nu\bar{\nu}}) \cdot \alpha''_{\bar{\nu}} \cdot (Q_\nu - Q_{\bar{\nu}}) + \alpha'_{\bar{\nu}} \\
&\cdot (Q_\nu - Q_{\bar{\nu}})(\nabla^T \cdot A'_{\nu\bar{\nu}}) - \alpha''_{\bar{\nu}} \cdot (Q_\nu - Q_{\bar{\nu}})(\nabla^T \cdot A''_{\nu\bar{\nu}}) + \frac{1}{2}(P_{\bar{\nu}} - P_\nu)(\nabla^T \cdot A'_{\nu\bar{\nu}}) \\
&+ \frac{1}{2}\sum_{\bar{\bar{\nu}}}(2\alpha''_{\bar{\nu}} \cdot (Q_\nu - Q_{\bar{\nu}})({A''_{\nu\bar{\bar{\nu}}}}^T \cdot A_{\bar{\bar{\nu}}\bar{\nu}}'') - 2\alpha''_{\bar{\nu}} \cdot (Q_\nu - Q_{\bar{\nu}})({A'_{\nu\bar{\bar{\nu}}}}^T \cdot A_{\bar{\bar{\nu}}\bar{\nu}}') - 2\alpha'_{\bar{\nu}} \\
&\cdot (Q_\nu - Q_{\bar{\nu}})({A'_{\nu\bar{\bar{\nu}}}}^T \cdot A_{\bar{\bar{\nu}}\bar{\nu}}'') - 2\alpha'_{\bar{\nu}} \cdot (Q_\nu - Q_{\bar{\nu}})({A''_{\nu\bar{\bar{\nu}}}}^T \cdot A_{\bar{\bar{\nu}}\bar{\nu}}') - (P_{\bar{\nu}} - P_\nu)({A''_{\nu\bar{\bar{\nu}}}}^T \\
&\cdot A_{\bar{\bar{\nu}}\bar{\nu}}') - (P_{\bar{\nu}} - P_\nu)({A'_{\nu\bar{\bar{\nu}}}}^T \cdot A_{\bar{\bar{\nu}}\bar{\nu}}'') + (\nabla {A'_{\nu\bar{\bar{\nu}}}}^T) \cdot A_{\bar{\bar{\nu}}\bar{\nu}}' - (\nabla {A''_{\nu\bar{\bar{\nu}}}}^T) \cdot A_{\bar{\bar{\nu}}\bar{\nu}}'' + (\nabla {A'_{\bar{\bar{\nu}}\bar{\nu}}}^T) \\
&\cdot A_{\nu\bar{\bar{\nu}}}{}' - (\nabla {A''_{\bar{\bar{\nu}}\bar{\nu}}}^T) \cdot A_{\nu\bar{\bar{\nu}}}{}'')\}
\end{aligned}
\tag{C.6}
$$

$$
\begin{aligned}
\dot{\alpha}'_\nu = &-\frac{1}{2}\nabla\nabla^T\varepsilon_\nu - 2\alpha'_\nu \cdot \alpha'_\nu + 2\alpha''_\nu \cdot \alpha''_\nu - \frac{1}{2}\sum_{\bar{\nu}} e^{-f''(\nu,\bar{\nu})}[\cos f'(\nu,\bar{\nu})\{(\nabla^T \cdot A'_{\nu\bar{\nu}}) \\
&\times (\alpha'_{\bar{\nu}} - \alpha'_\nu) - (\nabla^T \cdot A''_{\nu\bar{\nu}})(\alpha''_{\bar{\nu}} - \alpha''_\nu) - 2(\nabla^T \cdot A''_{\nu\bar{\nu}})(\alpha'_{\bar{\nu}} \cdot (Q_\nu - Q_{\bar{\nu}}) \\
&\times (Q_\nu - Q_{\bar{\nu}})^T \cdot \alpha'_{\bar{\nu}}) + 2(\nabla^T \cdot A''_{\nu\bar{\nu}})(\alpha''_{\bar{\nu}} \cdot (Q_\nu - Q_{\bar{\nu}}))((Q_\nu - Q_{\bar{\nu}})^T \cdot \alpha''_{\bar{\nu}}) \\
&- 2(\nabla^T \cdot A'_{\nu\bar{\nu}})(\alpha'_{\bar{\nu}} \cdot (Q_\nu - Q_{\bar{\nu}}))((Q_\nu - Q_{\bar{\nu}})^T \cdot \alpha''_{\bar{\nu}}) - 2(\nabla^T \cdot A'_{\nu\bar{\nu}})(\alpha''_{\bar{\nu}} \cdot (Q_\nu \\
&- Q_{\bar{\nu}}))((Q_\nu - Q_{\bar{\nu}})^T \cdot \alpha'_{\bar{\nu}}) - \frac{1}{2}(\nabla^T \cdot A''_{\nu\bar{\nu}})(P_{\bar{\nu}} - P_\nu)(P_{\bar{\nu}} - P_\nu)^T - (\nabla^T \cdot A'_{\nu\bar{\nu}}) \\
&\times (\alpha''_{\bar{\nu}} \cdot (Q_\nu - Q_{\bar{\nu}}))(P_{\bar{\nu}} - P_\nu)^T - (\nabla^T \cdot A''_{\nu\bar{\nu}})(\alpha'_{\bar{\nu}} \cdot (Q_\nu - Q_{\bar{\nu}}))(P_{\bar{\nu}} - P_\nu)^T \\
&- (\nabla^T \cdot A'_{\nu\bar{\nu}})(P_{\bar{\nu}} - P_\nu)((Q_\nu - Q_{\bar{\nu}})^T \cdot \alpha''_{\bar{\nu}}) - (\nabla^T \cdot A''_{\nu\bar{\nu}})(P_{\bar{\nu}} - P_\nu)((Q_\nu - Q_{\bar{\nu}})^T \\
&\cdot \alpha'_{\bar{\nu}}) - 2({A'_{\nu\bar{\nu}}}^T \cdot P_{\bar{\nu}})(\alpha''_{\bar{\nu}} - \alpha''_\nu) - 2({A''_{\nu\bar{\nu}}}^T \cdot P_{\bar{\nu}})(\alpha'_{\bar{\nu}} - \alpha'_\nu) - 4({A'_{\nu\bar{\nu}}}^T \cdot P_{\bar{\nu}})(\alpha'_{\bar{\nu}} \\
&\cdot (Q_\nu - Q_{\bar{\nu}}))((Q_\nu - Q_{\bar{\nu}})^T \cdot \alpha'_{\bar{\nu}}) + 4({A'_{\nu\bar{\nu}}}^T \cdot P_{\bar{\nu}})(\alpha''_{\bar{\nu}} \cdot (Q_\nu - Q_{\bar{\nu}}))((Q_\nu - Q_{\bar{\nu}})^T \cdot \alpha''_{\bar{\nu}})
\end{aligned}
$$

$$+ 4({A''_{\nu\bar{\nu}}}^T \cdot P_{\bar{\nu}})(\alpha'_{\bar{\nu}} \cdot (Q_\nu - Q_{\bar{\nu}}))((Q_\nu - Q_{\bar{\nu}})^T \cdot \alpha''_{\bar{\nu}}) + 4({A''_{\nu\bar{\nu}}}^T \cdot P_{\bar{\nu}})(\alpha''_{\bar{\nu}} \cdot (Q_\nu$$

$$- Q_{\bar{\nu}}))((Q_\nu - Q_{\bar{\nu}})^T \cdot \alpha'_{\bar{\nu}}) - ({A'_{\nu\bar{\nu}}}^T \cdot P_{\bar{\nu}})(P_{\bar{\nu}} - P_\nu)(P_{\bar{\nu}} - P_\nu)^T - 2({A'_{\nu\bar{\nu}}}^T \cdot P_{\bar{\nu}})(P_{\bar{\nu}}$$

$$- P_\nu)((Q_\nu - Q_{\bar{\nu}})^T \cdot \alpha'_{\bar{\nu}}) + 2({A''_{\nu\bar{\nu}}}^T \cdot P_{\bar{\nu}})(P_{\bar{\nu}} - P_\nu)((Q_\nu - Q_{\bar{\nu}})^T \cdot \alpha''_{\bar{\nu}}) - 2({A'_{\nu\bar{\nu}}}^T$$

$$\cdot P_{\bar{\nu}})(\alpha'_{\bar{\nu}} \cdot (Q_\nu - Q_{\bar{\nu}}))(P_{\bar{\nu}} - P_\nu)^T + 2({A''_{\nu\bar{\nu}}}^T \cdot P_{\bar{\nu}})(\alpha''_{\bar{\nu}} \cdot (Q_\nu - Q_{\bar{\nu}}))(P_{\bar{\nu}} - P_\nu)^T$$

$$- 4({A''_{\nu\bar{\nu}}}^T \cdot \alpha'_{\bar{\nu}} \cdot (Q_\nu - Q_{\bar{\nu}}))(\alpha'_{\bar{\nu}} - \alpha'_\nu) + 4({A''_{\nu\bar{\nu}}}^T \cdot \alpha''_{\bar{\nu}} \cdot (Q_\nu - Q_{\bar{\nu}}))(\alpha''_{\bar{\nu}} - \alpha''_\nu)$$

$$- 4({A'_{\nu\bar{\nu}}}^T \cdot \alpha'_{\bar{\nu}} \cdot (Q_\nu - Q_{\bar{\nu}}))(\alpha''_{\bar{\nu}} - \alpha''_\nu) - 4({A'_{\nu\bar{\nu}}}^T \cdot \alpha''_{\bar{\nu}} \cdot (Q_\nu - Q_{\bar{\nu}}))(\alpha'_{\bar{\nu}} - \alpha'_\nu)$$

$$- 8({A'_{\nu\bar{\nu}}}^T \cdot \alpha'_{\bar{\nu}} \cdot (Q_\nu - Q_{\bar{\nu}}))(\alpha'_{\bar{\nu}} \cdot (Q_\nu - Q_{\bar{\nu}}))((Q_\nu - Q_{\bar{\nu}})^T \cdot \alpha'_{\bar{\nu}}) + 8({A'_{\nu\bar{\nu}}}^T \cdot \alpha''_{\bar{\nu}}$$

$$\cdot (Q_\nu - Q_{\bar{\nu}}))(\alpha''_{\bar{\nu}} \cdot (Q_\nu - Q_{\bar{\nu}}))((Q_\nu - Q_{\bar{\nu}})^T \cdot \alpha'_{\bar{\nu}}) + 8({A''_{\nu\bar{\nu}}}^T \cdot \alpha'_{\bar{\nu}} \cdot (Q_\nu - Q_{\bar{\nu}}))(\alpha''_{\bar{\nu}}$$

$$\cdot (Q_\nu - Q_{\bar{\nu}}))((Q_\nu - Q_{\bar{\nu}})^T \cdot \alpha'_{\bar{\nu}}) + 8({A''_{\nu\bar{\nu}}}^T \cdot \alpha''_{\bar{\nu}} \cdot (Q_\nu - Q_{\bar{\nu}}))(\alpha'_{\bar{\nu}} \cdot (Q_\nu - Q_{\bar{\nu}}))((Q_\nu$$

$$- Q_{\bar{\nu}})^T \cdot \alpha'_{\bar{\nu}}) + 8({A'_{\nu\bar{\nu}}}^T \cdot \alpha'_{\bar{\nu}} \cdot (Q_\nu - Q_{\bar{\nu}}))(\alpha''_{\bar{\nu}} \cdot (Q_\nu - Q_{\bar{\nu}}))((Q_\nu - Q_{\bar{\nu}})^T \cdot \alpha''_{\bar{\nu}})$$

$$+ 8({A'_{\nu\bar{\nu}}}^T \cdot \alpha''_{\bar{\nu}} \cdot (Q_\nu - Q_{\bar{\nu}}))(\alpha'_{\bar{\nu}} \cdot (Q_\nu - Q_{\bar{\nu}}))((Q_\nu - Q_{\bar{\nu}})^T \cdot \alpha''_{\bar{\nu}}) + 8({A''_{\nu\bar{\nu}}}^T \cdot \alpha'_{\bar{\nu}}$$

$$\cdot (Q_\nu - Q_{\bar{\nu}}))(\alpha'_{\bar{\nu}} \cdot (Q_\nu - Q_{\bar{\nu}}))((Q_\nu - Q_{\bar{\nu}})^T \cdot \alpha''_{\bar{\nu}}) - 8({A''_{\nu\bar{\nu}}}^T \cdot \alpha''_{\bar{\nu}} \cdot (Q_\nu - Q_{\bar{\nu}}))(\alpha''_{\bar{\nu}}$$

$$\cdot (Q_\nu - Q_{\bar{\nu}}))((Q_\nu - Q_{\bar{\nu}})^T \cdot \alpha''_{\bar{\nu}}) - 2({A'_{\nu\bar{\nu}}}^T \cdot \alpha'_{\bar{\nu}} \cdot (Q_\nu - Q_{\bar{\nu}}))(P_{\bar{\nu}} - P_\nu)(P_{\bar{\nu}} - P_\nu)^T$$

$$+ 2({A''_{\nu\bar{\nu}}}^T \cdot \alpha''_{\bar{\nu}} \cdot (Q_\nu - Q_{\bar{\nu}}))(P_{\bar{\nu}} - P_\nu)(P_{\bar{\nu}} - P_\nu)^T - 4({A'_{\nu\bar{\nu}}}^T \cdot \alpha'_{\bar{\nu}} \cdot (Q_\nu - Q_{\bar{\nu}}))(\alpha'_{\bar{\nu}}$$

$$\cdot (Q_\nu - Q_{\bar{\nu}}))(P_{\bar{\nu}} - P_\nu)^T + 4({A'_{\nu\bar{\nu}}}^T \cdot \alpha''_{\bar{\nu}} \cdot (Q_\nu - Q_{\bar{\nu}}))(\alpha''_{\bar{\nu}} \cdot (Q_\nu - Q_{\bar{\nu}}))(P_{\bar{\nu}} - P_\nu)^T$$

$$+ 4({A''_{\nu\bar{\nu}}}^T \cdot \alpha'_{\bar{\nu}} \cdot (Q_\nu - Q_{\bar{\nu}}))(\alpha''_{\bar{\nu}} \cdot (Q_\nu - Q_{\bar{\nu}}))(P_{\bar{\nu}} - P_\nu)^T + 4({A''_{\nu\bar{\nu}}}^T \cdot \alpha''_{\bar{\nu}} \cdot (Q_\nu$$

$$- Q_{\bar{\nu}}))(\alpha'_{\bar{\nu}} \cdot (Q_\nu - Q_{\bar{\nu}}))(P_{\bar{\nu}} - P_\nu)^T - 4({A'_{\nu\bar{\nu}}}^T \cdot \alpha'_{\bar{\nu}} \cdot (Q_\nu - Q_{\bar{\nu}}))(P_{\bar{\nu}} - P_\nu)((Q_\nu$$

$$- Q_{\bar{\nu}})^T \cdot \alpha'_{\bar{\nu}}) + 4({A'_{\nu\bar{\nu}}}^T \cdot \alpha''_{\bar{\nu}} \cdot (Q_\nu - Q_{\bar{\nu}}))(P_{\bar{\nu}} - P_\nu)((Q_\nu - Q_{\bar{\nu}})^T \cdot \alpha''_{\bar{\nu}})$$

$$+ 4({A''_{\nu\bar{\nu}}}^T \cdot \alpha'_{\bar{\nu}} \cdot (Q_\nu - Q_{\bar{\nu}}))(P_{\bar{\nu}} - P_\nu)((Q_\nu - Q_{\bar{\nu}})^T \cdot \alpha''_{\bar{\nu}}) + 4({A''_{\nu\bar{\nu}}}^T \cdot \alpha''_{\bar{\nu}} \cdot (Q_\nu$$

$$- Q_{\bar{\nu}}))(P_{\bar{\nu}} - P_\nu)((Q_\nu - Q_{\bar{\nu}})^T \cdot \alpha'_{\bar{\nu}}) - 8(\alpha''_{\bar{\nu}} \cdot A'_{\nu\bar{\nu}})((Q_\nu - Q_{\bar{\nu}})^T \cdot \alpha'_{\bar{\nu}}) + 8(\alpha''_{\bar{\nu}}$$

$$\cdot A''_{\nu\bar{\nu}})((Q_\nu - Q_{\bar{\nu}})^T \cdot \alpha''_{\bar{\nu}}) - 8(\alpha'_{\bar{\nu}} \cdot A'_{\nu\bar{\nu}})((Q_\nu - Q_{\bar{\nu}})^T \cdot \alpha''_{\bar{\nu}}) - 8(\alpha'_{\bar{\nu}} \cdot A''_{\nu\bar{\nu}})((Q_\nu$$

$$- Q_{\bar{\nu}})^T \cdot \alpha'_{\bar{\nu}}) - 4(\alpha'_{\bar{\nu}} \cdot A''_{\nu\bar{\nu}})(P_{\bar{\nu}} - P_\nu)^T - 4(\alpha''_{\bar{\nu}} \cdot A'_{\nu\bar{\nu}})(P_{\bar{\nu}} - P_\nu)^T + 4(\nabla A'_{\nu\bar{\nu}}) \cdot \alpha'_{\bar{\nu}}$$

$$- 4(\nabla A''_{\nu\bar{\nu}}) \cdot \alpha''_{\bar{\nu}} - 4(\nabla A'_{\nu\bar{\nu}} \cdot P_{\bar{\nu}})((Q_\nu - Q_{\bar{\nu}})^T \cdot \alpha''_{\bar{\nu}}) - 4(\nabla A''_{\nu\bar{\nu}} \cdot P_{\bar{\nu}})((Q_\nu - Q_{\bar{\nu}})^T$$

$$\cdot \alpha'_{\bar{\nu}}) - 2(\nabla A''_{\nu\bar{\nu}} \cdot P_{\bar{\nu}})(P_{\bar{\nu}} - P_\nu)^T - 8(\nabla A''_{\nu\bar{\nu}} \cdot \alpha'_{\bar{\nu}} \cdot (Q_\nu - Q_{\bar{\nu}}))((Q_\nu - Q_{\bar{\nu}})^T \cdot \alpha'_{\bar{\nu}})$$

$$+ 8(\nabla A''_{\nu\bar{\nu}} \cdot \alpha''_{\bar{\nu}} \cdot (Q_\nu - Q_{\bar{\nu}}))((Q_\nu - Q_{\bar{\nu}})^T \cdot \alpha''_{\bar{\nu}}) - 8(\nabla A'_{\nu\bar{\nu}} \cdot \alpha'_{\bar{\nu}} \cdot (Q_\nu - Q_{\bar{\nu}}))((Q_\nu$$

$$- Q_{\bar{\nu}})^T \cdot \alpha''_{\bar{\nu}}) - 8(\nabla A'_{\nu\bar{\nu}} \cdot \alpha''_{\bar{\nu}} \cdot (Q_\nu - Q_{\bar{\nu}}))((Q_\nu - Q_{\bar{\nu}})^T \cdot \alpha'_{\bar{\nu}}) - 4(\nabla A'_{\nu\bar{\nu}} \cdot \alpha''_{\bar{\nu}} \cdot (Q_\nu$$

$$- Q_{\bar{\nu}}))(P_{\bar{\nu}} - P_\nu)^T - 4(\nabla A''_{\nu\bar{\nu}} \cdot \alpha'_{\bar{\nu}} \cdot (Q_\nu - Q_{\bar{\nu}}))(P_{\bar{\nu}} - P_\nu)^T$$

$$+ \sum_{\bar{\bar{\nu}}} [(A''_{\nu\bar{\bar{\nu}}}{}^T \cdot A_{\bar{\bar{\nu}}\bar{\nu}}{}'')(\alpha''_{\bar{\nu}} - \alpha''_\nu) - (A''_{\nu\bar{\bar{\nu}}}{}^T \cdot A_{\bar{\bar{\nu}}\bar{\nu}}{}')(\alpha'_{\bar{\nu}} - \alpha'_\nu) - (A'_{\nu\bar{\bar{\nu}}}{}^T \cdot A_{\bar{\bar{\nu}}\bar{\nu}}{}')(\alpha''_{\bar{\nu}} - \alpha''_\nu)$$

$$- (A'_{\nu\bar{\bar{\nu}}}{}^T \cdot A_{\bar{\bar{\nu}}\bar{\nu}}{}'')(\alpha'_{\bar{\nu}} - \alpha'_\nu) - 2(A'_{\nu\bar{\bar{\nu}}}{}^T \cdot A_{\bar{\bar{\nu}}\bar{\nu}}{}')(\alpha'_{\bar{\nu}} \cdot (Q_\nu - Q_{\bar{\nu}}))((Q_\nu - Q_{\bar{\nu}})^T \cdot \alpha'_{\bar{\nu}})$$

$$+ 2(A'_{\nu\bar{\bar{\nu}}}{}^T \cdot A_{\bar{\bar{\nu}}\bar{\nu}}{}'')(\alpha''_{\bar{\nu}} \cdot (Q_\nu - Q_{\bar{\nu}}))((Q_\nu - Q_{\bar{\nu}})^T \cdot \alpha'_{\bar{\nu}}) + 2(A''_{\nu\bar{\bar{\nu}}}{}^T \cdot A_{\bar{\bar{\nu}}\bar{\nu}}{}')(\alpha''_{\bar{\nu}} \cdot (Q_\nu - Q_{\bar{\nu}}))$$

$$\times ((Q_\nu - Q_{\bar{\nu}})^T \cdot \alpha'_{\bar{\nu}}) + 2(A''_{\nu\bar{\bar{\nu}}}{}^T \cdot A_{\bar{\bar{\nu}}\bar{\nu}}{}'')(\alpha'_{\bar{\nu}} \cdot (Q_\nu - Q_{\bar{\nu}}))((Q_\nu - Q_{\bar{\nu}})^T \cdot \alpha'_{\bar{\nu}}) + 2(A'_{\nu\bar{\bar{\nu}}}{}^T$$

$$\cdot A_{\bar{\bar{\nu}}\bar{\nu}}{}')(\alpha''_{\bar{\nu}} \cdot (Q_\nu - Q_{\bar{\nu}}))((Q_\nu - Q_{\bar{\nu}})^T \cdot \alpha''_{\bar{\nu}}) + 2(A'_{\nu\bar{\bar{\nu}}}{}^T \cdot A_{\bar{\bar{\nu}}\bar{\nu}}{}'')(\alpha'_{\bar{\nu}} \cdot (Q_\nu - Q_{\bar{\nu}}))((Q_\nu$$

$$- Q_{\bar{\nu}})^T \cdot \alpha''_{\bar{\nu}}) + 2(A''_{\nu\bar{\bar{\nu}}}{}^T \cdot A_{\bar{\bar{\nu}}\bar{\nu}}{}')(\alpha'_{\bar{\nu}} \cdot (Q_\nu - Q_{\bar{\nu}}))((Q_\nu - Q_{\bar{\nu}})^T \cdot \alpha''_{\bar{\nu}}) - 2(A''_{\nu\bar{\bar{\nu}}}{}^T \cdot A_{\bar{\bar{\nu}}\bar{\nu}}{}'')$$

$$\times (\alpha''_{\bar{\nu}} \cdot (Q_\nu - Q_{\bar{\nu}}))((Q_\nu - Q_{\bar{\nu}})^T \cdot \alpha''_{\bar{\nu}}) - \frac{1}{2}(A'_{\nu\bar{\bar{\nu}}}{}^T \cdot A_{\bar{\bar{\nu}}\bar{\nu}}{}')(P_{\bar{\nu}} - P_\nu)(P_{\bar{\nu}} - P_\nu)^T$$

$$+ \frac{1}{2}(A''_{\nu\bar{\bar{\nu}}}{}^T \cdot A_{\bar{\bar{\nu}}\bar{\nu}}{}'')(P_{\bar{\nu}} - P_\nu)(P_{\bar{\nu}} - P_\nu)^T - (A'_{\nu\bar{\bar{\nu}}}{}^T \cdot A_{\bar{\bar{\nu}}\bar{\nu}}{}')(\alpha'_{\bar{\nu}} \cdot (Q_\nu - Q_{\bar{\nu}}))(P_{\bar{\nu}} - P_\nu)^T$$

$$+ (A'_{\nu\bar{\bar{\nu}}}{}^T \cdot A_{\bar{\bar{\nu}}\bar{\nu}}{}'')(\alpha''_{\bar{\nu}} \cdot (Q_\nu - Q_{\bar{\nu}}))(P_{\bar{\nu}} - P_\nu)^T + (A''_{\nu\bar{\bar{\nu}}}{}^T \cdot A_{\bar{\bar{\nu}}\bar{\nu}}{}')(\alpha''_{\bar{\nu}} \cdot (Q_\nu - Q_{\bar{\nu}}))(P_{\bar{\nu}}$$

$$- P_\nu)^T + (A''_{\nu\bar{\bar{\nu}}}{}^T \cdot A_{\bar{\bar{\nu}}\bar{\nu}}{}'')(\alpha'_{\bar{\nu}} \cdot (Q_\nu - Q_{\bar{\nu}}))(P_{\bar{\nu}} - P_\nu)^T - (A'_{\nu\bar{\bar{\nu}}}{}^T \cdot A_{\bar{\bar{\nu}}\bar{\nu}}{}')(P_{\bar{\nu}} - P_\nu)((Q_\nu$$

$$- Q_{\bar{\nu}})^T \cdot \alpha'_{\bar{\nu}}) - (A'_{\nu\bar{\bar{\nu}}}{}^T \cdot A_{\bar{\bar{\nu}}\bar{\nu}}{}'')(P_{\bar{\nu}} - P_\nu)((Q_\nu - Q_{\bar{\nu}})^T \cdot \alpha''_{\bar{\nu}}) + (A''_{\nu\bar{\bar{\nu}}}{}^T \cdot A_{\bar{\bar{\nu}}\bar{\nu}}{}')(P_{\bar{\nu}} - P_\nu)$$

$$\times ((Q_\nu - Q_{\bar{\nu}})^T \cdot \alpha''_{\bar{\nu}}) + (A''_{\nu\bar{\bar{\nu}}}{}^T \cdot A_{\bar{\bar{\nu}}\bar{\nu}}{}'')(P_{\bar{\nu}} - P_\nu)((Q_\nu - Q_{\bar{\nu}})^T \cdot \alpha'_{\bar{\nu}}) - 2(\nabla A''_{\nu\bar{\bar{\nu}}}{}^T \cdot A_{\bar{\bar{\nu}}\bar{\nu}}{}')$$

$$\times ((Q_\nu - Q_{\bar{\nu}})^T \cdot \alpha'_{\bar{\nu}}) + 2(\nabla A''_{\nu\bar{\bar{\nu}}}{}^T \cdot A_{\bar{\bar{\nu}}\bar{\nu}}{}'')((Q_\nu - Q_{\bar{\nu}})^T \cdot \alpha''_{\bar{\nu}}) - 2(\nabla A'_{\nu\bar{\bar{\nu}}}{}^T \cdot A_{\bar{\bar{\nu}}\bar{\nu}}{}')((Q_\nu$$

$$- Q_{\bar{\nu}})^T \cdot \alpha''_{\bar{\nu}}) - 2(\nabla A'_{\nu\bar{\bar{\nu}}}{}^T \cdot A_{\bar{\bar{\nu}}\bar{\nu}}{}'')((Q_\nu - Q_{\bar{\nu}})^T \cdot \alpha'_{\bar{\nu}}) - 2(\nabla A''_{\bar{\bar{\nu}}\bar{\nu}}{}^T \cdot A_{\nu\bar{\bar{\nu}}}{}')((Q_\nu - Q_{\bar{\nu}})^T \cdot \alpha'_{\bar{\nu}})$$

$$+ 2(\nabla A''_{\bar{\bar{\nu}}\bar{\nu}}{}^T \cdot A_{\nu\bar{\bar{\nu}}}{}'')((Q_\nu - Q_{\bar{\nu}})^T \cdot \alpha''_{\bar{\nu}}) - 2(\nabla A'_{\bar{\bar{\nu}}\bar{\nu}}{}^T \cdot A_{\nu\bar{\bar{\nu}}}{}')((Q_\nu - Q_{\bar{\nu}})^T \cdot \alpha''_{\bar{\nu}}) - 2(\nabla A'_{\bar{\bar{\nu}}\bar{\nu}}{}^T$$

$$\cdot A_{\nu\bar{\bar{\nu}}}{}'')((Q_\nu - Q_{\bar{\nu}})^T \cdot \alpha'_{\bar{\nu}}) - (\nabla A'_{\nu\bar{\bar{\nu}}}{}^T \cdot A_{\bar{\bar{\nu}}\bar{\nu}}{}'')(P_{\bar{\nu}} - P_\nu)^T - (\nabla A''_{\nu\bar{\bar{\nu}}}{}^T \cdot A_{\bar{\bar{\nu}}\bar{\nu}}{}')(P_{\bar{\nu}} - P_\nu)^T$$

$$- (\nabla A'_{\bar{\bar{\nu}}\bar{\nu}}{}^T \cdot A_{\nu\bar{\bar{\nu}}}{}'')(P_{\bar{\nu}} - P_\nu)^T - (\nabla A''_{\bar{\bar{\nu}}\bar{\nu}}{}^T \cdot A_{\nu\bar{\bar{\nu}}}{}')(P_{\bar{\nu}} - P_\nu)^T + \nabla A'_{\nu\bar{\bar{\nu}}}{}^T \cdot \nabla A_{\bar{\bar{\nu}}\bar{\nu}}{}' - \nabla A''_{\nu\bar{\bar{\nu}}}{}^T$$

$$\cdot \nabla A_{\bar{\bar{\nu}}\bar{\nu}}{}'']\} - \sin f'(\nu,\bar{\nu})\{(\nabla^T \cdot A'_{\nu\bar{\nu}})(\alpha''_{\bar{\nu}} - \alpha''_\nu) + (\nabla^T \cdot A''_{\nu\bar{\nu}})(\alpha'_{\bar{\nu}} - \alpha'_\nu)$$

$$- 2(\nabla^T \cdot A''_{\nu\bar{\nu}})(\alpha'_{\bar{\nu}} \cdot (Q_\nu - Q_{\bar{\nu}}))((Q_\nu - Q_{\bar{\nu}})^T \cdot \alpha''_{\bar{\nu}}) - 2(\nabla^T \cdot A''_{\nu\bar{\nu}})(\alpha''_{\bar{\nu}} \cdot (Q_\nu - Q_{\bar{\nu}}))$$

$$\times ((Q_\nu - Q_{\bar{\nu}})^T \cdot \alpha'_{\bar{\nu}}) + 2(\nabla^T \cdot A'_{\nu\bar{\nu}})(\alpha'_{\bar{\nu}} \cdot (Q_\nu - Q_{\bar{\nu}}))((Q_\nu - Q_{\bar{\nu}})^T \cdot \alpha'_{\bar{\nu}})$$

$$
\begin{aligned}
&- 2(\nabla^T \cdot A'_{\nu\bar{\nu}})(\alpha''_{\bar{\nu}} \cdot (Q_\nu - Q_{\bar{\nu}}))((Q_\nu - Q_{\bar{\nu}})^T \cdot \alpha''_{\bar{\nu}}) + \frac{1}{2}(\nabla^T \cdot A'_{\nu\bar{\nu}})(P_{\bar{\nu}} - P_\nu)(P_{\bar{\nu}} - P_\nu)^T \\
&+ (\nabla^T \cdot A'_{\nu\bar{\nu}})(\alpha'_{\bar{\nu}} \cdot (Q_\nu - Q_{\bar{\nu}}))(P_{\bar{\nu}} - P_\nu)^T - (\nabla^T \cdot A''_{\nu\bar{\nu}})(\alpha''_{\bar{\nu}} \cdot (Q_\nu - Q_{\bar{\nu}}))(P_{\bar{\nu}} - P_\nu)^T \\
&+ (\nabla^T \cdot A'_{\nu\bar{\nu}})(P_{\bar{\nu}} - P_\nu)((Q_\nu - Q_{\bar{\nu}})^T \cdot \alpha'_{\bar{\nu}}) - (\nabla^T \cdot A''_{\nu\bar{\nu}})(P_{\bar{\nu}} - P_\nu)((Q_\nu - Q_{\bar{\nu}})^T \cdot \alpha''_{\bar{\nu}}) \\
&+ 2{A'_{\nu\bar{\nu}}}^T \cdot P_{\bar{\nu}})(\alpha'_{\bar{\nu}} - \alpha'_\nu) - 2({A''_{\nu\bar{\nu}}}^T \cdot P_{\bar{\nu}})(\alpha''_{\bar{\nu}} - \alpha''_\nu) - 4({A'_{\nu\bar{\nu}}}^T \cdot P_{\bar{\nu}})(\alpha'_{\bar{\nu}} \cdot (Q_\nu - Q_{\bar{\nu}}))((Q_\nu \\
&- Q_{\bar{\nu}})^T \cdot \alpha''_{\bar{\nu}}) - 4({A'_{\nu\bar{\nu}}}^T \cdot P_{\bar{\nu}})(\alpha''_{\bar{\nu}} \cdot (Q_\nu - Q_{\bar{\nu}}))((Q_\nu - Q_{\bar{\nu}})^T \cdot \alpha'_{\bar{\nu}}) - 4({A''_{\nu\bar{\nu}}}^T \cdot P_{\bar{\nu}})(\alpha'_{\bar{\nu}} \\
&\cdot (Q_\nu - Q_{\bar{\nu}}))((Q_\nu - Q_{\bar{\nu}})^T \cdot \alpha'_{\bar{\nu}}) + 4({A''_{\nu\bar{\nu}}}^T \cdot P_{\bar{\nu}})(\alpha''_{\bar{\nu}} \cdot (Q_\nu - Q_{\bar{\nu}}))((Q_\nu - Q_{\bar{\nu}})^T \cdot \alpha''_{\bar{\nu}}) \\
&- ({A''_{\nu\bar{\nu}}}^T \cdot P_{\bar{\nu}})(P_{\bar{\nu}} - P_\nu)(P_{\bar{\nu}} - P_\nu)^T - 2({A'_{\nu\bar{\nu}}}^T \cdot P_{\bar{\nu}})(P_{\bar{\nu}} - P_\nu)((Q_\nu - Q_{\bar{\nu}})^T \cdot \alpha''_{\bar{\nu}}) \\
&- 2({A''_{\nu\bar{\nu}}}^T \cdot P_{\bar{\nu}})(P_{\bar{\nu}} - P_\nu)((Q_\nu - Q_{\bar{\nu}})^T \cdot \alpha'_{\bar{\nu}}) - 2({A''_{\nu\bar{\nu}}}^T \cdot P_{\bar{\nu}})(\alpha'_{\bar{\nu}} \cdot (Q_\nu - Q_{\bar{\nu}}))(P_{\bar{\nu}} - P_\nu)^T \\
&- 2({A'_{\nu\bar{\nu}}}^T \cdot P_{\bar{\nu}})(\alpha''_{\bar{\nu}} \cdot (Q_\nu - Q_{\bar{\nu}}))(P_{\bar{\nu}} - P_\nu)^T - 4({A''_{\nu\bar{\nu}}}^T \cdot \alpha'_{\bar{\nu}} \cdot (Q_\nu - Q_{\bar{\nu}}))(\alpha''_{\bar{\nu}} - \alpha''_\nu) \\
&- 4({A''_{\nu\bar{\nu}}}^T \cdot \alpha''_{\bar{\nu}} \cdot (Q_\nu - Q_{\bar{\nu}}))(\alpha'_{\bar{\nu}} - \alpha'_\nu) + 4({A'_{\nu\bar{\nu}}}^T \cdot \alpha'_{\bar{\nu}} \cdot (Q_\nu - Q_{\bar{\nu}}))(\alpha'_{\bar{\nu}} - \alpha'_\nu) - 4({A'_{\nu\bar{\nu}}}^T \\
&\cdot \alpha''_{\bar{\nu}} \cdot (Q_\nu - Q_{\bar{\nu}}))(\alpha''_{\bar{\nu}} - \alpha''_\nu) - 8({A'_{\nu\bar{\nu}}}^T \cdot \alpha'_{\bar{\nu}} \cdot (Q_\nu - Q_{\bar{\nu}}))(\alpha'_{\bar{\nu}} \cdot (Q_\nu - Q_{\bar{\nu}}))((Q_\nu - Q_{\bar{\nu}})^T \\
&\cdot \alpha''_{\bar{\nu}}) + 8({A'_{\nu\bar{\nu}}}^T \cdot \alpha''_{\bar{\nu}} \cdot (Q_\nu - Q_{\bar{\nu}}))(\alpha''_{\bar{\nu}} \cdot (Q_\nu - Q_{\bar{\nu}}))((Q_\nu - Q_{\bar{\nu}})^T \cdot \alpha''_{\bar{\nu}}) + 8({A''_{\nu\bar{\nu}}}^T \cdot \alpha'_{\bar{\nu}} \\
&\cdot (Q_\nu - Q_{\bar{\nu}}))(\alpha''_{\bar{\nu}} \cdot (Q_\nu - Q_{\bar{\nu}}))((Q_\nu - Q_{\bar{\nu}})^T \cdot \alpha''_{\bar{\nu}}) + 8({A''_{\nu\bar{\nu}}}^T \cdot \alpha''_{\bar{\nu}} \cdot (Q_\nu - Q_{\bar{\nu}}))(\alpha'_{\bar{\nu}} \cdot (Q_\nu \\
&- Q_{\bar{\nu}}))((Q_\nu - Q_{\bar{\nu}})^T \cdot \alpha''_{\bar{\nu}}) - 8({A'_{\nu\bar{\nu}}}^T \cdot \alpha'_{\bar{\nu}} \cdot (Q_\nu - Q_{\bar{\nu}}))(\alpha''_{\bar{\nu}} \cdot (Q_\nu - Q_{\bar{\nu}}))((Q_\nu - Q_{\bar{\nu}})^T \cdot \alpha'_{\bar{\nu}}) \\
&- 8({A'_{\nu\bar{\nu}}}^T \cdot \alpha''_{\bar{\nu}} \cdot (Q_\nu - Q_{\bar{\nu}}))(\alpha'_{\bar{\nu}} \cdot (Q_\nu - Q_{\bar{\nu}}))((Q_\nu - Q_{\bar{\nu}})^T \cdot \alpha'_{\bar{\nu}}) - 8({A''_{\nu\bar{\nu}}}^T \cdot \alpha'_{\bar{\nu}} \cdot (Q_\nu \\
&- Q_{\bar{\nu}}))(\alpha'_{\bar{\nu}} \cdot (Q_\nu - Q_{\bar{\nu}}))((Q_\nu - Q_{\bar{\nu}})^T \cdot \alpha'_{\bar{\nu}}) + 8({A''_{\nu\bar{\nu}}}^T \cdot \alpha''_{\bar{\nu}} \cdot (Q_\nu - Q_{\bar{\nu}}))(\alpha''_{\bar{\nu}} \cdot (Q_\nu - Q_{\bar{\nu}})) \\
&\times ((Q_\nu - Q_{\bar{\nu}})^T \cdot \alpha'_{\bar{\nu}}) - 2({A'_{\nu\bar{\nu}}}^T \cdot \alpha''_{\bar{\nu}} \cdot (Q_\nu - Q_{\bar{\nu}}))(P_{\bar{\nu}} - P_\nu)(P_{\bar{\nu}} - P_\nu)^T - 2({A''_{\nu\bar{\nu}}}^T \cdot \alpha'_{\bar{\nu}} \\
&\cdot (Q_\nu - Q_{\bar{\nu}}))(P_{\bar{\nu}} - P_\nu)(P_{\bar{\nu}} - P_\nu)^T - 4({A'_{\nu\bar{\nu}}}^T \cdot \alpha'_{\bar{\nu}} \cdot (Q_\nu - Q_{\bar{\nu}}))(\alpha''_{\bar{\nu}} \cdot (Q_\nu - Q_{\bar{\nu}}))(P_{\bar{\nu}} \\
&- P_\nu)^T - 4({A'_{\nu\bar{\nu}}}^T \cdot \alpha''_{\bar{\nu}} \cdot (Q_\nu - Q_{\bar{\nu}}))(\alpha'_{\bar{\nu}} \cdot (Q_\nu - Q_{\bar{\nu}}))(P_{\bar{\nu}} - P_\nu)^T - 4({A''_{\nu\bar{\nu}}}^T \cdot \alpha'_{\bar{\nu}} \cdot (Q_\nu \\
&- Q_{\bar{\nu}}))(\alpha'_{\bar{\nu}} \cdot (Q_\nu - Q_{\bar{\nu}}))(P_{\bar{\nu}} - P_\nu)^T + 4({A''_{\nu\bar{\nu}}}^T \cdot \alpha''_{\bar{\nu}} \cdot (Q_\nu - Q_{\bar{\nu}}))(\alpha''_{\bar{\nu}} \cdot (Q_\nu - Q_{\bar{\nu}}))(P_{\bar{\nu}} \\
&- P_\nu)^T - 4({A'_{\nu\bar{\nu}}}^T \cdot \alpha'_{\bar{\nu}} \cdot (Q_\nu - Q_{\bar{\nu}}))(P_{\bar{\nu}} - P_\nu)((Q_\nu - Q_{\bar{\nu}})^T \cdot \alpha''_{\bar{\nu}}) - 4({A'_{\nu\bar{\nu}}}^T \cdot \alpha''_{\bar{\nu}} \cdot (Q_\nu \\
&- Q_{\bar{\nu}}))(P_{\bar{\nu}} - P_\nu)((Q_\nu - Q_{\bar{\nu}})^T \cdot \alpha'_{\bar{\nu}}) - ({A''_{\nu\bar{\nu}}}^T \cdot \alpha'_{\bar{\nu}} \cdot (Q_\nu - Q_{\bar{\nu}}))(P_{\bar{\nu}} - P_\nu)((Q_\nu - Q_{\bar{\nu}})^T \\
&\cdot \alpha'_{\bar{\nu}}) + 4({A''_{\nu\bar{\nu}}}^T \cdot \alpha''_{\bar{\nu}} \cdot (Q_\nu - Q_{\bar{\nu}}))(P_{\bar{\nu}} - P_\nu)((Q_\nu - Q_{\bar{\nu}})^T \cdot \alpha''_{\bar{\nu}}) - 8(\alpha''_{\bar{\nu}} \cdot A'_{\nu\bar{\nu}})((Q_\nu \\
&- Q_{\bar{\nu}})^T \cdot \alpha''_{\bar{\nu}}) - 8(\alpha''_{\bar{\nu}} \cdot A''_{\nu\bar{\nu}})((Q_\nu - Q_{\bar{\nu}})^T \cdot \alpha'_{\bar{\nu}}) + 8(\alpha'_{\bar{\nu}} \cdot A'_{\nu\bar{\nu}})((Q_\nu - Q_{\bar{\nu}})^T \cdot \alpha'_{\bar{\nu}})
\end{aligned}
$$

$$
\begin{aligned}
&- 8(\alpha'_{\bar{\nu}} \cdot A''_{\nu\bar{\nu}})((Q_\nu - Q_{\bar{\nu}})^T \cdot \alpha''_{\bar{\nu}}) + 4(\alpha'_{\bar{\nu}} \cdot A'_{\nu\bar{\nu}})(P_{\bar{\nu}} - P_\nu)^T - 4(\alpha''_{\bar{\nu}} \cdot A''_{\nu\bar{\nu}})(P_{\bar{\nu}} - P_\nu)^T \\
&+ 4\nabla A'_{\nu\bar{\nu}} \cdot \alpha''_{\bar{\nu}} + 4\nabla A''_{\nu\bar{\nu}} \cdot \alpha'_{\bar{\nu}} + 4(\nabla A'_{\nu\bar{\nu}} \cdot P_{\bar{\nu}})((Q_\nu - Q_{\bar{\nu}})^T \cdot \alpha'_{\bar{\nu}}) - 4(\nabla A''_{\nu\bar{\nu}} \cdot P_{\bar{\nu}})((Q_\nu \\
&- Q_{\bar{\nu}})^T \cdot \alpha''_{\bar{\nu}}) + 2(\nabla A'_{\nu\bar{\nu}} \cdot P_{\bar{\nu}})(P_{\bar{\nu}} - P_\nu)^T + 8(\nabla A'_{\nu\bar{\nu}} \cdot \alpha'_{\bar{\nu}} \cdot (Q_\nu - Q_{\bar{\nu}}))((Q_\nu - Q_{\bar{\nu}})^T \\
&\cdot \alpha'_{\bar{\nu}}) - 8(\nabla A'_{\nu\bar{\nu}} \cdot \alpha''_{\bar{\nu}} \cdot (Q_\nu - Q_{\bar{\nu}}))((Q_\nu - Q_{\bar{\nu}})^T \cdot \alpha''_{\bar{\nu}}) - 8(\nabla A''_{\nu\bar{\nu}} \cdot \alpha'_{\bar{\nu}} \cdot (Q_\nu - Q_{\bar{\nu}}))((Q_\nu \\
&- Q_{\bar{\nu}})^T \cdot \alpha''_{\bar{\nu}}) - 8(\nabla A''_{\nu\bar{\nu}} \cdot \alpha''_{\bar{\nu}} \cdot (Q_\nu - Q_{\bar{\nu}}))((Q_\nu - Q_{\bar{\nu}})^T \cdot \alpha'_{\bar{\nu}}) + 4(\nabla A'_{\nu\bar{\nu}} \cdot \alpha'_{\bar{\nu}} \cdot (Q_\nu \\
&- Q_{\bar{\nu}}))(P_{\bar{\nu}} - P_\nu)^T - 4(\nabla A''_{\nu\bar{\nu}} \cdot \alpha''_{\bar{\nu}} \cdot (Q_\nu - Q_{\bar{\nu}}))(P_{\bar{\nu}} - P_\nu)^T + \sum_{\bar{\bar{\nu}}}[({A'_{\nu\bar{\bar{\nu}}}}^T \cdot A_{\bar{\bar{\nu}}\bar{\nu}}')(\alpha'_{\bar{\nu}} \\
&- \alpha'_\nu) - ({A'_{\nu\bar{\bar{\nu}}}}^T \cdot A_{\bar{\bar{\nu}}\bar{\nu}}'')(\alpha''_{\bar{\nu}} - \alpha''_\nu) - ({A''_{\nu\bar{\bar{\nu}}}}^T \cdot A_{\bar{\bar{\nu}}\bar{\nu}}')(\alpha''_{\bar{\nu}} - \alpha''_\nu) - ({A''_{\nu\bar{\bar{\nu}}}}^T \cdot A_{\bar{\bar{\nu}}\bar{\nu}}'')(\alpha'_{\bar{\nu}} \\
&- \alpha'_\nu) - 2({A'_{\nu\bar{\bar{\nu}}}}^T \cdot A_{\bar{\bar{\nu}}\bar{\nu}}')(\alpha'_{\bar{\nu}} \cdot (Q_\nu - Q_{\bar{\nu}}))((Q_\nu - Q_{\bar{\nu}})^T \cdot \alpha''_{\bar{\nu}}) + 2({A'_{\nu\bar{\bar{\nu}}}}^T \cdot A_{\bar{\bar{\nu}}\bar{\nu}}'')(\alpha''_{\bar{\nu}} \cdot (Q_\nu \\
&- Q_{\bar{\nu}}))((Q_\nu - Q_{\bar{\nu}})^T \cdot \alpha''_{\bar{\nu}}) + 2({A''_{\nu\bar{\bar{\nu}}}}^T \cdot A_{\bar{\bar{\nu}}\bar{\nu}}')(\alpha''_{\bar{\nu}} \cdot (Q_\nu - Q_{\bar{\nu}}))((Q_\nu - Q_{\bar{\nu}})^T \cdot \alpha''_{\bar{\nu}}) \\
&+ 2({A''_{\nu\bar{\bar{\nu}}}}^T \cdot A_{\bar{\bar{\nu}}\bar{\nu}}'')(\alpha'_{\bar{\nu}} \cdot (Q_\nu - Q_{\bar{\nu}}))((Q_\nu - Q_{\bar{\nu}})^T \cdot \alpha''_{\bar{\nu}}) - 2({A'_{\nu\bar{\nu}}}^T \cdot A_{\bar{\nu}\bar{\nu}}')(\alpha''_{\bar{\nu}} \cdot (Q_\nu - Q_{\bar{\nu}})) \\
&\times ((Q_\nu - Q_{\bar{\nu}})^T \cdot \alpha'_{\bar{\nu}}) - 2({A'_{\nu\bar{\bar{\nu}}}}^T \cdot A_{\bar{\bar{\nu}}\bar{\nu}}'')(\alpha'_{\bar{\nu}} \cdot (Q_\nu - Q_{\bar{\nu}}))((Q_\nu - Q_{\bar{\nu}})^T \cdot \alpha'_{\bar{\nu}}) - 2({A''_{\nu\bar{\bar{\nu}}}}^T \\
&\cdot A_{\bar{\bar{\nu}}\bar{\nu}}')(\alpha'_{\bar{\nu}} \cdot (Q_\nu - Q_{\bar{\nu}}))((Q_\nu - Q_{\bar{\nu}})^T \cdot \alpha'_{\bar{\nu}}) + 2({A''_{\nu\bar{\bar{\nu}}}}^T \cdot A_{\bar{\bar{\nu}}\bar{\nu}}'')(\alpha''_{\bar{\nu}} \cdot (Q_\nu - Q_{\bar{\nu}}))((Q_\nu \\
&- Q_{\bar{\nu}})^T \cdot \alpha'_{\bar{\nu}}) - \frac{1}{2}({A'_{\nu\bar{\bar{\nu}}}}^T \cdot A_{\bar{\bar{\nu}}\bar{\nu}}'')(P_{\bar{\nu}} - P_\nu)(P_{\bar{\nu}} - P_\nu)^T - \frac{1}{2}({A''_{\nu\bar{\bar{\nu}}}}^T \cdot A_{\bar{\bar{\nu}}\bar{\nu}}')(P_{\bar{\nu}} - P_\nu)(P_{\bar{\nu}} \\
&- P_\nu)^T - ({A'_{\nu\bar{\bar{\nu}}}}^T \cdot A_{\bar{\bar{\nu}}\bar{\nu}}')(\alpha''_{\bar{\nu}} \cdot (Q_\nu - Q_{\bar{\nu}}))(P_{\bar{\nu}} - P_\nu)^T - ({A'_{\nu\bar{\bar{\nu}}}}^T \cdot A_{\bar{\bar{\nu}}\bar{\nu}}'')(\alpha'_{\bar{\nu}} \cdot (Q_\nu - Q_{\bar{\nu}})) \\
&\times (P_{\bar{\nu}} - P_\nu)^T - ({A''_{\nu\bar{\bar{\nu}}}}^T \cdot A_{\bar{\bar{\nu}}\bar{\nu}}')(\alpha'_{\bar{\nu}} \cdot (Q_\nu - Q_{\bar{\nu}}))(P_{\bar{\nu}} - P_\nu)^T + ({A''_{\nu\bar{\bar{\nu}}}}^T \cdot A_{\bar{\bar{\nu}}\bar{\nu}}'')(\alpha''_{\bar{\nu}} \cdot (Q_\nu \\
&- Q_{\bar{\nu}}))(P_{\bar{\nu}} - P_\nu)^T - ({A'_{\nu\bar{\nu}}}^T \cdot A_{\bar{\nu}\bar{\nu}}')(P_{\bar{\nu}} - P_\nu)((Q_\nu - Q_{\bar{\nu}})^T \cdot \alpha''_{\bar{\nu}}) - ({A'_{\nu\bar{\bar{\nu}}}}^T \cdot A_{\bar{\bar{\nu}}\bar{\nu}}'')(P_{\bar{\nu}} \\
&- P_\nu)((Q_\nu - Q_{\bar{\nu}})^T \cdot \alpha'_{\bar{\nu}}) - ({A''_{\nu\bar{\bar{\nu}}}}^T \cdot A_{\bar{\bar{\nu}}\bar{\nu}}')(P_{\bar{\nu}} - P_\nu)((Q_\nu - Q_{\bar{\nu}})^T \cdot \alpha'_{\bar{\nu}}) + ({A''_{\nu\bar{\bar{\nu}}}}^T \cdot A_{\bar{\bar{\nu}}\bar{\nu}}'') \\
&\times (P_{\bar{\nu}} - P_\nu)((Q_\nu - Q_{\bar{\nu}})^T \cdot \alpha''_{\bar{\nu}}) + 2(\nabla {A'_{\nu\bar{\bar{\nu}}}}^T \cdot A_{\bar{\bar{\nu}}\bar{\nu}}')((Q_\nu - Q_{\bar{\nu}})^T \cdot \alpha'_{\bar{\nu}}) - 2(\nabla {A'_{\nu\bar{\bar{\nu}}}}^T \cdot A_{\bar{\bar{\nu}}\bar{\nu}}'') \\
&\times ((Q_\nu - Q_{\bar{\nu}})^T \cdot \alpha''_{\bar{\nu}}) - 2(\nabla {A''_{\nu\bar{\bar{\nu}}}}^T \cdot A_{\bar{\bar{\nu}}\bar{\nu}}')((Q_\nu - Q_{\bar{\nu}})^T \cdot \alpha''_{\bar{\nu}}) - 2(\nabla {A''_{\nu\bar{\bar{\nu}}}}^T \cdot A_{\bar{\bar{\nu}}\bar{\nu}}'')((Q_\nu \\
&- Q_{\bar{\nu}})^T \cdot \alpha'_{\bar{\nu}}) + 2(\nabla {A'_{\bar{\bar{\nu}}\bar{\nu}}}^T \cdot A_{\nu\bar{\bar{\nu}}}')((Q_\nu - Q_{\bar{\nu}})^T \cdot \alpha'_{\bar{\nu}}) - 2(\nabla {A'_{\bar{\bar{\nu}}\bar{\nu}}}^T \cdot A_{\nu\bar{\bar{\nu}}}'')((Q_\nu - Q_{\bar{\nu}})^T \\
&\cdot \alpha''_{\bar{\nu}}) - 2(\nabla {A''_{\bar{\bar{\nu}}\bar{\nu}}}^T \cdot A_{\nu\bar{\bar{\nu}}}')((Q_\nu - Q_{\bar{\nu}})^T \cdot \alpha''_{\bar{\nu}}) - 2(\nabla {A''_{\bar{\bar{\nu}}\bar{\nu}}}^T \cdot A_{\nu\bar{\bar{\nu}}}'')((Q_\nu - Q_{\bar{\nu}})^T \cdot \alpha'_{\bar{\nu}}) \\
&+ (\nabla {A'_{\nu\bar{\bar{\nu}}}}^T \cdot A_{\bar{\bar{\nu}}\bar{\nu}}')(P_{\bar{\nu}} - P_\nu)^T - (\nabla {A''_{\nu\bar{\bar{\nu}}}}^T \cdot A_{\bar{\bar{\nu}}\bar{\nu}}'')(P_{\bar{\nu}} - P_\nu)^T + (\nabla {A'_{\bar{\bar{\nu}}\bar{\nu}}}^T \cdot A_{\nu\bar{\nu}}')(P_{\bar{\nu}} - P_\nu)^T \\
&- (\nabla {A''_{\bar{\bar{\nu}}\bar{\nu}}}^T \cdot A_{\nu\bar{\bar{\nu}}}'')(P_{\bar{\nu}} - P_\nu)^T + \nabla {A'_{\nu\bar{\bar{\nu}}}}^T \cdot \nabla A_{\bar{\bar{\nu}}\bar{\nu}}'' + \nabla {A''_{\nu\bar{\bar{\nu}}}}^T \cdot \nabla A_{\bar{\bar{\nu}}\bar{\nu}}']\}] \qquad \text{(C.7)}
\end{aligned}
$$

$$\dot{\alpha}''_\nu = -2\alpha'_\nu \cdot \alpha''_\nu - 2\alpha''_\nu \cdot \alpha'_\nu - \frac{1}{2}\sum_{\bar{\nu}} e^{-f''(\nu,\bar{\nu})}[\cos f'(\nu,\bar{\nu})\{(\nabla^T \cdot A'_{\nu\bar{\nu}})(\alpha''_{\bar{\nu}} - \alpha''_\nu)$$

$$+ (\nabla^T \cdot A''_{\nu\bar{\nu}})(\alpha'_{\bar{\nu}} - \alpha'_\nu) - 2(\nabla^T \cdot A''_{\nu\bar{\nu}})(\alpha'_{\bar{\nu}} \cdot (Q_\nu - Q_{\bar{\nu}}))((Q_\nu - Q_{\bar{\nu}})^T \cdot \alpha''_{\bar{\nu}})$$

$$- 2(\nabla^T \cdot A''_{\nu\bar{\nu}})(\alpha''_{\bar{\nu}} \cdot (Q_\nu - Q_{\bar{\nu}}))((Q_\nu - Q_{\bar{\nu}})^T \cdot \alpha'_{\bar{\nu}}) + 2(\nabla^T \cdot A'_{\nu\bar{\nu}})(\alpha'_{\bar{\nu}} \cdot (Q_\nu - Q_{\bar{\nu}}))$$

$$\times ((Q_\nu - Q_{\bar{\nu}})^T \cdot \alpha'_{\bar{\nu}}) - 2(\nabla^T \cdot A'_{\nu\bar{\nu}})(\alpha''_{\bar{\nu}} \cdot (Q_\nu - Q_{\bar{\nu}}))((Q_\nu - Q_{\bar{\nu}})^T \cdot \alpha''_{\bar{\nu}})$$

$$+ \frac{1}{2}(\nabla^T \cdot A'_{\nu\bar{\nu}})(P_{\bar{\nu}} - P_\nu)(P_{\bar{\nu}} - P_\nu)^T + (\nabla^T \cdot A'_{\nu\bar{\nu}})(\alpha'_{\bar{\nu}} \cdot (Q_\nu - Q_{\bar{\nu}}))(P_{\bar{\nu}} - P_\nu)^T$$

$$- (\nabla^T \cdot A''_{\nu\bar{\nu}})(\alpha''_{\bar{\nu}} \cdot (Q_\nu - Q_{\bar{\nu}}))(P_{\bar{\nu}} - P_\nu)^T + (\nabla^T \cdot A'_{\nu\bar{\nu}})(P_{\bar{\nu}} - P_\nu)((Q_\nu - Q_{\bar{\nu}})^T$$

$$\cdot \alpha'_{\bar{\nu}}) - (\nabla^T \cdot A''_{\nu\bar{\nu}})(P_{\bar{\nu}} - P_\nu)((Q_\nu - Q_{\bar{\nu}})^T \cdot \alpha''_{\bar{\nu}}) + 2({A'_{\nu\bar{\nu}}}^T \cdot P_{\bar{\nu}})(\alpha'_{\bar{\nu}} - \alpha'_\nu) - 2({A''_{\nu\bar{\nu}}}^T$$

$$\cdot P_{\bar{\nu}})(\alpha''_{\bar{\nu}} - \alpha''_\nu) - 4({A'_{\nu\bar{\nu}}}^T \cdot P_{\bar{\nu}})(\alpha'_{\bar{\nu}} \cdot (Q_\nu - Q_{\bar{\nu}}))((Q_\nu - Q_{\bar{\nu}})^T \cdot \alpha''_{\bar{\nu}}) - 4({A'_{\nu\bar{\nu}}}^T \cdot P_{\bar{\nu}})$$

$$\times (\alpha''_{\bar{\nu}} \cdot (Q_\nu - Q_{\bar{\nu}}))((Q_\nu - Q_{\bar{\nu}})^T \cdot \alpha'_{\bar{\nu}}) - 4({A''_{\nu\bar{\nu}}}^T \cdot P_{\bar{\nu}})(\alpha'_{\bar{\nu}} \cdot (Q_\nu - Q_{\bar{\nu}}))((Q_\nu - Q_{\bar{\nu}})^T$$

$$\cdot \alpha'_{\bar{\nu}}) + 4({A''_{\nu\bar{\nu}}}^T \cdot P_{\bar{\nu}})(\alpha''_{\bar{\nu}} \cdot (Q_\nu - Q_{\bar{\nu}}))((Q_\nu - Q_{\bar{\nu}})^T \cdot \alpha''_{\bar{\nu}}) - ({A''_{\nu\bar{\nu}}}^T \cdot P_{\bar{\nu}})(P_{\bar{\nu}} - P_\nu)$$

$$\times (P_{\bar{\nu}} - P_\nu)^T - 2({A'_{\nu\bar{\nu}}}^T \cdot P_{\bar{\nu}})(P_{\bar{\nu}} - P_\nu)((Q_\nu - Q_{\bar{\nu}})^T \cdot \alpha''_{\bar{\nu}}) - 2({A''_{\nu\bar{\nu}}}^T \cdot P_{\bar{\nu}})(P_{\bar{\nu}} - P_\nu)$$

$$\times ((Q_\nu - Q_{\bar{\nu}})^T \cdot \alpha'_{\bar{\nu}}) - 2({A''_{\nu\bar{\nu}}}^T \cdot P_{\bar{\nu}})(\alpha'_{\bar{\nu}} \cdot (Q_\nu - Q_{\bar{\nu}}))(P_{\bar{\nu}} - P_\nu)^T$$

$$- 2({A'_{\nu\bar{\nu}}}^T \cdot P_{\bar{\nu}})(\alpha''_{\bar{\nu}} \cdot (Q_\nu - Q_{\bar{\nu}}))(P_{\bar{\nu}} - P_\nu)^T - 4({A''_{\nu\bar{\nu}}}^T \cdot \alpha'_{\bar{\nu}} \cdot (Q_\nu - Q_{\bar{\nu}}))(\alpha''_{\bar{\nu}} - \alpha''_\nu)$$

$$- 4({A''_{\nu\bar{\nu}}}^T \cdot \alpha''_{\bar{\nu}} \cdot (Q_\nu - Q_{\bar{\nu}}))(\alpha'_{\bar{\nu}} - \alpha'_\nu) + 4({A'_{\nu\bar{\nu}}}^T \cdot \alpha'_{\bar{\nu}} \cdot (Q_\nu - Q_{\bar{\nu}}))(\alpha'_{\bar{\nu}} - \alpha'_\nu) - 4({A'_{\nu\bar{\nu}}}^T$$

$$\cdot \alpha''_{\bar{\nu}} \cdot (Q_\nu - Q_{\bar{\nu}}))(\alpha''_{\bar{\nu}} - \alpha''_\nu) - 8({A'_{\nu\bar{\nu}}}^T \cdot \alpha'_{\bar{\nu}} \cdot (Q_\nu - Q_{\bar{\nu}}))(\alpha'_{\bar{\nu}} \cdot (Q_\nu - Q_{\bar{\nu}}))((Q_\nu - Q_{\bar{\nu}})^T$$

$$\cdot \alpha''_{\bar{\nu}}) + 8({A'_{\nu\bar{\nu}}}^T \cdot \alpha''_{\bar{\nu}} \cdot (Q_\nu - Q_{\bar{\nu}}))(\alpha''_{\bar{\nu}} \cdot (Q_\nu - Q_{\bar{\nu}}))((Q_\nu - Q_{\bar{\nu}})^T \cdot \alpha''_{\bar{\nu}}) + 8({A''_{\nu\bar{\nu}}}^T \cdot \alpha'_{\bar{\nu}}$$

$$\cdot (Q_\nu - Q_{\bar{\nu}}))(\alpha''_{\bar{\nu}} \cdot (Q_\nu - Q_{\bar{\nu}}))((Q_\nu - Q_{\bar{\nu}})^T \cdot \alpha''_{\bar{\nu}}) + 8({A''_{\nu\bar{\nu}}}^T \cdot \alpha''_{\bar{\nu}} \cdot (Q_\nu - Q_{\bar{\nu}}))(\alpha'_{\bar{\nu}} \cdot (Q_\nu$$

$$- Q_{\bar{\nu}}))((Q_\nu - Q_{\bar{\nu}})^T \cdot \alpha''_{\bar{\nu}}) - 8({A'_{\nu\bar{\nu}}}^T \cdot \alpha'_{\bar{\nu}} \cdot (Q_\nu - Q_{\bar{\nu}}))(\alpha''_{\bar{\nu}} \cdot (Q_\nu - Q_{\bar{\nu}}))((Q_\nu - Q_{\bar{\nu}})^T \cdot \alpha'_{\bar{\nu}})$$

$$- 8({A'_{\nu\bar{\nu}}}^T \cdot \alpha''_{\bar{\nu}} \cdot (Q_\nu - Q_{\bar{\nu}}))(\alpha'_{\bar{\nu}} \cdot (Q_\nu - Q_{\bar{\nu}}))((Q_\nu - Q_{\bar{\nu}})^T \cdot \alpha'_{\bar{\nu}}) - 8({A''_{\nu\bar{\nu}}}^T \cdot \alpha'_{\bar{\nu}} \cdot (Q_\nu$$

$$- Q_{\bar{\nu}}))(\alpha'_{\bar{\nu}} \cdot (Q_\nu - Q_{\bar{\nu}}))((Q_\nu - Q_{\bar{\nu}})^T \cdot \alpha'_{\bar{\nu}}) + 8({A''_{\nu\bar{\nu}}}^T \cdot \alpha''_{\bar{\nu}} \cdot (Q_\nu - Q_{\bar{\nu}}))(\alpha''_{\bar{\nu}} \cdot (Q_\nu - Q_{\bar{\nu}}))$$

$$\times ((Q_\nu - Q_{\bar{\nu}})^T \cdot \alpha'_{\bar{\nu}}) - 2({A'_{\nu\bar{\nu}}}^T \cdot \alpha''_{\bar{\nu}} \cdot (Q_\nu - Q_{\bar{\nu}}))(P_{\bar{\nu}} - P_\nu)(P_{\bar{\nu}} - P_\nu)^T - 2({A''_{\nu\bar{\nu}}}^T \cdot \alpha'_{\bar{\nu}}$$

$$\cdot (Q_\nu - Q_{\bar\nu}))(P_{\bar\nu} - P_\nu)(P_{\bar\nu} - P_\nu)^T - 4({A'_{\nu\bar\nu}}^T \cdot \alpha'_{\bar\nu} \cdot (Q_\nu - Q_{\bar\nu}))(\alpha''_{\bar\nu} \cdot (Q_\nu - Q_{\bar\nu}))(P_{\bar\nu}$$

$$- P_\nu)^T - 4({A'_{\nu\bar\nu}}^T \cdot \alpha''_{\bar\nu} \cdot (Q_\nu - Q_{\bar\nu}))(\alpha'_{\bar\nu} \cdot (Q_\nu - Q_{\bar\nu}))(P_{\bar\nu} - P_\nu)^T - 4({A''_{\nu\bar\nu}}^T \cdot \alpha'_{\bar\nu} \cdot (Q_\nu$$

$$- Q_{\bar\nu}))(\alpha'_{\bar\nu} \cdot (Q_\nu - Q_{\bar\nu}))(P_{\bar\nu} - P_\nu)^T + 4({A''_{\nu\bar\nu}}^T \cdot \alpha''_{\bar\nu} \cdot (Q_\nu - Q_{\bar\nu}))(\alpha''_{\bar\nu} \cdot (Q_\nu - Q_{\bar\nu}))(P_{\bar\nu}$$

$$- P_\nu)^T - 4({A'_{\nu\bar\nu}}^T \cdot \alpha'_{\bar\nu} \cdot (Q_\nu - Q_{\bar\nu}))(P_{\bar\nu} - P_\nu)((Q_\nu - Q_{\bar\nu})^T \cdot \alpha''_{\bar\nu}) - 4({A'_{\nu\bar\nu}}^T \cdot \alpha''_{\bar\nu} \cdot (Q_\nu$$

$$- Q_{\bar\nu}))(P_{\bar\nu} - P_\nu)((Q_\nu - Q_{\bar\nu})^T \cdot \alpha'_{\bar\nu}) - ({A''_{\nu\bar\nu}}^T \cdot \alpha'_{\bar\nu} \cdot (Q_\nu - Q_{\bar\nu}))(P_{\bar\nu} - P_\nu)((Q_\nu - Q_{\bar\nu})^T$$

$$\cdot \alpha'_{\bar\nu}) + 4({A''_{\nu\bar\nu}}^T \cdot \alpha''_{\bar\nu} \cdot (Q_\nu - Q_{\bar\nu}))(P_{\bar\nu} - P_\nu)((Q_\nu - Q_{\bar\nu})^T \cdot \alpha''_{\bar\nu}) - 8(\alpha''_{\bar\nu} \cdot A'_{\nu\bar\nu})((Q_\nu$$

$$- Q_{\bar\nu})^T \cdot \alpha''_{\bar\nu}) - 8(\alpha''_{\bar\nu} \cdot A''_{\nu\bar\nu})((Q_\nu - Q_{\bar\nu})^T \cdot \alpha'_{\bar\nu}) + 8(\alpha'_{\bar\nu} \cdot A'_{\nu\bar\nu})((Q_\nu - Q_{\bar\nu})^T \cdot \alpha'_{\bar\nu})$$

$$- 8(\alpha'_{\bar\nu} \cdot A''_{\nu\bar\nu})((Q_\nu - Q_{\bar\nu})^T \cdot \alpha''_{\bar\nu}) + 4(\alpha'_{\bar\nu} \cdot A'_{\nu\bar\nu})(P_{\bar\nu} - P_\nu)^T - 4(\alpha''_{\bar\nu} \cdot A''_{\nu\bar\nu})(P_{\bar\nu} - P_\nu)^T$$

$$+ 4\nabla A'_{\nu\bar\nu} \cdot \alpha''_{\bar\nu} + 4\nabla A''_{\nu\bar\nu} \cdot \alpha'_{\bar\nu} + 4(\nabla A'_{\nu\bar\nu} \cdot P_{\bar\nu})((Q_\nu - Q_{\bar\nu})^T \cdot \alpha'_{\bar\nu}) - 4(\nabla A''_{\nu\bar\nu} \cdot P_{\bar\nu})((Q_\nu$$

$$- Q_{\bar\nu})^T \cdot \alpha''_{\bar\nu}) + 2(\nabla A'_{\nu\bar\nu} \cdot P_{\bar\nu})(P_{\bar\nu} - P_\nu)^T + 8(\nabla A'_{\nu\bar\nu} \cdot \alpha'_{\bar\nu} \cdot (Q_\nu - Q_{\bar\nu}))((Q_\nu - Q_{\bar\nu})^T$$

$$\cdot \alpha'_{\bar\nu}) - 8(\nabla A'_{\nu\bar\nu} \cdot \alpha''_{\bar\nu} \cdot (Q_\nu - Q_{\bar\nu}))((Q_\nu - Q_{\bar\nu})^T \cdot \alpha''_{\bar\nu}) - 8(\nabla A''_{\nu\bar\nu} \cdot \alpha'_{\bar\nu} \cdot (Q_\nu - Q_{\bar\nu}))((Q_\nu$$

$$- Q_{\bar\nu})^T \cdot \alpha''_{\bar\nu}) - 8(\nabla A''_{\nu\bar\nu} \cdot \alpha''_{\bar\nu} \cdot (Q_\nu - Q_{\bar\nu}))((Q_\nu - Q_{\bar\nu})^T \cdot \alpha'_{\bar\nu}) + 4(\nabla A'_{\nu\bar\nu} \cdot \alpha'_{\bar\nu} \cdot (Q_\nu$$

$$- Q_{\bar\nu}))(P_{\bar\nu} - P_\nu)^T - 4(\nabla A''_{\nu\bar\nu} \cdot \alpha''_{\bar\nu} \cdot (Q_\nu - Q_{\bar\nu}))(P_{\bar\nu} - P_\nu)^T + \sum_{\bar{\bar\nu}} [({A'_{\nu\bar{\bar\nu}}}^T \cdot A_{\bar{\bar\nu}\bar\nu}')(\alpha'_{\bar\nu}$$

$$- \alpha'_\nu) - ({A'_{\nu\bar{\bar\nu}}}^T \cdot A_{\bar{\bar\nu}\bar\nu}'')(\alpha''_{\bar\nu} - \alpha''_\nu) - ({A''_{\nu\bar{\bar\nu}}}^T \cdot A_{\bar{\bar\nu}\bar\nu}')(\alpha''_{\bar\nu} - \alpha''_\nu) - ({A''_{\nu\bar{\bar\nu}}}^T \cdot A_{\bar{\bar\nu}\bar\nu}'')(\alpha'_{\bar\nu}$$

$$- \alpha'_\nu) - 2({A'_{\nu\bar{\bar\nu}}}^T \cdot A_{\bar{\bar\nu}\bar\nu}')(\alpha'_{\bar\nu} \cdot (Q_\nu - Q_{\bar\nu}))((Q_\nu - Q_{\bar\nu})^T \cdot \alpha''_{\bar\nu}) + 2({A'_{\nu\bar{\bar\nu}}}^T \cdot A_{\bar{\bar\nu}\bar\nu}'')(\alpha''_{\bar\nu} \cdot (Q_\nu$$

$$- Q_{\bar\nu}))((Q_\nu - Q_{\bar\nu})^T \cdot \alpha''_{\bar\nu}) + 2({A''_{\nu\bar{\bar\nu}}}^T \cdot A_{\bar{\bar\nu}\bar\nu}')(\alpha''_{\bar\nu} \cdot (Q_\nu - Q_{\bar\nu}))((Q_\nu - Q_{\bar\nu})^T \cdot \alpha''_{\bar\nu})$$

$$+ 2({A''_{\nu\bar{\bar\nu}}}^T \cdot A_{\bar{\bar\nu}\bar\nu}'')(\alpha'_{\bar\nu} \cdot (Q_\nu - Q_{\bar\nu}))((Q_\nu - Q_{\bar\nu})^T \cdot \alpha''_{\bar\nu}) - 2({A'_{\nu\bar{\bar\nu}}}^T \cdot A_{\bar{\bar\nu}\bar\nu}')(\alpha''_{\bar\nu} \cdot (Q_\nu - Q_{\bar\nu}))$$

$$\times ((Q_\nu - Q_{\bar\nu})^T \cdot \alpha'_{\bar\nu}) - 2({A'_{\nu\bar{\bar\nu}}}^T \cdot A_{\bar{\bar\nu}\bar\nu}'')(\alpha'_{\bar\nu} \cdot (Q_\nu - Q_{\bar\nu}))((Q_\nu - Q_{\bar\nu})^T \cdot \alpha'_{\bar\nu}) - 2({A''_{\nu\bar{\bar\nu}}}^T$$

$$\cdot A_{\bar{\bar\nu}\bar\nu}')(\alpha'_{\bar\nu} \cdot (Q_\nu - Q_{\bar\nu}))((Q_\nu - Q_{\bar\nu})^T \cdot \alpha'_{\bar\nu}) + 2({A''_{\nu\bar{\bar\nu}}}^T \cdot A_{\bar{\bar\nu}\bar\nu}'')(\alpha''_{\bar\nu} \cdot (Q_\nu - Q_{\bar\nu}))((Q_\nu$$

$$- Q_{\bar\nu})^T \cdot \alpha'_{\bar\nu}) - \frac{1}{2}({A'_{\nu\bar{\bar\nu}}}^T \cdot A_{\bar{\bar\nu}\bar\nu}'')(P_{\bar\nu} - P_\nu)(P_{\bar\nu} - P_\nu)^T - \frac{1}{2}({A''_{\nu\bar{\bar\nu}}}^T \cdot A_{\bar{\bar\nu}\bar\nu}')(P_{\bar\nu} - P_\nu)(P_{\bar\nu}$$

$$- P_\nu)^T - ({A'_{\nu\bar{\bar\nu}}}^T \cdot A_{\bar{\bar\nu}\bar\nu}')(\alpha''_{\bar\nu} \cdot (Q_\nu - Q_{\bar\nu}))(P_{\bar\nu} - P_\nu)^T - ({A'_{\nu\bar{\bar\nu}}}^T \cdot A_{\bar{\bar\nu}\bar\nu}'')(\alpha'_{\bar\nu} \cdot (Q_\nu - Q_{\bar\nu}))$$

$$\times (P_{\bar\nu} - P_\nu)^T - ({A''_{\nu\bar{\bar\nu}}}^T \cdot A_{\bar{\bar\nu}\bar\nu}')(\alpha'_{\bar\nu} \cdot (Q_\nu - Q_{\bar\nu}))(P_{\bar\nu} - P_\nu)^T + ({A''_{\nu\bar{\bar\nu}}}^T \cdot A_{\bar{\bar\nu}\bar\nu}'')(\alpha''_{\bar\nu} \cdot (Q_\nu$$

$$- Q_{\bar\nu}))(P_{\bar\nu} - P_\nu)^T - ({A'_{\nu\bar{\bar\nu}}}^T \cdot A_{\bar{\bar\nu}\bar\nu}')(P_{\bar\nu} - P_\nu)((Q_\nu - Q_{\bar\nu})^T \cdot \alpha''_{\bar\nu}) - ({A'_{\nu\bar{\bar\nu}}}^T \cdot A_{\bar{\bar\nu}\bar\nu}'')(P_{\bar\nu}$$

$$
\begin{aligned}
&- P_\nu)((Q_\nu - Q_{\bar\nu})^T \cdot \alpha'_{\bar\nu}) - ({A''_{\nu\bar\nu}}^T \cdot A_{\bar\nu\bar\nu}{}')(P_{\bar\nu} - P_\nu)((Q_\nu - Q_{\bar\nu})^T \cdot \alpha'_{\bar\nu}) + ({A''_{\nu\bar\nu}}^T \cdot A_{\bar\nu\bar\nu}{}'')\\
&\times (P_{\bar\nu} - P_\nu)((Q_\nu - Q_{\bar\nu})^T \cdot \alpha''_{\bar\nu}) + 2(\nabla {A'_{\nu\bar\nu}}^T \cdot A_{\bar\nu\bar\nu}{}')((Q_\nu - Q_{\bar\nu})^T \cdot \alpha'_{\bar\nu}) - 2(\nabla {A'_{\nu\bar\nu}}^T \cdot A_{\bar\nu\bar\nu}{}'')\\
&\times ((Q_\nu - Q_{\bar\nu})^T \cdot \alpha''_{\bar\nu}) - 2(\nabla {A''_{\nu\bar\nu}}^T \cdot A_{\bar\nu\bar\nu}{}')((Q_\nu - Q_{\bar\nu})^T \cdot \alpha''_{\bar\nu}) - 2(\nabla {A''_{\nu\bar\nu}}^T \cdot A_{\bar\nu\bar\nu}{}'')((Q_\nu\\
&- Q_{\bar\nu})^T \cdot \alpha'_{\bar\nu}) + 2(\nabla {A'_{\bar\nu\bar\nu}}^T \cdot A_{\nu\bar\nu}{}')((Q_\nu - Q_{\bar\nu})^T \cdot \alpha'_{\bar\nu}) - 2(\nabla {A'_{\bar\nu\bar\nu}}^T \cdot A_{\nu\bar\nu}{}'')((Q_\nu - Q_{\bar\nu})^T\\
&\cdot \alpha''_{\bar\nu}) - 2(\nabla {A''_{\bar\nu\bar\nu}}^T \cdot A_{\nu\bar\nu}{}')((Q_\nu - Q_{\bar\nu})^T \cdot \alpha''_{\bar\nu}) - 2(\nabla {A''_{\bar\nu\bar\nu}}^T \cdot A_{\nu\bar\nu}{}'')((Q_\nu - Q_{\bar\nu})^T \cdot \alpha'_{\bar\nu})\\
&+ (\nabla {A'_{\nu\bar\nu}}^T \cdot A_{\bar\nu\bar\nu}{}')(P_{\bar\nu} - P_\nu)^T - (\nabla {A''_{\nu\bar\nu}}^T \cdot A_{\bar\nu\bar\nu}{}'')(P_{\bar\nu} - P_\nu)^T + (\nabla {A'_{\bar\nu\bar\nu}}^T \cdot A_{\nu\bar\nu}{}')(P_{\bar\nu} - P_\nu)^T\\
&- (\nabla {A''_{\bar\nu\bar\nu}}^T \cdot A_{\nu\bar\nu}{}'')(P_{\bar\nu} - P_\nu)^T + \nabla {A'_{\nu\bar\nu}}^T \cdot \nabla A_{\bar\nu\bar\nu}{}'' + \nabla {A''_{\nu\bar\nu}}^T \cdot \nabla A_{\bar\nu\bar\nu}{}']\}\\
&+ \sin f'(\nu,\bar\nu)\{(\nabla^T \cdot A'_{\nu\bar\nu})(\alpha'_{\bar\nu} - \alpha'_\nu) - (\nabla^T \cdot A''_{\nu\bar\nu})(\alpha''_{\bar\nu} - \alpha''_\nu) - 2(\nabla^T \cdot A''_{\nu\bar\nu})\\
&\times (\alpha'_{\bar\nu} \cdot (Q_\nu - Q_{\bar\nu})(Q_\nu - Q_{\bar\nu})^T \cdot \alpha'_{\bar\nu}) + 2(\nabla^T \cdot A''_{\nu\bar\nu})(\alpha''_{\bar\nu} \cdot (Q_\nu - Q_{\bar\nu}))((Q_\nu - Q_{\bar\nu})^T\\
&\cdot \alpha''_{\bar\nu}) - 2(\nabla^T \cdot A'_{\nu\bar\nu})(\alpha'_{\bar\nu} \cdot (Q_\nu - Q_{\bar\nu}))((Q_\nu - Q_{\bar\nu})^T \cdot \alpha''_{\bar\nu}) - 2(\nabla^T \cdot A'_{\nu\bar\nu})(\alpha''_{\bar\nu} \cdot (Q_\nu\\
&- Q_{\bar\nu}))((Q_\nu - Q_{\bar\nu})^T \cdot \alpha'_{\bar\nu}) - \frac{1}{2}(\nabla^T \cdot A''_{\nu\bar\nu})(P_{\bar\nu} - P_\nu)(P_{\bar\nu} - P_\nu)^T - (\nabla^T \cdot A'_{\nu\bar\nu})\\
&\times (\alpha''_{\bar\nu} \cdot (Q_\nu - Q_{\bar\nu}))(P_{\bar\nu} - P_\nu)^T - (\nabla^T \cdot A''_{\nu\bar\nu})(\alpha'_{\bar\nu} \cdot (Q_\nu - Q_{\bar\nu}))(P_{\bar\nu} - P_\nu)^T\\
&- (\nabla^T \cdot A'_{\nu\bar\nu})(P_{\bar\nu} - P_\nu)((Q_\nu - Q_{\bar\nu})^T \cdot \alpha''_{\bar\nu}) - (\nabla^T \cdot A''_{\nu\bar\nu})(P_{\bar\nu} - P_\nu)((Q_\nu - Q_{\bar\nu})^T\\
&\cdot \alpha'_{\bar\nu}) - 2({A'_{\nu\bar\nu}}^T \cdot P_{\bar\nu})(\alpha''_{\bar\nu} - \alpha''_\nu) - 2({A''_{\nu\bar\nu}}^T \cdot P_{\bar\nu})(\alpha'_{\bar\nu} - \alpha'_\nu) - 4({A'_{\nu\bar\nu}}^T \cdot P_{\bar\nu})(\alpha'_{\bar\nu}\\
&\cdot (Q_\nu - Q_{\bar\nu}))((Q_\nu - Q_{\bar\nu})^T \cdot \alpha'_{\bar\nu}) + 4({A'_{\nu\bar\nu}}^T \cdot P_{\bar\nu})(\alpha''_{\bar\nu} \cdot (Q_\nu - Q_{\bar\nu}))((Q_\nu - Q_{\bar\nu})^T \cdot \alpha''_{\bar\nu})\\
&+ 4({A''_{\nu\bar\nu}}^T \cdot P_{\bar\nu})(\alpha'_{\bar\nu} \cdot (Q_\nu - Q_{\bar\nu}))((Q_\nu - Q_{\bar\nu})^T \cdot \alpha''_{\bar\nu}) + 4({A''_{\nu\bar\nu}}^T \cdot P_{\bar\nu})(\alpha''_{\bar\nu} \cdot (Q_\nu\\
&- Q_{\bar\nu}))((Q_\nu - Q_{\bar\nu})^T \cdot \alpha'_{\bar\nu}) - ({A'_{\nu\bar\nu}}^T \cdot P_{\bar\nu})(P_{\bar\nu} - P_\nu)(P_{\bar\nu} - P_\nu)^T - 2({A'_{\nu\bar\nu}}^T \cdot P_{\bar\nu})(P_{\bar\nu}\\
&- P_\nu)((Q_\nu - Q_{\bar\nu})^T \cdot \alpha'_{\bar\nu}) + 2({A''_{\nu\bar\nu}}^T \cdot P_{\bar\nu})(P_{\bar\nu} - P_\nu)((Q_\nu - Q_{\bar\nu})^T \cdot \alpha''_{\bar\nu}) - 2({A'_{\nu\bar\nu}}^T\\
&\cdot P_{\bar\nu})(\alpha'_{\bar\nu} \cdot (Q_\nu - Q_{\bar\nu}))(P_{\bar\nu} - P_\nu)^T + 2({A''_{\nu\bar\nu}}^T \cdot P_{\bar\nu})(\alpha''_{\bar\nu} \cdot (Q_\nu - Q_{\bar\nu}))(P_{\bar\nu} - P_\nu)^T\\
&- 4({A''_{\nu\bar\nu}}^T \cdot \alpha'_{\bar\nu} \cdot (Q_\nu - Q_{\bar\nu}))(\alpha'_{\bar\nu} - \alpha'_\nu) + 4({A''_{\nu\bar\nu}}^T \cdot \alpha''_{\bar\nu} \cdot (Q_\nu - Q_{\bar\nu}))(\alpha''_{\bar\nu} - \alpha''_\nu)\\
&- 4({A'_{\nu\bar\nu}}^T \cdot \alpha'_{\bar\nu} \cdot (Q_\nu - Q_{\bar\nu}))(\alpha''_{\bar\nu} - \alpha''_\nu) - 4({A'_{\nu\bar\nu}}^T \cdot \alpha''_{\bar\nu} \cdot (Q_\nu - Q_{\bar\nu}))(\alpha'_{\bar\nu} - \alpha'_\nu)\\
&- 8({A'_{\nu\bar\nu}}^T \cdot \alpha'_{\bar\nu} \cdot (Q_\nu - Q_{\bar\nu}))(\alpha'_{\bar\nu} \cdot (Q_\nu - Q_{\bar\nu}))((Q_\nu - Q_{\bar\nu})^T \cdot \alpha'_{\bar\nu}) + 8({A'_{\nu\bar\nu}}^T \cdot \alpha''_{\bar\nu}\\
&\cdot (Q_\nu - Q_{\bar\nu}))(\alpha''_{\bar\nu} \cdot (Q_\nu - Q_{\bar\nu}))((Q_\nu - Q_{\bar\nu})^T \cdot \alpha'_{\bar\nu}) + 8({A''_{\nu\bar\nu}}^T \cdot \alpha'_{\bar\nu} \cdot (Q_\nu - Q_{\bar\nu}))(\alpha''_{\bar\nu}\\
&\cdot (Q_\nu - Q_{\bar\nu}))((Q_\nu - Q_{\bar\nu})^T \cdot \alpha'_{\bar\nu}) + 8({A''_{\nu\bar\nu}}^T \cdot \alpha''_{\bar\nu} \cdot (Q_\nu - Q_{\bar\nu}))(\alpha'_{\bar\nu} \cdot (Q_\nu - Q_{\bar\nu}))((Q_\nu
\end{aligned}
$$

$$
\begin{aligned}
&- Q_{\bar{\nu}})^T \cdot \alpha'_{\bar{\nu}}) + 8({A'_{\nu\bar{\nu}}}^T \cdot \alpha'_{\bar{\nu}} \cdot (Q_\nu - Q_{\bar{\nu}}))(\alpha''_{\bar{\nu}} \cdot (Q_\nu - Q_{\bar{\nu}}))((Q_\nu - Q_{\bar{\nu}})^T \cdot \alpha''_{\bar{\nu}}) \\
&+ 8({A'_{\nu\bar{\nu}}}^T \cdot \alpha''_{\bar{\nu}} \cdot (Q_\nu - Q_{\bar{\nu}}))(\alpha'_{\bar{\nu}} \cdot (Q_\nu - Q_{\bar{\nu}}))((Q_\nu - Q_{\bar{\nu}})^T \cdot \alpha''_{\bar{\nu}}) + 8({A''_{\nu\bar{\nu}}}^T \cdot \alpha'_{\bar{\nu}} \\
&\cdot (Q_\nu - Q_{\bar{\nu}}))(\alpha'_{\bar{\nu}} \cdot (Q_\nu - Q_{\bar{\nu}}))((Q_\nu - Q_{\bar{\nu}})^T \cdot \alpha''_{\bar{\nu}}) - 8({A''_{\nu\bar{\nu}}}^T \cdot \alpha''_{\bar{\nu}} \cdot (Q_\nu - Q_{\bar{\nu}}))(\alpha''_{\bar{\nu}} \\
&\cdot (Q_\nu - Q_{\bar{\nu}}))((Q_\nu - Q_{\bar{\nu}})^T \cdot \alpha''_{\bar{\nu}}) - 2({A'_{\nu\bar{\nu}}}^T \cdot \alpha'_{\bar{\nu}} \cdot (Q_\nu - Q_{\bar{\nu}}))(P_{\bar{\nu}} - P_\nu)(P_{\bar{\nu}} - P_\nu)^T \\
&+ 2({A''_{\nu\bar{\nu}}}^T \cdot \alpha''_{\bar{\nu}} \cdot (Q_\nu - Q_{\bar{\nu}}))(P_{\bar{\nu}} - P_\nu)(P_{\bar{\nu}} - P_\nu)^T - 4({A'_{\nu\bar{\nu}}}^T \cdot \alpha'_{\bar{\nu}} \cdot (Q_\nu - Q_{\bar{\nu}}))(\alpha'_{\bar{\nu}} \\
&\cdot (Q_\nu - Q_{\bar{\nu}}))(P_{\bar{\nu}} - P_\nu)^T + 4({A'_{\nu\bar{\nu}}}^T \cdot \alpha''_{\bar{\nu}} \cdot (Q_\nu - Q_{\bar{\nu}}))(\alpha''_{\bar{\nu}} \cdot (Q_\nu - Q_{\bar{\nu}}))(P_{\bar{\nu}} - P_\nu)^T \\
&+ 4({A''_{\nu\bar{\nu}}}^T \cdot \alpha'_{\bar{\nu}} \cdot (Q_\nu - Q_{\bar{\nu}}))(\alpha''_{\bar{\nu}} \cdot (Q_\nu - Q_{\bar{\nu}}))(P_{\bar{\nu}} - P_\nu)^T + 4({A''_{\nu\bar{\nu}}}^T \cdot \alpha''_{\bar{\nu}} \cdot (Q_\nu \\
&- Q_{\bar{\nu}}))(\alpha'_{\bar{\nu}} \cdot (Q_\nu - Q_{\bar{\nu}}))(P_{\bar{\nu}} - P_\nu)^T - 4({A'_{\nu\bar{\nu}}}^T \cdot \alpha'_{\bar{\nu}} \cdot (Q_\nu - Q_{\bar{\nu}}))(P_{\bar{\nu}} - P_\nu)((Q_\nu \\
&- Q_{\bar{\nu}})^T \cdot \alpha'_{\bar{\nu}}) + 4({A'_{\nu\bar{\nu}}}^T \cdot \alpha''_{\bar{\nu}} \cdot (Q_\nu - Q_{\bar{\nu}}))(P_{\bar{\nu}} - P_\nu)((Q_\nu - Q_{\bar{\nu}})^T \cdot \alpha''_{\bar{\nu}}) \\
&+ 4({A''_{\nu\bar{\nu}}}^T \cdot \alpha'_{\bar{\nu}} \cdot (Q_\nu - Q_{\bar{\nu}}))(P_{\bar{\nu}} - P_\nu)((Q_\nu - Q_{\bar{\nu}})^T \cdot \alpha''_{\bar{\nu}}) + 4({A''_{\nu\bar{\nu}}}^T \cdot \alpha''_{\bar{\nu}} \cdot (Q_\nu \\
&- Q_{\bar{\nu}}))(P_{\bar{\nu}} - P_\nu)((Q_\nu - Q_{\bar{\nu}})^T \cdot \alpha'_{\bar{\nu}}) - 8(\alpha''_{\bar{\nu}} \cdot A'_{\nu\bar{\nu}})((Q_\nu - Q_{\bar{\nu}})^T \cdot \alpha'_{\bar{\nu}}) + 8(\alpha''_{\bar{\nu}} \\
&\cdot A''_{\nu\bar{\nu}})((Q_\nu - Q_{\bar{\nu}})^T \cdot \alpha''_{\bar{\nu}}) - 8(\alpha'_{\bar{\nu}} \cdot A'_{\nu\bar{\nu}})((Q_\nu - Q_{\bar{\nu}})^T \cdot \alpha''_{\bar{\nu}}) - 8(\alpha'_{\bar{\nu}} \cdot A''_{\nu\bar{\nu}})((Q_\nu \\
&- Q_{\bar{\nu}})^T \cdot \alpha'_{\bar{\nu}}) - 4(\alpha'_{\bar{\nu}} \cdot A''_{\nu\bar{\nu}})(P_{\bar{\nu}} - P_\nu)^T - 4(\alpha''_{\bar{\nu}} \cdot A'_{\nu\bar{\nu}})(P_{\bar{\nu}} - P_\nu)^T + 4(\nabla A'_{\nu\bar{\nu}}) \cdot \alpha'_{\bar{\nu}} \\
&- 4(\nabla A''_{\nu\bar{\nu}}) \cdot \alpha''_{\bar{\nu}} - 4(\nabla A'_{\nu\bar{\nu}} \cdot P_{\bar{\nu}})((Q_\nu - Q_{\bar{\nu}})^T \cdot \alpha''_{\bar{\nu}}) - 4(\nabla A''_{\nu\bar{\nu}} \cdot P_{\bar{\nu}})((Q_\nu - Q_{\bar{\nu}})^T \\
&\cdot \alpha'_{\bar{\nu}}) - 2(\nabla A''_{\nu\bar{\nu}} \cdot P_{\bar{\nu}})(P_{\bar{\nu}} - P_\nu)^T - 8(\nabla A''_{\nu\bar{\nu}} \cdot \alpha'_{\bar{\nu}} \cdot (Q_\nu - Q_{\bar{\nu}}))((Q_\nu - Q_{\bar{\nu}})^T \cdot \alpha'_{\bar{\nu}}) \\
&+ 8(\nabla A''_{\nu\bar{\nu}} \cdot \alpha''_{\bar{\nu}} \cdot (Q_\nu - Q_{\bar{\nu}}))((Q_\nu - Q_{\bar{\nu}})^T \cdot \alpha''_{\bar{\nu}}) - 8(\nabla A'_{\nu\bar{\nu}} \cdot \alpha'_{\bar{\nu}} \cdot (Q_\nu - Q_{\bar{\nu}}))((Q_\nu \\
&- Q_{\bar{\nu}})^T \cdot \alpha''_{\bar{\nu}}) - 8(\nabla A'_{\nu\bar{\nu}} \cdot \alpha''_{\bar{\nu}} \cdot (Q_\nu - Q_{\bar{\nu}}))((Q_\nu - Q_{\bar{\nu}})^T \cdot \alpha'_{\bar{\nu}}) - 4(\nabla A'_{\nu\bar{\nu}} \cdot \alpha''_{\bar{\nu}} \cdot (Q_\nu \\
&- Q_{\bar{\nu}}))(P_{\bar{\nu}} - P_\nu)^T - 4(\nabla A''_{\nu\bar{\nu}} \cdot \alpha'_{\bar{\nu}} \cdot (Q_\nu - Q_{\bar{\nu}}))(P_{\bar{\nu}} - P_\nu)^T \\
&+ \sum_{\bar{\bar{\nu}}} [({A''_{\nu\bar{\bar{\nu}}}}^T \cdot A_{\bar{\bar{\nu}}\bar{\nu}}'')(\alpha''_{\bar{\nu}} - \alpha''_\nu) - ({A''_{\nu\bar{\bar{\nu}}}}^T \cdot A_{\bar{\bar{\nu}}\bar{\nu}}')(\alpha'_{\bar{\nu}} - \alpha'_\nu) - ({A'_{\nu\bar{\bar{\nu}}}}^T \cdot A_{\bar{\bar{\nu}}\bar{\nu}}')(\alpha''_{\bar{\nu}} - \alpha''_\nu) \\
&- ({A'_{\nu\bar{\bar{\nu}}}}^T \cdot A_{\bar{\bar{\nu}}\bar{\nu}}'')(\alpha'_{\bar{\nu}} - \alpha_\nu') - 2({A'_{\nu\bar{\bar{\nu}}}}^T \cdot A_{\bar{\bar{\nu}}\bar{\nu}}')(\alpha'_{\bar{\nu}} \cdot (Q_\nu - Q_{\bar{\nu}}))((Q_\nu - Q_{\bar{\nu}})^T \cdot \alpha'_{\bar{\nu}}) \\
&+ 2({A'_{\nu\bar{\bar{\nu}}}}^T \cdot A_{\bar{\bar{\nu}}\bar{\nu}}'')(\alpha''_{\bar{\nu}} \cdot (Q_\nu - Q_{\bar{\nu}}))((Q_\nu - Q_{\bar{\nu}})^T \cdot \alpha'_{\bar{\nu}}) + 2({A''_{\nu\bar{\bar{\nu}}}}^T \cdot A_{\bar{\bar{\nu}}\bar{\nu}}')(\alpha''_{\bar{\nu}} \cdot (Q_\nu - Q_{\bar{\nu}})) \\
&\times ((Q_\nu - Q_{\bar{\nu}})^T \cdot \alpha'_{\bar{\nu}}) + 2({A''_{\nu\bar{\bar{\nu}}}}^T \cdot A_{\bar{\bar{\nu}}\bar{\nu}}'')(\alpha'_{\bar{\nu}} \cdot (Q_\nu - Q_{\bar{\nu}}))((Q_\nu - Q_{\bar{\nu}})^T \cdot \alpha'_{\bar{\nu}}) + 2({A'_{\nu\bar{\bar{\nu}}}}^T \\
&\cdot A_{\bar{\bar{\nu}}\bar{\nu}}')(\alpha''_{\bar{\nu}} \cdot (Q_\nu - Q_{\bar{\nu}}))((Q_\nu - Q_{\bar{\nu}})^T \cdot \alpha''_{\bar{\nu}}) + 2({A'_{\nu\bar{\bar{\nu}}}}^T \cdot A_{\bar{\bar{\nu}}\bar{\nu}}'')(\alpha'_{\bar{\nu}} \cdot (Q_\nu - Q_{\bar{\nu}}))((Q_\nu \\
&- Q_{\bar{\nu}})^T \cdot \alpha''_{\bar{\nu}}) + 2({A''_{\nu\bar{\bar{\nu}}}}^T \cdot A_{\bar{\bar{\nu}}\bar{\nu}}')(\alpha'_{\bar{\nu}} \cdot (Q_\nu - Q_{\bar{\nu}}))((Q_\nu - Q_{\bar{\nu}})^T \cdot \alpha''_{\bar{\nu}}) - 2({A''_{\nu\bar{\bar{\nu}}}}^T \cdot A_{\bar{\bar{\nu}}\bar{\nu}}'')
\end{aligned}
$$

$$\times (\alpha''_{\bar{\nu}} \cdot (Q_\nu - Q_{\bar{\nu}}))((Q_\nu - Q_{\bar{\nu}})^T \cdot \alpha''_{\bar{\nu}}) - \frac{1}{2}({A'_{\nu\bar{\nu}}}^T \cdot A_{\bar{\nu}\nu}')(P_{\bar{\nu}} - P_\nu)(P_{\bar{\nu}} - P_\nu)^T$$

$$+ \frac{1}{2}({A''_{\nu\bar{\nu}}}^T \cdot A_{\bar{\nu}\nu}'')(P_{\bar{\nu}} - P_\nu)(P_{\bar{\nu}} - P_\nu)^T - ({A'_{\nu\bar{\nu}}}^T \cdot A_{\bar{\nu}\nu}')(\alpha'_{\bar{\nu}} \cdot (Q_\nu - Q_{\bar{\nu}}))(P_{\bar{\nu}} - P_\nu)^T$$

$$+ ({A'_{\nu\bar{\nu}}}^T \cdot A_{\bar{\nu}\nu}'')(\alpha''_{\bar{\nu}} \cdot (Q_\nu - Q_{\bar{\nu}}))(P_{\bar{\nu}} - P_\nu)^T + ({A''_{\nu\bar{\nu}}}^T \cdot A_{\bar{\nu}\nu}')(\alpha''_{\bar{\nu}} \cdot (Q_\nu - Q_{\bar{\nu}}))(P_{\bar{\nu}}$$

$$- P_\nu)^T + ({A''_{\nu\bar{\nu}}}^T \cdot A_{\bar{\nu}\nu}'')(\alpha'_{\bar{\nu}} \cdot (Q_\nu - Q_{\bar{\nu}}))(P_{\bar{\nu}} - P_\nu)^T - ({A'_{\nu\bar{\nu}}}^T \cdot A_{\bar{\nu}\nu}')(P_{\bar{\nu}} - P_\nu)((Q_\nu$$

$$- Q_{\bar{\nu}})^T \cdot \alpha'_{\bar{\nu}}) - ({A'_{\nu\bar{\nu}}}^T \cdot A_{\bar{\nu}\nu}'')(P_{\bar{\nu}} - P_\nu)((Q_\nu - Q_{\bar{\nu}})^T \cdot \alpha''_{\bar{\nu}}) + ({A''_{\nu\bar{\nu}}}^T \cdot A_{\bar{\nu}\nu}')(P_{\bar{\nu}} - P_\nu)$$

$$\times ((Q_\nu - Q_{\bar{\nu}})^T \cdot \alpha''_{\bar{\nu}}) + ({A''_{\nu\bar{\nu}}}^T \cdot A_{\bar{\nu}\nu}'')(P_{\bar{\nu}} - P_\nu)((Q_\nu - Q_{\bar{\nu}})^T \cdot \alpha'_{\bar{\nu}}) - 2(\nabla {A''_{\nu\bar{\nu}}}^T \cdot A_{\bar{\nu}\nu}')$$

$$\times ((Q_\nu - Q_{\bar{\nu}})^T \cdot \alpha'_{\bar{\nu}}) + 2(\nabla {A''_{\nu\bar{\nu}}}^T \cdot A_{\bar{\nu}\nu}'')((Q_\nu - Q_{\bar{\nu}})^T \cdot \alpha''_{\bar{\nu}}) - 2(\nabla {A'_{\nu\bar{\nu}}}^T \cdot A_{\bar{\nu}\nu}')((Q_\nu$$

$$- Q_{\bar{\nu}})^T \cdot \alpha''_{\bar{\nu}}) - 2(\nabla {A'_{\nu\bar{\nu}}}^T \cdot A_{\bar{\nu}\nu}'')((Q_\nu - Q_{\bar{\nu}})^T \cdot \alpha'_{\bar{\nu}}) - 2(\nabla {A''_{\bar{\nu}\nu}}^T \cdot A_{\nu\bar{\nu}}')((Q_\nu - Q_{\bar{\nu}})^T$$

$$\cdot \alpha'_{\bar{\nu}}) + 2(\nabla {A''_{\bar{\nu}\nu}}^T \cdot A_{\nu\bar{\nu}}'')((Q_\nu - Q_{\bar{\nu}})^T \cdot \alpha''_{\bar{\nu}}) - 2(\nabla {A'_{\bar{\nu}\nu}}^T \cdot A_{\nu\bar{\nu}}')((Q_\nu - Q_{\bar{\nu}})^T \cdot \alpha''_{\bar{\nu}})$$

$$- 2(\nabla {A'_{\bar{\nu}\nu}}^T \cdot A_{\nu\bar{\nu}}'')((Q_\nu - Q_{\bar{\nu}})^T \cdot \alpha'_{\bar{\nu}}) - (\nabla {A'_{\nu\bar{\nu}}}^T \cdot A_{\bar{\nu}\nu}'')(P_{\bar{\nu}} - P_\nu)^T - (\nabla {A''_{\nu\bar{\nu}}}^T \cdot A_{\bar{\nu}\nu}')$$

$$\times (P_{\bar{\nu}} - P_\nu)^T - (\nabla {A'_{\bar{\nu}\nu}}^T \cdot A_{\nu\bar{\nu}}'')(P_{\bar{\nu}} - P_\nu)^T - (\nabla {A''_{\bar{\nu}\nu}}^T \cdot A_{\nu\bar{\nu}}')(P_{\bar{\nu}} - P_\nu)^T + \nabla {A'_{\nu\bar{\nu}}}^T$$

$$\cdot \nabla A_{\bar{\nu}\nu}' - \nabla {A''_{\nu\bar{\nu}}}^T \cdot \nabla A_{\bar{\nu}\nu}'']\}] \tag{C.8}$$

APPENDIX D

COMPUTATIONAL CONSIDERATIONS IN THE FVB/GB

The numerical integration of the equations of motion for bath wave-packets under a FVB/GB treatment proved to be sensitive to the method of integration and precision of parameters. A fourth-order Runge-Kutta scheme was found to be sufficient for successful integration. The propagation of bath wave packets accompanying vibrational levels with very little population necessitates the use of a software package that allows for multiple-precision floating-point computation. The Gnu Multiple Precision package (GMP, ver. 4.3.2) was used in conjunction with the MPFR library (ver. 2.4.2) to provide 96 significant digits (384 bits) along with the corresponding arithmetic operations.

Below is a representative program, written in c++, used to propagate one-dimensional bath wave packets under the FVB/GB theory with conditions consistent with case D, presented in Ch. IV Sec. E.

File: "main.cc"

```
//Main fvb/gb program
#include "fvb.h"

int main(int argc, char *argv[])
{
cout<<"**********************"<<endl;
cout<<":::::   hello   ::::::"<<endl;
cout<<"**********************"<<endl;

switch (argc) {
case 1: {
cout<<"********** No input parameters.  Using defaults. **********"<<endl;
fvb();
break;
}
case 8: {
cout<<"********** Parameters provided from file: "<<"'"<<argv[2]<<"', "<<
"'"<<argv[3]<<", '"<<argv[4]<<", '"<<argv[5]<<", '"<<argv[6]<<", '"<<argv[7]<<endl;
fvb(argv);
break;
}
default: {
cout<<" Usage: fvb.exe"<<endl;
cout<<"        fvb.exe -wfile 'parameter_file'"<<endl;
}
}
}
```

File: "fvb.cc"

```
//fvb program
#include "fvb.h"

//default program
void fvb()
{
cout.precision(16);
```

```
/************************
 * Declare constants
 */
fvbConstants c;
c.set_basis_size(11);
c.set_xmin(-30.);
c.set_xmax(30.);
c.set_npoints(2000.);
c.set_dx();

/************************
 * Declare potential
 * parameters
 * this is for the excited state.
 * In this case there is only propagation
 * on the excited state so we only need
 * one potential defined
  * Note the initial displacements are negative.
  * this is because the internuclear distance
  * in the excited electronic state is greater
  * than in the ground state
 */

fvbPotentials fp;
fp.set_sys_freq(1);
fp.set_bath_freq(0.333333333333*fp.omega_sys_);
fp.set_coupling(0.05);
fp.set_sys_eq(-sqrt(3));
//fp.set_ve_qe_(0.5);
fp.set_bath_Qe(-sqrt(3)); //set bath displacement
fp.hermites_s = new double[c.npoints() * c.nbasis];
fp.wfpolys_s = new double[c.npoints() * c.nbasis];
fp.ground_wf = new double[c.npoints()];
fp.gamma = new double[c.nbasis];

/*****************************
 * Get position rep wf's
 * of system
```

```
 */
fp.pos_rep_sys(c);
fp.pos_rep_sys_g(c);
fp.calculate_overlap(c);

/*****************************
 * Declare bath wave packets
 * each accompanying a system
 * vibrational level
 */

fvbWavePacket *gwp = new fvbWavePacket[c.nbasis];

/*****************************
 * Create some operators
 * creation, annhilation,
 * position, momentum, etc...
 */

fvbOperators *operators = new fvbOperators[1];
operators[0].setops(c,fp);

/****************************************
 * Initialize wave packet parameters
 */

for (int i=0; i<c.nbasis; i++) {
gwp[i].Initialize(i,operators,fp.qe_.get_d(),fp);
}

/*****************************
 * Set up time variables
 */

fvbTimeParameters ft;
   ft.tdt_.set_prec(precision);
ft.tmn_.set_prec(precision);
ft.tmx_.set_prec(precision);
ft.tnstep_.set_prec(precision);
```

```
ft.set_tmin(0);
ft.set_tmax(200*(2*M_PI));
//ft.set_tsteps(100);
//ft.set_dt();
   ft.tdt_ = "1.e-5";
   ft.set_dt(ft.tdt_.get_d());
ft.set_tsteps();




/**********************************
 * How often to write data when
 * using quality controlled
 * runge-kutta and gmp
 */

ft.every_dt_.set_prec(precision);
mpfr_class dummy("0",precision);
dummy = "0.1";
//dummy *= (2*M_PI);
ft.every_dt_ = dummy;

/*****************************
 * Declare Propagator object
 */

fvbPropagate prop;

//~ //set initial population
//~ prop[0].totnorm = 0.;
//~ for (int i=0; i<c.nbasis; i++)
//~ {
//~ gwp[i].calculate_norm(i);
//~ prop[0].totnorm += gwp[i].norm;
//~ }
//~ prop[0].initnorm = prop[0].totnorm;
```

```
/*******************************
 * Propagate wave packets from
 * tmin to tmax, writing at dt
 */

prop.forward(gwp,c,ft,fp);
};

/*****************************************************
*
* Using input from Gui
*/

void fvb(char *opts[])
{
cout.precision(20);

//constants
fvbConstants c;

//set up time grid
fvbTimeParameters t;

//get stuff from gui
get_input(opts, c, t);

//bath wave packets
fvbWavePacket *gwp = new fvbWavePacket[c.nbasis];

//some operators (raising, lowering, etc...)
fvbOperators operators;
// operators.setops(c,fp);

//sets appropriate time variables
//t.dt(t.tdt/*((2*M_PI)/c.omega_sys)*/);
//t.dt_set_steps();

//initialize wave packet parameters
// for (int i=0; i<c.nbasis; i++)
```

```
// {
// gwp[i].Initialize(i,operators,c.disp,c);
// }
//exit(1);
//propagate wave packets
// fvbPropagate prop(c);

//set initial population
/*  prop.totnorm = 0.;
 *  for (int i=0; i<c.nbasis; i++)
 *  {
 *  gwp[i].calculate_norm(i);
 *  prop.totnorm += gwp[i].norm;
 *  }
 *  prop.initnorm = prop.totnorm;
 */

//propagation routine
// prop.forward(gwp,c,t);
}

void get_input(char *opts[], fvbConstants &c, fvbTimeParameters &t)
{
/*****************************
* Gets Parameters Set by
* The UI and sets the
*  Appropriate Variables
*/

ifstream insyspot, inbathpot, ingeneral, intime, inwp, incoupling;

insyspot.open(opts[2]);
inbathpot.open(opts[3]);
ingeneral.open(opts[4]);
intime.open(opts[5]);
inwp.open(opts[6]);
incoupling.open(opts[7]);

if (insyspot.fail() || inbathpot.fail() || ingeneral.fail()
```

```
|| intime.fail() || inwp.fail() || incoupling.fail() ) {
cout<<"invalid filename"<<endl;
exit(1);
}

char systype[100], bathtype[50],coupling[50];
int freq;
insyspot>>systype;
char h[] = "Harmonic";
char bl[] = "Bilinear";

cout<<" *************************"<<endl;
cout<<"sys pot: "<<systype;
/*****************
* System
*/
if (!strcmp(systype,h)) {
insyspot>>c.omega_sys;
c.omega_sys_ = c.omega_sys;
cout<<" w/ freq = "<<c.omega_sys<<" "<<c.omega_sys_<<endl;
}

/*******************
* Bath
*/
cout<<" *************************"<<endl;
inbathpot>>bathtype;
cout<<"bath pot: "<<bathtype;

if (!strcmp(bathtype,h)) {
inbathpot>>c.omega_bath;
c.omega_bath_ = c.omega_bath;
cout<<" w/ freq = "<<c.omega_bath<<" "<<c.omega_bath_<<endl;
}

/******************
* Coupling
*/
cout<<" *************************"<<endl;
```

```
incoupling>>coupling;
cout<<"coupling : "<<coupling;

if ( !strcmp(coupling,bl) ) {
char hold[10];
incoupling>>hold;
c.coupling_ = hold;
c.coupling = c.coupling_.get_d();
//c.coupling_ = c.coupling;
cout<<" w/ J= "<<c.coupling<<" "<<c.coupling_<<endl;
}

/******************
* General Parameters
*/
cout<<" *************************"<<endl;
ingeneral>>c.sysmodes>>c.nbath>>c.nbasis>>c.disp>>c.bath_disp;
c.disp_ = c.disp;
cout<<"bath dim = "<<c.nbath<<endl;
cout<<"sys basis = "<<c.nbasis<<endl;
cout<<"sys displacement = "<<c.disp<<endl;
cout<<"*************************"<<endl;

/*********************
* Time Parameters
*/
/* t.tdt_.set_prec(precision);
t.tmn_.set_prec(precision);
t.tmx_.set_prec(precision);
t.tnstep_.set_prec(precision);

double tstep;
cout<<" *************************"<<endl;
char tmin[16], tmax[16], tsteps_n[16], tnstep_n[16];
intime>>tmin>>tmax>>tsteps_n>>tnstep_n;
//intime>>t.tmn>>t.tmx>>tstep>>t.tnstep;
t.tdt_ = tsteps_n;
t.tmn_ = tmin;
t.tmx_ = tmax;
```

```
t.tnstep_ = tnstep_n;
double test = t.tdt_.get_d();

t.dt(test);
t.tmn = t.tmn_.get_d();
t.tmx = t.tmx_.get_d();

cout<<"start time = "<<t.tmn<<endl;
cout<<"finish time = "<<t.tmx<<" sys vibrational periods"<<endl;
cout<<"step size = "<<t.tdt<<" x sys vib period"<<" "<<t.tdt_<<endl;
cout<<"# of steps = "<<t.tnstep<<endl;
*/
/************************
* close files
*/

insyspot.close(); inbathpot.close(); ingeneral.close(); incoupling.close(); intime.close();
inwp.close();

//exit(1);
}

int func(double t, const double y[], double f[], void *params) {

gslholder *gslh = (gslholder *) params;

//for (int i=0; i < gslh->cs.nbasis; i++) {
gslh->dvs[0].get_derivs(gslh->cs,y,f);
//}
       return GSL_SUCCESS;
}

int jac (double t, const double y[], double *dfdy,
          double dfdt[], void *params)
     {

       return GSL_SUCCESS;
     }
```

File: "fvb.h"

```
#ifndef _FVB_H
#define _FVB_H

//includes
#include <iostream>
#include <fstream>
#include <cstdlib>
#include <math.h>
#include <string>
#include <climits>
using namespace std;
#include <cblas.h>
#include <complex>
#include <gsl/gsl_errno.h>
#include <gsl/gsl_odeiv.h>
#include <gsl/gsl_sf_gamma.h>
#include <gmp.h>
#include <gmpfrxx.h>

//definitions
typedef complex<double> dcomp;
#define Kronecker(a,b) (( a == b ? 1 : 0))
//precision (in bits) for GMP
static const unsigned long precision = 384;

#define MAXSTP 10000000

#define MAX(a,b) ((a<b ? (a) : (b)))

//#define RK45
//#define RKCONST
//#define GMP
//#define DOUBLEFINITE
#define GMPRK4
//#define RK4QC

//classes
```

```
#include "fvbConstants.h"
#include "fvbPotentials.h"
#include "fvbOperators.h"
#include "fvbWavePackets.h"
#include "fvbTimeParameters.h"
#include "fvbDerivatives.h"

class gslholder
{
public:
int level;
fvbWavePacket *wps;
fvbDerivatives *dvs;
fvbConstants cs;
double *all_params, *all_params_i;

gslholder() {};
~gslholder(){};
};
#include "fvbPropagate.h"

//function prototypes
void get_input(char *opts[], fvbConstants &c, fvbTimeParameters &t);
void fvb();
void fvb(char *opts[]);
int func(double t, const double y[], double f[], void *params);

int jac (double t, const double y[], double *dfdy,
         double dfdt[], void *params);
#endif
```

File: "fvbConstants.h"

```
/*************************************************************************
 *            fvbConstants.h
 *
 *  Wed Dec  3 12:32:59 2008
 *  Copyright  2008  Craig Chapman
 *  cchapma2@uoregon.edu
```

```
 ***************************************************************************/
//#include "fvb.h"

class fvbConstants
{
public:
//static const unsigned long precision = 128;
int sysmodes;
int nbasis;//= 11;  //how many system levels to populate initially
int nbath;
double omega_sys;// =1;//6.283185307179586; //system frequency
mpfr_class omega_sys_;
double omega_bath; //bath frequency set in initializer
mpfr_class omega_bath_;
double coupling; //bilinear coupling constant
mpfr_class coupling_;
double disp; //displace system coord by this much
mpfr_class disp_;
double bath_disp;  //does nothing for now
mpfr_class gmpbath_disp;
double x_max, x_min,d_x;
int n_points;

void set_sys_freq(mpfr_class x) {omega_sys_ = x;};
void set_bath_freq(mpfr_class x) {omega_bath_ = x;};
void set_coupling(mpfr_class x) {coupling_ = x;};
void set_basis_size(int x) {nbasis = x;};
void set_xmax(double x) {x_max = x;};
void set_xmin(double x) {x_min = x;};
void set_npoints(int x) {n_points = x;};
void set_dx() {d_x = (x_max - x_min)/n_points;};

double xmax() {return x_max;};
double xmin() {return x_min;};
int npoints() {return n_points;};
double dx() {return d_x;};

fvbConstants();
~fvbConstants() {};
```

```
};
```

File: "fvbConstants.cc"

```
/*************************************************************************
 *            fvbConstants.cc
 *
 *  Wed Jan 14 11:08:13 2009
 *  Copyright  2009  Craig Chapman
 *  cchapma2@uoregon.edu
 *************************************************************************/
#include "fvb.h"

fvbConstants::fvbConstants()
{
omega_sys_.set_prec(precision);
coupling_.set_prec(precision);
disp_.set_prec(precision);
omega_bath_.set_prec(precision);
};
```

File: "fvbDerivatives.h"

```
/*************************************************************************
 *            fvbDerivatives.h
 *
 *  Wed Dec  3 12:28:40 2008
 *  Copyright  2008  Craig Chapman
 *  cchapma2@uoregon.edu
 *************************************************************************/
//#include "fvb.h"

class fvbDerivatives
{
double usb, divusb, divdivusb, ub, divub, divdivub;
mpfr_class usb_, divusb_, divdivusb_, ub_, divub_, divdivub_;
double fim, fre;
mpfr_class fim_, fre_;
double sumgre, sumgim, sumP, sumQ, sumaim, sumare;
mpfr_class sumgre_, sumgim_, sumP_, sumQ_, sumaim_, sumare_;
double qnnb;
```

```
mpfr_class qnnb_;
double holder, holder1;
mpfr_class holder_, holder1_;
mpfr_class half_;
mpfr_class exp_fim_;
mpfr_class damp_;

public:
//Functions are overloaded for GSL ODE propagation and GMP usage
//Re(f)
double freal(int one, int two, fvbWavePacket *gwp);
void freal(mpfr_class *gmpfre, int one, int two, fvbWavePacket *gwp);
double freal(int one, int two, const double y[]);
void freal(mpfr_class *gmpfre, int one, int two, const double y[]);
//Im(f)
double fimaginary(int one, int two, fvbWavePacket *gwp);
void fimaginary(mpfr_class *fim_, int one, int two, fvbWavePacket *gwp);
double fimaginary(int one, int two, const double y[]);
void fimaginary(mpfr_class fim_, int one, int two, const double y[]);
//sets linear time derivatives - used for finite difference
void get_derivs(int level, fvbWavePacket *gwp, fvbConstants c);
void get_derivs_gmp(int level, fvbWavePacket *gwp, fvbConstants c,fvbPotentials);
//sets linear time derivatives - used for gsl routines
void get_derivs(fvbConstants c, const double y[], double f[]);
//sets ubath, divubath, divdivubath
void ubath(int one, fvbWavePacket *gwp, fvbConstants c);
void ubath_gmp(mpfr_class *ub_, mpfr_class *divub_, mpfr_class *divdivub_,
int one, fvbWavePacket *gwp, fvbPotentials c);
void ubath(int one, fvbConstants c, const double y[]);
//sets uint, divuint, divdivuint
void uint(int one, int two, fvbWavePacket *gwp, fvbConstants c);
void uint_gmp(mpfr_class *usb_, mpfr_class *divusb_,
              mpfr_class *divdivusb_, int one, int two, fvbWavePacket *gwp,
              fvbConstants c, fvbPotentials fp);
void uint(int one, int two, fvbConstants c, const double y[]);


fvbOperators *deriv_ops;
```

```
fvbDerivatives();
~fvbDerivatives() {};
};
```

File: "fvbDerivatives.cc"

```
/*************************************************************************
 *            fvbDerivatives.cc
 *
 *  Thu Oct  2 18:29:34 2008
 *  Copyright  2008  Craig Chapman
 *  cchapma2@uoregon.edu
 *************************************************************************/

#include "fvb.h"

fvbDerivatives::fvbDerivatives()
{
sumgim_.set_prec(precision);
sumgre_.set_prec(precision);
sumQ_.set_prec(precision);
sumP_.set_prec(precision);
sumare_.set_prec(precision);
sumaim_.set_prec(precision);
fim_.set_prec(precision);
fre_.set_prec(precision);
usb_.set_prec(precision);
divusb_.set_prec(precision);
divdivusb_.set_prec(precision);
ub_.set_prec(precision);
divub_.set_prec(precision);
divdivub_.set_prec(precision);
holder_.set_prec(precision);
holder1_.set_prec(precision);
half_.set_prec(precision);
exp_fim_.set_prec(precision);
damp_.set_prec(precision);
}

void fvbDerivatives::get_derivs(int nu, fvbWavePacket *gwp, fvbConstants c)
```

```
{
sumgim = 0.;
sumgre = 0.;
sumQ = 0.;
sumP = 0.;
sumare = 0.;
sumaim = 0.;

for (int nubar = 0; nubar < c.nbasis; nubar ++)
if (nubar != nu)
{
uint(nu,nubar, gwp,c); //sets usb, divusb, divdivusb
qnnb = gwp[nu].Q - gwp[nubar].Q;
fre = freal(nu,nubar, gwp);
fim = fimaginary(nu,nubar, gwp);

/*********************************
* Real gamma
*********************************/

sumgre += exp(-fim) * (cos(freal(nu,nubar, gwp))*(-usb +( usb * qnnb * gwp[nubar].are *
+ 0.5 * usb* (gwp[nubar].P - gwp[nu].P)) * (1./gwp[nu].aim) * gwp[nu].P)
+sin(freal(nu,nubar, gwp)) * ((0.5 * divusb - usb * qnnb * gwp[nubar].aim)
* (1./gwp[nu].aim) * gwp[nu].P));

/*********************************
* Imaginary gamma
*********************************/

sumgim += exp(-fim) * sin(fre) * usb;
// cout<<exp (-fim)<<" "<<sin(fre)<<" "<<usb<<endl;

/*********************************
* P
*********************************/

sumP += exp (-fim) * ( cos(fre) * (divusb + usb *(-2.*gwp[nubar].aim * qnnb)
- (gwp[nu].are/gwp[nu].aim) *(2. * gwp[nubar].are * qnnb + gwp[nubar].P - gwp[nu].P)
* usb) - sin(fre) * (usb * (2. * gwp[nubar].are * qnnb +  gwp[nubar].P - gwp[nu].P)
```

```
+ (gwp[nu].are/gwp[nu].aim) * (divusb - usb * (2. * gwp[nubar].aim * qnnb))));

/*********************************
* Q
*********************************/

sumQ += exp(-fim) * ( cos(fre) * (( 2. * gwp[nubar].are * qnnb + gwp[nubar].P
- gwp[nu].P) * usb)
+ sin(fre) * (divusb + usb * (-2. * gwp[nubar].aim * qnnb)));

/*********************************
* Real alpha
*********************************/

holder = (0.5 * divdivusb + divusb * (-2. * gwp[nubar].aim * qnnb)
+ usb * (-2. * (gwp[nubar].are * gwp[nubar].are - gwp[nubar].aim * gwp[nubar].aim) * qnnb * qnnb
-gwp[nubar].aim + gwp[nu].aim - 2. * gwp[nubar].are * qnnb *  (gwp[nubar].P - gwp[nu].P)
-0.5 * ( gwp[nubar].P - gwp[nu].P)*( gwp[nubar].P - gwp[nu].P)));

holder1 = (divusb * (2. * gwp[nubar].are * qnnb +  gwp[nubar].P - gwp[nu].P) + usb
* (-2. * (gwp[nubar].are * gwp[nubar].aim + gwp[nubar].are * gwp[nubar].aim) * qnnb * qnnb
+ gwp[nubar].are - gwp[nu].are - 2. * gwp[nubar].aim * qnnb *  (gwp[nubar].P - gwp[nu].P)));

sumare += exp(-fim) * ( cos(fre) * holder
- sin(fre) * holder1);

/*********************************
* Imaginary alpha
*********************************/

sumaim += exp(-fim) * (cos(fre) * holder1 + sin(fre) * holder);
}; //done with off diagonal parts
//cout<<sumP<<endl;

//set other quantities
uint(nu,nu, gwp,c); //sets uint(nu,nu), ...
ubath(nu, gwp,c); //sets ub, divub, divdivub

gwp[nu].dgre = 0.5 * gwp[nu].P * gwp[nu].P - deriv_ops[0].sysevals[nu] - usb - gwp[nu].aim
```

```
- ub + sumgre;
gwp[nu].dgim = gwp[nu].are - sumgim;
gwp[nu].dQ = gwp[nu].P + (0.5 / gwp[nu].aim) * sumQ;
gwp[nu].dP = -divusb - divub - sumP;
gwp[nu].dare = -0.5 * (divdivub + divdivusb) - 2. * gwp[nu].are * gwp[nu].are + 2. *gwp[nu].aim
*gwp[nu].aim - sumare;
gwp[nu].daim = -4. * gwp[nu].are * gwp[nu].aim - sumaim;

//cout<<gwp[nu].dP<<endl;
};

void fvbDerivatives::get_derivs_gmp(int nu, fvbWavePacket *gwp, fvbConstants c,
                                    fvbPotentials fp)
{
sumgim_ = "0";
sumgre_ = "0";
sumQ_ = "0";
sumP_ = "0";
sumare_ = "0";
sumaim_ = "0";
half_ = "0.5";
ub_ = "0";
divub_ = "0";
divdivub_ = "0";
damp_ = "0";

//cout<<sumP_<<" ";
for (int nubar = 0; nubar < c.nbasis; nubar ++)
if (nubar != nu)
if (Kronecker(nu,nubar+1) != 0 || Kronecker(nu,nubar-1)!= 0)
{
//cout<<nubar<<" "<<nubar+1<<" "<<nubar-1<<endl;
uint_gmp(&usb_, &divusb_, &divdivusb_,nu,nubar, gwp,c,fp); //sets usb_, divusb_, divdivusb_
qnnb_ = gwp[nu].gmp_Q - gwp[nubar].gmp_Q;
freal(&fre_, nu, nubar, gwp);
fimaginary(&fim_,nu,nubar, gwp);
exp_fim_ = exp(-fim_);

//cout<<qnnb_<<" "<<fre_<<" "<<fim_<<" "<<usb_<<" "<<divusb_<<" "<<divdivusb_<<endl;
```

```
//exit(1);

/*********************************
* Real gamma
*********************************/

sumgre_ += exp_fim_ * (cos(fre_)*(-usb_ +( usb_ * qnnb_ * gwp[nubar].gmp_are
+ half_ * usb_* (gwp[nubar].gmp_P - gwp[nu].gmp_P)) * (gwp[nu].gmp_P/gwp[nu].gmp_aim))
+sin(fre_) * ((half_ * divusb_ - usb_ * qnnb_ * gwp[nubar].gmp_aim)
* (gwp[nu].gmp_P/gwp[nu].gmp_aim) ));

/*********************************
* Imaginary gamma
*********************************/

sumgim_ += exp_fim_ * sin(fre_) * usb_;
// cout<<exp (-fim)<<" "<<sin(fre)<<" "<<usb<<endl;

/*********************************
* P
*********************************/

sumP_ += exp_fim_ * ( cos(fre_) * (divusb_ + usb_ *(-2.*gwp[nubar].gmp_aim * qnnb_)
- (gwp[nu].gmp_are/gwp[nu].gmp_aim) *(2 * gwp[nubar].gmp_are * qnnb_ + gwp[nubar].gmp_P - gwp[nu].gmp_P)
* usb_) - sin(fre_) * (usb_ * (2 * gwp[nubar].gmp_are * qnnb_ +  gwp[nubar].gmp_P - gwp[nu].gmp_P)
+ (gwp[nu].gmp_are/gwp[nu].gmp_aim) * (divusb_ - usb_ * (2 * gwp[nubar].gmp_aim * qnnb_))));

/*********************************
* Q
*********************************/

sumQ_ += exp_fim_ * ( cos(fre_) * (( 2 * gwp[nubar].gmp_are * qnnb_ + gwp[nubar].gmp_P
- gwp[nu].gmp_P) * usb_)
+ sin(fre_) * (divusb_ + usb_ * (-2 * gwp[nubar].gmp_aim * qnnb_)));

//cout<<sumQ_<<" "<<fim_<<" "<<fre_<<endl;

/*********************************
* Real alpha
```

```
**********************************/

holder_ = (half_ * divdivusb_ + divusb_ * (-2 * gwp[nubar].gmp_aim * qnnb_)
+ usb_ * (-2 * (gwp[nubar].gmp_are * gwp[nubar].gmp_are - gwp[nubar].gmp_aim * gwp[nubar].gmp_aim)
* qnnb_ * qnnb_-gwp[nubar].gmp_aim + gwp[nu].gmp_aim - 2 * gwp[nubar].gmp_are * qnnb_ *  (gwp[nubar]
.gmp_P - gwp[nu].gmp_P)-half_ * ( gwp[nubar].gmp_P - gwp[nu].gmp_P)*( gwp[nubar].gmp_P
- gwp[nu].gmp_P)));

holder1_ = (divusb_ * (2 * gwp[nubar].gmp_are * qnnb_ +  gwp[nubar].gmp_P - gwp[nu].gmp_P) + usb_
* (-4 * (gwp[nubar].gmp_are * gwp[nubar].gmp_aim) * qnnb_ * qnnb_
+ gwp[nubar].gmp_are - gwp[nu].gmp_are - 2 * gwp[nubar].gmp_aim * qnnb_ *  (gwp[nubar].gmp_P
- gwp[nu].gmp_P)));

sumare_ += exp_fim_ * ( cos(fre_) * holder_
- sin(fre_) * holder1_);

/**********************************
* Imaginary alpha
**********************************/

sumaim_ += exp_fim_ * (cos(fre_) * holder1_ + sin(fre_) * holder_);
}; //done with off diagonal parts


//set other quantities
//uint(nu,nu, gwp,c); //sets uint(nu,nu), ... NB : uint = 0 for bilinear coupling
ubath_gmp(&ub_, &divub_, &divdivub_,nu, gwp,fp); //sets ub, divub, divdivub

gwp[nu].dgre_ = half_ * gwp[nu].gmp_P * gwp[nu].gmp_P - deriv_ops[0].sysevals_[nu]  - gwp[nu].gmp_aim
- ub_ + sumgre_;
gwp[nu].dgim_ = gwp[nu].gmp_are - sumgim_;
gwp[nu].dQ_ = gwp[nu].gmp_P + half_ * (sumQ_ / gwp[nu].gmp_aim);
gwp[nu].dP_ =- divub_ - sumP_;

gwp[nu].dare_ = -half_ * (divdivub_ ) - 2 * gwp[nu].gmp_are * gwp[nu].gmp_are + 2 *gwp[nu].gmp_aim
*gwp[nu].gmp_aim - sumare_;
gwp[nu].daim_ = -4 * gwp[nu].gmp_are * gwp[nu].gmp_aim - sumaim_;

};
```

```
void fvbDerivatives::get_derivs(fvbConstants c, const double y[],double f[])
{
for (int nu=0; nu<c.nbasis; nu++) {
sumgim = 0.;
sumgre = 0.;
sumQ = 0.;
sumP = 0.;
sumare = 0.;
sumaim = 0.;

double qn = y[2+nu*6];
double pn = y[3+nu*6];
double aren = y[4+nu*6];
double aimn = y[5+nu*6];

for (int nubar = 0; nubar < c.nbasis; nubar ++)
if (nubar != nu)
{
if (Kronecker(nu,nubar+1) != 0 || Kronecker(nu,nubar-1) != 0) {

double qnn = y[2+nubar*6];
double pnn = y[3+nubar*6];
double arenn = y[4+nubar*6];
double aimnn = y[5+nubar*6];

uint(nu,nubar,c,y); //sets usb, divusb, divdivusb
qnnb = qn-qnn;
fre = freal(nu,nubar, y);
fim = fimaginary(nu,nubar, y);

/*********************************
* Real gamma
*********************************/

sumgre += exp(-fim) * (cos(fre)*(-usb +( usb * qnnb * arenn *
+ 0.5 * usb* (pnn - pn)) * (1./aimn) * pn)
+sin(fre) * ((0.5 * divusb - usb * qnnb * aimnn)
* (1./aimn) * pn));
```

```
/**********************************
* Imaginary gamma
**********************************/

sumgim += exp(-fim) * sin(fre) * usb;

/**********************************
* P
**********************************/

sumP += exp (-fim) * ( cos(fre) * (divusb + usb *(-2.*aimn * qnnb)
- (aren/aimn) *(2. * arenn * qnnb + pnn - pn)
* usb) - sin(fre) * (usb * (2. * arenn * qnnb +  pnn - pn)
+ (aren/aimn) * (divusb - usb * (2. * aimnn * qnnb))));

/**********************************
* Q
**********************************/

sumQ += exp(-fim) * ( cos(fre) * (( 2. * arenn * qnnb + pnn
- pn) * usb)
+ sin(fre) * (divusb + usb * (-2. * aimnn * qnnb)));

/**********************************
* Real alpha
**********************************/

holder = (0.5 * divdivusb + divusb * (-2. * aimnn * qnnb)
+ usb * (-2 * (arenn*arenn - aimnn*aimnn) * qnnb * qnnb
-aimnn + aimn - 2 * arenn * qnnb *  (pnn - pn)
-0.5 * ( pnn - pn)*( pnn - pn)));

holder1 = (divusb * (2 * arenn * qnnb +  pnn - pn) + usb
* (-2 * (arenn*aimnn + arenn*aimnn) * qnnb * qnnb
+ arenn - aren - 2 * aimnn * qnnb *  (pnn - pn)));

sumare += exp(-fim) * ( cos(fre) * holder
- sin(fre) * holder1);
```

```
/*********************************
* Imaginary alpha
*********************************/

sumaim += exp(-fim) * (cos(fre) * holder1 + sin(fre) * holder);
}
else
continue;
}; //done with off diagonal parts
//cout<<sumP<<endl;

//set other quantities
uint(nu,nu,c,y); //sets uint(nu,nu), ...
ubath(nu,c,y); //sets ub, divub, divdivub

      //gre
f[0+nu*6] = 0.5 * pn * pn - deriv_ops[0].sysevals[nu] /*- usb*/ - aimn
- ub + sumgre;
//gim
      f[1+nu*6] = aren - sumgim;
      //Q
f[2+nu*6] = pn + (1 /(2 * aimn)) * sumQ;
      //P
f[3+nu*6] = /*-divusb*/ - divub - sumP;
      //are
f[4+nu*6] = -0.5 * (divdivub /*+ divdivusb*/) - 2. * aren * aren + 2. *aimn
*aimn - sumare;
      //aim
f[5+nu*6] = -4. * aren * aimn - sumaim;

}//end nu
};


//real part of f
double fvbDerivatives::freal(int one, int two, fvbWavePacket *gwp)
{
return (gwp[one].Q - gwp[two].Q)*(gwp[one].Q - gwp[two].Q)*gwp[two].are
+ (gwp[one].Q - gwp[two].Q) * gwp[two].P
```

```
+ gwp[two].gre - gwp[one].gre;
}

void fvbDerivatives::freal(mpfr_class *fre_, int one, int two, fvbWavePacket *gwp)
{
*fre_ = (gwp[one].gmp_Q - gwp[two].gmp_Q)*(gwp[one].gmp_Q - gwp[two].gmp_Q)*gwp[two].gmp_are
+ (gwp[one].gmp_Q - gwp[two].gmp_Q) * gwp[two].gmp_P
+ gwp[two].gmp_gre - gwp[one].gmp_gre;
}

double fvbDerivatives::freal(int one, int two, const double y[])
{
return pow((y[2+one*6] - y[2+two*6]),2) /** (y[2+one*6] - y[2+two*6])*/*y[4+two*6]
+ (y[2+one*6] - y[2+two*6]) * y[3+two*6]
+ y[0+two*6] - y[0+one*6];
}

void fvbDerivatives::freal(mpfr_class *gmpfre, int one, int two, const double y[])
{
*gmpfre = pow((y[2+one*6] - y[2+two*6]),2) /** (y[2+one*6] - y[2+two*6])*/*y[4+two*6]
+ (y[2+one*6] - y[2+two*6]) * y[3+two*6]
+ y[0+two*6] - y[0+one*6];
}

double fvbDerivatives::fimaginary(int one, int two, fvbWavePacket *gwp)
{
return  (gwp[one].Q - gwp[two].Q)* (gwp[one].Q - gwp[two].Q)*gwp[two].aim
+ gwp[two].gim - gwp[one].gim;
}

void fvbDerivatives::fimaginary(mpfr_class *fim_, int one, int two, fvbWavePacket *gwp)
{
*fim_ =  (gwp[one].gmp_Q - gwp[two].gmp_Q)* (gwp[one].gmp_Q - gwp[two].gmp_Q)*gwp[two].gmp_aim
+ gwp[two].gmp_gim - gwp[one].gmp_gim;
}

double fvbDerivatives::fimaginary(int one, int two, const double y[])
{
return  pow((y[2+one*6] - y[2+two*6]),2) /** (y[2+one*6] - y[2+two*6])*/*y[5+two*6]
```

```
+ y[1+two*6] - y[1+one*6];
}

void fvbDerivatives::ubath(int one, fvbWavePacket *gwp, fvbConstants c)
{
ub = 0.5 * c.omega_bath * c.omega_bath * gwp[one].Q * gwp[one].Q;
divub = c.omega_bath * c.omega_bath * gwp[one].Q;
divdivub = c.omega_bath * c.omega_bath;

ub_ = 0.5 * c.omega_bath_ * c.omega_bath_ * gwp[one].gmp_Q * gwp[one].gmp_Q;
divub_ = c.omega_bath_ * c.omega_bath_ * gwp[one].gmp_Q;
divdivub_ = c.omega_bath_ * c.omega_bath_;
};
void fvbDerivatives::ubath_gmp(mpfr_class *ub_, mpfr_class *divub_, mpfr_class *divdivub_,
int one, fvbWavePacket *gwp, fvbPotentials c)
{

*ub_ = 0.5 * c.omega_bath_ * c.omega_bath_ * gwp[one].gmp_Q * gwp[one].gmp_Q;
*divub_ = c.omega_bath_ * c.omega_bath_ * gwp[one].gmp_Q;
*divdivub_ = c.omega_bath_ * c.omega_bath_;
};


void fvbDerivatives::ubath(int one, fvbConstants c, const double y[])
{
ub = 0.5 * c.omega_bath * c.omega_bath * y[2+one*6];
divub = c.omega_bath * c.omega_bath * y[2+one*6];
divdivub = c.omega_bath * c.omega_bath;
};

void fvbDerivatives::uint(int one, int two, fvbWavePacket *gwp, fvbConstants c)
{
if (Kronecker(one, two+1)!= 0  || Kronecker(one, two-1)!= 0) {
usb = c.coupling * gwp[one].Q * deriv_ops[0].q[one + two * c.nbasis];
divusb = c.coupling * deriv_ops[0].q[one + two * c.nbasis];
divdivusb = 0.;

damp_ = cos((M_PI/2)*(one-6)/(c.nbasis-6));
```

```
usb_ =damp_* c.coupling * gwp[one].gmp_Q * deriv_ops[0].q_[one + two * c.nbasis];
divusb_ = damp_*c.coupling * deriv_ops[0].q_[one + two * c.nbasis];
divdivusb_ = 0.;
}
else {
usb = 0.;
divusb = 0.;
divdivusb = 0.;

usb_ = "0";
divusb_ = "0";
divdivusb_ = "0";
}

};
void fvbDerivatives::uint_gmp(mpfr_class *usb_, mpfr_class *divusb_,
mpfr_class *divdivusb_, int one, int two, fvbWavePacket *gwp, fvbConstants c,
                              fvbPotentials fp)
{
if (Kronecker(one, two+1)!= 0  || Kronecker(one, two-1)!= 0) {
/* if (one >= 3) {
damp_ = cos((M_PI/2)*(one-3)/((c.nbasis-1)-3));

*usb_ = damp_*fp.coupling_ * gwp[one].gmp_Q * deriv_ops[0].q_[one + two * c.nbasis];
*divusb_ = damp_*fp.coupling_ * deriv_ops[0].q_[one + two * c.nbasis];
*divdivusb_ = "0";
} else {*/
*usb_ = fp.coupling_ * gwp[one].gmp_Q * deriv_ops[0].q_[one + two * c.nbasis];
*divusb_ = fp.coupling_ * deriv_ops[0].q_[one + two * c.nbasis];
*divdivusb_ = "0";
//}
}
else {
*usb_ = "0";
*divusb_ = "0";
*divdivusb_ = "0";
}
};
void fvbDerivatives::uint(int one, int two, fvbConstants c, const double y[])
```

```
{
if (Kronecker(one, two+1)!= 0  || Kronecker(one, two-1)!= 0) {
usb = c.coupling * y[2+one*6] * deriv_ops[0].q[one + two * c.nbasis];
divusb = c.coupling * deriv_ops[0].q[one + two * c.nbasis];
divdivusb = 0.;
} else {
usb = 0.;
divusb = 0.;
divdivusb = 0.;
}
};
```

File: "fvbOperators.h"

```
/*************************************************************************
 *            fvbOperators.h
 *
 *  Wed Dec  3 12:25:28 2008
 *  Copyright  2008  Craig Chapman
 *  cchapma2@uoregon.edu
 *************************************************************************/
//#include "fvb.h"

class fvbOperators
{
public:
//system momentum
double *p,*p2,*p3,*p4,*p5,*p6,*p7,*p8,*p9,*p10,*p11,*p12,*qt,*qt2;
double *q;
mpfr_class *q_;
//ladder operators
double *at,*a;
mpfr_class *at_, *a_;
//displacement operator
double *disp_operator;
//system eigenvalues
double *sysevals;
mpfr_class *sysevals_;

//multiply two square double precision arrays of size m
```

```
//returns a pointer to new double array
double *multmm(double *one,double *two,int m);
//same but for matrix*vector
double *multmv(double *one,double *two,int m);

double factorial(int number) {double temp;
if(number <= 1)
return 1.;
temp = number * factorial(number - 1);
return temp;}

void setops(fvbConstants, fvbPotentials);

fvbOperators();
~fvbOperators() {};
};
```

File: "fvbOperators.cc"

```
/*************************************************************************
 *            fvbOperators.cc
 *
 *  Thu Oct  2 17:28:45 2008
 *  Copyright  2008  Craig Chapman
 *  cchapma2@uoregon.edu
 *************************************************************************/
#include "fvb.h"

fvbOperators::fvbOperators()
{

}

void fvbOperators::setops(fvbConstants c,fvbPotentials fp)
{
a = new double[c.nbasis*c.nbasis];
at = new double[c.nbasis*c.nbasis];

a_ = new mpfr_class[c.nbasis*c.nbasis];
at_ = new mpfr_class[c.nbasis*c.nbasis];
```

```
sysevals = new double[c.nbasis];
sysevals_ = new mpfr_class[c.nbasis];
disp_operator = new double[c.nbasis*c.nbasis];
p = new double[c.nbasis*c.nbasis];
q = new double[c.nbasis*c.nbasis];
q_ = new mpfr_class[c.nbasis*c.nbasis];
cout.precision(32);

//sets precision of gmp stuff
for (int i=0; i<c.nbasis*c.nbasis; i++)
{
a_[i].set_prec(precision);
at_[i].set_prec(precision);
q_[i].set_prec(precision);
}

for (int i=0; i<c.nbasis; i++)
for (int j=0; j<c.nbasis; j++){
double row = 1.*i;
double col = 1.*j;
char row1_[10];
char col1_[10];
sprintf(row1_,"%i",i);
sprintf(col1_,"%i",j);

mpfr_class row_ (row1_,precision);
mpfr_class col_ (col1_,precision);

//raising and lowering operators
a[i+j*c.nbasis] = sqrt(col) * Kronecker(row, col-1);
at[i+j*c.nbasis] = sqrt(row) * Kronecker(row, col+1);

a_[i+j*c.nbasis] = sqrt(col_) * Kronecker(row,col-1);
at_[i+j*c.nbasis] = sqrt(row_) * Kronecker(row,col+1);

// system and bath position operators
p[i+j*c.nbasis] = sqrt(fp.omega_bath_.get_d()/2) * (at[i+j*c.nbasis] - a[i+j*c.nbasis]);
q[i+j*c.nbasis] = (at[i+j*c.nbasis] + a[i+j*c.nbasis]) * (1/sqrt(fp.omega_sys_.get_d()*2));
```

```
q_[i+j*c.nbasis] = (at_[i+j*c.nbasis] + a_[i+j*c.nbasis]) * (1/sqrt(2*fp.omega_sys_));
}

p2 = multmm(p,p,c.nbasis);
p3 = multmm(p2,p,c.nbasis);
p4 = multmm(p3,p,c.nbasis);
p5 = multmm(p4,p,c.nbasis);
p6 = multmm(p5,p,c.nbasis);
p7 = multmm(p6,p,c.nbasis);
p8 = multmm(p7,p,c.nbasis);
p9 = multmm(p8,p,c.nbasis);
p10= multmm(p9,p,c.nbasis);
p11 = multmm(p10,p,c.nbasis);
p12 = multmm(p11,p,c.nbasis);

/*********************************
 * Create Displacement operator
 */

for (int i=0; i<c.nbasis; i++) {
for (int j=0; j<c.nbasis; j++) {
disp_operator[i+j*c.nbasis] = p[i+j*c.nbasis] * fp.ve_qe_.get_d()
;/* + p2[i+j*c.nbasis] * (1./gsl_sf_fact(2)) * pow(fp.ve_qe_.get_d(),2)
+ p3[i+j*c.nbasis] * (1./gsl_sf_fact(3)) * pow(fp.ve_qe_.get_d(),3)
+ p4[i+j*c.nbasis] * (1./gsl_sf_fact(4)) * pow(fp.ve_qe_.get_d(),4)
+ p5[i+j*c.nbasis] * (1./gsl_sf_fact(5)) * pow(fp.ve_qe_.get_d(),5)
;/*+ p6[i+j*c.nbasis] * (1./gsl_sf_fact(6)) * pow(fp.ve_qe_.get_d(),6)
+ p7[i+j*c.nbasis] * (1./gsl_sf_fact(7)) * pow(fp.ve_qe_.get_d(),7)
+ p8[i+j*c.nbasis] * (1./gsl_sf_fact(8)) * pow(fp.ve_qe_.get_d(),8)
+ p9[i+j*c.nbasis] * (1./gsl_sf_fact(9)) * pow(fp.ve_qe_.get_d(),9)
+ p10[i+j*c.nbasis] * (1./gsl_sf_fact(10)) * pow(fp.ve_qe_.get_d(),10)
+ p11[i+j*c.nbasis] * (1./gsl_sf_fact(11)) * pow(fp.ve_qe_.get_d(),11)
+ p12[i+j*c.nbasis] * (1./gsl_sf_fact(12)) * pow(fp.ve_qe_.get_d(),12);
          */
}
disp_operator[i+i*c.nbasis] += 1.;
}

qt = new double[c.nbasis*c.nbasis];//multmm(q,disp_operator,c.nbasis);
```

```
   qt2=new double[c.nbasis*c.nbasis];

   cblas_dgemm(CblasColMajor,CblasNoTrans,CblasNoTrans,
   c.nbasis,c.nbasis,c.nbasis,1.0,q,
            c.nbasis,disp_operator,c.nbasis,0,qt,c.nbasis);

   cblas_dgemm(CblasColMajor,CblasNoTrans,CblasNoTrans,
   c.nbasis,c.nbasis,c.nbasis,1.0,disp_operator,
            c.nbasis,qt,c.nbasis,0,qt2,c.nbasis);

   //qt2 = multmm(disp_operator,qt,c.nbasis);

for (int i=0; i<c.nbasis; i++) {
for (int j=0; j<c.nbasis; j++) {
//cout<<i<<" "<<j<<" "<<q[i+j*c.nbasis]<<" "<<disp_operator[i+j*c.nbasis]<<endl;
}
}
//exit(0);
//system eigenvalues
for (int i=0; i<c.nbasis; i++) {
sysevals[i] = fp.omega_sys_.get_d() * (i + 0.5);
sysevals_[i] = fp.omega_sys_ * (i + 0.5);
}



};

double *fvbOperators::multmm(double *one,double *two,int m)
{
double *res = new double[m*m];

cblas_dgemm(CblasColMajor,CblasNoTrans,CblasNoTrans,
m,m,m,1.0,one,
            m,two,m,0,res,m);

return res;
};

double *fvbOperators::multmv(double *one,double *two,int m)
```

```
{
double *res = new double[m];

//~ cblas_dgemv(CblasColMajor,CblasNoTrans,
//~ m, m, 1, one, m, two, 1, 0, res, 1);

//~ //return result
return res;
};
```

File: "fvbPotentials.h"

```
/*****************************************************************************
 *            fvbPotentials.h
 *
 *  Wed Dec  3 12:32:59 2008
 *  Copyright  2008  Craig Chapman
 *  cchapma2@uoregon.edu
 *****************************************************************************/

 class fvbPotentials
{
public:
mpfr_class omega_sys_,omega_bath_,coupling_,qe_,Qe_,ve_qe_;

double * hermites_s;
double * wfpolys_s;
double * ground_wf;
double * gamma;

void set_sys_freq(mpfr_class x) {omega_sys_ = x;};
void set_bath_freq(mpfr_class x) {omega_bath_ = x;};
void set_coupling(mpfr_class x) {coupling_ = x;};
void set_bath_Qe();
void set_bath_Qe(mpfr_class x) {Qe_ = x;};
void set_sys_eq(mpfr_class x) {qe_ = x;};
void set_ve_qe_(mpfr_class x) {ve_qe_ = x;};

void pos_rep_sys(fvbConstants);
double hermite_s(int n, int pos, double x, fvbConstants);
```

```
double hermite(int n, int pos, double x);
double hermite(int n, double pos);
void pos_rep_sys_g(fvbConstants c);
void calculate_overlap(fvbConstants);

fvbPotentials();
~fvbPotentials() {};
};
```

File: "fvbPotentials.cc"

```
/*****************************************************************************
 *            fvbPotentials.cc
 *
 *  Wed Jan 14 11:08:13 2009
 *  Copyright  2009  Craig Chapman
 *  cchapma2@uoregon.edu
 *****************************************************************************/
#include "fvb.h"

fvbPotentials::fvbPotentials()
{
ve_qe_.set_prec(precision);
qe_.set_prec(precision);
Qe_.set_prec(precision);
omega_sys_.set_prec(precision);
coupling_.set_prec(precision);
omega_bath_.set_prec(precision);
};

void fvbPotentials::set_bath_Qe()
{
}

void fvbPotentials::pos_rep_sys(fvbConstants c)
{
double beta=sqrt(omega_sys_.get_d());
double coeff=sqrt(beta/sqrt(M_PI));

    //Initialize first two basis functions
```

```
for (int n=0;n<2;n++) {
double hold=n;
double coeff2=1./(sqrt(pow(2,hold)*gsl_sf_fact(n)));

for (int point=0;point<c.npoints();point++) {
hermites_s[point + n*c.npoints()]=hermite(n, beta*(c.xmin()+point*c.dx()));
wfpolys_s[point + n*c.npoints()]=coeff*coeff2*exp(-0.5*(pow((c.xmin()+point*c.dx())*beta,2)))
*hermites_s[point + (c.npoints()*n)];
}
}

   //Now the rest
for (int n=2;n<c.nbasis;n++) {

int which = 0;
double hold=n;
double coeff2=1./(sqrt(pow(2,hold)*gsl_sf_fact(n)));

for (int point=0;point<c.npoints();point++) {
hermites_s[point + n*c.npoints()]=hermite_s(n,point,beta*(c.xmin()+point*c.dx()),c);
wfpolys_s[point + n*c.npoints()]=coeff*coeff2*exp(-0.5*(pow((c.xmin()+point*c.dx())*beta,2)))
*hermites_s[point + n*c.npoints()];
}
}
}

void fvbPotentials::pos_rep_sys_g(fvbConstants c)
{
double beta=sqrt(omega_sys_.get_d());
double coeff=sqrt(beta/sqrt(M_PI));

   //Initialize first basis functions
double hold=0;
double coeff2=1./(sqrt(pow(2,hold)*gsl_sf_fact(0)));

for (int point=0;point<c.npoints();point++) {
hermites_s[point]=hermite(0, beta*((c.xmin() - qe_.get_d())+point*c.dx()));
ground_wf[point]=coeff*coeff2*exp(-0.5*(pow(((c.xmin() - qe_.get_d()) +point*c.dx())*beta,2)))
*hermites_s[point];
```

```
}
   ofstream oscfunc;
   oscfunc.open("posrep_s", ios::out);
//for (int nf=0;nf<c.nbasis;nf++)
for (int point=0;point<c.npoints();point++)
oscfunc<<(c.xmin()+point*c.dx())<<" "<<ground_wf[point]<<" "<<wfpolys_s[point+c.npoints()]<<endl;

oscfunc.close();
// exit(0);
}

double fvbPotentials::hermite(int n, double pos)
{
if (n==0) {
return 1.;
}
else if (n==1) {
return 2.*pos;
}
else {
double number;//=2.*pos*hermite(n-1,pos)-2.*(n-1)*hermite(n-2,pos);
return number;
}
}
double fvbPotentials::hermite(int n, int pos, double x)
{
double number;//=2.*x*hermites[pos][n-1]-2.*(n-1)*hermites[pos][n-2];
return number;
}
double fvbPotentials::hermite_s(int n, int pos, double x, fvbConstants c)
{
double number=2.*x*hermites_s[pos + (n-1)*c.npoints()]-2.*(n-1)*hermites_s[pos + (n-2) * c.npoints()];
//if (n==2)
// cout<<number<<endl;
return number;
}

void fvbPotentials::calculate_overlap(fvbConstants c)
{
```

```
for (int i=0; i<c.npoints(); i++)
for (int j=0; j<c.nbasis; j++) {
wfpolys_s[i+j*c.npoints()] *= c.dx();
//holder[i+j*npoints]=wfpolys_s[i][j];
}

cblas_dgemv (CblasColMajor,CblasTrans
,c.npoints(),c.nbasis,1,wfpolys_s
,c.npoints(),ground_wf,1,0,gamma,1);

// exit(0);
}
```

File: "fvbPropagate.h"

```
/*****************************************************************************
 *            fvbPropagate.h
 *
 *  Wed Dec  3 12:44:26 2008
 *  Copyright  2008  Craig Chapman
 *  cchapma2@uoregon.edu
 *****************************************************************************/

//#include "fvb.h"

class fvbPropagate
{
fvbDerivatives *derivs;
double factor;

public:
//for calculating overlaps
dcomp A, B, C, exp_arg, exp_pre, overlap;

void forward(fvbWavePacket *gwp,fvbConstants &c, fvbTimeParameters t, fvbPotentials);
void renormalize(fvbWavePacket *gwp, fvbConstants c);
dcomp calculate_overlap(int one, int two, fvbWavePacket *gwp);
dcomp calculate_overlap_init(int one, int two, fvbWavePacket *gwp);
void check_purity(fvbWavePacket *gwp, fvbConstants c);
```

```
double totnorm;
double initnorm;
double purity;
double *all_params;

void set_allparams(gslholder gsl, fvbWavePacket *gwp, fvbConstants c);
void update_array(gslholder gslstuff, fvbWavePacket *gwp, fvbConstants c);
void revert(gslholder gslstuff, fvbConstants c);
       void rk4_step(fvbDerivatives *derivs,fvbWavePacket * gwp,
                     fvbWavePacket *gwp_t, fvbConstants &c,
                         mpfr_class time_step, mpfr_class dydx[],
                         mpfr_class dyt[], mpfr_class dym[], mpfr_class y[],
                      fvbPotentials);
void odeint(mpfr_class y[], fvbDerivatives *derivs, fvbWavePacket *gwp,
            fvbWavePacket *gwp_t, fvbConstants &c, mpfr_class *timeh_, mpfr_class t2,
mpfr_class h1_, mpfr_class dydx[], mpfr_class dyt[],
            mpfr_class dym[],fvbPotentials fp);

void rkqc(fvbDerivatives *derivs,fvbWavePacket * gwp,
          fvbWavePacket *gwp_t, fvbConstants &c, mpfr_class *time_step,
          mpfr_class dydx[], mpfr_class dyt[], mpfr_class dym[],
          mpfr_class y[], mpfr_class *x, mpfr_class yscal[],
          mpfr_class *hnext, fvbPotentials);
double q(fvbWavePacket *, fvbConstants, double*,fvbPotentials);
dcomp qt(fvbWavePacket *, fvbConstants);

fvbPropagate() {};
~fvbPropagate() {};
};
```

File: "fvbPropagate.cc"

```
/*************************************************************************
 *            fvbPropagate.cc
 *
 *  Thu Oct  2 18:07:04 2008
 *  Copyright  2008  Craig Chapman
 *  cchapma2@uoregon.edu
 *************************************************************************/
#include "fvb.h"
```

```
void fvbPropagate::forward(fvbWavePacket *gwp, fvbConstants &c,
                           fvbTimeParameters t, fvbPotentials fp)
{

ofstream grefile, gimfile, Qfile, Pfile, arefile, aimfile, normfile,
purityfile,q0file,qtfile;
grefile.open("gre",fstream::ate);
gimfile.open("gim",fstream::ate); gimfile.precision(16);
Qfile.open("Q", fstream::ate);  Qfile.precision(16);
Pfile.open("P", fstream::ate);
arefile.open("are",fstream::ate);
aimfile.open("aim",fstream::ate);  aimfile.precision(16);
normfile.open("norm",fstream::ate);  normfile.precision(16);
purityfile.open("purity",fstream::ate); purityfile.precision(16);
q0file.open("q0"); q0file.precision(16);
qtfile.open("qt"); qtfile.precision(16);

double time = t.tmin();
double timeh;
double h = 1e-4;
double hmin = 1e-8;
double timem;
double timestop = 400000;

/*****************************************************************************
*****************************************************************************
* Runge Kutta Techniques, non-GMP, uses gsl
*/

#ifdef RK45
/*************************
 * propagation routine */
const gsl_odeiv_step_type * T = gsl_odeiv_step_rkf45;
gsl_odeiv_step *stepper = gsl_odeiv_step_alloc(T,6*c.nbasis);
/*********************
 * error limits */
gsl_odeiv_control *controller =gsl_odeiv_control_standard_new (1e-25,1.e-12,.0,1);
/*************
```

```
 * evolver */
gsl_odeiv_evolve *evolver = gsl_odeiv_evolve_alloc(6*c.nbasis);

/*********************************
 * Object that calculates all
 *  of the time derivatives.
 * In the case of RK45, all of the
 *  WP parameters are in a single
 * array of size 6*nbasis
 */

derivs = new fvbDerivatives[1];
for (int i=0; i<1; i++) {
derivs[i].deriv_ops = new fvbOperators[1];
derivs[i].deriv_ops[0].setops(c,fp);
}
#else
/*********************************
 * In the case of no RK45 each
 * basis state gets its own
 * derivative object
 */

derivs = new fvbDerivatives[c.nbasis];
for (int i=0; i<c.nbasis; i++) {
derivs[i].deriv_ops = new fvbOperators[1];
derivs[i].deriv_ops[0].setops(c,fp);
}
#endif

#ifdef RK45
gslholder gslstuff;
gslstuff.wps = gwp;
gslstuff.dvs = derivs;
gslstuff.cs = c;
/*************************
 *  this holds all of the
 * current wp parameters
 */
```

```
gslstuff.all_params = new double[6*c.nbasis];
/*************************
 * This holds the initial
 * wp parameters
 */
gslstuff.all_params_i = new double[6*c.nbasis];
set_allparams(gslstuff,gslstuff.wps,c);
gsl_odeiv_system syst = {func, jac, 6*c.nbasis, &gslstuff};
#endif

#ifdef RKCONST
double y_err[6*c.nbasis];
double dydt_in[6*c.nbasis], dydt_out[6*c.nbasis];

//GSL_ODEIV_FN_EVAL(&syst, time, gslstuff.all_params, dydt_in);
int marker=0;

while (time < timestop) {
timeh = time / (2*M_PI);
if (((marker % 10000) == 0) || marker == 0) {
grefile<<timeh<<" ";
gimfile<<timeh<<" ";
Qfile<<timeh<<" ";
Pfile<<timeh<<" ";
arefile<<timeh<<" ";
aimfile<<timeh<<" ";
normfile<<timeh<<" ";
purityfile<<timeh<<" ";
q0file<<gwp[0].Q<<endl;

//write out wp parameters at current time
for (int i=0; i<c.nbasis; i++)
{
grefile<<gwp[i].gre<<" ";
gimfile<<gwp[i].gim<<" ";
Qfile<<gwp[i].Q<<" ";
Pfile<<gwp[i].P<<" ";
arefile<<gwp[i].are<<" ";
aimfile<<gwp[i].aim<<" ";
```

```
}

totnorm = 0.;
for (int i=0; i<c.nbasis; i++)
{
//calculate populations and total norm
gwp[i].calculate_norm(i);
totnorm += gwp[i].norm;

//write ith norm
normfile<<gwp[i].norm<<" ";
}

//Calculate trace_sys {rho^2}
check_purity(gwp,c);

//write purity to file
purityfile<<purity;

//start new line in files
grefile<<endl; gimfile<<endl; Qfile<<endl; Pfile<<endl; arefile<<endl; aimfile<<endl;
purityfile<<endl;

//write total norm to end of line in normfile
normfile<<totnorm<<endl;
}

int status = gsl_odeiv_step_apply (stepper,time,h,gslstuff.all_params,y_err,
                                   dydt_in, dydt_out, &syst);
update_array(gslstuff,gwp,c);

if (status != GSL_SUCCESS)
break;

for (int i=0; i<c.nbasis*6; i++) {
dydt_in[i] = dydt_out[i];
}

time += h;
```

```
marker ++;

cout<<time<<endl;
}
exit(1);
#endif

#ifdef RK45
for (int i= 1; i<timestop; i++) {

double ti = i * .1;

timeh = time / (2*M_PI);

grefile<<timeh<<" ";
gimfile<<timeh<<" ";
Qfile<<timeh<<" ";
Pfile<<timeh<<" ";
arefile<<timeh<<" ";
aimfile<<timeh<<" ";
normfile<<timeh<<" ";
purityfile<<timeh<<" ";
q0file<<gwp[0].Q<<endl;

//write out wp parameters at current time
for (int i=0; i<c.nbasis; i++)
{
grefile<<gwp[i].gre<<" ";
gimfile<<gwp[i].gim<<" ";
Qfile<<gwp[i].Q<<" ";
Pfile<<gwp[i].P<<" ";
arefile<<gwp[i].are<<" ";
aimfile<<gwp[i].aim<<" ";
}

totnorm = 0.;
for (int i=0; i<c.nbasis; i++)
{
//calculate populations and total norm
```

```
gwp[i].calculate_norm(i);
totnorm += gwp[i].norm;

//write ith norm
normfile<<gwp[i].norm<<" ";
}

//Calculate trace_sys {rho^2}
check_purity(gwp,c);

//write purity to file
purityfile<<purity;

//start new line in files
grefile<<endl; gimfile<<endl; Qfile<<endl; Pfile<<endl; arefile<<endl; aimfile<<endl;
purityfile<<endl;

//write total norm to end of line in normfile
normfile<<totnorm<<endl;

//end writing arrays
while (time < ti) {
int status = gsl_odeiv_evolve_apply
(evolver, controller, stepper, &syst, &time, ti,
&h, gslstuff.all_params);

update_array(gslstuff,gwp,c);
cout<<time/(2*M_PI)<<" "<<h<<endl;
}

}
exit(1);
#endif

/*****************************************************************************
*****************************************************************************
* Finite Difference
*/
/*****************************************
```

```
*******************************************
* Non - gmp first
*/

#ifdef DOUBLEFINITE

//main time loop
for (int total_step = 0; total_step < 1e12; total_step ++)
{
timeh = t.min() + (t.dt() * total_step)/(2*M_PI);
double inttime;

if ((total_step %  10000) == 0  )
{
cout<<timeh<<endl;

grefile<<timeh<<" ";
gimfile<<timeh<<" ";
Qfile<<timeh<<" ";
Pfile<<timeh<<" ";
arefile<<timeh<<" ";
aimfile<<timeh<<" ";
normfile<<timeh<<" ";
purityfile<<timeh<<" ";
q0file<<gwp[0].Q<<endl;

//write out wp parameters at current time
for (int i=0; i<c.nbasis; i++)
{
grefile<<gwp[i].gre<<" ";
gimfile<<gwp[i].gim<<" ";
Qfile<<gwp[i].Q<<" ";
Pfile<<gwp[i].P<<" ";
arefile<<gwp[i].are<<" ";
aimfile<<gwp[i].aim<<" ";
}

totnorm = 0.;
for (int i=0; i<c.nbasis; i++)
```

```
{
//calculate populations and total norm
gwp[i].calculate_norm(i);
totnorm += gwp[i].norm;

//write ith norm
normfile<<gwp[i].norm<<" ";
}

//Calculate trace_sys {rho^2}
check_purity(gwp,c);

//write purity to file
purityfile<<purity;

//start new line in files
grefile<<endl; gimfile<<endl; Qfile<<endl; Pfile<<endl; arefile<<endl; aimfile<<endl;
purityfile<<endl;

//write total norm to end of line in normfile
normfile<<totnorm<<endl;

} //end writing arrays

//get derivatives
for (int i=0; i<c.nbasis; i++)
derivs[i].get_derivs(i,gwp,c,derivs[0].deriv_ops[0].q);

//step forward one time step of length dt
for (int i=0; i<c.nbasis; i++)
{
gwp[i].gre += t.dt() * gwp[i].dgre;
gwp[i].gim += t.dt() * gwp[i].dgim;
gwp[i].Q += t.dt() * gwp[i].dQ;
gwp[i].P += t.dt() * gwp[i].dP;
gwp[i].are += t.dt() * gwp[i].dare;
gwp[i].aim += t.dt() * gwp[i].daim;
}
```

```
//renormalize wave packets
totnorm = 0.;
for (int i=0; i<c.nbasis; i++)
{
gwp[i].calculate_norm(i);
totnorm += gwp[i].norm;
}

//renormalize(gwp);

}// end total time

//close files
arefile.close(); aimfile.close(); grefile.close(); gimfile.close(); Qfile.close(); Pfile.close();
purityfile.close();
exit(0);
#endif

/*********************************************************
**********************************************************
* Now for GMP
*/

#ifdef GMP
mpfr_class timeh_;
//main time loop
for (int total_step = 0; total_step < 1e12; total_step ++)
{
timeh_ = t.min() + (t.dt() * total_step)/(2*M_PI);
double inttime;

//cout<<timeh_<<" "<<gwp[0].gmp_Q<<endl;

if ((total_step %  100) == 0  )
{
cout<<"time = "<<timeh_<<endl;

grefile<<timeh_<<" ";
gimfile<<timeh_<<" ";
```

```
Qfile<<timeh_<<" ";
Pfile<<timeh_<<" ";
arefile<<timeh_<<" ";
aimfile<<timeh_<<" ";
normfile<<timeh_<<" ";
purityfile<<timeh_<<" ";
//q0file<<gwp[0].gmp_Q<<endl;

//write out wp parameters at current time
for (int i=0; i<c.nbasis; i++)
{
grefile<<gwp[i].gmp_gre<<" ";
gimfile<<gwp[i].gmp_gim<<" ";
Qfile<<gwp[i].gmp_Q<<" ";
Pfile<<gwp[i].gmp_P<<" ";
arefile<<gwp[i].gmp_are<<" ";
aimfile<<gwp[i].gmp_aim<<" ";
}

totnorm = 0.;
/*  for (int i=0; i<c.nbasis; i++)
{
//calculate populations and total norm
gwp[i].calculate_norm(i);
totnorm += gwp[i].norm;

//write ith norm
normfile<<gwp[i].norm<<" ";
} */

//Calculate trace_sys {rho^2}
// check_purity(gwp,c);

//write purity to file
purityfile<<purity;

//start new line in files
grefile<<endl; gimfile<<endl; Qfile<<endl; Pfile<<endl; arefile<<endl; aimfile<<endl;
purityfile<<endl;
```

```
//write total norm to end of line in normfile
normfile<<totnorm<<endl;

} //end writing arrays

//get derivatives
for (int i=0; i<c.nbasis; i++)
derivs[i].get_derivs_gmp(i,gwp,c);

//step forward one time step of length dt
for (int i=0; i<c.nbasis; i++)
{
gwp[i].gmp_gre += t.tdt_ * gwp[i].dgre_;
gwp[i].gmp_gim += t.tdt_ * gwp[i].dgim_;
gwp[i].gmp_Q += t.tdt_ * gwp[i].dQ_;
gwp[i].gmp_P += t.tdt_ * gwp[i].dP_;
gwp[i].gmp_are += t.tdt_ * gwp[i].dare_;
gwp[i].gmp_aim += t.tdt_ * gwp[i].daim_;
}

//renormalize wave packets
totnorm = 0.;
for (int i=0; i<c.nbasis; i++)
{
gwp[i].calculate_norm(i);
totnorm += gwp[i].norm;
}

//renormalize(gwp);

}// end total time

//close files
arefile.close(); aimfile.close(); grefile.close(); gimfile.close(); Qfile.close(); Pfile.close();
purityfile.close();
exit(0);
#endif
```

```
/*************************************************************************
*************************************************************************
* Runge Kutta for GMP
*  Fixed or adaptive step size chosen by defining
    *  RK4QC (adaptive) or not (fixed) in fvb.h, both have
    *  GMPRK4 defined
*************************************************************************
*************************************************************************
*/

#ifdef GMPRK4
cout<<"Using rk4 with gmp precision of "<<precision<<" bits"<<endl;
mpfr_class timeh_("0", precision);
mpfr_class htry("0.0001", precision);
//bath wave packets
fvbWavePacket *gwp_t = new fvbWavePacket[c.nbasis];
mpfr_class dydx[6*c.nbasis];
mpfr_class dyt[6*c.nbasis];
mpfr_class dym[6*c.nbasis];
   mpfr_class y[6*c.nbasis];

  for (int i=0; i<6*c.nbasis; i++){
dydx[i].set_prec(precision);
dyt[i].set_prec(precision);
dym[i].set_prec(precision);
         y[i].set_prec(precision);
}
   for (int i=0; i<c.nbasis; i++) {
y[0+i*6] = gwp[i].gmp_gre ;
y[1+i*6] = gwp[i].gmp_gim ;
y[2+i*6] = gwp[i].gmp_Q ;
y[3+i*6] = gwp[i].gmp_P ;
y[4+i*6] = gwp[i].gmp_are ;
y[5+i*6] = gwp[i].gmp_aim ;
}

//main time loop
int total_step = 0;
//for (int total_step = 0; total_step < 1e12; total_step ++)
```

```
while (timeh_ <= t.tmax())
{
#ifndef RK4QC
timeh_ = t.tmin() + (t.tdt_ * total_step)/(2*M_PI);
double inttime;



if ((total_step %  10000) == 0  )
{
#endif
cout<<"time is "<<timeh_/(2*M_PI) <<endl;

grefile<<timeh_/(2*M_PI)<<" ";
gimfile<<timeh_/(2*M_PI)<<" ";
Qfile<<timeh_/(2*M_PI)<<" ";
Pfile<<timeh_/(2*M_PI)<<" ";
arefile<<timeh_/(2*M_PI)<<" ";
aimfile<<timeh_/(2*M_PI)<<" ";
normfile<<timeh_/(2*M_PI)<<" ";
purityfile<<timeh_/(2*M_PI)<<" ";
q0file<<timeh_/(2*M_PI)<<" ";
qtfile<<timeh_/(2*M_PI)<<" ";


//write out wp parameters at current time
for (int i=0; i<c.nbasis; i++)
{
grefile<<gwp[i].gmp_gre<<" ";
gimfile<<gwp[i].gmp_gim<<" ";
Qfile<<gwp[i].gmp_Q<<" ";
Pfile<<gwp[i].gmp_P<<" ";
arefile<<gwp[i].gmp_are<<" ";
aimfile<<gwp[i].gmp_aim<<" ";
}

mpfr_class totnorm_("0", precision);

  for (int i=0; i<c.nbasis; i++)
```

```
{
//calculate populations and total norm
gwp[i].calculate_norm_gmp(i);
totnorm_ += gwp[i].norm_;

//write ith norm
normfile<<gwp[i].norm_<<" ";
}

//set double wp params to the gmp values
for (int i=0; i<c.nbasis; i++) {
gwp[i].gmp_to_double();
}

//calculate average value of system coordinate
//and write it to a file
double qavg = q(gwp,c,derivs[0].deriv_ops[0].q,fp);
q0file<<qavg;

dcomp qta = qt(gwp,c);

//fourier_trans(qta);

qtfile<<real(qta)<<" "<<imag(qta);

//Calculate trace_sys {rho^2}
// check_purity(gwp,c);

//write purity to file
purityfile<<purity;

//start new line in files
grefile<<endl; gimfile<<endl; Qfile<<endl; Pfile<<endl; arefile<<endl; aimfile<<endl;
purityfile<<endl;q0file<<endl;qtfile<<endl;

//write total norm to end of line in normfile
normfile<<totnorm_<<endl;
#ifndef RK4QC
} //end writing arrays
```

```
#endif
#ifndef RK4QC
      //Take one step of size t.tdt_
      rk4_step(derivs, gwp, gwp_t, c, t.tdt_, dydx, dyt, dym, y,fp);
#else
  mpfr_class dt(t.every_dt_);
mpfr_class t2 ( timeh_ + t.every_dt_, precision);
odeint(y, derivs, gwp, gwp_t, c, &timeh_, t2, htry, dydx, dyt, dym,fp);
#endif
total_step ++;
}// end total time

//close files
arefile.close(); aimfile.close(); grefile.close(); gimfile.close(); Qfile.close(); Pfile.close();
purityfile.close();
exit(0);
#endif

};

void fvbPropagate::odeint(mpfr_class ystart[], fvbDerivatives *derivs, fvbWavePacket *gwp,
fvbWavePacket *gwp_t, fvbConstants &c, mpfr_class *timeh_, mpfr_class t2,
   mpfr_class h1_, mpfr_class dydx[],
                           mpfr_class dyt[], mpfr_class dym[],fvbPotentials fp)
{
mpfr_class x(*timeh_);
mpfr_class y[6*c.nbasis], yscal[6*c.nbasis];
    mpfr_class tiny(1e-30, precision);
    mpfr_class hnext("0", precision);
    mpfr_class hmin("1e-100", precision);

for (int i=0; i<6*c.nbasis; i++) {
y[i].set_prec(precision);
yscal[i].set_prec(precision);
y[i] = ystart[i];
}

/***************************************
 * Step forward until a predefined max
```

```
 * number of steps (per dt event)
 * is reached
 */

for (int nstp = 1; nstp <= MAXSTP; nstp++) {
/***********************
 * get initial derivs
 */

for (int i=0; i<c.nbasis; i++)
derivs[i].get_derivs_gmp(i,gwp,c,fp);

for (int i=0; i<c.nbasis; i++) {
dydx[0+i*6] = gwp[i].dgre_;
dydx[1+i*6] = gwp[i].dgim_;
dydx[2+i*6] = gwp[i].dQ_;
dydx[3+i*6] = gwp[i].dP_;
dydx[4+i*6] = gwp[i].dare_;
dydx[5+i*6] = gwp[i].daim_;
}

for (int i=0; i<6*c.nbasis; i++)
yscal[i] = abs(y[i]) + abs(dydx[i] * h1_) + tiny;

if ((x+h1_-t2)*(x+h1_-*timeh_) > 0) {
h1_ = t2 - x;
      }
rkqc(derivs, gwp, gwp_t, c, &h1_, dydx, dyt, dym, y,
           &x, yscal, &hnext,fp);
      if ((x-t2)*(t2-*timeh_) >= 0) {
         *timeh_ = x;
         return;
      }
      if (abs(hnext)<hmin) {
         cout<<"h < hmin in fvbPropagate::odeint()"<<endl;
         cout<<"h = "<<hnext<<", hmin = "<<hmin<<endl;
         exit(1);
      }
      h1_ = hnext;
```

```
   }
   cout<<"too many steps in fvbPropagate::odeint()"<<endl;
   exit(1);

}
void fvbPropagate::rkqc(fvbDerivatives *derivs,fvbWavePacket * gwp,
                            fvbWavePacket *gwp_t, fvbConstants &c,
                            mpfr_class *time_step, mpfr_class dydx[],
                            mpfr_class dyt[], mpfr_class dym[], mpfr_class y[],
                           mpfr_class *x, mpfr_class yscal[], mpfr_class *hnext,
                       fvbPotentials fp)
{
mpfr_class safety(0.75, precision);
    mpfr_class pshrink(-.25, precision);
    mpfr_class pgrow(-.2, precision);
    mpfr_class errcon(6e-8, precision);
    mpfr_class eps("1e-20", precision);
mpfr_class xsav(*x);
mpfr_class ysave[6*c.nbasis];
    mpfr_class ytemp[6*c.nbasis];
mpfr_class hh(*time_step/2, precision);
    mpfr_class errmax("0", precision);

for (int i=0; i<6*c.nbasis; i++) {
ysave[i].set_prec(precision);
       ytemp[i].set_prec(precision);
   }

for (int i=0; i<c.nbasis; i++) {
ysave[0+i*6] = gwp[i].gmp_gre ;
ysave[1+i*6] = gwp[i].gmp_gim ;
ysave[2+i*6] = gwp[i].gmp_Q ;
ysave[3+i*6] = gwp[i].gmp_P ;
ysave[4+i*6] = gwp[i].gmp_are ;
ysave[5+i*6] = gwp[i].gmp_aim ;

     ytemp[0+i*6] = gwp[i].gmp_gre ;
ytemp[1+i*6] = gwp[i].gmp_gim ;
ytemp[2+i*6] = gwp[i].gmp_Q ;
```

```
ytemp[3+i*6] = gwp[i].gmp_P ;
ytemp[4+i*6] = gwp[i].gmp_are ;
ytemp[5+i*6] = gwp[i].gmp_aim ;
}

for(;;) {
    hh = *time_step/2;
    for (int i=0; i<c.nbasis; i++) {
     ytemp[0+i*6] = ysave[0+i*6] ;
        ytemp[1+i*6] = ysave[0+i*6] ;
        ytemp[2+i*6] = ysave[0+i*6] ;
        ytemp[3+i*6] = ysave[0+i*6] ;
        ytemp[4+i*6] = ysave[0+i*6] ;
        ytemp[5+i*6] = ysave[0+i*6] ;

        y[0+i*6] = ysave[0+i*6] ;
        y[1+i*6] = ysave[0+i*6] ;
        y[2+i*6] = ysave[0+i*6] ;
        y[3+i*6] = ysave[0+i*6] ;
        y[4+i*6] = ysave[0+i*6] ;
        y[5+i*6] = ysave[0+i*6] ;

        gwp[i].gmp_gre = ysave[0+i*6];
        gwp[i].gmp_gim = ysave[1+i*6];
        gwp[i].gmp_Q = ysave[2+i*6];
        gwp[i].gmp_P = ysave[3+i*6];
        gwp[i].gmp_are = ysave[4+i*6];
        gwp[i].gmp_aim = ysave[5+i*6];
}
      /*****************************
* take a half step
* using the array 'ytemp'
*/
rk4_step(derivs, gwp, gwp_t, c, hh, dydx, dyt, dym, ytemp,fp);
    //get derivs
for (int i=0; i<c.nbasis; i++)
derivs[i].get_derivs_gmp(i,gwp,c,fp);
     /*****************************
* take a half step
```

```
* using the array 'ytemp'
*/
rk4_step(derivs, gwp, gwp_t, c, hh, dydx, dyt, dym, ytemp,fp);
    //step time variable and check if step is too small
*x = xsav + *time_step;
if ( *x == xsav) {
cout<<"stepsize too small in fvbPropagate::rkqc()"<<endl;
        cout<<*time_step<<" was the time step"<<endl;
exit(1);
}

    //revert gwp to pre-half-step values
    for (int i=0; i<c.nbasis; i++) {
gwp[i].gmp_gre = ysave[0+i*6];
gwp[i].gmp_gim = ysave[1+i*6];
gwp[i].gmp_Q = ysave[2+i*6];
gwp[i].gmp_P = ysave[3+i*6];
gwp[i].gmp_are = ysave[4+i*6];
gwp[i].gmp_aim = ysave[5+i*6];
    }

    //get derivs
    for (int i=0; i<c.nbasis; i++)
derivs[i].get_derivs_gmp(i,gwp,c,fp);
    /*****************************
* take a whole step
* using the array 'y'
*/

rk4_step(derivs, gwp, gwp_t, c, *time_step, dydx, dyt, dym, y,fp);
    //evaluate error
    errmax = "0";
    for (int i=0; i<6*c.nbasis; i++) {
       ytemp[i] = y[i] - ytemp[i];
       errmax = MAX(errmax, abs(ytemp[i]/yscal[i]));
    }
       errmax /= eps;
       if (errmax > 1) {
         *time_step = safety * *time_step * (pow(errmax, pshrink));
```

```
          continue;
        } else {
          // hdid = time_step;
          if (errmax > errcon) {
             *hnext = safety * *time_step * (pow(errmax, pgrow));
          } else {
            *hnext = 1.5 * *time_step;
          }
         break;
        }
break;
}

   for (int i=0; i<6*c.nbasis; i++)
      y[i] += ytemp[i] * (1/15);
}
void fvbPropagate::rk4_step(fvbDerivatives *derivs,fvbWavePacket * gwp,
                            fvbWavePacket *gwp_t, fvbConstants &c,
                            mpfr_class time_step, mpfr_class dydx[],
                            mpfr_class dyt[], mpfr_class dym[], mpfr_class y[],
                            fvbPotentials fp)
{
 #ifndef RK4QC
//Get derivatives for first step
for (int i=0; i<c.nbasis; i++)
derivs[i].get_derivs_gmp(i,gwp,c,fp);

for (int i=0; i<c.nbasis; i++) {
dydx[0+i*6] = gwp[i].dgre_;
dydx[1+i*6] = gwp[i].dgim_;
dydx[2+i*6] = gwp[i].dQ_;
dydx[3+i*6] = gwp[i].dP_;
dydx[4+i*6] = gwp[i].dare_;
dydx[5+i*6] = gwp[i].daim_;
}
#endif
for (int i=0; i<c.nbasis; i++) {
gwp_t[i].gmp_are = gwp[i].gmp_are + gwp[i].dare_ * (time_step  / 2);
gwp_t[i].gmp_aim = gwp[i].gmp_aim + gwp[i].daim_ *( time_step  / 2);
```

```
gwp_t[i].gmp_Q = gwp[i].gmp_Q + gwp[i].dQ_ * (time_step  / 2);
gwp_t[i].gmp_P = gwp[i].gmp_P + gwp[i].dP_ *( time_step  / 2);
gwp_t[i].gmp_gre = gwp[i].gmp_gre + gwp[i].dgre_ * (time_step  / 2);
gwp_t[i].gmp_gim = gwp[i].gmp_gim + gwp[i].dgim_ * (time_step  / 2);
}

// for (int i=0; i<c.nbasis; i++) {
// cout<<time_step<<" "<<gwp_t[i].gmp_aim<<" "<<gwp_t[i].gmp_Q<<" "<<gwp_t[i].gmp_P<<endl;
// }
// exit(1);

//Get derivatives for second step
for (int i=0; i<c.nbasis; i++)
derivs[i].get_derivs_gmp(i,gwp_t,c,fp);

for (int i=0; i<c.nbasis; i++) {
dyt[0 + i*6] = gwp_t[i].dgre_;
dyt[1+i*6] = gwp_t[i].dgim_;
dyt[2+i*6] = gwp_t[i].dQ_;
dyt[3+i*6] = gwp_t[i].dP_;
dyt[4+i*6] = gwp_t[i].dare_;
dyt[5+i*6] = gwp_t[i].daim_;
}

for (int i=0; i<c.nbasis; i++) {
gwp_t[i].gmp_gre = gwp[i].gmp_gre + dyt[0+i*6] * time_step  / 2;
gwp_t[i].gmp_gim = gwp[i].gmp_gim + dyt[1+i*6] * time_step  / 2;
gwp_t[i].gmp_Q = gwp[i].gmp_Q + dyt[2+i*6] * time_step  / 2;
gwp_t[i].gmp_P = gwp[i].gmp_P + dyt[3+i*6] * time_step  / 2;
gwp_t[i].gmp_are = gwp[i].gmp_are + dyt[4+i*6] * time_step  / 2;
gwp_t[i].gmp_aim = gwp[i].gmp_aim + dyt[5+i*6] * time_step  / 2;
}



//Get derivatives for third step
for (int i=0; i<c.nbasis; i++)
derivs[i].get_derivs_gmp(i,gwp_t,c,fp);
```

```
for (int i=0; i<c.nbasis; i++) {
dym[0 + i*6] = gwp_t[i].dgre_;
dym[1+i*6] = gwp_t[i].dgim_;
dym[2+i*6] = gwp_t[i].dQ_;
dym[3+i*6] = gwp_t[i].dP_;
dym[4+i*6] = gwp_t[i].dare_;
dym[5+i*6] = gwp_t[i].daim_;
}

for (int i=0; i<c.nbasis; i++) {
gwp_t[i].gmp_gre = gwp[i].gmp_gre + dym[0+i*6] * time_step;
gwp_t[i].gmp_gim = gwp[i].gmp_gim + dym[1+i*6] * time_step;
gwp_t[i].gmp_Q = gwp[i].gmp_Q + dym[2+i*6] * time_step;
gwp_t[i].gmp_P = gwp[i].gmp_P + dym[3+i*6] * time_step;
gwp_t[i].gmp_are = gwp[i].gmp_are + dym[4+i*6] * time_step;
gwp_t[i].gmp_aim = gwp[i].gmp_aim + dym[5+i*6] * time_step;

dym[0+i*6] += dyt[0 +i*6];
dym[1+i*6] += dyt[1 +i*6];
dym[2+i*6] += dyt[2 +i*6];
dym[3+i*6] += dyt[3 +i*6];
dym[4+i*6] += dyt[4 +i*6];
dym[5+i*6] += dyt[5 +i*6];
}

//Fourth step
for (int i=0; i<c.nbasis; i++)
derivs[i].get_derivs_gmp(i,gwp_t,c,fp);

for (int i=0; i<c.nbasis; i++) {
dyt[0 + i*6] = gwp_t[i].dgre_;
dyt[1+i*6] = gwp_t[i].dgim_;
dyt[2+i*6] = gwp_t[i].dQ_;
dyt[3+i*6] = gwp_t[i].dP_;
dyt[4+i*6] = gwp_t[i].dare_;
dyt[5+i*6] = gwp_t[i].daim_;
}

for (int i=0; i<c.nbasis; i++) {
```

```
gwp[i].gmp_gre += (2*dym[0+i*6] + dyt[0+i*6] + dydx[0+i*6])* (time_step/6);
gwp[i].gmp_gim += (2*dym[1+i*6] + dyt[1+i*6] + dydx[1+i*6])* (time_step/6);
gwp[i].gmp_Q += (2*dym[2+i*6] + dyt[2+i*6] + dydx[2+i*6])* (time_step/6);
gwp[i].gmp_P += (2*dym[3+i*6] + dyt[3+i*6] + dydx[3+i*6])* (time_step/6);
gwp[i].gmp_are += (2*dym[4+i*6] + dyt[4+i*6] + dydx[4+i*6])* (time_step/6);
gwp[i].gmp_aim += (2*dym[5+i*6] + dyt[5+i*6] + dydx[5+i*6])* (time_step/6);

        y[0+i*6] = gwp[i].gmp_gre ;
y[1+i*6] = gwp[i].gmp_gim ;
y[2+i*6] = gwp[i].gmp_Q ;
y[3+i*6] = gwp[i].gmp_P ;
y[4+i*6] = gwp[i].gmp_are ;
y[5+i*6] = gwp[i].gmp_aim ;
}

   for (int i=0; i<c.nbasis; i++) {
        y[0+i*6] = gwp[i].gmp_gre ;
y[1+i*6] = gwp[i].gmp_gim ;
y[2+i*6] = gwp[i].gmp_Q ;
y[3+i*6] = gwp[i].gmp_P ;
y[4+i*6] = gwp[i].gmp_are ;
y[5+i*6] = gwp[i].gmp_aim ;
}

}

void fvbPropagate::renormalize(fvbWavePacket *gwp, fvbConstants c)
{
factor = 0.5*(log(totnorm)-log(initnorm));

for (int i=0; i<c.nbasis; i++)
gwp[i].gim += factor;
};

dcomp fvbPropagate::calculate_overlap(int one, int two, fvbWavePacket *gwp)
{
//Calculate A, B, and C in expression 40-43 in JCP
A = dcomp(gwp[one].aim + gwp[two].aim, gwp[one].are - gwp[two].are);
```

```
B = dcomp(2.*gwp[one].aim*gwp[one].Q + 2.*gwp[two].aim*gwp[two].Q,
2.*gwp[one].are*gwp[one].Q - 2.*gwp[two].are*gwp[two].Q - gwp[one].P
+ gwp[two].P);

C = dcomp(-gwp[one].aim*gwp[one].Q*gwp[one].Q - gwp[two].aim*gwp[two].Q*gwp[two].Q
-gwp[one].gim - gwp[two].gim,
-gwp[one].are*gwp[one].Q*gwp[one].Q
+ gwp[two].are*gwp[two].Q*gwp[two].Q + gwp[one].Q*gwp[one].P
- gwp[two].Q*gwp[two].P -gwp[one].gre + gwp[two].gre);

//exponential argument and prefactor
exp_arg = 0.25*A*B*B + C;
exp_pre =  sqrt(M_PI/A);

//cout<<one<<" "<<two<<" "<<A<<" "<<B<<" "<<C<<" "<<exp_arg<<endl;

return exp(real(exp_arg)) * dcomp(cos(imag(exp_arg))*real(exp_pre) - sin(imag(exp_arg))
* imag(exp_pre), cos(imag(exp_arg))* imag(exp_pre) + sin(imag(exp_arg))*real(exp_pre));
};

dcomp fvbPropagate::calculate_overlap_init(int one, int two, fvbWavePacket *gwp)
{
//Calculate A, B, and C in expression 40-43 in JCP
A = dcomp(gwp[one].aimi + gwp[two].aim, gwp[one].arei - gwp[two].are);

B = dcomp(2.*gwp[one].aimi*gwp[one].Qi + 2.*gwp[two].aim*gwp[two].Q,
2.*gwp[one].arei*gwp[one].Qi - 2.*gwp[two].are*gwp[two].Q - gwp[one].Pi
+ gwp[two].P);

C = dcomp(-gwp[one].aimi*gwp[one].Qi*gwp[one].Qi - gwp[two].aim*gwp[two].Q*gwp[two].Q
-gwp[one].gimi - gwp[two].gim,
-gwp[one].arei*gwp[one].Qi*gwp[one].Qi
+ gwp[two].are*gwp[two].Q*gwp[two].Q + gwp[one].Qi*gwp[one].Pi
- gwp[two].Q*gwp[two].P -gwp[one].grei + gwp[two].gre);

//exponential argument and prefactor
exp_arg = 0.25*A*B*B + C;
exp_pre =  sqrt(M_PI/A);
```

```
//cout<<one<<" "<<two<<" "<<A<<" "<<B<<" "<<C<<" "<<exp_arg<<endl;

return exp(real(exp_arg)) * dcomp(cos(imag(exp_arg))*real(exp_pre) - sin(imag(exp_arg))
* imag(exp_pre), cos(imag(exp_arg))* imag(exp_pre) + sin(imag(exp_arg))*real(exp_pre));
};

void fvbPropagate::check_purity(fvbWavePacket *gwp, fvbConstants c)
{
purity = 0.;
//Loop over pairs of vibrational states
for (int i=0; i<c.nbasis; i++)
for (int j=0; j<c.nbasis; j++)
{
overlap = calculate_overlap(i,j,gwp);
purity += real(overlap*conj(overlap));
// cout<<i<<" "<<j<<" "<<overlap<<" "<<real(overlap*conj(overlap))<<endl;
}
// exit(1);
};

void fvbPropagate::set_allparams(gslholder gslstuff, fvbWavePacket *gwp, fvbConstants c)
{
for (int i=0; i<c.nbasis; i++) {
gslstuff.all_params[0+i*6] = gwp[i].gre;
gslstuff.all_params[1+i*6] = gwp[i].gim;
gslstuff.all_params[2+i*6] = gwp[i].Q;
gslstuff.all_params[3+i*6] = gwp[i].P;
gslstuff.all_params[4+i*6] = gwp[i].are;
gslstuff.all_params[5+i*6] = gwp[i].aim;

gslstuff.all_params_i[0+i*6] = gwp[i].gre;
gslstuff.all_params_i[1+i*6] = gwp[i].gim;
gslstuff.all_params_i[2+i*6] = gwp[i].Q;
gslstuff.all_params_i[3+i*6] = gwp[i].P;
gslstuff.all_params_i[4+i*6] = gwp[i].are;
gslstuff.all_params_i[5+i*6] = gwp[i].aim;
}
}
```

```
void fvbPropagate::update_array(gslholder gslstuff, fvbWavePacket *gwp, fvbConstants c)
{
for (int i=0; i<c.nbasis; i++) {
gwp[i].gre = gslstuff.all_params[0+i*6];
gwp[i].gim = gslstuff.all_params[1+i*6];
gwp[i].Q = gslstuff.all_params[2+i*6];
gwp[i].P = gslstuff.all_params[3+i*6];
gwp[i].are = gslstuff.all_params[4+i*6];
gwp[i].aim = gslstuff.all_params[5+i*6];
}
gslstuff.wps = gwp;
}

void fvbPropagate::revert(gslholder gslstuff, fvbConstants c)
{
for (int i=0; i<c.nbasis; i++) {
gslstuff.all_params[0+i*6] = gslstuff.all_params_i[0+i*6];
gslstuff.all_params[1+i*6] = gslstuff.all_params_i[1+i*6];
gslstuff.all_params[2+i*6] = gslstuff.all_params_i[2+i*6];
gslstuff.all_params[3+i*6] = gslstuff.all_params_i[3+i*6];
gslstuff.all_params[4+i*6] = gslstuff.all_params_i[4+i*6];
gslstuff.all_params[5+i*6] = gslstuff.all_params_i[5+i*6] ;
}
}

double fvbPropagate::q(fvbWavePacket *gwp, fvbConstants c, double *q, fvbPotentials fp)
{
double sum = 0.;

for (int i=0; i<c.nbasis-1; i++) {
for (int j=i+1; j<c.nbasis; j++) {
sum += q[i+j*c.nbasis] * 2 * real(calculate_overlap(i,j,gwp));
}
sum += gwp[i].get_norm() * q[i+i*c.nbasis];
}

return sum;
}
```

```
dcomp fvbPropagate::qt(fvbWavePacket *gwp, fvbConstants c)
{
dcomp sum = dcomp(0.,0.);

for (int i=0; i<c.nbasis; i++) {
sum += calculate_overlap_init(i,i,gwp)/*/gwp[i].get_norm()*/;
}

return sum;
}
```

File: "fvbTimeParameters.h"

```
/*************************************************************************
 *            fvbTimeParameters.h
 *
 *  Wed Dec  3 12:27:28 2008
 *  Copyright  2008  Craig Chapman
 *  cchapma2@uoregon.edu
 *************************************************************************/
//#include "fvb.h"

class fvbTimeParameters
{
public:
double tmn, tmx, tdt;
mpfr_class tmn_, tmx_, tdt_, every_dt_;
double tnstep;
mpfr_class tnstep_;
public:
//get/set min or max values
double tmin();
void set_tmin(double x);
double tmax();
void set_tmax(double x);

//get/set time step
//dt_set_steps sets number of steps
//according to min, max, and dt
double dt();
```

```
void set_dt(double x);
void set_dt();

//get/set number of steps
//dt_set_steps sets dt
//according to min, max, and tsteps
double tsteps();
void tsteps(double x);
void set_tsteps();

fvbTimeParameters();
~fvbTimeParameters() {};
};
```

File: "fvbTimeParameters.cc"

```
/*****************************************************************************
 *            fvbTimeParameters.cc
 *
 *  Thu Oct  2 18:03:44 2008
 *  Copyright  2008  Craig Chapman
 *  cchapma2@uoregon.edu
 *****************************************************************************/

#include "fvb.h"

fvbTimeParameters::fvbTimeParameters()
{

}

double fvbTimeParameters::tmin()
{
return tmn;
}

void fvbTimeParameters::set_tmin(double x)
{
tmn = x;
}
```

```
double fvbTimeParameters::tmax()
{
return tmx;
}

void fvbTimeParameters::set_tmax(double x)
{
tmx = x;
}

double fvbTimeParameters::dt()
{
return tdt;
}

void fvbTimeParameters::set_dt(double x)
{
tdt = x;
}

//set an integer number of steps, closest to
//the full range without going over
void fvbTimeParameters::set_tsteps()
{
tnstep = floor((tmx-tmn)/tdt);
};

//set nsteps w/o dt
double fvbTimeParameters::tsteps()
{
return tnstep;
}

void fvbTimeParameters::tsteps(double x)
{
tnstep = x;
}
```

```
//sets dt according to tmax,min, and number
// of desired steps
void fvbTimeParameters::set_dt()
{
tdt = (tmx-tmn)/tnstep;
};
```

File: "fvbWavePackets.h"

```
/*************************************************************************
 *            fvbWavePackets.h
 *
 *  Wed Dec  3 12:26:50 2008
 *  Copyright  2008  Craig Chapman
 *  cchapma2@uoregon.edu
 *************************************************************************/
//#include "fvb.h"

class fvbWavePacket
{
public:
//wp parameters
double gim, gre,are,aim,P,Q, *all_params;
mpfr_class gmp_gim, gmp_gre, gmp_are, gmp_aim, gmp_P, gmp_Q, *all_params_gmp;
    mpfr_class *y;
double gimi,grei,arei,aimi,Qi,Pi;



//param derivs
double dgim, dgre, dare, daim, dP, dQ;
mpfr_class dgim_, dgre_, dare_, daim_, dP_, dQ_;
//other wp stuff
double norm;
       mpfr_class norm_;
void calculate_norm(int level);
       void calculate_norm_gmp(int level);

//initial conditions
void Initialize(int level, fvbOperators * , double dis, fvbPotentials);
```

```
        //convert gmp to double for calculating populations, etc...
        void gmp_to_double();

double get_norm();

fvbWavePacket();
~fvbWavePacket() {};
};
```

File: "fvbWavePackets.cc"

```
/*************************************************************************
 *            fvb.cc
 *
 *  Thu Oct  2 17:15:44 2008
 *  Copyright  2008  Craig Chapman
 *  cchapma2@uoregon.edu
 *************************************************************************/
#include "fvb.h"

fvbWavePacket::fvbWavePacket()
{
dgim_.set_prec(precision);
dgre_.set_prec(precision);
dQ_.set_prec(precision);
dP_.set_prec(precision);
dare_.set_prec(precision);
daim_.set_prec(precision);
   norm_.set_prec(precision);
}
void fvbWavePacket::Initialize(int level, fvbOperators ops[], double dis, fvbPotentials c)
{
aim = c.omega_bath_.get_d()*0.5;
are = 0.;

//gim = -0.25*log(c.omega_bath_/M_PI)  +0.5*log(gsl_sf_fact(level))
// - level*log(sqrt(c.omega_sys_/2.)*c.qe_)
// + (c.omega_sys_/4)*c.qe_*c.qe_;

gre = 0.;
```

```
P=0.;
Q=0.;

/*
*set precision of wp parameters (gmp)
*/
gmp_gim.set_prec(precision);
gmp_gre.set_prec(precision);
gmp_Q.set_prec(precision);
gmp_P.set_prec(precision);
gmp_are.set_prec(precision);
gmp_aim.set_prec(precision);

gmp_Q = c.Qe_;
gmp_P = "0";

gmp_are = "0";

if (c.gamma[level] > 0)
gmp_gre = "0";
else
gmp_gre = M_PI;

gmp_aim = c.omega_bath_/2;
gmp_gim = -0.25*log(c.omega_bath_/M_PI)  /*+0.5*log(gsl_sf_fact(level))
- level*log(sqrt(c.omega_sys_/2)*c.qe_) */
-log(abs(c.gamma[level]))
;//+ (c.omega_sys_/4)*c.qe_*c.qe_;

Qi=gmp_Q.get_d();
Pi = gmp_P.get_d();
arei = gmp_are.get_d();
aimi = gmp_aim.get_d();
gimi = gmp_gim.get_d();
grei = gmp_gre.get_d();

//cout<<level<<" "<<gmp_gim<<endl;
};
```

```
void fvbWavePacket::calculate_norm(int level)
{
norm = sqrt(M_PI/(2*aim)) * exp (-2. * gim);
};

void fvbWavePacket::calculate_norm_gmp(int level)
{
   norm_ = sqrt(M_PI/(2*gmp_aim)) * exp (-2 * gmp_gim);
}

double fvbWavePacket::get_norm()
{
return sqrt(M_PI/(2*aim)) * exp (-2. * gim);
}

void fvbWavePacket::gmp_to_double()
{
   gre = gmp_gre.get_d();
   gim = gmp_gim.get_d();
   Q = gmp_Q.get_d();
   P = gmp_P.get_d();
   are = gmp_are.get_d();
   aim = gmp_aim.get_d();
};
```

REFERENCES

V. A. Apkarian and N. Schwentner. Molecular photodynamics in rare gas solids. *Chem. Rev.*, 99(6):1481, 1999.

I. Sh. Averbukh, M. Shapiro, C. Leichtle, and W. P. Schleich. Reconstructing wave packets by quantum-state holography. *Phys. Rev. A*, 59(3):2163–2173, 1999.

Joel S. Bader and B. J. Berne. Quantum and classical relaxation rates from classical simulations. *J. Chem. Phys.*, 100(11):8359, 1994.

Richard F. Barrow and Kim K. Yee. $B^3_{0+u}X^1_{+g}$ system of $^{127}I_2$: Rotational analysis and long-range potential in the B^3_{0+u} state. *J. Chem. Soc. Faraday Trans. 2*, 69:684, 1973.

Peter F. Bernath. *Spectra of Atoms and Molecules.* Oxford University Press, NY, 1995.

Z. Bihary, M. Karavitis, and V. Ara Apkarian. Onset of decoherence: Six-wave mixing measurements of vibrational decoherence on the excited electronic state of I_2 in solid argon. *J. Chem. Phys.*, 120(17):8144, 2004.

Z. Bihary, R. Zadoyan, M. Karavitis, and V. A. Apkarian. Dynamics and the breaking of a driven cage: I_2 in solid Ar. *J. Chem. Phys.*, 120(16):7576, 2004.

M. Born and J. R. Oppenheimer. On the quantum theory of molecules. *Ann. Phys.*, 84(427), 1927.

H. G. Breunig, G. Urbasch, and K.-M. Weitzel. Phase control of molecular fragmentation with a pair of femtosecond-laser pulses. *J. Chem. Phys.*, 128(12):121101, 2008.

Victoria Buch. Exploration of multidimensional variational gaussian wave packets as a simulation tool. *J. Chem. Phys.*, 117(10):4738, 2002.

Victoria Buch. Calculation of infrared absorption spectra using gaussian variational wave packets. *J. Chem. Phys.*, 121(14):6961, 2004.

C. T. Chapman and J. A. Cina. Semiclassical treatments for small-molecule dynamics in low-temperature crystals using fixed and adiabatic vibrational bases. *J. Chem. Phys.*, 127:114502, 2007.

J. A. Cina, Jr. T. J. Smith, and V. Romero-Rochin. Time-resolved optical tests for electronic geometric phase development. *Adv. Chem. Phys.*, 83:1, 1993.

Jeffrey A. Cina and Robert A. Harris. On the preparation and measurement of superpositions of chiral amplitudes. *J. Chem. Phys.*, 100(4):2531, 1994.

Rob D. Coalson and Martin Karplus. Multidimensional variational gaussian wave packet dynamics with application to photodissociation spectroscopy. *J. Chem. Phys.*, 93(6):3919, 1990.

Pavel Frantsuzov, Arnold Neumaier, and Vladimir A. Mandelshtam. Gaussian resolutions for equilibrium density matrices. *Chem. Phys. Lett.*, 381(1-2):117, 2003.

Pavel A. Frantsuzov and Vladimir A. Mandelshtam. Quantum statistical mechanics with gaussians: Equilibrium properties of van der waals clusters. *J. Chem. Phys.*, 121(19):9247, 2004.

M Fushitani, M Bargheer, M Guhr, H Ibrahim, and N Schwentner. Control of chromophore-to-bath coupling by interferometry: Cl_2 vibrational wave packets in solid Ar. *J. Phys. B: At. Mol. Opt. Phys.*, 41(7):074013, 2008.

M. Fushitani, M. Bargheer, M. Gühr, and N. Schwentner. Pump-probe spectroscopy with phase-locked pulses in the condensed phase: Decoherence and control of vibrational wavepackets. *Phy. Chem. Chem. Phys.*, 7:3143, 2005.

I. U. Goldschleger, V. Senekerimyan, M. S. Krage, H. Seferyan, K. C. Janda, and V. A. Apkarian. Quenched by ice: Transient grating measurements of vibronic dynamics in bromine-doped ice. *J. Chem. Phys.*, 124(20):204507, 2006.

I. U. Goldschleger, V. Senekerimyan, M. S. Krage, H. Seferyan, K. C. Janda, and V. A. Apkarian. Quenched by ice: Transient grating measurements of vibronic dynamics in bromine-doped ice. *J. Chem. Phys.*, 124(20):204507, 2006.

M. Gühr, M. Bargheer, and N. Schwentner. Generation of coherent zone boundary phonons by impulsive excitation of molecules. *Phys. Rev. Lett.*, 91(8):085504, Aug 2003.

M. Gühr, M. Bargheer, and N. Schwentner. Coherent phonon dynamics: Br_2 in solid Ar. *Phys. Chem. Chem. Phys.*, 7:760, 2004.

M. Gühr and N. Schwentner. Effective chromophore potential, dissipative trajectories, and vibrational energy relaxation: Br_2 in Ar matrix. *J. Chem. Phys.*, 123(24):244506, 2005.

E. J. Heller, R. L. Sundberg, and D. Tannor. Simple aspects of Raman scattering. *J. Phys. Chem.*, 86:1822, 1982.

Eric J. Heller. Time-dependent approach to semiclassical dynamics. *J. Chem. Phys.*, 62(4):1544, 1975.

Eric J. Heller. Quantum corrections to classical photodissociation models. *J. Chem. Phys.*, 68(5):2066, 1978.

Eric J. Heller. The semiclassical way to molecular spectroscopy. *Acc. Chem. Res.*, 14(12):368, December 1981.

Travis S. Humble and Jeffrey A. Cina. Nonlinear wave-packet interferometry and molecular state reconstruction in a vibrating and rotating diatomic molecule. *J. Phys. Chem. B*, 110(38):18879, 2006.

M. Karavitis and V. A. Apkarian. Vibrational coherence of I_2 in solid Kr. *J. Chem. Phys.*, 120(1):292, 2004.

M. Karavitis, T. Kumada, I. U. Goldschleger, and V. A. Apkarian. Vibrational dissipation and dephasing of $I_2(v = 119)$ in solid Kr. *Phys. Chem. Chem. Phys.*, 7:791, 2005.

M. Karavitis, D. Segale, Z. Bihary, M. Pettersson, and V. A. Apkarian. Time-resolved CARS measurements of the vibrational decoherence of I_2 isolated in an Ar matrix. *Low Temp. Phys.*, 29(9):814–821, 2003.

M. Karavitis, R. Zadoyan, and V. Ara Apkarian. Time resolved coherent anti-stokes raman scattering of i_2 isolated in matrix argon: Vibrational dynamics on the ground electronic state. *J. Chem. Phys.*, 114(9):4131, 2001.

Hiroyuki Katsuki, Hisashi Chiba, Bertrand Girard, Christoph Meier, and Kenji Ohmori. Visualizing picometric quantum ripples of ultrafast wave-packet interference. *Science*, 311(5767):1589, 2006.

Hiroyuki Katsuki, Hisashi Chiba, Bertrand Girard, Christoph Meier, and Kenji Ohmori. Visualizing picometric quantum ripples of ultrafast wave-packet interference. *Science*, 311(5767):1589, 2006.

Tiina Kiviniemi, Jukka Aumanen, Pasi Myllyperkiö, V. A. Apkarian, and Mika Pettersson. Time-resolved coherent anti-stokes raman-scattering measurements of I_2 in solid Kr: Vibrational dephasing on the ground electronic state at 2.6—32 K. *J. Chem. Phys.*, 123(6):064509, 2005.

Oliver Kuhn and Nancy Makri. Forward—backward semiclassical calculation of spectral line shapes: I_2 in a rare gas cluster. *J. Phys. Chem. A*, 103(47):9487, November 1999.

C. P. Lawrence, A. Nakayama, N. Makri, and J. L. Skinner. Quantum dynamics in simple fluids. *J. Chem. Phys.*, 120(14):6621, 2004.

Soo-Y. Lee and Eric J. Heller. Exact time-dependent wave packet propagation: Application to the photodissociation of methyl iodide. *J. Chem. Phys.*, 76(6):3035, 1982.

C. Leichtle, W. P. Schleich, I. Sh. Averbukh, and M. Shapiro. Quantum state holography. *Phys. Rev. Lett.*, 80(7):1418, 1998.

Robert J. LeRoy. Spectroscopic reassignment and ground-state dissociation energy of molecular iodine. *J. Chem. Phys.*, 52(5):2678, 1970.

Todd J. Martinez. Insights for light-driven molecular devices from ab initio multiple spawning excited-state dynamics of organic and biological chromophores. *Acc. Chem. Res.*, 39(2):119, February 2006.

C. Alden Mead. The geometric phase in molecular systems. *Rev. Mod. Phys.*, 64(1):51, Jan 1992.

A. Messiah. *Quantum Mechanics.* Dover Pulications, Mineola, New York, 1999.

William H. Miller. Including quantum effects in the dynamics of complex (i.e., large) molecular systems. *J. Chem. Phys.*, 125(13):132305, 2006.

Takamasa Momose, Mizuho Fushitani, and Hiromichi Hoshina. Chemical reactions in quantum crystals. *International Reviews in Physical Chemistry*, 24(3):533, 2005.

John Moody, A. Shapere, and Frank Wilczek. Realizations of magnetic-monopole gauge fields: Diatoms and spin precession. *Phys. Rev. Lett.*, 56(9):893, Mar 1986.

Shaul Mukamel. *Principles of Nonlinear Optical Spectroscopy.* Oxford University Press, 1999.

Anne B. Myers, Robert A. Harris, and Richard A. Mathies. Resonance raman excitation profiles of bacteriorhodopsin. *J. Chem. Phys.*, 79(2):603, 1983.

Kenji Ohmori, Hiroyuki Katsuki, Hisashi Chiba, Masahiro Honda, Yusuke Hagihara, Katsutoshi Fujiwara, Yukinori Sato, and Kiyoshi Ueda. Real-time observation of phase-controlled molecular wave-packet interference. *Phys. Rev. Lett.*, 96(9):093002, Mar 2006.

Kenji Ohmori, Yukinori Sato, Evgueni E. Nikitin, and Stuart A. Rice. High-precision molecular wave-packet interferometry with HgAr dimers. *Phys. Rev. Lett.*, 91(24):243003, 2003.

M. Ovchinnikov and V. A. Apkarian. Mixed-order semiclassical dynamics in coherent state representation: The connection between phonon sidebands and guest—host dynamics. *J. Chem. Phys.*, 108(6):2277, 1998.

M. Ovchinnikov, V. A. Apkarian, and Gregory A. Voth. Semiclassical molecular dynamics computation of spontaneous light emission in the condensed phase: Resonance Raman spectra. *J. Chem. Phys.*, 114(16):7130, 2001.

David W. Oxtoby. Vibrational population relaxation in liquids. page 487, 2007.

George C. Pimentel. Reaction kinetics by the matrix isolation method: Diffusion in argon; cis-trans isomerization of nitrous acid. *J. Am. Chem. Soc.*, 80(1):62, 1958.

W. T. Pollard, A. K. Felts, and R. A. Friesner. Time-resolved optical tests for electronic geometric phase development. *Adv. Chem. Phys.*, 93:77, 1996.

Sandu Popescu, Anthony J. Short, and Andreas Winter. Entanglement and the foundations of statistical mechanics. *Nature Physics*, 2(11):754, 2006.

Sandu Popescu, Anthony J. Short, and Andreas Winter. The foundations of statistical mechanics from entanglement: Individual states vs. averages. *http://arxiv.org/abs/quant-ph/0511225v3*, 2006.

P. R. Poulin and K. A. Nelson. Irreversible organic crystalline chemistry monitored in real time. *Science*, 313:1756, 2006.

William Press, Saul Teukolsky, William Vetterling, and Brian Flannery. *Numerical Recipes in C.* Cambridge University Press, Cambridge, UK, 2nd edition, 1992.

O. V. Prezhdo and Y. V. Pereverzev. Quantized Hamilton dynamics for a general potential. *J. Chem. Phys.*, 116(11):4450, 2002.

Oleg Prezhdo. Quantized hamilton dynamics. *Theor. Chem. Acc.*, 116(1):206, August 2006.

Jeanne M. Riga, Erick Fredj, and Craig C. Martens. Quantum vibrational state-dependent potentials for classical many-body simulations. *J. Chem. Phys.*, 122(17):174107, 2005.

Mary A. Rohrdanz and Jeffrey A. Cina. Probing intermolecular communication via lattice phonons with time-resolved coherent anti-Stokes Raman scattering. *Mol. Phys.*, 104(8):1161, 2006.

S. Sawada and H. Metiu. A multiple trajectory theory for curve crossing problems obtained by using a gaussian wave packet representation of the nuclear motion. *J. Chem. Phys.*, 84(1):227–238, 1986.

Roland Schanz. Virgiliu Boţan, and Peter Hamm. A femtosecond study of the infrared-driven cis-trans isomerization of nitrous acid (HONO). *J. Chem. Phys.*, 122(4):044509, 2005.

N. F. Scherer, A. Matro, L. D. Ziegler, M. Du, R. J. Carlson, J. A. Cina, and G. R. Fleming. Fluorescence-detected wave packet interferometry. II. role of rotations and determination of the susceptibility. *J. Chem. Phys.*, 96(6):4180, 1992.

Norbert F. Scherer, Roger J. Carlson, Alexander Matro, Mei Du, Anthony J. Ruggiero, Victor Romero-Rochin, Jeffrey A. Cina, Graham R. Fleming, and Stuart A. Rice. Fluorescence-detected wave packet interferometry: Time resolved molecular spectroscopy with sequences of femtosecond phase-locked pulses. *J. Chem. Phys.*, 95(3):1487, 1991.

Yu-Chen Shen and Jeffrey A. Cina. What can short-pulse pump-probe spectroscopy tell us about Franck-Condon dynamics? *J. Chem. Phys.*, 110(20):9793, 1999.

Qiang Shi and Eitan Geva. A semiclassical generalized quantum master equation for an arbitrary system-bath coupling. *J. Chem. Phys.*, 120(22):10647, 2004.

Robert Silbey and Robert A. Harris. Tunneling of molecules in low-temperature media: An elementary description. *J. Phys. Chem.*, 93(20):7062, October 1989.

T. J. Smith and J. A. Cina. Toward preresonant impulsive raman preparation of large amplitude vibrational motion. *J. Chem. Phys.*, 104(4):1272, 1996.

Lowell W. Ungar and Jeffrey A. Cina. The relaxation dynamics and short-time optical response of a multimode open system. *J. Phys. Chem. A*, 102(38):7382, 1998.

Eric Whittle, David A. Dows, and George C. Pimentel. Matrix isolation method for the experimental study of unstable species. *J. Chem. Phys.*, 22(11):1943, 1954.

Yi Jing Yan and Shaul Mukamel. Semiclassical dynamics in Liouville space: Application to molecular electronic spectroscopy. *J. Chem. Phys.*, 88(9):5735, 1988.